Modulators of Auditory Responses in *Drosophila*: From the Ear to Behaviour via the Clock?

Assel Kashkenbayeva

A dissertation submitted in partial fulfilment of the requirements for the degree of
Doctor of Philosophy
of
University College London

London Interdisciplinary Doctorial Training Programme (Lido)

I, Assel Kashkenbayeva, confirm that the work presented in this thesis is my own. Where information has been derived from other sources, I confirm that this has been indicated and appropriately referenced within this work.

Acknowledgements

Firstly, thank you to the BBSRC for sponsoring my PhD and to everyone who is part of the LiDo programme for curating such an interdisciplinary, demanding yet rewarding doctoral programme.

I would like to thank my supervisors Prof Joerg Albert and Prof Jonathan Ashmore for supporting me throughout this PhD. You have always emphasised that this is 'my research', and even in the most uncertain times you have always guided rather than instructed me along the right path; I am grateful that you gave me both intellectual and resource freedoms to discuss, explore and execute ideas. The importance you place on my personal development hasn't gone unnoticed and has led me to become a better researcher.

Thank you to the past and present lab members: Marta Andres, Nick Boyd-Gibbins, Alyona Keder, Ryan Kaville, Matthew Su and Camille Tardieu who have helped introduce me to the world of *Drosophila* and given me the knowledge and skills to execute this work. A special thank-you to Jason Somers who has on many occasions acted as my supervisor in his own right.

Thank you to my friends who have listened to me talk about my PhD far too much. Especially Irina Ionescu, not only was your career advice and support instrumental in my securing a fantastic PIPs placement but you have also kept me in good supply of snacks throughout this whole period. I am glad to have shared this PhD journey with Mariann Angola, Brynna Hoggard and Laura Stennett who have all helped provide much needed entertainment along the way.

And finally, the biggest thank-you is to my whole family. Thank you for always encouraging me to be curious and allowing me to thoroughly explore whichever path those curiosities lead me down. To Ben, who has always been patient, supportive and loving; your contribution to this research can be found on every page of this thesis. To my brother Max, you have always shown such care and concern for my future; thank you for always believing in me and encouraging me to

do better. To my father, thank you for the innumerable cups of tea over the last few months. And finally, to my mother, without your hard work, encouragement and persistent support I wouldn't have had the privilege to follow this academic path in the first place. Thank you for not only providing me with the best example of how to reach my goals but also with the resources to help build the brightest future.

This work might have been written by me but was enabled by all of you, for which I am infinitely grateful.

Contents

Contents

Contents

Contents

List of Figures

Contents

Contents

11

Contents

List of Tables

Contents

Abstract

Mechanoelectrical transduction (MET) is the crucial process underlying hearing. *Drosophila melanogaster* perform elaborate courtship rituals in which the male engages in the production of auditory courtship signals by vibrating his wings (Spieth, 1974). Playback of these sounds results in observable changes in locomotor activity in both male and female flies (von Schilcher, 1976; Yoon, Matsuo, Yamada, Mizuno, & Morimoto, 2013). Overall, *Drosophila* demonstrate robust activity patterns (Tataroglu & Emery, 2014). This behavioural rhythmicity is regulated by the circadian clock (Helfrich-Förster, 2001). To probe whether auditory-induced locomotor behaviour is also under clock control, here I present a novel behavioural assay to study the intersection between these two systems.

I begin by quantifying this method and subsequently uncover several factors which regulate auditory-induced locomotor activity. Light exposure and the 'naturalness' of the stimulus were identified as key modulators. Additionally, I find that the behavioural response to sound stimuli does indeed does show periodic changes over a 24-h cycle. These oscillations showed a unique rhythm in comparison to the periodicity of non-sound-induced locomotor activity and were abolished in clock-disrupted conditions; suggesting that auditory-induced locomotor activity is also regulated by the circadian clock.

Functional imaging using GCaMP reporters was performed in different subsets of Johnston's Organ (JO) neurons to probe whether the key regulators of sound-induced behaviour directly modulate the function of the auditory neurons. Calcium responses to sound stimuli were found to be modulated by both the naturalness of stimuli and the environmental light conditions.

Impact statement

The work presented within this thesis is of direct benefit and relevance in the mechanosensory and chronobiology research fields as well as outside academia. The project was not solely motivated by advancing knowledge and understanding of auditory processing and auditory-induced behaviours in *Drosophila,* but also to provide novel experimental tools to probe the function of sensory systems.

By quantifying a novel auditory behavioural assay and developing a data analysis protocol to extract meaningful insights, this paradigm can be applied directly in other studies investigating auditory processing. Due to the simplicity of the experimental protocol and direct link between primary sensory processing and behaviour, this assay can also be utilized for screening drugs which impact these systems. With a few more preliminary investigations into this behavioural assay, it also has the potential to be used as a paradigm for exploring other processes such as learning and memory, since one of the greatest advantages of the approach is that it allows for prolonged monitoring of behaviour. Though this thesis did not investigate this assay within that capacity, it lays the foundations for this work.

The findings in this thesis demonstrate that there are key modulators of auditory-induced behaviours which also interact with the primary auditory processing organ. The ability of environmental factors to influence mechanisms of sound transduction and behaviour show the adaptability (as well as highlighting the complexity of) the auditory system. The finding that there is circadian modulation of auditory-induced behaviours is perhaps a factor that has been overlooked in previous studies within the field. This calls for future investigations of these behaviours in *Drosophila* to ensure that the the time of observation controlled for within experimental protocols. This finding may help explain why there are contradicting observations within the field relating to auditory-induced behaviours.

Lastly, the broader impact of this research is that it poses the same questions to mammalian systems. Are there certain points of the day at which we hear better and is this sensitivity mediated directly by the primary sensory organ? If so, what

mechanisms underlie this process and how can they be independently targeted to improve hearing? To use a specific example from the experiments detailed within this thesis, I observed that constant light exposure led to an increased behavioural and physiological responsiveness to sound stimuli. If this effect is conserved in mammals, this would suggest an immediate relevance for humans. Our urban lives expose us to a wide range of sensory stimuli that has moved away from natural diurnal patterns of e.g. light and temperature. If these self-created environments affect our ability to perceive the world, it leads to interesting possibilities to exploit this interaction to improve human work place safety and general wellbeing.

In conclusion, I would posit that this research may find wider usage within several different fields of *Drosophila* investigation and with potential impacts on mammalian work and thus on the broader field of audiology.

Chapter 1

Background: *Drosophila* mechanosensory processing

1.1 Evolutionary importance of auditory & mechanosensory processing

Mechanosensation starts with the elementary process of transducing a mechanical stimulus into an intracellular signal (Eatock, Corey, Hudspeth, & Fettiplace, 1987). This process forms the basis of two primary senses key for survival; hearing and touch. An organism exploits these senses to interact with their environment allowing them to feed, mate and detect danger. Besides the use of these sensory modalities to gain information about their physical and social surroundings (Cocroft, 2001); mechanosensory processing also underpins proprioception (Cheng, Song, Looger, Jan, & Jan, 2010) – the sense of self movement and body position. Needless to say, the ability to detect and perceive mechanical signals is a process which is important for the evolutionary success of an organism.

Table 1: Relevant mechanosensory terminology

Abbreviation	Term	Description
A1	1st Antennal segment/ Scape	Forms one of the antennal components. Positioned dorsally, the antennal nerve consisting of all axons from A2 and A3 passes through this segment leading to higher processing regions in the brain.
A2	2nd Antennal segment/ Pedicel	Forms one of the antennal components. The JO is housed within this distal part of the antenna.
A3	3rd Antennal segment/ Funiculus	Forms one of the antennal components. This segment houses the olfactory organ.
–	Antenna	The antenna is an anatomical structure located on the head of the fruit fly which is composed of 3 segments.
AMMC	Antennal Mechanosensory & Motor Centre	Located in the deutocerebrum in the fly brain. The output from the antennal nerve synapses here. This is the central auditory processing region.
–	Arista/ Sound receiver	This feather-like structure extends out from the 3rd antennal segment. It detects particle velocity changes & forms the first stage of the transduction process.
CAP	Compound Action Potential	Extracellular electrophysiological recording of the sum activity within the JO obtained by inserting an electrode into the antennal joint behind A1 in close proximity the antennal nerve.
ChO	Chordotonal Organ	A sensory organ present in insects. Chordotonal organs have a diverse morphology. These organs consist of multiple repeats of multicellular scolopidia.
IP	Inter-Pulse Frequency	As part of a courtship ritual, male fruit flies produce a courtship song by movement of their wing. The IPF is the frequency of the produced sound

IPI	Inter-Pulse Interval	Pulse trains form part of a courtship signal. The IPI is the time interval between two sound pulses. This feature is species-specific and for *D. Melanogaster* the preferred IPI is 34ms.
JO	Johnston's Organ	The largest chordotonal organ of the fruit fly. It is the auditory processing organ. This structure functions analogously to the cochlea in mammals.
JON	Johnston's Organ Neurons	The comprising sensory neurons of the JO. There is a heterogenous population of mechanosensory neurons within the JO which function as auditory and wind/gravity detectors.
MET	Mechanoelectrical transduction	The process by which a mechanical stimulus is transduced into an electrical current.
–	Scolopidium	A composite structure which forms the functional unit of the mechanosensory receptor.

1.2 Anatomical dissection of mechanosensory processing in *Drosophila*
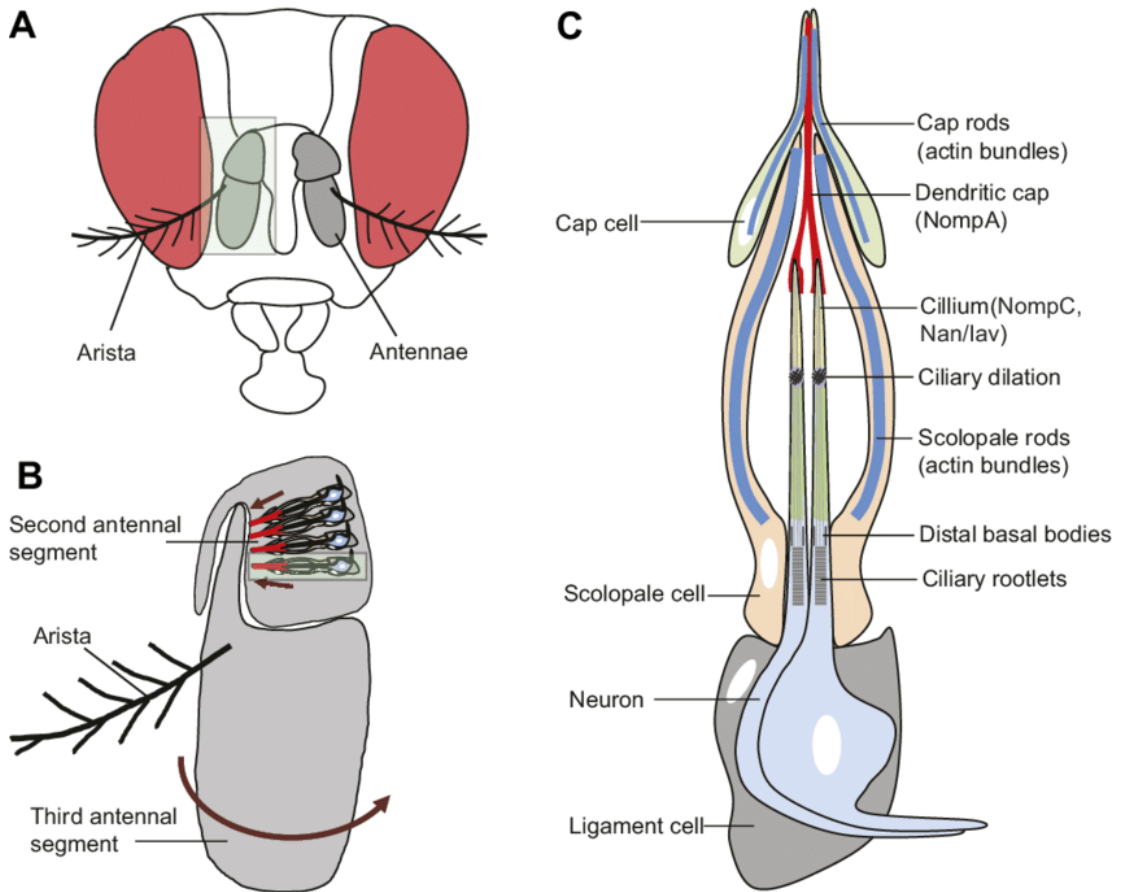
Figure 1: Schematic of antenna & morphological structure of a scolopidium.
A: A diagram to show the positioning of the antennae on the *Drosophila* head with the arista extending out laterally out below the second antennal segment. **B:** A diagram of the pedicel and funiculus with an arrow to demonstrate the rotation of the structure when presented with a sound stimulus. **C:** A depiction of the different components of the mechanoreceptive structures within the JO. (Figure adapted from (Li, Bellen, & Groves, 2018)).

Drosophila have a vast variety of mechanoreceptive organs (Yack, 2004). Insect and thus fruit fly mechanoreceptors can be classified into two groups, type I and type II. The composite structure of a type I sensory organ (bristles and scolopidia) comprises of multiple cells: sensory neurons, each with a single ciliated dendrite supported by accessory cells (**Fig 1C**). These ciliated stretch receptor sub-units are responsible for transducing mechanical distortions into electrical signals within the external sensory organs (es organs) such as the bristles and chordotonal organs

(ChO organs) (Gillespie & Walker, 2001). The main distinction between es and ChO organs is that the former has external sensilla whereas the latter is internally innervated by mechanoreceptors.

Conversely, type II sensory neurons are morphologically dissimilar and possess multi-dendritic non-ciliated projections. Furthermore, there are no accessory cells associated with type II mechanoreceptors (Bodmer et al., 1987; Crozatier & Vincent, 2007). Since the current work focuses on ChO mediated mechanosensation, the former type of mechanoreceptors bears most relevance to this thesis.

The largest chordotonal organ of the fruit fly is the Johnston's Organ (JO). It houses the auditory neurons within the antennal ear (Eberl, Duyk, & Perrimon, 1997; Kamikouchi et al., 2009) (**Fig 1B**). Housed within the 2nd antennal segment (A2), it consists of ~227 scolopidia (Kamikouchi, Shimada, & Ito, 2006). The arista branches laterally from the upper part of the 3rd antennal segment (A3) (Todi, Sharma, & Eberl, 2004) (**Fig 2A**). The latter is a club-shaped structure, which is positioned below A2 and also houses the primary olfactory organ. Despite their pronounced morphological differences, the JO and these associated structures are analogous to the structure and function of the mammalian ear (Albert & Kozlov, 2016).

A hooked cuticular stalk extends from the basilar part of A3 into A2 making direct connections to the scolopidia within JO (**Fig 2B**). These sensory sub-units project radially from the hooked joint which forms the only anatomical connection between the two antennal segments (Eberl, Hardy, & Kernan, 2000a) (**Fig 2C**). The arista, together with A3, functions as a sound receiver forming the first part of the transduction process (Göpfert & Robert, 2001). The pendular movement of the sound receiver and the tangential rotation of A3 in response to particle velocity distortions translate to the hook, activating and deactivating the mechanically-coupled stretch receptors positioned in two topographically distinct arrays within the JO (Göpfert & Robert, 2002; Kamikouchi *et al.*, 2009) (**Fig 2**). Removing the arista or A3 results in severely dampened receptivity to sound stimuli (Göpfert & Robert, 2002; von Schilcher, 1976).
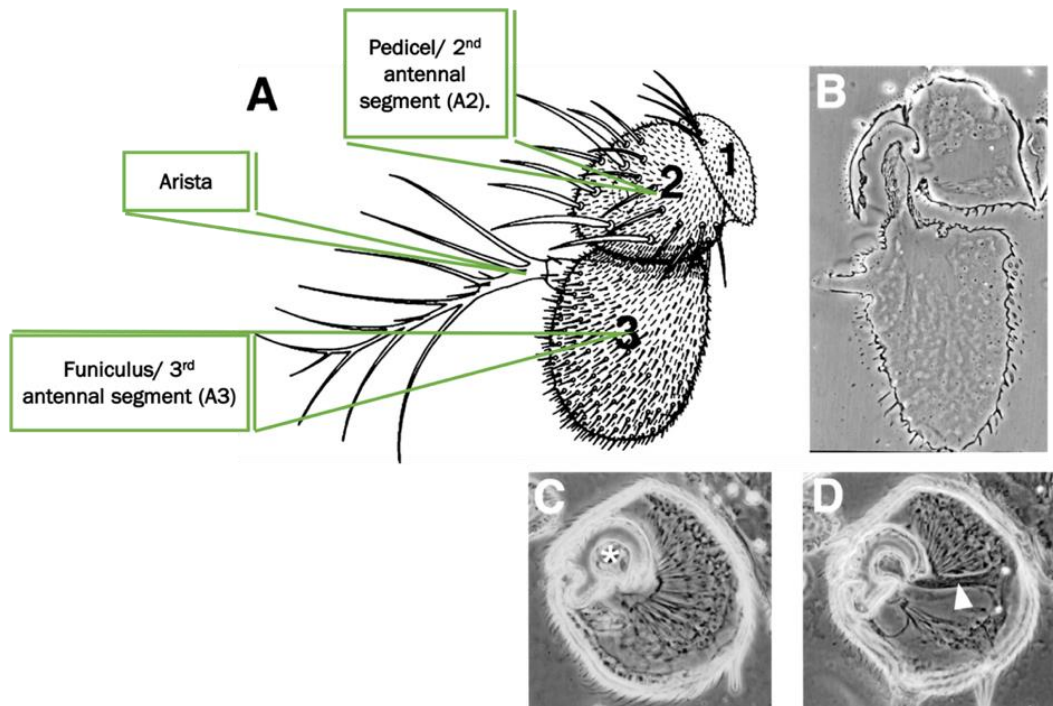
Figure 2: Structure of the antennae & phase contrast images of sectioned antennae to show the distribution of scolopidia within the JO.
A: An illustration to show the different components of the antennae. B: Frontal sections through the antenna to show the hook from the funiculus extending into the pedicel. C: Cross-section through the pedicel showing the scolopidia distributed radially inside the JO. The asterisk shows the stalk extending from the 3$_{rd}$ to the 2$_{nd}$ antennal segment. D: Another cross-section through the second antennal segment. The arrow shows the antennal nerve projections. (Figure adapted from (Eberl, Hardy, & Kernan, 2000)).

Each JO scolopidium is a self-contained sensory unit which can harbour up to 3 sensory neurons. Variants of scolopidia are dispersed throughout the organ and the reason for this diversity in neuronal number per receptor unit is so far unknown (Todi *et al.*, 2004). JO neurons (JONs) are bipolar with two cytoplasmic extensions lengthening from the soma (**Fig 3**). The apical dendrite makes connections with the cap cells which scaffolds this stretch receptor to the underside of the cuticular plate, keeping it under tension (**Fig 3**). The basal axon projects into the central brain processing region, the antennal mechanosensory and motor centre (AMMC).
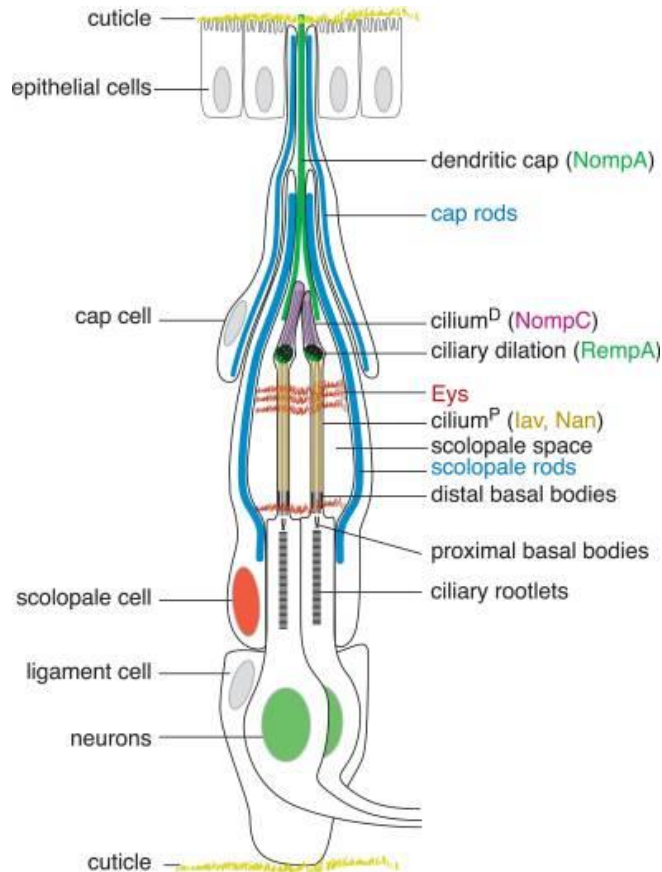
Figure 3: Schematic to show the detailed structure of a scolopidia & the proposed involvement of proteins within this structure.
Reference for illustration (Boekhoff-Falk & Eberl, 2014)

The ciliary endings of these neurons are encased by a fluid-filled capsule known as the scolopale which maintains and regulates the ionic composition of the endolymph (Boekhoff-Falk & Eberl, 2014). There is an ionic gradient between the lumen and the distal cilium due to the receptor lymph being high in potassium (K_+) and low in calcium (Ca_{2+}) (Grunert & Gnatzy, 1987). This disparity drives the receptor current upon channel opening (Field & Matheson, 1998).

Due to the short latency of auditory transduction, it is predicted that JONs are directly gated by force rather than through the use of a second messenger (Albert, Nadrowski, & Göpfert, 2007; Lehnert, Baker, Gaudry, Chiang, & Wilson, 2013; Walker, Willingham, & Zuker, 2000). It is hypothesised that mechanical stimulation results in the direct opening of cation channels. The subsequent influx ion (probably K_+) results in neuronal depolarisation and generation of receptor potentials.

By inserting an electrode close to the antennal nerve, sound-evoked compound action potentials (CAPs) can be recorded. When presented with a pulse stimulus, the aggregate product of the CAP recordings reflects the pulse pattern of the given sound stimulus (Eberl, Hardy, & Kernan, 2000b). In this way, the stretch-sensitive neurons in the fly antenna are directly coupled to the presented mechanical forces (Caldwell & Eberl, 2002; Kamikouchi et al., 2009; Todi et al., 2004).

There is a heterogeneous population of ~500 JONs functioning as sound, wind and gravity detectors (Armstrong, Texada, Munjaal, Baker, & Beckingham, 2006; (Budick, 2006); Field & Matheson, 1998; Kamikouchi et al., 2009; Kernan, 2007). The different sub-populations have been identified based on their distinct synapse formation within the brain, molecular composition and response mechanics (Yorozu et al., 2009).

The antennal nerve carries the JON projections via the scape to the AMMC; the brain region located in the ventral side of the fly brain essential for auditory processing (Tootoonian, Coen, Kawai, & Murthy, 2012). Kamikouchi, Shimada, & Ito (2006) distinguished between five different mechanosensory populations (labelled A-E) in the JO based on the spatially-segregated synapsing formation in the AMMC (**Fig 4**).
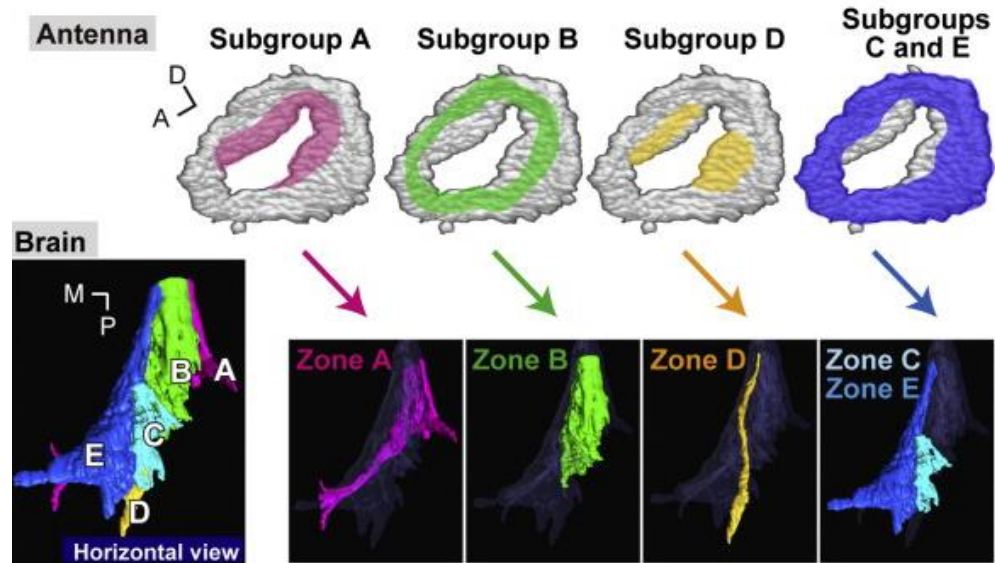
Figure 4: Illustration to show the mapping of the heterogenous populations of sensory neurons within the antenna & brain.
The top panel shows the approximate distribution of the sensory neurons within the antenna and the bottom panel demonstrates the distinct regions within the AMMC where these sub-populations of sensory neurons synapse. (Reference for illustration (Kamikouchi, 2013)

Different types of receptor movements trigger activation of cellularly distinct JONs. A and B sub-population neurons respond to a broad range of frequency vibrations of 19 Hz to 952 Hz whereas the C and E neurons respond preferentially to static deflections (Kamikouchi et al., 2009)

1.3 Molecular & biomechanical dissection of mechanosensory processing in *Drosophila*

The hearing organ of a fly is not a passive system. Active processes enhance sensitivity of the antennal ear, leading to amplification of the mechanical signal (Göpfert, Humphris, Albert, Robert, & Hendrich, 2005). The nonlinearity of the system and motility of the mechanosensory neurons within the JO can be observed by measuring the vibrations of the arista in response to both Brownian motion and during acoustic stimulation (**Fig 5**).

Figure 5: Graphs to show the frequency tuning & gating compliance of *Drosophila* antennal ears.
A: Graph to show the free mechanical fluctuations (without stimulus) of the antennal receiver in its active and passive states. The fly has been anaesthetized with CO_2 in the passive state. **B:** Shows the gating compliance of the sound receiver where smaller distortions of the arista are amplified compared to larger displacements. (Reference for panel **A** (Riabinina, Dai, Duke, & Albert, 2011) & for panel **B** (Albert et al., 2007)).

In conditions where the fly is dead, sedated or a mechanosensory mutant, the resonant frequency of the sound receiver becomes purely reflective of the stiffness of the mechanical coupling of the anatomical modules within the JO (Nadrowski, Albert, & Göpfert, 2008) (**Fig 5A**).

Unlike the cochlea amplifier, which is known to rely on efferent feedback, the fly's antennal ear appears to be independent of efferent chemical signalling. Mechanical power gain and electrophysiological response properties to sound stimuli are not affected by neurotransmission blockage to or from the JO (Albert, Göpfert, & Kamikouchi, 2010).

Taken together, these findings suggest that *Drosophila* auditory mechanotransduction is a two-part process. Firstly, there is mechanical-signal-to-electrical-impulse conversion and secondly, active amplification for positive mechanical feedback. The latter boosts antennal vibration which is controlled peripherally within the ear (**Fig 5B**).

In mammals and fruit flies, a variety of signalling processes are reliant on transient receptor potential (TRP) channels (Christensen & Corey, 2007). Three primary TRP channels are expressed in JONs which have been identified as key molecular components of *Drosophila* ChO mechanotransduction (Kim et al., 2003; Lee, Moon, Cha, & Chung, 2010; Lehnert et al., 2013). The TRPN1 gene *nompC* and the heterodimeric channel formed by the two TRP vanilloid (TRPV) channels *nanchung (nan)* and *inactive (iav)*, all of which contribute to the mechanosensory processing. The exact role of these proteins within the mechanotransducer complex is not fully clear and there is dispute within the field as to which proteins are involved directly in the mechanotransduction process and which in the amplification apparatus (Albert & Göpfert, 2015). Nevertheless, they provide viable genetic targets to investigate mechanosensory processing in *Drosophila.*

1.4 Auditory-induced behaviours in *Drosophila*

Despite morphological and topographical differences, both auditory and touch pathways have shared genetic elements (Eberl et al, 2000a) and a common evolutionary origin (Merritt, 1997). Touch insensitivity, incoordination and impaired gravitaxis are all indicators of mechanosensory defects. Many mutants displaying these touch deficiencies are also associated with hearing deficits (Eberl et al., 2000b).

At times it is difficult to determine whether behavioural deficiencies are a direct consequence of primary sensory deficits, since a mutation can act at any point within the system; altering the processing of initial input as well as the generation of behavioural output. However, impairments in auditory-induced behaviours are often associated with the reduction or abolishment of sound-evoked mechanoreceptor potentials from the JO (Eberl et al., 2000a; Walker, 200; Eberl, Duyk, & Perrimon, 1997).
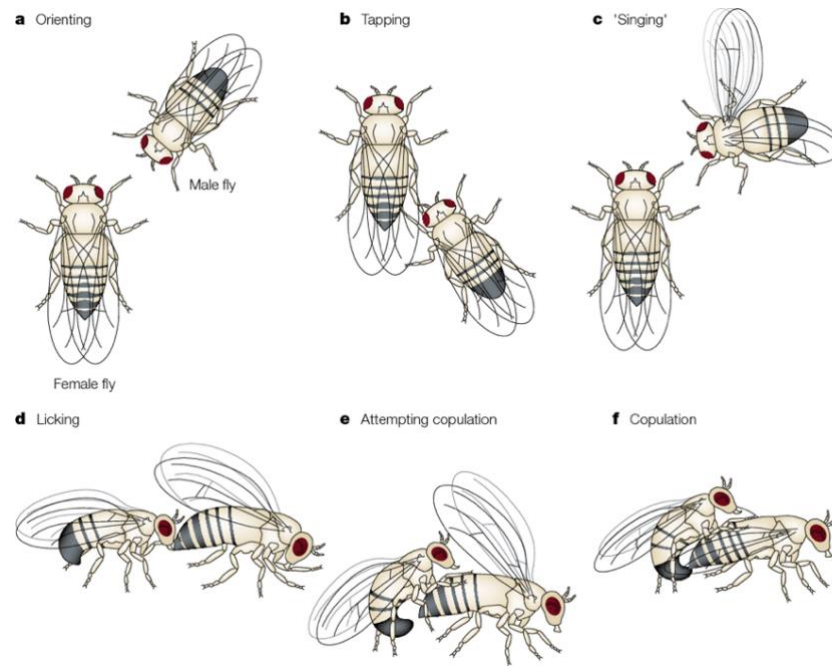
Figure 6: Schematic to show the stages within a courtship ritual in *Drosophila*
Hearing is an integral part of the courtship process whereby the male uses its wing to produce a courtship song. Copulation is highly dependent on successful reception of this sensory signal. (Adapted from (Sokolowski, 2001)).

Mating success and courtship behaviour is strongly correlated with auditory processing (von Schilcher, 1976). Male *Drosophila* show overt signs of courtship behaviour. Starting by tapping the female and positioning himself close, the male fruit fly proceeds to produce a courtship song by extension and vibration of his wings (Spieth, 1974) (**Fig 6**). The full courtship sequence is described in detail in Manning (1955). The importance of the males' wings in a courtship display was first identified by Sturtevant in 1915, whereas the significance of the courtship song as an auditory stimulus within the courtship ritual was established by Shorey (1962).

Courtship behaviour requires the function of a number of sensory modalities. Visual, auditory and chemical cues are relevant during courtship rituals (Ewing, 1983). Immobilizing or removing the antennal ear or the arista results in a dramatic reduction in sound-evoked courtship behaviour and an increase in mating latency (Kamikouchi et al., 2009; Eberl et al., 1997; Eberl et al., 2000a; Hall, 1994). Amputating the wings to varying degrees also results in latency in copulation due to the attenuation of the wing-generated air borne distortions (Cook, 1973).

30

The effect of the courtship song on behaviour is determined to be sexual in nature since the playback of sound stimulus results in increased attempts at copulation (von Schilcher, 1976). Male *Drosophila* show a steady increase in locomotor activity in response to courtship stimuli which are sustained over a long period of time (von Schilcher, 1976). Whereas agonistic sound stimuli (which resemble the song produced during male aggressive behaviour) also produce bursts of increased locomotion, the observed effect is brief (Ishikawa, Okamoto, Yoneyama, Maeda, & Kamikouchi, 2019) (**Fig 7D**). Conversely, the main indicator of female receptibility to copulation is the slowing of locomotor activity (Spieth, 1974). It is hypothesised that the slowing of movement of a female fly facilitates courtship and copulation (Cook, 1973, Markow and Hanson, 1981).

The courtship song is primarily composed of two parts, the pulse and the sine components (Ewing, 1967) (**Fig 7C**). By extension of a single wing, the male produces a so called 'pulse train' which can last in bouts for several seconds and is interspersed with sine components. Since it was observed that out of 76 interactions directly preceded by the pulse song, 75 ended in copulation (Schilcher, 1976a), it was hypothesised that the pulse part of the courtship song acts as a trigger, and is described as the active part of the song.

The pulse train, which forms a part of the courtship song, can be characterised by the inter-pulse interval (IPI) and the inter-pulse frequency (IPF or also referred to as the carrier frequency). The IPI is the duration between pulses and the IPF is the carrier frequency of the produced pulses. There is variation in these parameters in the production of a courtship signal among different *Drosophila* species (Markow & O'Grady, 2005; Saarikettu, Liimatainen, & Hoikkala, 2005). The IPI in particular is the parameter that distinguishes species-specific courtship songs (Bennet-Clark and Ewing, 1969; Kyriacou and Hall, 1986) (**Fig 7 A&B**).

Both the production and detection of species-specific signals are under neuronal control (Bennet-Clark, 1967; Cowling & Burnet, 1981). JO neurons have been found to be selectively responsive to species-specific signals (Yoon et al., 2013). Riabinina, Dai, Duke, & Albert (2011) reported that there is mechanical tuning to conspecific courtship signals in a number of *D. melanogaster* sub-species.

It has been identified that for *D. melanogaster* the preferred IPI is 34ms (Kyriacou & Hall, 1984). As well as there being physiological priming to species-specific signals, the exposure to the correct species-specific signals affects behaviour. Presentation of a 34ms pulse train to *D. melanogaster* increased female receptibility and has been shown to induce greater courtship behaviour from males (Moulin, Aubin, & Jallon, 2004; Rybak, Sureau, & Aubin, 2002).
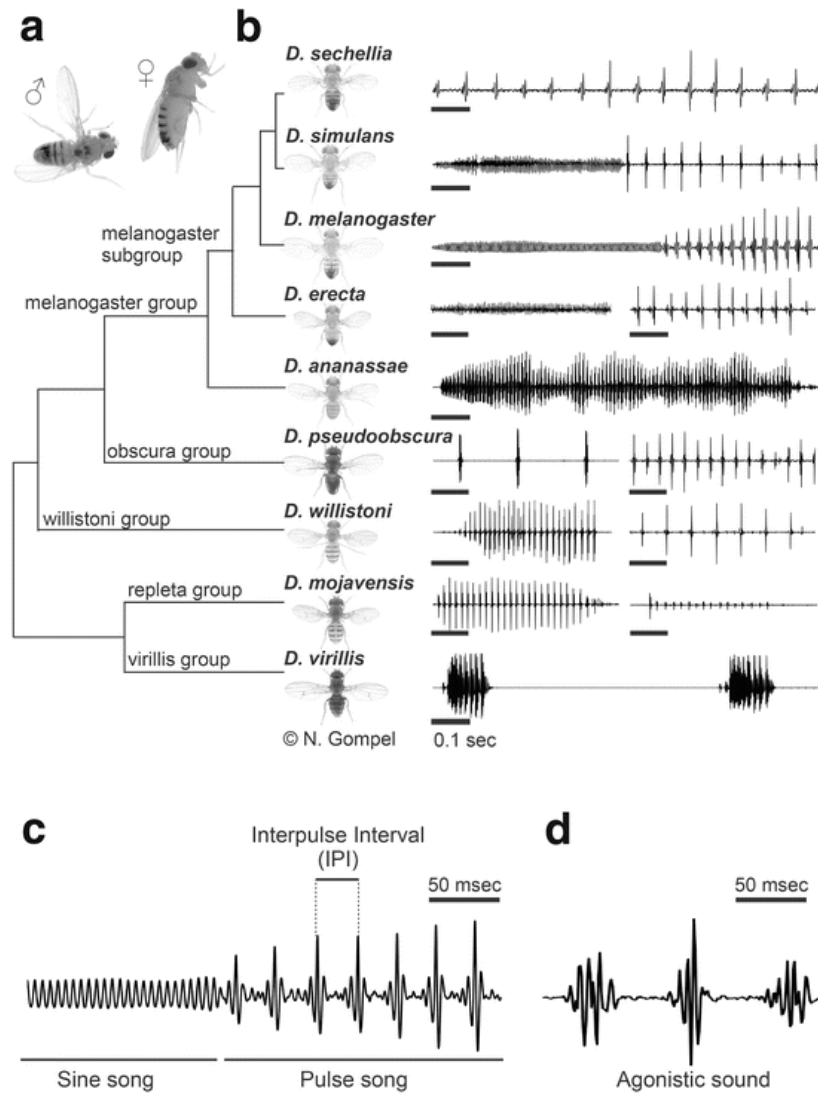
Figure 7: Differences in courtship song between *Drosophila* species.
A: schematic to show a male fruit fly extending its wing to produce a courtship song for the female. The courtship signal of *Drosophila* consists of two components: the sine and pulse song (C). Each *Drosophila* species has differences in the expression of these two modes of signal and there are also species-specific differences in the IPI (B). An agonistic sound has distinctly different sound features compared to the courtship signals (D). (Reference for figure (Kamikouchi & Ishikawa, 2016)).

Chapter 2

Background: *Drosophila* Chronobiology

Part of the work presented in this report falls into the area of chronobiology, thus a brief introduction into the topic and the current understanding of the molecular circuitry of the *Drosophila* circadian oscillator is covered within this chapter.

Table 2: Relevant circadian terminology

Abbreviation	*Term*	*Description*
–	Circadian rhythm/ oscillation/ periodicity	A process which undergoes changes over a 24-h time period. This process is governed by the endogenous clock, thus this oscillatory behaviour is not dependent on external cues.
CT	Circadian Time	Standard time based on the internal clock rhythm. In the absence of external time-giving cues; the CT of an entrained animal would follow the pattern of the external cue to which the internal clock was aligned.
DD	24-h Dark conditions	This is an environmental condition where the animal is not exposed to light.
–	Entrainment	The synchronization of the internal circadian oscillator to the external time-giving cue.
–	Freerun	The state of self-sustaining oscillations in the absence of time-giving cues.
D	12-h light/ 12-h dark cycle	A 24-h light dark cycle which follows a 12-h light and then 12-h dark pattern. This environmental condition simulates the presence and absence of light in real world conditions.

LL	24-h constant light	This is an environmental condition where the animal is constantly exposed to light.
–	Masking	An expression of overt rhythms which obscures the activity as governed by the endogenous clock. This usually refers to locomotor behaviour where there is a direct effect of an environmental cue on the behavioural output.
–	Zeitgeber	A rhythmic environmental cue which acts to regulate circadian rhythms. Zeitgeber translates as 'time giver' from German.
ZT	Zeitgeber time	Standard time based on the period of a Zeitgeber. The beginning of this corresponds with the onset of the external cue. Usually ZT1 refers to the first hour of light in an LD cycle.

2.1 Evolutionary importance of the clock.

The passage of time is a difficult concept to grasp and a process often quantified and associated with the day cycle. Earth is governed by a 24-hour periodicity where each revolution on its longitudinal axis results in a shift from light to dark, warm to cold, presence to absence of sustenance. These oscillations determine the rhythmicity by which all organisms of all phyla modulate their behaviour and biological function, known as their circadian rhythm.

Circadian rhythms are defined as endogenous daily oscillations of physiology and behaviour. They can be entrained by environmental cues, yet persist in their absence. The field of chronobiology in *Drosophila* evolved following the discovery that pupal eclosion (the process of emergence of an adult fly from the puparium), demonstrates the key principles of circadian regulation.

In entrained 12-h light/12-h dark (LD) (**Table 2**) environmental conditions, there is an emergence pattern with the highest rate of pupal eclosion occurring in bursts following dawn (Pittendrigh, 1954). This pattern was found to persist in constant environmental conditions and could also be reset by shifting the subjective dawn. These observations lead to the hypothesis that *Drosophila* have an endogenous clock.

2.2 Molecular basis of clock function

Based on the initial observations on pupal eclosion, a mutagenesis screen conducted by Konopka and Benzer (1971) uncovered the first clock mutants and identified the fundamental molecular player in circadian clock function. Mutations with shortened, lengthened and abolished periodicity were isolated in this seminal work (**Fig 8**). All these mutations were mapped to the same gene on the X chromosome named *Period (per)*.
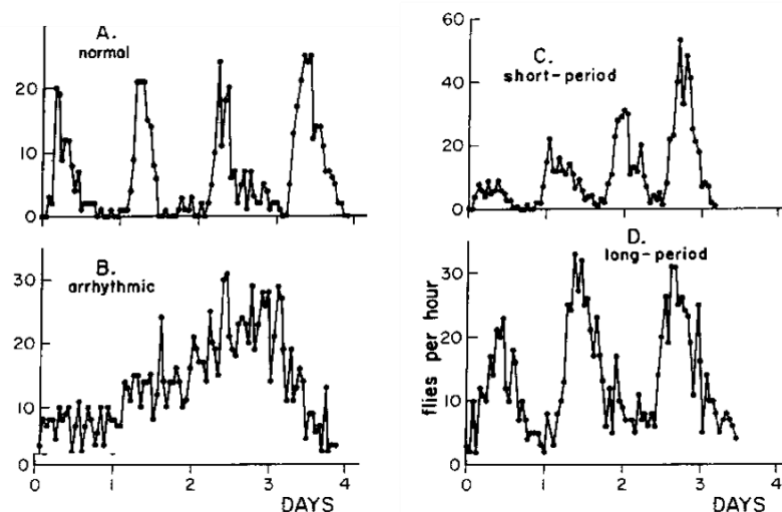
Figure 8: The locomotor rhythms of *period* mutants as observed by Konopka & Benzer 1971.
Figure is from the original paper introducing the *period* mutant (Reference for figure: (Konopka & Benzer, 1971)).

Levels of locomotor activity show daily rhythmic cycles in *Drosophila* (Klarsfeld, Leloup, & Rouyer, 2003). Mutations to *period* affect both eclosion and locomotor rhythms, demonstrating that an operative biological clock is the determinant of active periods in *Drosophila* locomotor behaviour (Qiu & Hardin, 1996).

Both *per* primary transcript and gene product display oscillatory behaviour in wild-type flies with there being a delay in abundance between the two. Antibody binding revealed that native *per* expression can be both cytoplasmic and nuclear, with temporal changes taking place in subcellular localisation of this protein (PER) (Siwicki, Eastman, Petersen, Rosbash, & Hall, 1988).

In 1994, Sehgal, Price, Man, & Young characterised a second clock gene located on the second chromosome named *timeless (tim)*. RNA cycles of *tim* occur in phase and at the same amplitude as *per* and shows similar posttranslational lag between primary transcript and protein abundance. The temporal expression pattern of the *tim* protein (TIM) in the nucleus correlates with that of *period* and the tim_{01} null mutation was also found to produce the same behavioural phenotype (Sehgal et al., 1995).

There is no nuclear localisation of PER in tim_{01} mutants nor nuclear expression of TIM in per_{01} mutants (Siwicki et al., 1971). Additionally, *per* and *tim* contain a PAS domain which mediates protein-protein interactions (Huang, Edery, & Rosbash, 1993). Collectively, these findings lead to the assumption that there is PER-TIM dimerization and that rhythmic abundance of these proteins is dependent on the correct localisation of the gene product (Vosshall, Price, Sehgal, Saez, & Young, 1994).

Mutations to the third chromosomal gene *doubletime* (*DBT*) have been found to disrupt the circadian oscillations of PER and TIM (Suri et al 2000). Following translocation of PER-TIM dimers to the nucleus, there is a sharp increase of nuclear DBT (Kloss, Rothenfluh, Young, & Saez, 2001). Through this mechanism, DBT helps determine the timing of *per* phosphorylation and turnover in the nucleus.

The *mClock* gene is one of the core molecular components in the mammalian circadian clock (Kondratov et al., 2003). This sequence region was found to be remarkedly conserved between mammal and fly when the *Drosophila* homolog of *mClock* simply called *clock (clk)* was discovered by Allada, White, Venus So, Hall, & Rosbash (1998). In mammalian systems, the *mClock* protein (mCLOCK) forms a heterodimer through its interaction with BMAL1 (Kondratov et al., 2003). This

heterodimeric interaction is also conserved in *Drosophila* systems. The homolog for BMAL1 named *cycle (cyc)* was discovered by the work of Rutila et al (1998). CLK-CYC protein complexes bind to *per* and *tim* via the E-box sequence to modulate transcription of these circadian clock genes (Darlington et al., 1998).

This transcriptional feedback loop is also reversed since PER-TIM complexes interact with CLK-CYC to inhibit the activity of these transcription factors. Throughout the day there is an increase in abundance of PER-TIM in the cytoplasm which gradually translocates to the nucleus throughout this period. As the day falls into night, PER-TIM complexes interact with CLK- CYC in the nucleus which inhibits CLK-CYC-dependent binding to the E-box containing circadian enhancer element on *per* and *tim* (Lee et al., 1998). This results in an antiphase pattern of CLK-CYC expression which is found to be maximal around ZT24 and undetectable at ZT11 (Lee et al., 1998) (**Fig 9**).
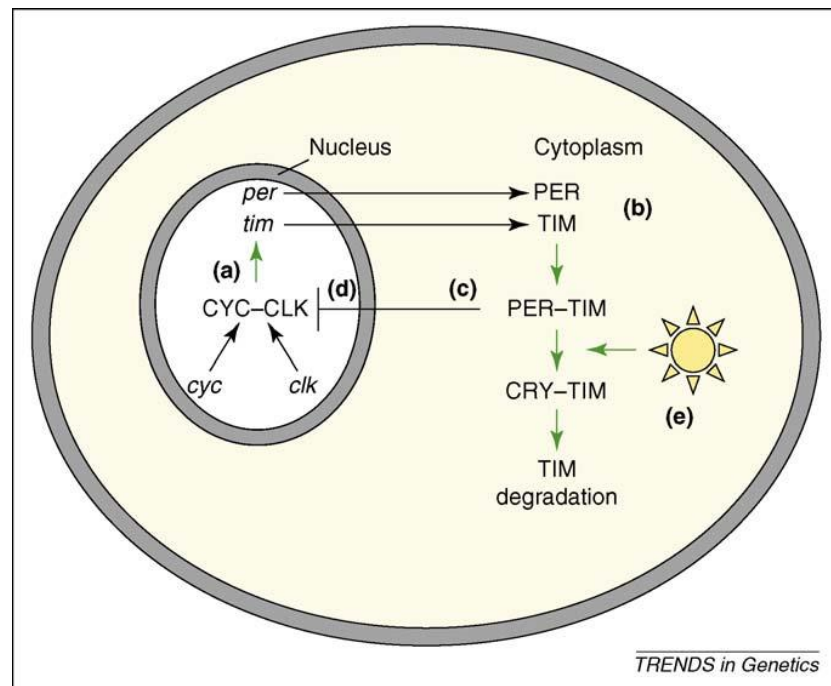
Figure 9: A simplified schematic of the transcription- translation feedback loop (TTFL) of *period & timeless* expression.

The CLK-CYC heterodimer promotes transcription of *per* and *tim*. mRNA for these is transported into the cytoplasm in the early evening. Within the cytoplasm PER and TIM proteins form a heterodimer by interaction via the PAS domain. These structures re-enter the nucleolus to interact with the CLK-CYC to inhibit the transcription of PER and TIM. Additionally, TIM is degraded in the cytoplasm by the binding of TIM to CRY which prevents its binding to PER (Reference for image (Emerson, Bradshaw, & Holzapfel, 2009).

In summary, a comprehensive model of the molecular regulation of circadian rhythmicity has been developed through the collective work of several decades. The molecular players form the basis of the series of transcriptional/ translational feedback loops (TTFL) which drive autonomous oscillators and autoregulate expression of key genes. In summary, a comprehensive model of the molecular regulation of circadian rhythmicity has been developed through the collective work of several decades. The molecular players form the basis of the series of transcriptional/translational feedback loops (TTFL) which drive autonomous oscillators and autoregulate expression (**Fig 9**). There are other factors that contribute to proper circadian function (Somers, Harper, & Albert, 2018) which prolong, delay and reset the clock (Koh, Zheng, & Sehgal, 2006; Rosato, Tauber, & Kyriacou, 2006; Tang, Hinteregger, Shang, & Rosbash, 2010) but *per, tim, doubletime, clock* and *cycle* form the main molecular basis of circadian rhythms in *Drosophila.*

2.3 The central clock

Around 150 neurons within the *Drosophila* brain make up the central clock. This architecture consists of several distinct subgroups which function together to form the central pacemaker (Helfrich-Förster & Homberg, 1993). There are seven distinct cell groups named according to morphological description and anatomical location. These are the small and large ventral lateral neurons (s-LNv, l-LNv), dorsal lateral neurons (LNd), the first, second, and third dorsal neuron groups (DN1, DN2, and DN3) and the lateral posterior neurons (LPNs) (Nitabach & Taghert, 2008) (**Fig 10**). These central components have all been identified through cytological staining of clock genes therefore show robust cycling of key molecular components (Helfrich-Förster & Homberg, 1993).
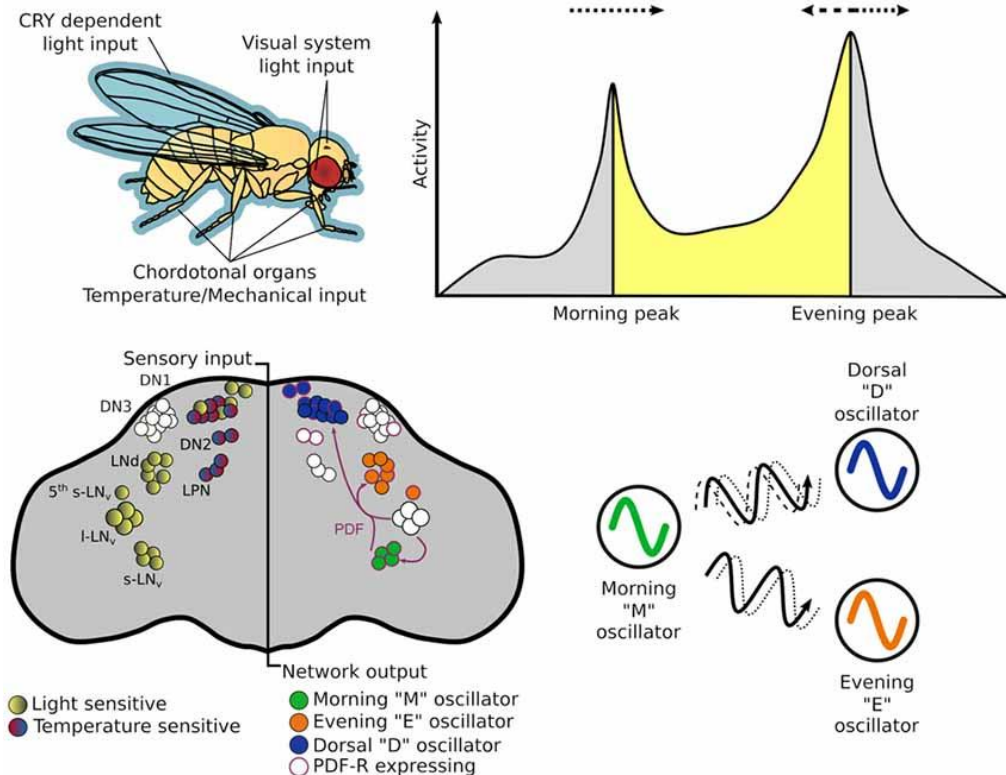
Figure 10: Diagram of the circuitry of the central clock.
Different central pacemaker neurons control the morning and evening activity peaks. The illustration shows the clusters of the central pacemaker cells and specifies whether these neurons have been found to be light or temperature sensitive and whether they express PDF. (Reference for figure: (Somers et al., 2018)).

In LD conditions, there are two prominent peaks in locomotor activity. A Morning (M) peak associated with the dark to light environmental transition and the Evening (E) peak associated with the light to dark environmental transition. These behavioural rhythms are driven by the central pacemaker neurons (Frisch, Hardin, Hamblen-Coyle, Rosbash, & Hall, 1994). One of the key distinctions amongst the network of the central clock neurons is whether the cells are pigment dispersing factor (PDF) secreting. PDF is a neuropeptide which has been found to be expressed in around 10% of the central clock neurons (Helfrich-Förster, 2004). Inhibition of PDF or ablation of PDF-positive neurons results in the suppression of the morning locomotor activity peak as well as a shift of the evening peak activity (Renn, Park, Rosbash, Hall, & Taghert, 1999). On the other hand, the evening activity peak is regulated by the LNd's and the PDF negative s-LNv (Grima, Chélot, Xia, & Rouyer, 2004). These findings demonstrate the differential contribution from separate groups of neurons in the control of behavioural rhythms.

Despite a number of peripheral tissues having independent clock function, these core components within the CNS have been found to be regulators of the rhythmicity of some tissues. For example, the prothoracic gland (PC), which is essential for eclosion rhythms has been found to have a functional clock. However, the interaction between the lateral neurons (forming part of the central control) and this peripheral clock has been found vital for the establishment of the eclosion rhythms (Myers, Yu, & Sehgal, 2003).

Similarly, metabolic processes in *Drosophila* were also found to be under the control of both the central and peripheral clocks. The fat body, which is a tissue that is highly relevant to metabolic control, was found to have independent clock function yet required interaction with the central clock for normal metabolic function within this tissue (Sehgal, 2016).

The clock is comprised of a hierarchy of oscillators. Functioning on a cellular, tissue and systems level, these oscillators regulate biological rhythms. The integration and communication of these clocks contributes to the fine tuning and robustness of the circadian rhythms in *Drosophila*.

2.4 The peripheral clock

The fly circadian system can be conceptually subdivided into two parts, the central and the peripheral clocks. Although there are a cluster of central pacemaker neurons within the brain, many tissues within the fly show tissue-autonomous circadian oscillations (Plautz, Kaneko, Hall, & Kay, 1997). Malphigian tubes, ring glands and sensory tissues such as mechanoreceptive bristles and wings have all been found to have cycling of the key molecular clock components (Giebultowicz, Stanewsky, Hall, & Hege, 2000; Ito & Tomioka, 2016; Plautz et al., 1997). These examples demonstrate that some systems are able to sustain rhythmic cycling and entrain directly to external stimuli independent of central clock components.

Circadian changes in physiology can be observed in some sensory systems. The work of Krishnan, Dryer, & Hardin (1999) found that wild-type flies have robust diurnal rhythms in the electroantennogram (EAG) responses to odorants. This oscillatory behaviour was found to be independent of the central clock since inhibition of the lateral neurons (which makes up part of the central pacemaker circuitry) had no effect on rhythmicity of the olfactory system (Krishnan, Dryer, & Hardin, 1999). Unlike the chemosensory sensilla, the visual system relies on a combination of inputs from the peripheral and central clocks to establish rhythmic behaviour. Rhythmic variation in electrophysiological responses to visual stimuli was found to persist in clock mutants with impaired central clock components (Nippe, Wade, Elliott, & Chawla, 2017). However, the persisting rhythm was weakened, indicating that the central oscillators contribute to, but do not govern the circadian changes in responsiveness of the visual system (Nippe, Wade, Elliott, & Chawla, 2017).

There are differential properties in the oscillatory machinery of varying tissues in *Drosophila*. There is no clear explanation for this diversification amongst tissue but it is evident that some peripheral clocks are cell-autonomous, directly light-entrainable and independent of the central oscillator whereas others are less so. This heterogeneity of peripheral systems demonstrates the complexity of circadian function in *Drosophila* (Ito & Tomioka, 2016)

2.5 Circadian control of behaviour

As established in the previous sections, *Drosophila* locomotor activity is under circadian control (Allada & Chung, 2011). Wild-type flies with a functioning endogenous oscillator show anticipatory behaviour where increases in activity are an adjustment of physiology and behaviour in anticipation to environmental changing conditions (**Fig 11**).
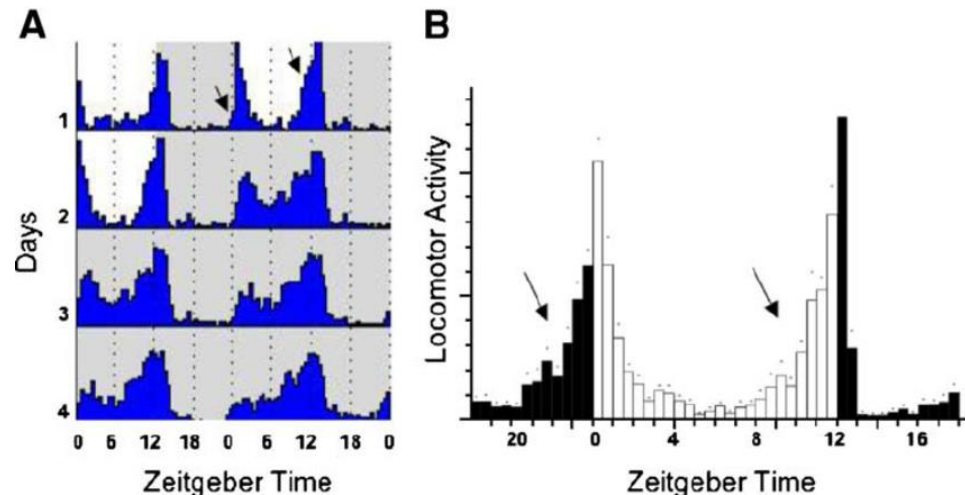
Figure 11: Activity rhythms of wild-type flies in LD & DD conditions.
　　A: Shows actograms of the activity rhythms of wild-type flies kept in LD conditions and then transferred to DD. There is a decrease in morning peak over the series of consecutive days.
　　B: Shows the activity of wild-type flies in LD conditions with arrows to show the anticipatory behaviour leading to the morning (M) and evening (E) peaks in activity (Reference for figure: (Dubruille & Emery, 2008)).

Entrainment is the ability of an organism to synchronize the endogenous oscillator to exogenous environmental stimuli. Rhythmic external stimuli capable of synchronizing the internal oscillator are called zeitgebers. Light is the most dominant zeitgeber, capable of shifting, resetting and prolonging endogenous circadian rhythms.

Constant light is known to lengthen the period of the activity rhythm, finally leading to arrhythmicity (Konopka et al., 1989). Prolonged exposure to this environmental condition also results in the inhibition of cycling of the fundamental clock genes. Upon transfer to constant light, there is a gradual decay in the oscillations of *per* and *tim* (Marrus, Zeng, & Rosbash, 1996; Zerr, Hall, Rosbash, & Siwickil, 1990).

Multiple studies have shown that physiologically blind (*norpA*) and anatomically eyeless (so) mutants demonstrate robust behavioural and molecular oscillations and are able to entrain to exogenous light transitions (Hamblen-Coyle et al., 1989; Wheeler, Hamblen-Coyle, Dushay, & Hall, 1993a). Based on the observation that flies lacking visual inputs were able to entrain to light/dark cycles, nonvisual pathway for photoreception were suggested (Yang, Emerson, Su, & Sehgal, 1998) (**Fig 12**).
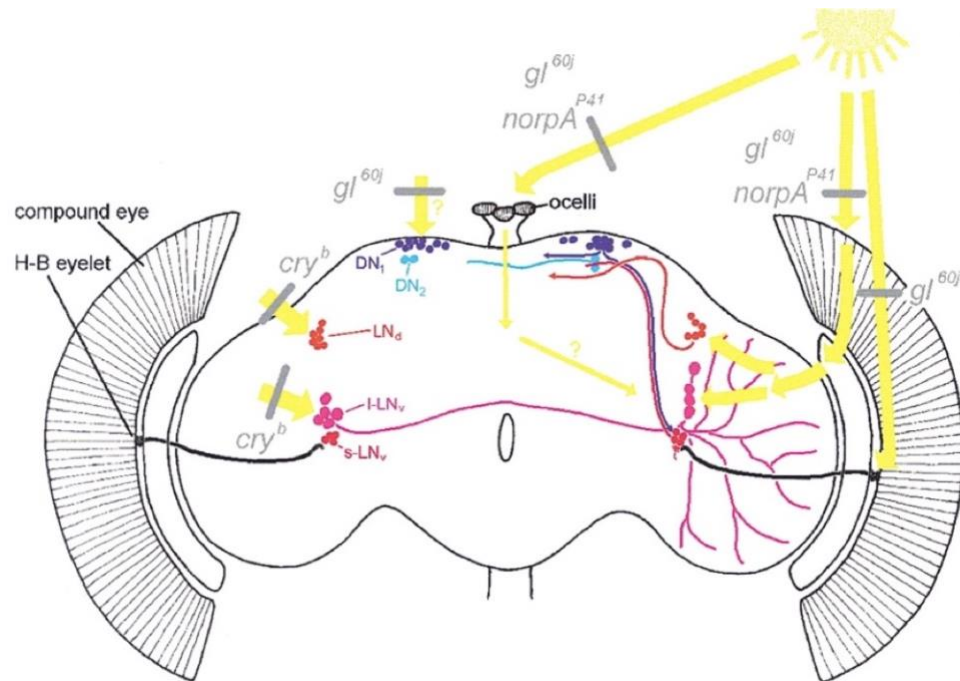
Figure 12: Illustration to show the multiple light input pathways in *Drosophila*.
The varying light input pathways have interactions with distinct central pacemaker neurons. Light through the compound eye, H-B eyelet, ocelli and directly through the cuticle contribute to synchronising the internal clock with the external environment. (Reference for figure: (Helfrich-Förster, Winter, Hofbauer, Hall, & Stanewsky, 2001)).

The Hofbauer- Buchner eyelet (H-B eyelet) has been identified as being a putative extraretinal photoreceptor contributing to the entrainment of circadian pacemaker neurons (Veleri, Rieger, Helfrich-Förster, & Stanewsky, 2007). Manipulating the synaptic transmission from the H-B eyelet to clock neurons results in the inability of PER-TIM protein oscillations to synchronize to light within these central pacemakers (Veleri et al., 2007); suggesting that the H-B eyelet is a second phototransduction pathway to contribute to abiotic entrainment.

The third phototransduction pathway is directly involved in light entrainment and is intricately implicated in the molecular core clock mechanism. Due to the compact size of *Drosophila* and its light-permeable cuticle, non-visual photoreceptors such as cryptochrome receive direct light input. Cryptochrome is a flavin-binding, blue light photoreceptor expressed in clock neurons in the lateral brain as well as in peripheral tissue. Stanewsky et al (1998) presented a third chromosomal deletion called *cry*baby (*cry*b) a missense mutation which produces defects in circadian photosensitivity resulting in behavioural arrhythmicity.

Rieger, Stanewsky, & Helfrich-Förster (2003) found that mutants lacking compound eyes struggled to entrain to long photoperiods whereas cryptochrome mutants were impaired in short photoperiod entrainment trials (**Fig 13**). It is possible that each photoreceptor is responsible for entrainment at different points within the cycle. These multiple light input pathways are capable of entraining to the locomotor rhythm to varying degrees, however the inhibition of these collectively leads to the inability of the animal to entrain to photic environmental cues (Veleri, Brandes, Helfrich-Förster, Hall, & Stanewsky, 2003).
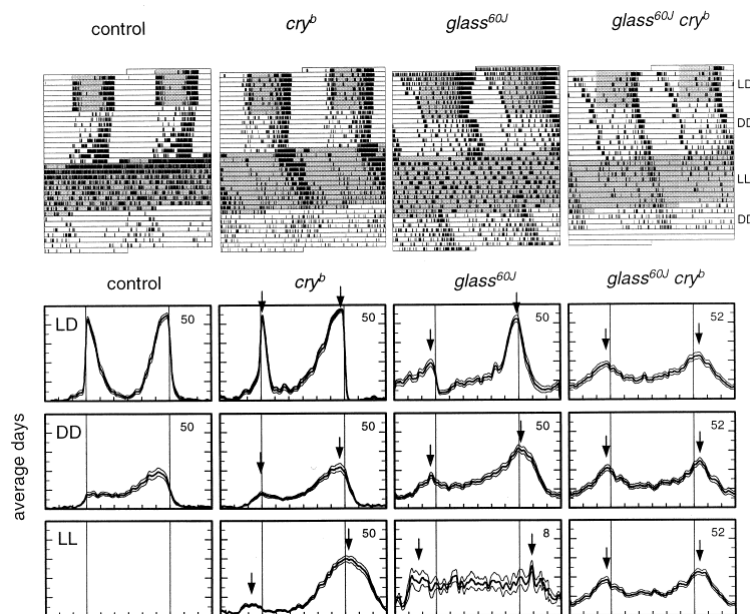
Figure 13: Actograms to show the changes to locomotor behaviour of flies with deficits in the various photoreceptor pathways in different environmental conditions.
Typical actograms of individual flies. The activity of *cry_b* mutants remains oscillatory in LL conditions. Whereas *glass_60j* have a diminished morning activity peak due to the inhibition of the visual phototransduction pathway. The activity of the double mutant remains unchanged in all the environmental light conditions thus independent of this external cue (Reference for figure: (Helfrich-Förster, Winter, Hofbauer, Hall, & Stanewsky, 2001)).

These three light input pathways allow for light entrainment, but how does this light translate to interact with the molecular components of the circadian clock? Cryptochrome RNA levels peak towards the evening light transition and plateau at a high level during the night in wild-type flies (Emery, So, Kaneko, Hall, & Rosbash, 1998). It has been proposed that CRY influences the circadian oscillator by undergoing a light-dependent conformational change which promotes CRY-TIM binding and proteomic degradation of TIM (Stanewsky et al., 1998).

In the natural world, the daily cycles of light are accompanied with cycles of temperature fluctuations. Diurnal temperature variations change with season but most commonly, temperature is raised during the day and decreased during the night. Similar to light, ambient temperature fluctuations can serve as a synchronization signal for the endogenous clock.

Anticipatory behaviour to temperature entrainment cycles can be observed indicating this exogenous cue is a zeitgeber (Wheeler et al., 1993). In constant darkness, the fluctuations of PER and TIM proteins synchronize to warm/cold cycles (Stanewsky et al., 1998). The mechanism of temperature entrainment is however not as direct as light on the molecular clock. Rapid degradation of PER and TIM protein is only observed after exposure to artificially exaggerated heat pulses which are outside the physiological range (Sidote, Majercak, Parikh, And, & Edery, 1998). It was found that *period* is receptive only to heat, whereas *timeless* is receptive to both heat and light. This supports the assumption that the individual clock components have differences in their sensitivity and work together to reset the clock to temporal cues.

The temperature entrainment pathway has been found to be independent of the main thermosensory region within the 3rd antennal segment (Glaser & Stanewsky, 2005; Zars, 2001). Chordotonal organs are key structures in transducing the thermal signal to the circadian temperature entrainment pathway. Downregulation of *nocte (no circadian temperature regulation)* in the peripheral tissue as well as other mutations which affect these sensory structures result in defects in temperature entrainment (Sehadova et al., 2009; Glaser & Stanewsky, 2005).

The circadian temperature entrainment pathway is a tissue-autonomous process which relies on nocte and *norpA* for correct transduction from the periphery to the central pacemakers in the CNS (Sehadova et al., 2009).

Collectively, these findings indicate that there are a number of input pathways which feed into the circadian clock. Peripheral tissue and structures such as chordotonal organs have been found to contribute to this process. Undoubtedly, in natural conditions, the clock uses photic and thermal input as well as other yet-to-be-identified pathways to correctly regulate and synchronize its internal machinery. These direct and indirect pathways have all been proven to modulate the key fundamental molecular oscillators, *period* and *timeless*.

.

Chapter 3

Project aims & objectives

A vast body of work has been done towards understanding mechanosensation in *Drosophila*. Even though significant efforts have been made to uncover the biological underpinnings of auditory-induced behaviour, many knowledge gaps remain with regards to the systemic properties linking behaviour to physiology and understanding the complex neurobiological systems behind the behaviour. Furthermore, *Drosophila* has been the pre-eminent model organism for the advances in understanding biological time keeping, but the interaction between the respective fields of mechanosensory processing and chronobiology has been limited thus far, leaving many questions unresolved. My research aims to expand upon the existing body of work on the underpinnings of auditory behaviour with an emphasis on merging the two fields of chronobiology and auditory neuroscience. To address this problem and fill the knowledge gap, the aims of this thesis build on one another in progress.

1. Develop a novel behavioural assay to probe auditory behaviour in *Drosophila*. Quantify and qualify a method to be used as a readout for mechanosensory processing (**Chapter 5**).
2. Identify the key modulators of auditory behaviour and conduct a cross comparison of which properties influence mechanosensory processing (**Chapter 6**).
3. Determine the biological underpinnings of auditory behaviour. Quantify whether the same modulators of auditory behaviour influence auditory processing within the JO and examine if the changes observed within the behavioural assay are influenced by changes in the physiological processing of signal (**Chapter 7**).

Chapter 4

Experimental Methodological Overview

Within this chapter I provide an overview of the key methodologies used within my experimental research. A general synopsis of the approaches that have universal application and span multiple chapters are discussed here, whereas specifics of experimental protocols and adopted methodologies are discussed in more detail along with the experimental results within their respective chapters.

4.1 Fly Stocks

Unless specifically stated, all flies used in the experiments presented in this thesis were kept in a 12-h light/ 12-h dark regime maintained at 25˚C in temperature and light controlled incubators prior to experimental procedures. Male and female flies were kept together in vials, allowing them to breed. Each vial was populated with approximately 10 flies. Fly food consisting of yeast, sugar and cornmeal was dispensed on the bottom of the plastic vials in which they were housed.

4.2 Locomotor Assay

Drosophila show robust daily locomotor rhythms that are under the regulation of the circadian clock (Klarsfeld et al., 2003). Locomotor monitoring is a powerful experimental tool utilised extensively within the field of chronobiology as this behavioural output permits the investigation of circadian oscillations.

It has been reported that male *Drosophila* show an increase in locomotor activity during the playback of conspecific auditory signals (Kowalski, Aubin, & Martin, 2004). Based upon this finding, I considered whether the same tools currently used

for behavioural monitoring in chronobiology research might also be utilised for studying auditory processing. Evaluating and establishing locomotor activity as a readout for auditory processing has formed a large part of this thesis and was used extensively in this work.

4.3 Activity monitoring

Locomotor activity measurements were obtained using the *Drosophila* Activity Monitoring (DAM) system produced by Trikinetics (Walham, USA) (**Fig 14A**). This system allows for continuous monitoring of fly locomotor activity within individually spaced tubes at specified time intervals. The movement record providing a measure of intensity of locomotor activity within each tube was maintained on a host computer. This widely-used locomotor assay is popular in studies investigating circadian clock function, owing to its ability to yield large amounts of continuous data collected over several days.
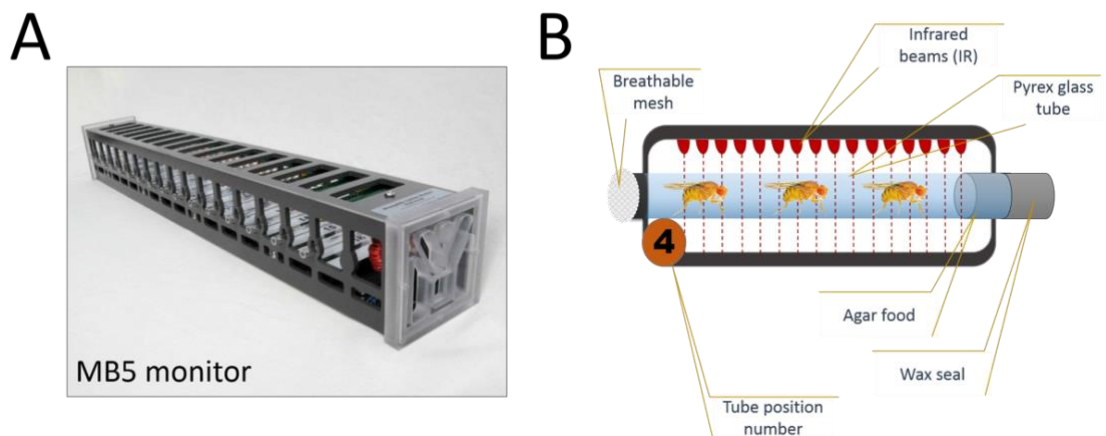
Figure 14: Photo & illustration of the Trikinetics MB5 monitor used for investigating *Drosophila* locomotor activity.
A: Photo to show the MB5 monitors used to assay *Drosophila* locomotor activity in response to presentation of sound stimuli. B: An illustration of how the MB5 monitors capture locomotor activity, 17 infrared beams intersect a glass tube. Movement within the glass tube results in beam breaks. At each tube position, a readout of the number of beam breaks within a given timeframe is produced. The more recorded beam breaks, the more movement within the tube.

To conduct the measurements, flies were housed in Pyrex® 50mm x 65mm glass tubes. One end of the tube was sealed with an acoustically transparent mesh and the other with food consisting of 5% sucrose and 2% agar medium occupying approximately a quarter of the tube. The side of the tube containing food was sealed with wax to prevent drying out. The glass tubes were then loaded into the MB5 activity monitors (**Fig 14A**). This specific model has a multi-beam system that has 17 independent infrared (IR) beams bisecting each tube at 3-mm intervals producing a high-fidelity record of the activity within each tube (**Fig 14B**). Through the use of DAMSystem software, the detector was set to count the number of beam breaks every minute over a time series. Thus, the greater number of beam breaks recorded, the more active the fly is within the tube. Activity counts were registered independently at each beam position within a tube, allowing for the generation of counts from separate beam positions simultaneously, which permits an accurate readout of activity from a tube with multiple flies. To maximise data collection, 3 MB5 monitors were stacked together forming a grid allowing me to record from 36 tubes simultaneously over the course of a single experiment (**Fig 15**).
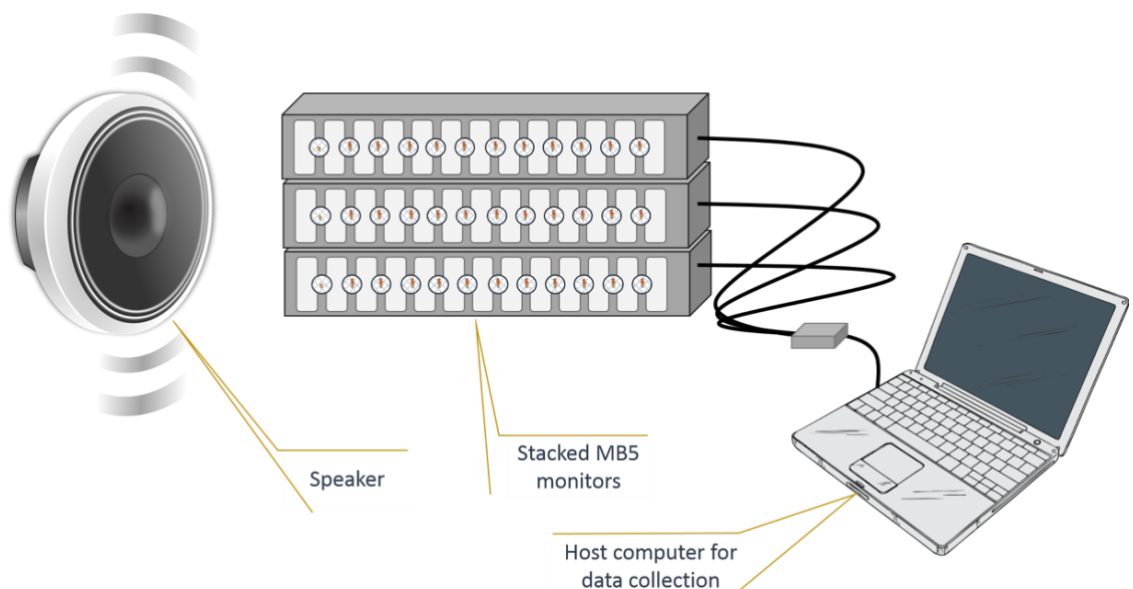
Figure 15: Illustration of experimental set up for the auditory-induced locomotor assay.
The experiment was conducted by placing 3 stacked MB5 monitors in front of a speaker. The sound stimulus would be played through the speaker. A host computer connects to the MB5 monitors to record the number of beam breaks within each tube in the monitors.

4.4 Sound stimulus

The effect of sound stimulation on general locomotor activity was investigated. The monitors were placed in front of a 381mm diameter, 400W speaker (Eminence Delta 15 (400W, 15" Driver, 8 Ω)) connected to an amplifier (Prosound 1600W amplifier). To avoid vibratory interference from the environment disturbing the recordings, the monitors were placed onto a vibration isolation table. The monitors were positioned centrally with the audio-transparent mesh of the tubes facing the speaker at a distance of ~60mm from the speaker rim. Initially the optimal distance was determined by measuring the output of the speaker by a sound level meter (CEL- 450) to be approximately 90dB sound pressure level (SPL) at the level of the monitors. This SPL is consistent with the sound amplitudes used for other auditory behavioural assays (Inagaki, Kamikouchi, & Ito, 2010; Ishikawa et al., 2019; Yorozu et al., 2009).

Further efforts were made to identify any distortions between input waveform and output sound through the speaker. A particle velocity meter (Knowles NR-23150-000) was used to assess this in addition to quantifying the differences in power spectrum between the different positions within the behavioural monitors. Nine measurements were performed at different points around the stacked monitors. There was little variability in measurements between different positions, however there was a shift in peak frequency between input waveform and output sound. Both variants of sound stimuli used in the experiments had an original waveform with a peak at ~170 Hz, however this was shifted to ~200 Hz when assessing the power spectrum of the recorded speaker output (**Fig 16**). This shift is still within the normal best frequency range as recorded for wild-type *Drosophila melanogaster* (Göpfert & Robert, 2003)*.*
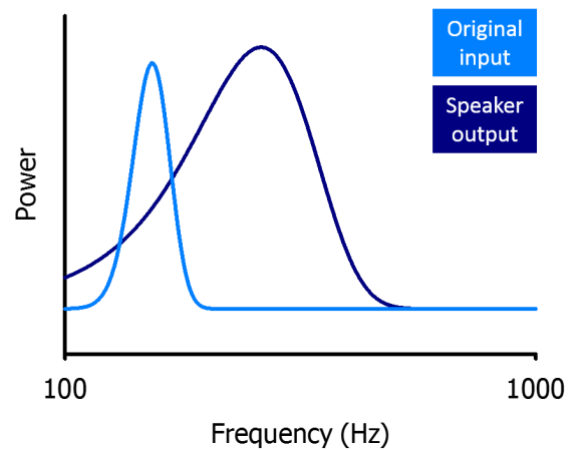
Figure 16: Power spectrum to show the frequency distribution of the input waveform compared to speaker output.

There is a shift in the peak frequency between the input waveform and the output waveform recorded from the speaker. This shift shows there is a distortion of the input sound waveform however the peak frequency of the output is still within normal hearing frequency range for *Drosophila melanogaster.*

The sound stimulus was controlled using Spike2 software. There were 3 primary sound stimuli used for the behavioural assay which are described below. The peak-to-peak amplitude between the sound stimuli was normalised so that the output waveform had a similar voltage.

4.4.1 Artificial Pulse Train (APT) stimulus

 An single artificial pulse was composed by averaging over ~1000 pulses recorded within a sound chamber from 10 *Drosophila melanogaster*. A 2s pulse train constructed out of the artificial pulse with a 40-ms inter-pulse interval (IPI) followed by a 2s silence period was played continuously for 15 min at the beginning of every hour during the behavioural experiments (**Fig 17**).
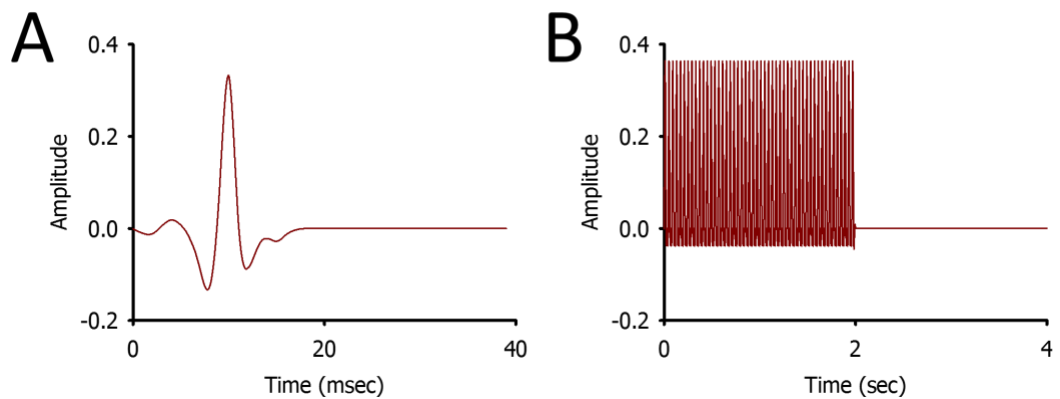
Figure 17: Time series graph to show the APT sound stimulus. An artificial single pulse constructed out of averaging a range of pulses from 10 *Drosophilae* forms the bases of a pulse train. **A**: Single pulse as constructed by averaging a range of pulses by 10 *Drosophilae* as recorded in a sound chamber. **B:** 2 s pulse train followed by a 2 s pause. The inter-pulse interval (IPI) is 40 ms between the pulses in the train.

4.4.2 Real Courtship Song (RCS) stimulus

A 9 s extract of an Oregon-R courtship recording obtained within a sound chamber was used (**Fig 18A**). The recording contained interspersed pulse and sine fragments (**Fig 18 B&C**). The criteria for extract selection was based on resulting copulation success which was determined from an accompanying video. This extract was taken as a typical representative sample of real courtship song and to allow for direct comparison to the averaged artificial pulse train, the peak to peak amplitude for the pulses within the natural song were identical for both the natural courtship extract and artificial pulse train.
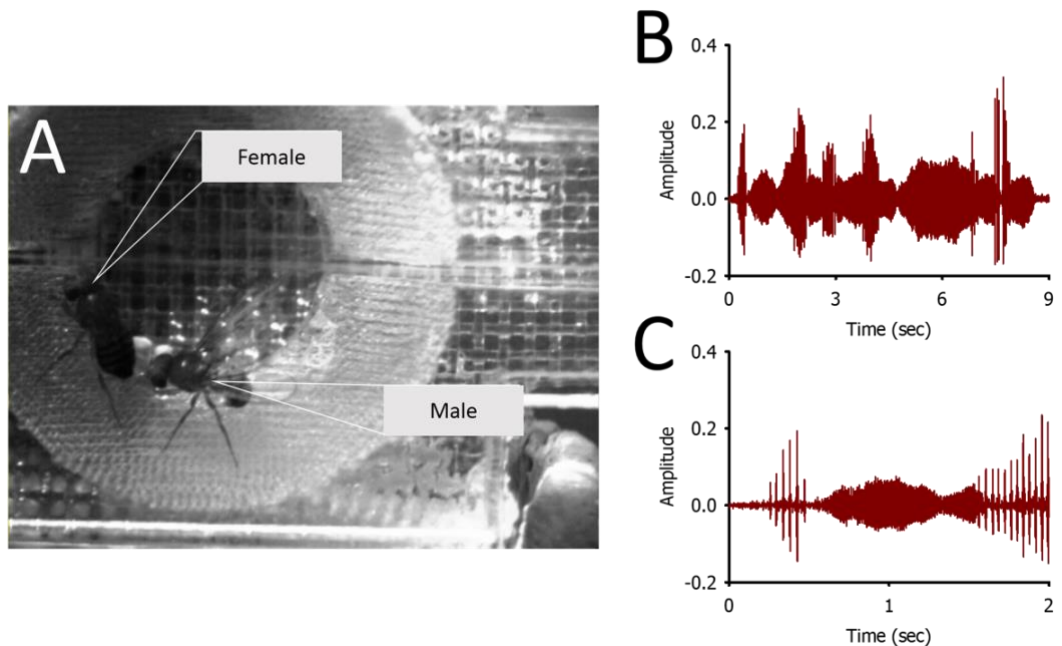
Figure 18: Time series graph to show the RCS stimulus. RCS stimuli consists of a 9 s extract of an Oregon-R courtship song.
 A: A snapshot of a video of the sound chamber associated with the recording of the courtship song extract. **B:** The 9s courtship song recording tested on the behavioral assay. **C:** A zoomed in version of B to show the pulse and sine components of the natural courtship song.

4.4.3 White noise (WN) stimulus

A white noise sound stimulus was also used in the behavioural experiments to determine whether locomotor behaviour is mediated purely by the presence of a sound, irrelevant of species specificity. An online platform was used to generate a white noise fragment (**Fig 19**). This signal was composed of random frequencies with equal intensity.
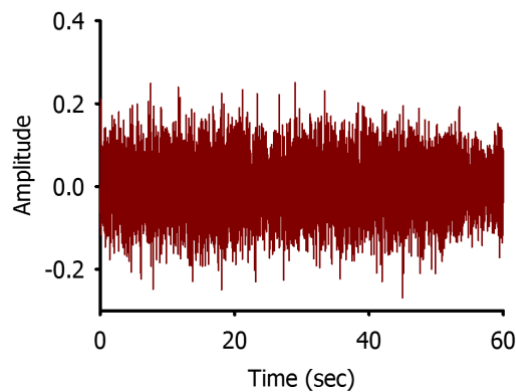
Figure 19: The input waveform of the white noise stimulus used in the behavioural assay.
An online platform was used to generate a white noise stimulus waveform which was then calibrated to the other two stimuli where the max and min peaks matched those of APT and RCS stimuli.

Within the results figures in **Chapter 5**, icons are used to denote which sound stimulus was presented in the reported section. The table below shows the icons used.

Figure 20: Table of icons used in the results graphs to demonstrate which sound stimulus was use.

4.5 Protocol for auditory behavioural assay

It is well documented that the exposure to courtship sound stimuli induces male flies to mimic wing movements to also produce a mating call (von Schilcher, 1976). To ensure the flies were only exposed to the sound stimulus during the experiment, experimental flies were anaesthetized using CO_2 and wing clipped 2-4 days prior to the initiation of the experiment. At least 2/3 of the wing was removed using microdissection scissors. After allowing time for healing post procedure, the flies were anesthetized again using the same methods and were housed into the glass tubes before being placed into the MB5 monitors.

Flies were exposed to a continuous sound stimulus for 15 min of every hour. 15 min of sound stimulus followed by 45 min of silence was looped throughout the whole duration of the experiment (**Fig 21**). Flies were exposed to the sound stimulus as soon as they were placed into the monitors however data only began to be recorded starting from the first morning light transition. Experimental animals thus had ~12-h to adapt to the stimulus, new environment and recover from any after-effects of CO_2 exposure since the monitors were loaded in the evening and data collection would begin from the following morning light transition. Data was collected for 48 hours after this equilibration stage.
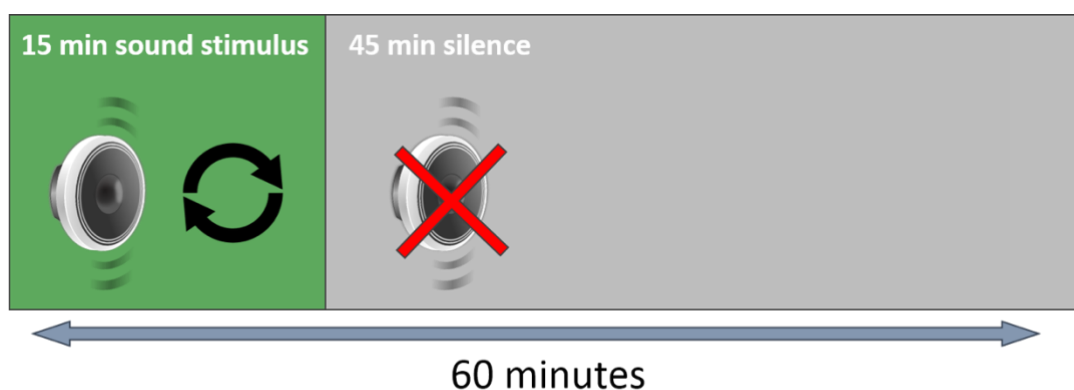
Figure 21: Schematic to show the stimulus protocol for the experimental period.
Each hour there is a 15 min sound stimulus presentation which is looped for this duration followed by a 45 min silence interval.

The room in which the recordings took place was held at a constant 25˚C and followed a 12-h light, 12-h dark cycle which was kept consistent with the previous entrainment regime.

4.6 Data analysis

Even though pre-existing MATLAB toolbox libraries exist for the analysis of locomotor data in *Drosophila* (Levine, Funes, Dowse, & Hall, 2002) these approaches are primarily applied to circadian data and were found not to be useful when applying it to the readouts obtained for auditory-induced locomotor behaviour. Thus, I designed a new analysis protocol to extract meaningful insights from the raw data collected from the Trikinetics monitors (**Supplementary 1**).

Each sampling tube is associated with its own position number within the monitors (**Fig 14**) and with an individual readout of all the occurred beam breaks within that sampling tube is recorded to a host computer. Any sampling tubes with logged fly death at the end of an experiment or which remained empty were excluded at this stage. For ease of understanding, from this point onwards I shall refer to each sampling tube as a sample. First the raw data from the DAMSystem program was rearranged to separate out the activity for each sample over the two experimental days (**Table 3**). Each experimental day was treated separately thus separate files were created for each 24-h period. Data from samples in the same experimental conditions in separate trials was concatenated.

Table 3: A: is an example able of the typical data structure of the raw data as recorded by the DAMSystem program. B: is a table indicating of how the data is restructured to be used for further processing.

A

Time	Position	Activity Count
08:00	1	46
08:00	2	45
08:00	3	79
08:00	4	41
08:00	5	24
08:00	6	5
08:00	7	38
::::	::::	::::
08:01	1	95
08:01	2	38

B

Time	Position 1	Position 2	Position 3	Position 4
08:00	46	45	79	41
08:01	95	38	45	12
08:02	34	5	79	63
08:03	24	34	41	2
08:04	53	32	24	53
08:05	64	14	58	4
08:06	7		38	

4.6.1 Circadian corrected hourly activity

Drosophila show fluctuations in locomotor activity throughout a 24-h cycle (Klarsfeld et al., 2003). Steps were taken to correct for this modulation to make it possible to explore the overall response to the sound stimuli over the whole experimental day independent of circadian changes of activity.

For each individual sample, there was a readout of activity for every minute over a 24-h range. The median for each minute over a 24-h range was calculated to provide the median hourly activity for each sample. For simplicity, I will refer to this measure as **individual hourly activity.** With this procedure, it was possible to assess the dynamics of the overall response activity of individual samples to the sound stimulus (**Fig 22A, Fig 23A** the responses in grey show the average hourly activity for individual samples).

A

Minute	ZT1	ZT2	ZT3	ZT4	ZT5	ZT6	:	Sample 1 median hourly response
				Sample 1			:	
1	13	12	24	12	23	34	:	20
2	14	5	3	53	4	2	:	5
3	16	25	14	24	5	6	:	14
4	2	33	6	6	78	4	:	16
5	35	5	7	73	4	34	:	34
6	7	2	34	67	32	2	:	52
7	8	3	6	3	4	5	:	61

B

Minute	Sample 1 median hourly response	Sample 2 median hourly response	Sample 3 median hourly response	Sample 4 median hourly response	Sample 5 median hourly response	Sample 6 median hourly response	:	Circadian corrected hourly activity
				Experimental condition			:	
1	13	12	24	12	23	34	:	18
2	14	5	3	53	4	2	:	4.5
3	16	25	14	24	5	6	:	15
4	2	33	6	6	78	4	:	6
5	35	5	7	73	4	34	:	20.5
6	7	2	34	67	32	2	:	19.5
7	8	3	6	3	4	5	:	4.5

Figure 22: Illustration to show how the individual hourly activity & circadian corrected hourly activity was calculated.
A: For individual samples, each hour within a 24-h cycle was split into separate columns with 1 to 60 min in the rows. The individual hourly activity was calculated by taking the median for each minute 1 to 60 over a 24-h range. Once this was done for all the samples within one experimental condition, a median for the whole group was taken amongst the samples (**B**). So the circadian-corrected hourly activity was the taken as a the median of individual hourly activity for all the samples in an experimental condition.

To assess the response dynamics for an overall experimental condition, a median of the **individual hourly activity** was taken to make a single representative hourly median response for all the samples in that experimental condition (**Fig 22B, Fig 23B,** where for the latter, the red line represents the median hourly activity for the whole sample). This measure was referred to as **circadian-corrected hourly activity.**

These individual hourly activity medians were used for data filtering (**section 4.6.2**) and the circadian-corrected hourly activity was used to compare the response dynamics between conditions.
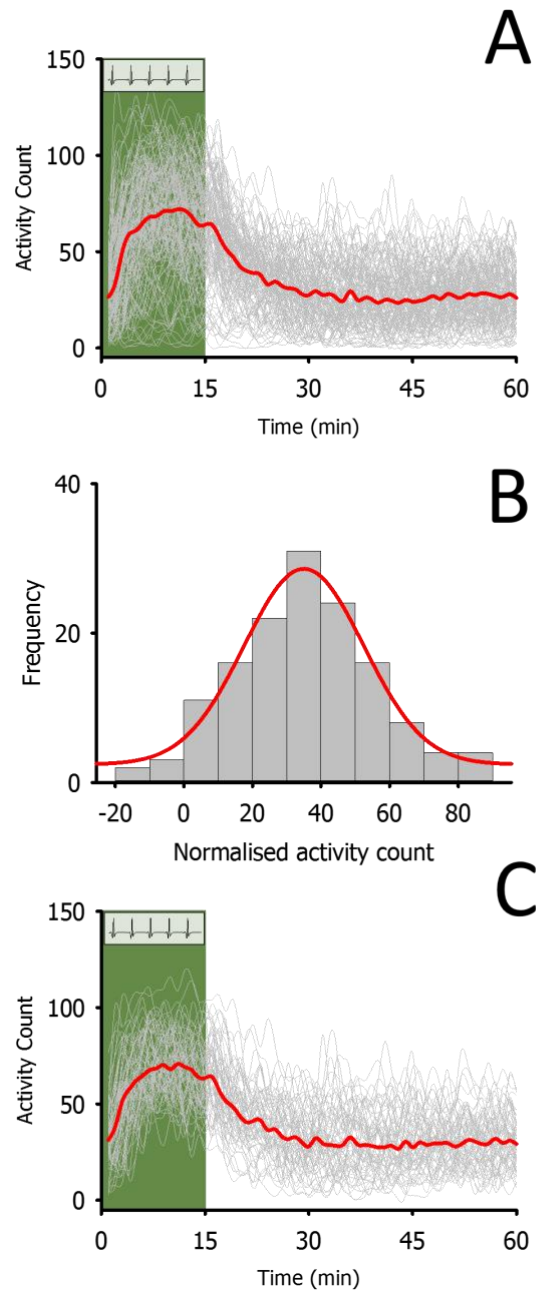
Figure 23: Series of graphs to show the filtering procedure used to minimise noise in the recorded data.
A: Shows the average hourly activity of 130 samples with the green section to demonstrate the stimulus presentation and red line is the median hourly activity of the whole population. **B:** Shows a histogram with curve fit to show the distribution of subtraction normalized values for the whole population. **C:** Is a graph to show the average hourly activity of 75 samples as selected by filtering 50% from the original collected data to be further used for data analysis.

4.6.2 Filtering

Once the raw data was collected, it was filtered to reduce noise prior to further analysis. Within chronobiology research some form of filtering is typically applied to the collected data to disentangle the signal from noise. As with most behaviours, locomotor activity in a general sample of wildtype *Drosophila* falls into a normal distribution (**Fig 23B**). It was decided to exclude extremes from the standard deviations furthest away from the average activity patterns since it is likely that the behaviours within these ranges were due to non-natural factors. For example, since flies were wing clipped and loaded into the activity tubes, it is possible that the antennae were damaged during these pre-experimental procedures. In studies utilising *Drosophila,* it is common practice to exclude samples which do not display the investigated behaviours (Stern, 2014) and sample filtering prior to analysis is often used in chronobiology studies to exclude outliers such as wildtype flies which do not show robust locomotor activity patterns in entrained conditions (Simoni et al., 2014). These sample selection procedures are commonly done by manually inspecting recordings. I posit that the filtering procedure used within this work builds upon the practices commonly used in both researches conducted on *Drosophila* and chronobiology research and provides an objective way to conduct sample selection.

First **individual hourly activity** was calculated as described in **4.6.1**. From the **individual hourly activity**, the median activity of the first 15 min and the last 15 min was calculated for each sample. Since the sound stimulus was presented during the first 15 min of every hour and the last 15 min of every hour had the longest post-stimulus recovery time; these measures gave a readout of activity during stimulus presentation and baseline activity respectively. I then subtracted baseline activity from the activity during stimulus for each sample. This provided a normalised, **baseline subtracted activity** measure for each sample. The baseline subtracted activity for all the samples in the experimental condition was plotted onto a histogram and I fitted a 4-parameter Gaussian curve to the data using Sigmaplot (**Fig 23B**). To safeguard from bias and to exclude outliers, I discarded 50% of the samples. A representative population within one-standard deviation around the peak of the curve was used for further data analysis (**Fig 23C**).

4.6.3 Analysis for testing general responsiveness to sound stimuli

The selected samples remaining after the filtering protocol described in **4.6.2** were used to derive 4 key metrics from the raw data. First, the activity for each sample was summed into 15-min bins over a 24-h period (**Table 4**).

Table 4: **Sum activity for an individual sample with the column in green representing the activity during stimulus presentation and the last column showing the sum of activity at baseline.** The activity throughout the day was binned into 15 min intervals for each individual sample. The first 15 min of every hour was taken as the activity during stimulus presentation, and the last 15 min was taken as the activity during baseline. To get an overall measure of responsiveness to the sound stimulus; a median for these two readouts was calculated by taking the median activity throughout the whole day (ZT1-24).

		Sample 1		
ZT	**1 -15 min SUM**	**16 -30 min SUM**	**31 -45 min SUM**	**46 – 60 min SUM**
1	1281	196	319	279
2	1260	426	345	239
3	690	388	181	44
4	231	250	52	36
5	36	304	76	16
6	995	643	183	69
:	::	::	::	::
Average	947.5	641	268	292

4.6.3.1 Activity at baseline

The last 15 min sum of every hour represents the activity at baseline (B_{base}) (**Table 4**). To get a better measure of locomotor activity at baseline, an interpolating baseline was calculated for each hour. A simple 2-hourly moving average was used to calculate the interpolating baseline for each sample (**Eq. 1**). Then to calculate the overall baseline activity, a median of the interpolating baseline over the 24-h range was taken for each sample. This value represented the overall **activity at baseline**.

Equation 1: Simple moving average used to calculate the interpolating baseline activity.

$$\{-1 < ZT < 24\} \qquad B_{interpolating\ baseline} = \frac{B_{ZT-1\ base} + B_{ZT\ base}}{2} \qquad (1)$$

4.6.3.2 Activity during stimulus

The sum of the first 15 min of every hour was taken to be the **activity during stimulus** $A_{stim.}$ A median of the activity during stimulus was calculated over a 24-h period for each sample.

4.6.3.3 Baseline subtracted activity

The baseline subtracted activity ($A_{baseline\_subtracted}$) provided a normalised activity value. To obtain this metric, the interpolating baseline was subtracted from the activity during stimulus presentation response for each hour (**Eq. 2**).

Equation 2: Baseline subtracted activity was calculated by subtracting the interpolating baseline from the

$$A_{baseline\_subtracted} = A_{stim} - B_{interpolating\ baseline} \qquad (2)$$

To get an overall impression of the responsiveness of the sample to sound stimulus, this value was calculated for each hour and then the median was taken over the 24-h period for each sample. The larger this value, the greater the increase in locomotor activity above baseline during stimulus presentation. This metric is referred to as **baseline subtracted activity** or **auditory-induced locomotor activity** in the results sections.

4.6.3.4 Activity gain

Since the baseline locomotor activity is oscillating throughout the day, it was difficult to assess whether changes in baseline subtracted activity were reflective of overall systemic changes or specific to the sound stimulus response. Hence the **activity gain** was also used as a metric to assess the relative change in activity in

relation to baseline. The activity gain was calculated by dividing the baseline subtracted activity for each hour by the corresponding interpolating baseline for each sample (**Eq. 3**). The activity gain matric is represented by a percentage. If baseline subtracted metric is equivalent to the interpolating baseline, then the activity gain is 100%.

Equation 3: The gain was calculated by dividing through the baseline subtracted activity by the interpolating baseline.

$$A_{gain} = \left. A_{baseline\_subtracted} \middle/ B_{interpolating\ baseline} \right. \tag{3}$$

To get an impression of overall activity gain, a median activity gain was taken over a 24-h period for each sample.

4.6.4 Analysis maintaining circadian periodicity in locomotor behaviour

The metrics described in **4.6.3** provide insight into the overall baseline and auditory-induced activity. Since these measures were calculated by taking a readout of the whole day, they do not account for the circadian changes occurring over a 24-h cycle.

The same key metrics as described above were used to give a readout of circadian locomotor behaviour. However, to keep the crucial time dimension; the median across samples for each hour was calculated instead.

After the filtering procedure described in **4.6.2**, the data was binned into 15 min intervals over the 48-h experimental period. The activity at baseline, activity during stimulus, baseline subtracted and activity gain were calculated for each hour as described in **4.6.3** however instead of taking the median across the whole day for each sample, a median across all samples was calculated for each hour (**Table 5**). This provided the possibility to examine the **activity at baseline, activity during stimulus, baseline subtracted and activity gain** for each ZT time point over a 48-h period.

Table 5: A table to show the averaging procedure for circadian analysis.
The key metrics were derived by averaging across samples for each time point of a day. The median activity of each metric (activity at baseline, during stimulus presentation, baseline subtracted and activity gain) was calculated for each hour by taking the median activity of samples within the same experimental condition.

	Sample 1		Sample 2			Activity at baseline
ZT	1 -15 min SUM	46 - 60 min SUM	1 – 15 min SUM	46 – 60 min SUM	:	
1	1281	196	319	279	::	800
2	1260	426	345	239	::	752.5
3	690	388	181	44	::	435.5
4	231	250	52	36	::	141.5
5	36	304	76	16	::	56
6	995	643	183	69	::	589
:	::	::	::	::	::	::

4.7 Statistics & hypothesis testing

A variety of statistical methods were used within this thesis to test hypotheses. The decision of which test should be applied to the data was governed by the hypothesis being tested, the relationship between the test groups and the criterion for the use of applied statistical method. Both parametric and non-parametric approaches were used (**Fig 24**).
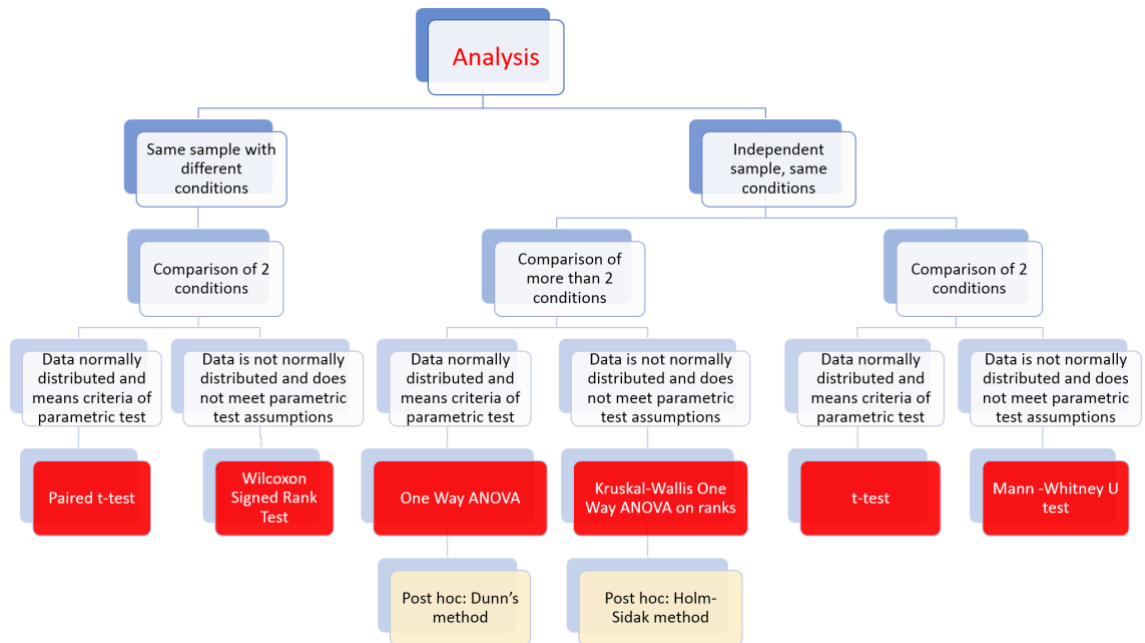
Figure 24: A flow chart to show which statistical tests were used for hypothesis testing.
A number of statistical tests were used based on how many experimental conditions there were, whether the same experimental sample was exposed to different experimental conditions and whether the sample was normally distributed.

4.7.1 Statistical tests for independent conditions

To compare between two independent groups tested in the same condition a Student's t-test was used. If the number of experimental groups exceeded two, a One-Way Analysis of Variance (ANOVA) was used. These statistical methods test whether there is a significant difference in the means between the groups. If the null hypothesis was rejected by the ANOVA test, the Holm-Sidak method was used to make multiple pairwise comparisons between the experimental groups. Applying the Holm-Sidak method allowed to determination of which groups were significantly different from one another.

Both of the approaches described above are parametric tests and assume that the samples have been drawn from a population of normal distribution with equal variances. Thus, both these tests were only employed based on the sample meeting the criterion that the sampled population was normally distributed and showed equal variance. The Shapiro-Wilk test of normality was used to test the assumption of normal distribution and the Brown-Forsyth test of equal variance assumption test was used to check the variability about the group means.

66

If there were violations of either assumptions, non-parametric measures were taken instead. Mann-Whitney Rank Sum test was taken as an alternative to the t-test and the Kruskal-Wallis One Way ANOVA on ranks was used instead of one-way ANOVA. If the null hypothesis was rejected by the ANOVA test, the Dunn's method was used to make multiple pairwise comparisons between the experimental groups

4.7.2 Statistical tests for dependent conditions

If the same sample was exposed to different treatment conditions, a paired t-test was used to determine whether there was a significant effect. If the sample failed to meet the normality and equal variance distribution assumption of this parametric test, a Wilcoxon Signed Rank test was used as an alternative.

4.7.3 Descriptives

Descriptive statistics are reported within the body of the results section. For parametric tests the mean and standard error are reported section together with the p-value. If a non-parametric approach was used, only the median and p-value are reported. Since activity counts are a discrete measure, these descriptive values were round up to whole numbers.

Chapter 5

A novel behavioural assay for investigating auditory-induced behaviours

5.1 Introduction

For many animals, elaborate courtship displays involve auditory cues to aid with sexual selection (Bretman, Rouse, Westmancoat, & Chapman, 2017). Documenting the courtship rituals of fruit flies, Manning (1955) observed that with the vibration of its wing, a male creates an auditory signal. The reception of this signal is dependent on the hearing organ and results in stereotyped behaviours in both males and females. Removing the arista and its related structures inhibits auditory sensitivity (von Schilcher, 1976). Courtship behaviour in hearing-impaired flies is only exhibited in response to auditory courtship signals of greater intensities. This demonstrates that there is a link between the antennal ear, auditory reception and behaviour.

5.1.1 Quantifying auditory-induced behaviours in *Drosophila*

Early work exploring auditory behaviour in *Drosophila* was done by inferring auditory sensitivity by recording instances of courtship interactions. A courtship interaction was classified by the animal exhibiting previously described sexual behaviours such as tapping, chasing and copulation attempts. A full description of these pre-copulatory behaviours was initially made by Shorey (1962).

Von Schilcher (1976) made two other observations which provided the foundation for the development of behavioural assays to test auditory sensitivity. Within this seminal work he demonstrated that firstly, male fruit flies show increases in locomotor behaviour in response to playback of simulated courtship song (this effect was especially pronounced for wingless flies) and secondly, that in the presence of other males, playback of simulated courtship song results in vigorous courting at other males, resulting in chaining behaviour.

Utilising the finding that playback of courtship signal results in increases in locomotor behaviour, Kowalski, Aubin, & Martin (2004) developed a paradigm using video tracking to quantify auditory sensitivity through analysis of this behaviour. Distance moved and duration were interpreted as indicators of activity level. This work confirmed that playback of courtship song results in strong stimulating effects on levels of activity. In particular, it was found that the pulse component of the courtship signal has a greater effect on locomotor output.

Playback of courtship stimuli results in differential behavioural responses in between male and female fruit flies. Initial observations by Cook (1973) found courtship song playback induces reductions in female locomotor activity. It was hypothesised that this inhibition of activity is a sign of receptivity and an act which facilitates copulation. Further probing of this hypothesis by Kowalski et al (2004) found that this effect was only observable in more 'naturalistic' conditions: females would demonstrate this behaviour only in the physical presence of a male. Otherwise, auditory courtship stimulus playback did not change female locomotor behaviour. Clearly, female propensity to exhibit inhibitory locomotor effects in response to auditory courtship signals is dependent upon visual and chemosensory pathways too. This reveals the complexities of this behaviour and how input from a number of senses can contribute to auditory-induced behaviour. Additionally, this demonstrates the benefit of applying a paradigm quantifying locomotor behaviour to better understand the properties of auditory and courtship behaviour.

5.1.2 Mating chain assay

The tendency of males to show courtship interactions towards other males was also used as the basis to develop auditory assays which are frequently used to assess auditory sensitivity in *Drosophila* (von Schilcher, 1976). A chaining assay was developed by Eberl, Duyk, & Perrimon (1997) which quantified auditory-induced behaviour by scoring the number of males within a cohort involved in chaining behaviour during playback of a courtship stimulus. Chaining behaviour was quantified by attributing a score to the number of flies engaged in courtship events within an observation chamber every 3 seconds and then summed in 30 second increments. Following and orientation were events captured by the courtship index. The higher the courtship index, the greater the number of observed courtship events, thus the sensitivity to the given stimulus is considered larger (Inagaki, Kamikouchi, & Ito, 2010). The scoring of courtship events was done by replaying the video recording, which is a long and laborious process prone to experimenter bias. The process was automated by further developments to this assay whereby the courtship index score was generated through the use of video tracking software (Yoon, Matsuo, Yamada, Mizuno, & Morimoto, 2013).
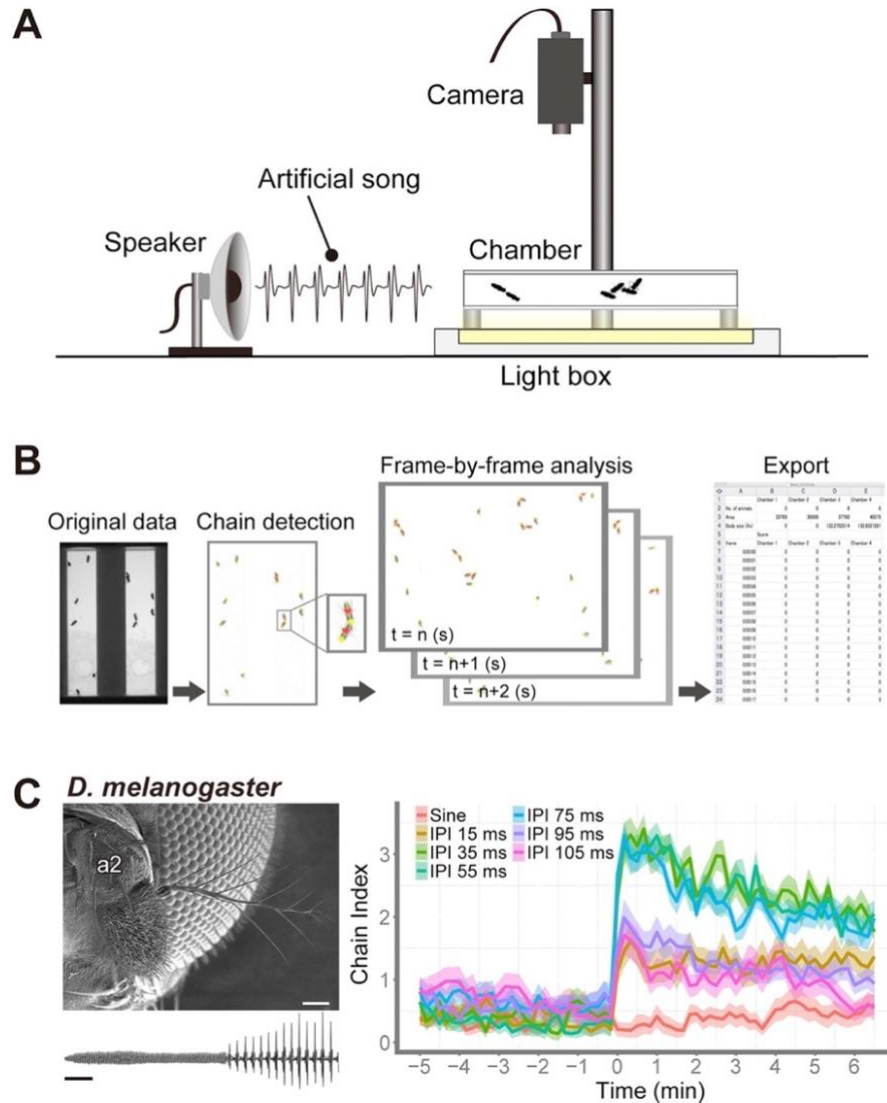
Figure 25: Series of diagrams to show the mating chain assay protocol & the responses of *D melanogaster* to various sound stimuli as observed in this assay.
A: Demonstrates the mating chain set up. A courtship sound stimulus is played through a speaker and cohorts of male wing-clipped flies are observed in a chamber. The response of these flies is recorded by the video tracker positioned above the chamber. Chain detector software analyses the interactions between flies and analysis is done frame by frame (**B**). The IPI encodes a species-specific signal where it was found that *D melanogaster* show the greatest chain index to species specific IPIs (**C**).

Both methods described above provide the opportunity to explore auditory-induced behaviour in *Drosophila*. Auditory behaviour is a high-level function which involves a number of processes amongst mechanosensation to execute. It can also be influenced by a number of factors. Despite this, auditory-induced behaviours provide a convenient output to assess initial sensory processing. This chapter introduces a new method which can be used to supplement previous findings on auditory-induced behaviour.

5.2 Methods

Unless specifically stated, all experiments within this chapter were done on Canton-S (CS) flies. This strain was taken as the wild-type. All the flies sampled were 7-12 days old on the first day of the experiment. During the experiments, unless specifically stated, all experiments were done in cohorts of 3 wing-clipped male flies per tube. The light/dark conditions within the experimental room were synchronized to the regime that flies were exposed to during maturation and the temperature was at a constant 25ºC.

For all the results presented within this chapter, the metrics were derived following the protocol described in **Methods 4.6.4 (page 62)**. The metrics were calculated from the data collected on the first experimental day only. To test the outcomes for statistical significance, appropriate statistical measures were taken in accordance with data structures and assumption testing. Full rationale is given within **Methods, 4.7 (page 63)**.

5.2.1 Methods for 5.3.2: Application of pymetrozine & antenna removal

These methods are relating to the results presented in **5.3.2 (page 74)**. For the pymetrozine condition flies were put onto agar medium topped with diluted pymetrozine solution 24 hours prior to the experiment. 60µL of 1mM solution was used. For the antenna-removed condition, the antenna was removed with forceps during the wing clipping procedure (**methods 4.5**, **page 54**).

5.2.2 Methods for 5.3.5: Selection of virgin & mated samples

These methods are relating to the results presented in **5.3.5 (page 87)**. For experiments testing virgin flies, the sexes were separated within 6 hours post-eclosion and matured in separate vials. For mated conditions, male and female flies were reared together allowing for flies to mate. Both virgin and mated flies were matured accordingly to 7-12 days before testing.

5.3 Results

5.3.1: Increased locomotor activity is observed in response to sound stimulation

To confirm the findings of Kowalski, Aubin, & Martin (2004) and von Schilcher (1976) and to determine whether exposure to sound stimuli produces an observable effect on male locomotor behaviour, the activity of two wild-type strains was assessed in response to playback of an artificial pulse train (APT).
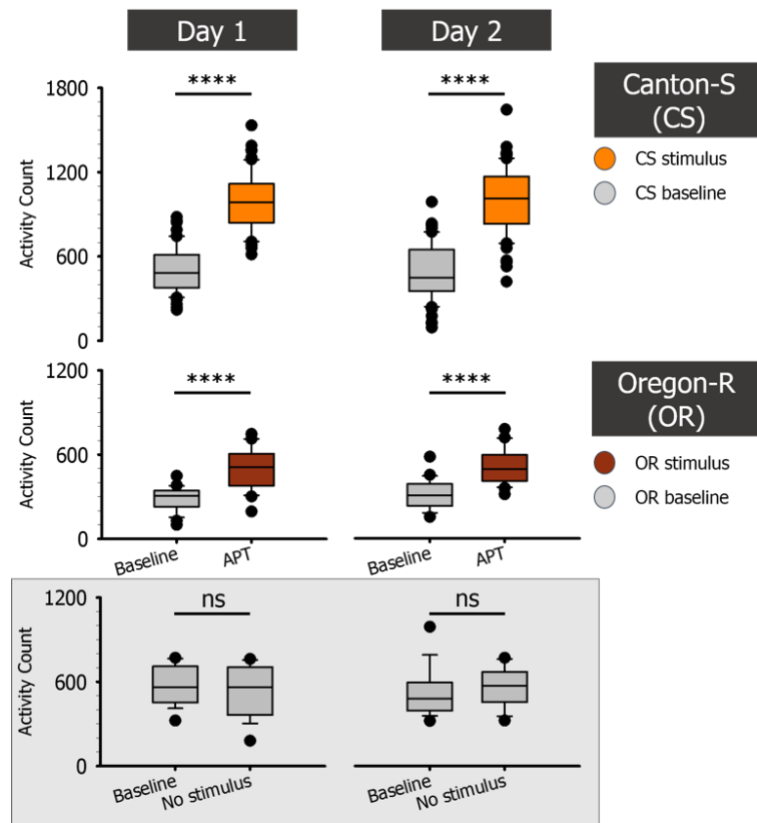
Figure 26: Graph to show auditory-induced locomotor response to sound stimulus presentation in male wild-type flies.
CS and OR wild-type male flies showed significant increases in locomotor activity when presented with an artificial pulse train (APT) stimulus. The same response behavior was observed for both experimental days. There were no changes in activity of flies that were not presented with a sound stimulus. (CS: n=70, OR: n=22, no stim: n=18) (**** = p<0.0001). Data shown is of male flies tested in LD environmental conditions.

Presentation of APT stimulus resulted in increases in locomotor activity in both Canton-S (CS) and Oregon-R (OR) *Drosophila melanogaster* flies (**Fig: 26**). For the

first experimental day, CS males had a mean activity of 503 ± 162 at baseline which increased to 994 ± 202 during stimulus presentation [t(69)= -37.988, p<0.0001, Paired t-test]. The same was observed for OR males. The mean activity at baseline was 287 ± 82 which increased to 500 ± 144 during APT presentation [t(21)= -11.077, p<0.0001, Paired t-test]. Though the response of OR males was weaker, the difference in the activity at baseline and during stimulus presentation remained statistically significant.

Both CS and OR showed similarly higher levels of activity during APT stimulus presentation on the second experimental day. There were no significant differences in the activity at baseline between the two experimental days for CS and OR samples nor were there any significant differences for activity during stimulus presentation. This demonstrates that the effect of APT sound stimulus on locomotor behaviour is constant and stable over experimental days. Implying that there is no decrease in sensitivity to the sound stimuli over the experimental days.

There were differences in activity at baseline between CS and OR. The median baseline activity for OR was 306 which was significantly lower compared to CS 483 [U=165.5, p<0.001, Mann-Whitney-U test] for the first experimental day. The same trend was observed for the second experimental day [OR: 305, CS: 450, U= 328, p<0.001, Mann-Whitney-U test].

To ensure that the observed difference in locomotor activity between baseline and during stimulus presentation were not artefacts of data processing, the same data handling procedure was applied to CS males which were exposed to exactly the same experimental conditions, but were not presented with a sound stimulus. Predictably, this group showed no increases in locomotor activity when there was no stimulus presentation. The locomotor activity count sampled during all the time intervals was ~550.

Interestingly, the mean activity at baseline for unstimulated CS flies was 574 ± 136 which was greater compared to the mean baseline activity of stimulated CS flies 503 ± 162. However, these differences were not found to be significant [t(89)= -1.696, p=0.09, t-test].

The circadian-corrected hourly activity (refer to **methods 4.6.1, page 56**) for further details on data analysis) shows that median activity for CS flies begins to ramp up from APT stimulus onset (**Fig: 27A**). The exponential increase in activity was observed to reach a peak ~11-min into stimulus presentation. There is a slight decay in activity beyond this point despite the presence of APT stimuli. After APT stimulus offset, there is an exponential decay in activity which takes ~15 min to return back to baseline. All individual CS samples showed the same pattern of responsiveness to APT stimulus (**Fig: 27B**)
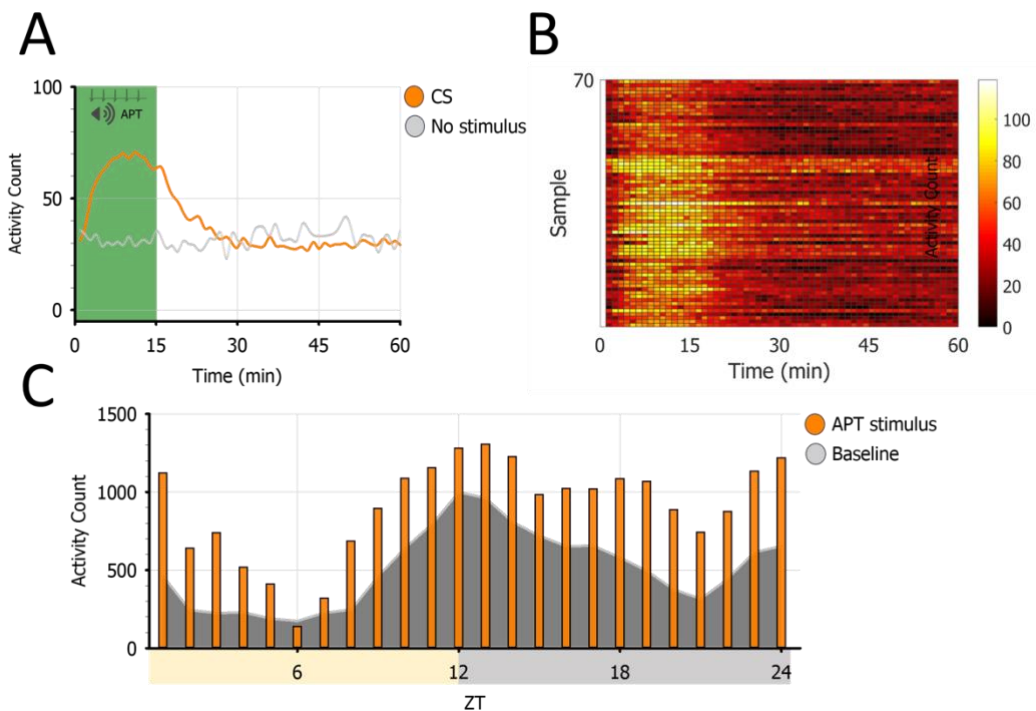
Figure 27: Response properties of auditory-induced locomotor activity in CS male flies.
A: Time series graph to show circadian-corrected hourly activity. An increase in locomotor activity can be observed during the first 15 min of APT stimulus presentation. CS male flies not exposed to sound stimulus did not show this behaviour (n=18). B: Tile plot to show the average hourly activity for individual CS samples (n=70). Averages for both graphs were calculated by taking the median activity for each time point over a circadian period (24-h). C: Elevated activity during APT stimulus presentation was evident at nearly all points throughout a 24-h cycle in male wild-type flies in LD conditions. The area plot shows the activity at baseline binned over a 15 min interval and the bars demonstrate the 15 min binned activity count during stimulus presentation. Data shown is of male flies tested in LD environmental conditions.

The baseline activity pattern of CS flies showed typical circadian modulation ((**Fig: 27C**). This variation in baseline activity over a 24-h cycle is consistent with

behaviour reported in the literature (Helfrich-Förster, 2000; Klarsfeld et al., 2003; Wheeler et al., 1993a). Increases in locomotor activity in response to APT were evident at almost all hours within a 24-h cycle. However, it is clear that there is a variation in response throughout the circadian day. This observation is explored and elaborated further in **Chapter 6.3.2 (page 105)**.

In summary, the findings above demonstrate that APT stimulation elicits a behavioural response whereby the flies show increased locomotor activity during the presentation of a sound stimulus. This behaviour is robust and the response to the stimulus can be observed on an individual sample level, as well as in population medians (**Fig: 27 A&B**). This behaviour is evident in two wild-type strains tested, CS and OR. For the rest of the results within this report, CS is taken as the wild-type.

5.3.2: Sound-induced locomotor activity is antenna-dependent

In the previous section it was demonstrated that wild-type flies show robust increases in locomotor activity in response to APT sound stimulus. However, there are many processes which might contribute to the generation of locomotor behaviour. It was investigated whether the antenna is directly involved in the production of this behavioural response. To test whether the behavioural response is dependent on the detection of the sound stimulus by the antennal sensory organ (i.e. by mechanosensory neurons of JO), JO function was ablated by two means: a) by the removal of the whole antenna and b) by pharmacological means through treating the flies with pymetrozine. Pymetrozine is an insecticide with an inhibitory effect on mechanosensory neurons. It is an irreversible agonist of the heterodimeric *nan/iav* channels which are specific and essential for chordotonal organ function (Ausborn, Wolf, Mader, & Kayser, 2005; Nesterov et al., 2015).

There were no significant differences found in the baseline activity between the conditions (**Fig: 28A, Table 6**) [$F_{(2,91)}= 0.606$, $p= 0.547$, one way ANOVA]. Since the activity at baseline was comparable between untreated (CTRL), pymetrozine-treated (PYM) and antenna ablated (-ANT) flies, it suggests that the interventions of the treatment groups did not have a general adverse effect on the animals.

There were significant differences between the conditions in the activity during APT stimulus presentation [$F_{(2,91)}=30.474$, $p<0.001$, one way ANOVA] (**Fig: 28B**). Post hoc comparisons using the Holm-Sidak method indicated that the mean activity for the untreated wild-type condition 994 ± 202 was significantly higher compared to both PYM 567 ± 284 and -ANT 588 ± 299 ($p<0.001$ for both).
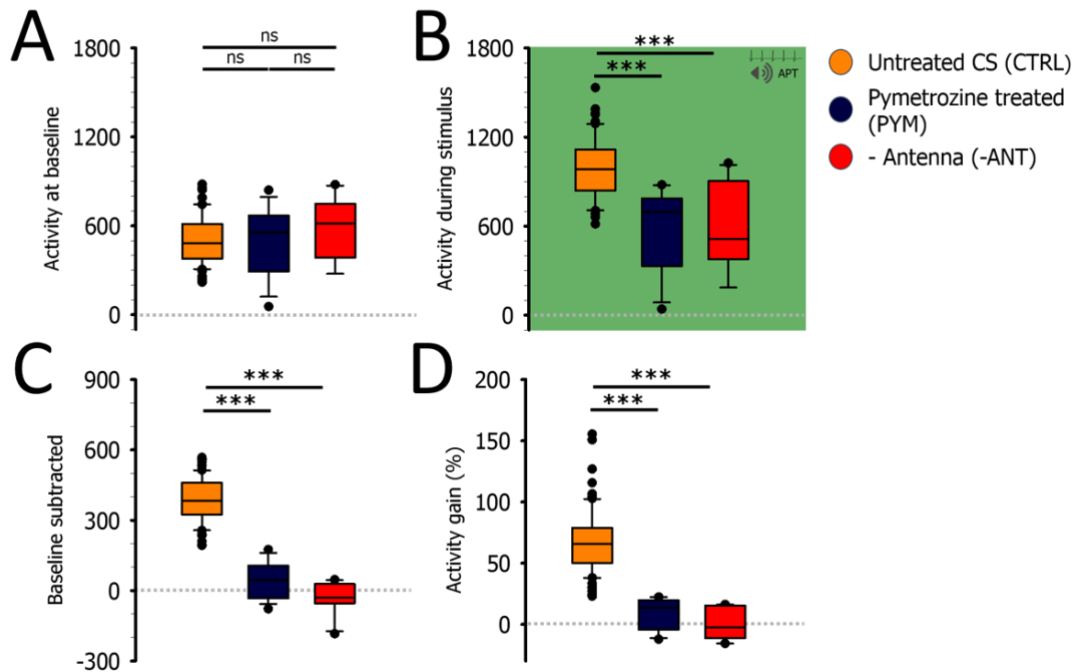
Figure 28: Box plots to show sound-induced locomotor activity is antenna-dependent. Graphs to show the locomotor activity of pymetrozine-treated (PYM), antenna-removed (-ANT) and untreated wild-type flies (CTRL).
A: Box plot to show the activity at baseline of PYM, -ANT and CTRL male wild-type flies. There were no significant differences between conditions in baseline activity. **B**: Box plots to show the activity during APT stimulus presentation. **C**: Box plots to show the baseline subtracted activity and D shows the activity gain for the 3 conditions. CTRL had significantly greater sound-induced locomotor activity compared to the treatment conditions (**B,C,D**). (CTRL: n=70, PYM: n=14, -ANT: n=10) (*** = *p<0.001*). Data shown is of male flies tested in LD environmental conditions.

The difference between the groups was found to be more pronounced in baseline subtracted activity [$F_{(2,91)}=154.58$, $p<0.001$, one way ANOVA] (**Fig: 28C**). The baseline subtracted activity for the untreated condition was 385 ± 94 which was significantly greater compared to the PYM condition 44 ± 76 and -ANT condition -28 ± 69 ($p<0.001$ for both, post hoc comparisons using the Holm-Sidak method).

Table 6: A table to summarise the locomotor activity of pymetrozine-treated, antenna-removed and untreated wild-type male flies in response to APT sound stimulus.

	CTRL (n=70)	PYM (n=14)	-ANT (n=10)
Activity at baseline	483	503	569
Activity during stimulus	994 ± 202	567 ± 284	588 ± 299
Baseline subtracted activity	385 ± 94	44 ± 76	-28 ± 69
Activity gain (%)	65.5	13.6	-2.56

Significant differences in the activity gain were observed between the conditions also [χ_2(2)=51.524, p<0.001, Kruskal-Wallis one way ANOVA] (**Fig: 28D**). The median activity gain for the untreated condition was 65.5%, which was significantly greater compared to both the median for PYM condition 13.6% and -ANT condition -2.56% (p<0.001, Dunn's method used for post hoc comparisons).

Despite there being such a strong disparity in the responses between treated and untreated flies, animals exposed to PYM were found to respond to APT sound stimuli. For the pymetrozine condition, the activity at baseline was 503 ± 235 which increased to 567 ± 284 during APT stimulus presentation [t(13)= -2.528, p= 0.025, Paired t-test]. However, there were no significant differences in the activity at baseline and during stimulus for -ANT flies [t(9)= -0.440, p= 0.670, Paired t-test]. These findings indicate that there was an attenuated but present sound-induced increase in locomotor activity in the PYM treatment condition. Conversely, in antenna-ablated flies, the behavioural response is totally abolished.

The effect of pymetrozine and antennal ablation was evident throughout the whole 24-h cycle. The activity during stimulus presentation rarely exceeded activity at baseline (**Fig: 29 B&C**). The flies in the treatment conditions showed normal oscillatory baseline activity patterns in a 12-h light/dark cycle. Interestingly, the evening activity peak appears more pronounced in the antenna-ablated condition. This suggests that antenna removal effects baseline locomotor activity patterns.

In summary, these findings show that inhibition of the JO results in an inhibition of sound-induced locomotor activity. This suggests that the behavioural response to APT sound stimulus is dependent on the antennal chordotonal organ.
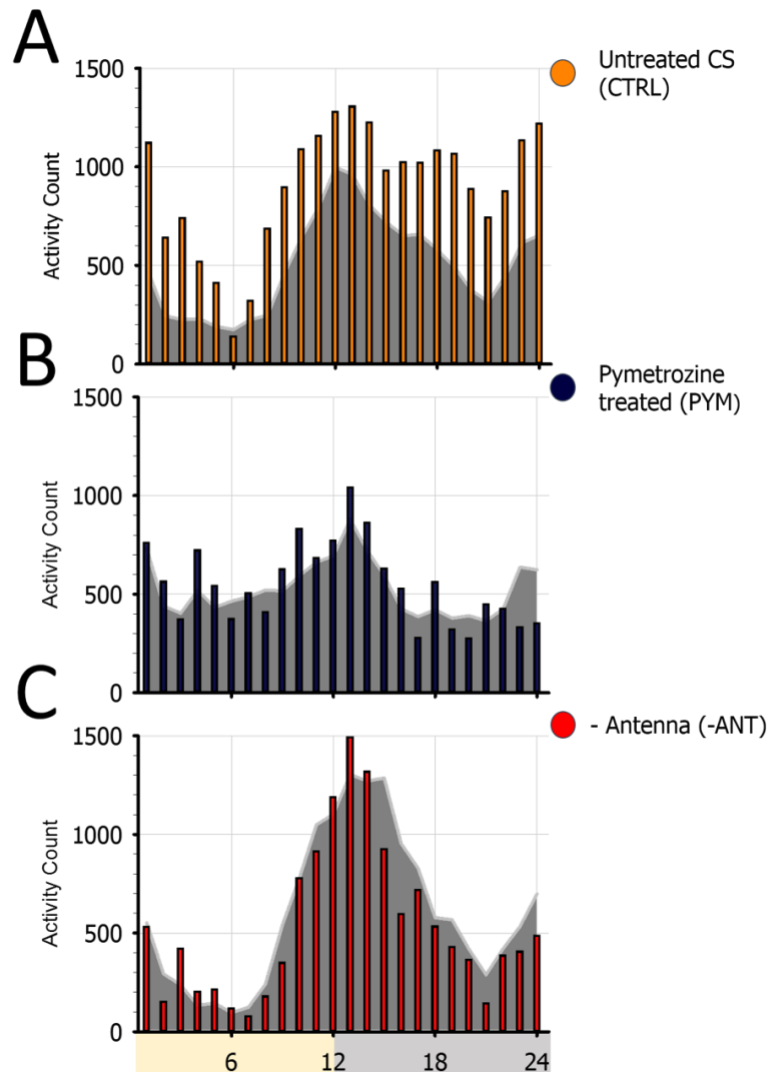
Figure 29: Actograms showing the median baseline and APT stimulus-induced locomotor activity of CTRL, PYM & -ANT male flies.
A: Modified actogram to show the baseline activity of wild-type flies in grey with an overlaying bar graph to show the activity during stimulus presentation binned over 15 min intervals. Time is on the x-axis with the light switch at ZT12. **B** & **C:** Actograms to show the activity of pymetrozine-treated and antenna-removed flies. The effect of pymetrozine and antenna removal on behavior is evident throughout a 24-h period. Data shown is of male flies tested in LD environmental conditions.

5.3.3 Increases in locomotor behaviour are modulated by the nature of the sound presented

Within the previous sections in this chapter, it was determined that there are increases in locomotor behaviour in response to the presentation of APT sound stimulus and that this behaviour is dependent on JO function.

79

To further explore the properties of this stimulus-induced locomotor behaviour, it was explored whether the magnitude of response to the stimulus is regulated by the perceived sound. To test this, wild-type flies were presented with white noise (WN, artificial pulse train (APT) or a real courtship song (RCS). Furthermore, comparisons were made to wild-type flies in unstimulated (-STIM) conditions to explore the effects of sound stimulation on overall behaviour.

The activity at baseline was found to be significantly different between the different treatment conditions [χ_2 (3)=26.647, p<0.001, Kruskal-Wallis one-way ANOVA on ranks]. The median baseline activity of flies in the -STIM condition was 561. Using the Dunn's method for pairwise post-hoc comparisons revealed this baseline activity were significantly greater compared to the WN condition (326, p<0.001) and RCS stimulus condition (363, p<0.001). Furthermore, the baseline activity of flies in the APT condition (483) was also found to be significantly greater compared to WN and RCS (p=0.003 and p=0.008 respectively) (**Fig: 30A, Table 7**).

The activity during stimulus was found to be significantly greater for both APT and RCS compared to WN and -STIM conditions [χ_2 (3)=66.418, p<0.001, Kruskal-Wallis one-way ANOVA on ranks]. RCS had the highest median activity during stimulus presentation (985) followed by APT (929). Post hoc comparisons using the Dunn's method found both of these conditions to be significantly different when compared to the median of WN (503) and unstimulated condition (560, p<0.001 for all comparisons) (**Fig: 30B**).

There were significant differences in the baseline subtracted activity between the conditions [χ_2 (2)=42.139, p<0.001, Kruskal-Wallis one-way ANOVA on ranks]. Post hoc comparisons using the Dunn's method showed that the baseline subtracted activity of flies in the RCS (438) and APT (384) conditions was significantly greater compared to baseline subtracted activity of WN condition (54, p<0.001 for both comparisons) (**Fig: 30C**).
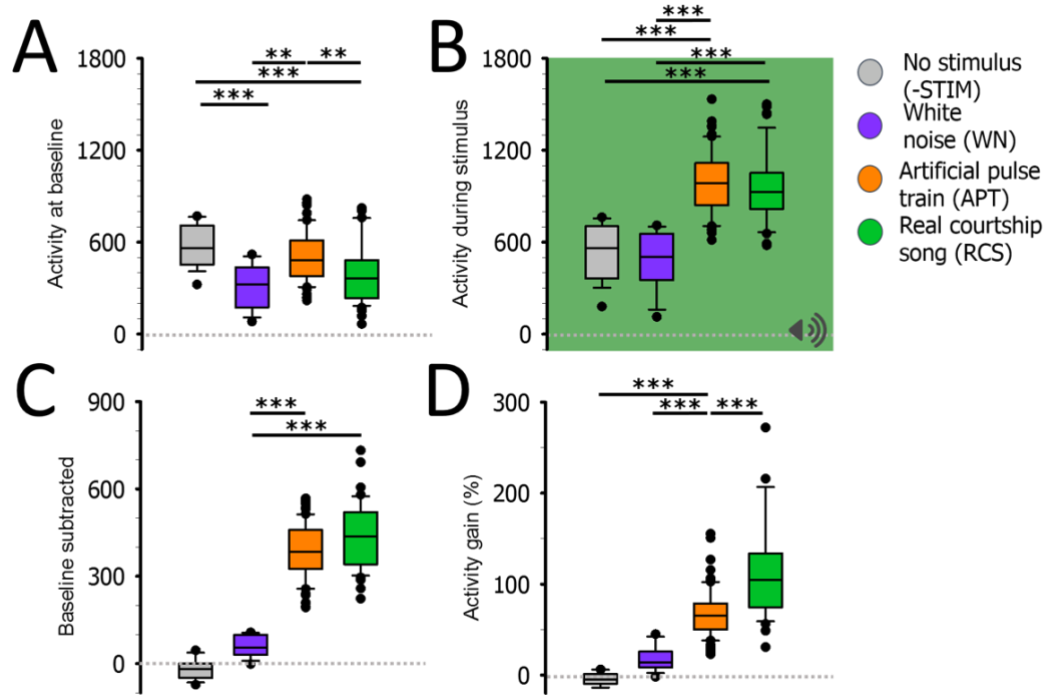
Figure 30: Box plots to show the differences in auditory-induced locomotor activity of male wild-type flies in response to no stimulus (-STIM), white noise (WN), artificial pulse train (APT) & real courtship song (RCS).

A: Box plot showing the activity at baseline for wild-type flies in -STIM, WN, APT and RCS conditions. -STIM conditions show a significantly elevated baseline activity. B: Box plots to show the activity during stimulus presentation. APT and RCS elicit largest changes in locomotor activity. Baseline subtracted activity demonstrates the locomotor response to APT and RCS is significantly higher compared to WN responses (C). D: Box plots showing responses to APT and RCS have a larger activity gain compared to WN (-STIM: n=18, WN: n=14, APT: n=70, RCS: n=46) (*** = p <0.001, ** = p <0.01). Data shown is of male flies tested in LD environmental conditions.

Table 7: Summary of median baseline and auditory-induced activity of male wild-type flies in response to APT, RCS and WN stimuli.

	APT (n=70)	RCS (n=46)	WN (n=14)
Activity at baseline	483	367	326
Activity during stimulus	929	985	503
Baseline subtracted activity	384	438	54
Activity gain (%)	65.5	104.4	13.8

The activity gain was also found to be significantly different between conditions [χ_2 (2)=58.157, p<0.001, Kruskal-Wallis one-way ANOVA on ranks]. The median activity gain for the RCS condition was 104.4% was significantly greater compared to WN (13.8%, p<0.001). The median activity gain for APT conditions (65.5%) was also significantly greater compared to WN, likewise it was found to be significantly lower compared to RCS (p<0.001 for both) (comparisons were made using the Dunn's method) (**Fig: 30D**).

Given these differences between conditions, it is unsurprising that wild-type flies in the RCS condition showed largest increases in locomotor activity during sound stimulus presentation. The activity during RCS stimulus presentation was 949 ± 227 which was significantly higher compared to activity at baseline 399 ± 198 [t(45)= -26.916, p<0.0001, Paired t-test]. There was also a significant increase in locomotor activity observed in WN conditions. Activity at baseline within these conditions was 314 ± 138 which increased to 484 ± 191 during WN stimulus presentation [t(13)= -6.267, p<0.0001,, Paired t-test].

From these findings, it is possible to infer that the response magnitude of locomotor behaviour is linked to the biological relevance of the given stimulus. Both APT and RCS stimuli can be considered biologically relevant. These stimuli carry elements of the courtship signals whereas WN stimuli do not encode any such information. The 'naturalness' of the presented stimulus is positively correlated with the levels of response activity. However, since there is a significant increase in locomotor activity in response to WN stimulus, it is evident that this behavioural response, though weakened, is also observable to sound stimuli with no biologically meaningful signals.
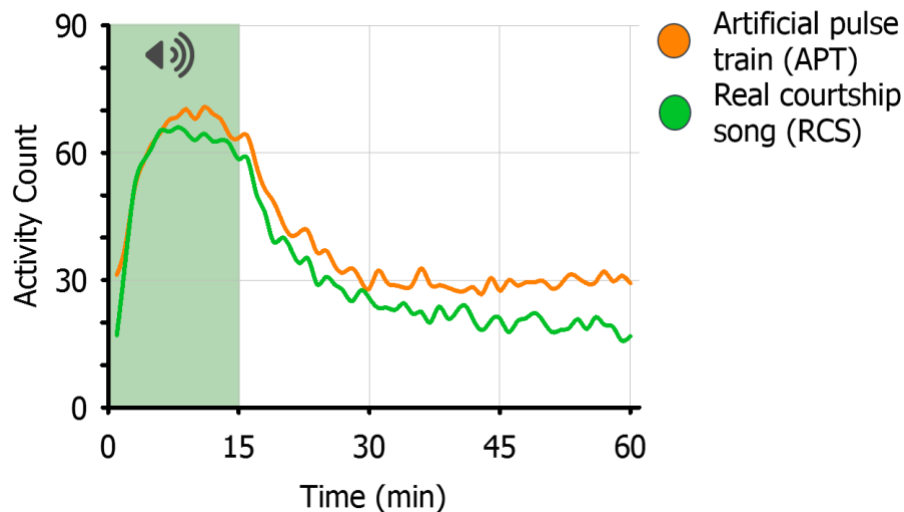
Figure 31: Time series graph to show median activity of male wild-type flies in response to APT & RCS stimulus.
The graph shows that the median activity to both stimuli follows a similar response pattern with an exponential rise during the stimulus presentation period followed by an exponential decay in activity to baseline. Data shown is of male flies tested in LD environmental conditions.

As well as the given stimulus affecting the response magnitude, it was assessed whether the temporal response pattern is changed as a result of exposure to different sound stimuli. Despite the significant differences in response magnitude, the temporal response pattern for both APT and RCS conditions remain comparable. From **Figure 31** is it evident that both stimuli induce similar response dynamics within the two conditions – an exponential rise aligned with stimulus onset followed by a decay period following stimulus offset. It should be noted, however, that during stimulus presentation, there is an increase to similar activity levels for both stimuli yet the baseline activity for RCS appears lower (**Fig: 30A, 31, 32**).

In conclusion, these findings suggest that the locomotor response to sound stimulus is modulated by the type of stimulus given. This effect is on the magnitude rather than the dynamics of the response. The changes to baseline between the conditions could show that exposure to particular sound stimuli such as RCS change the overall behaviour of the animal.
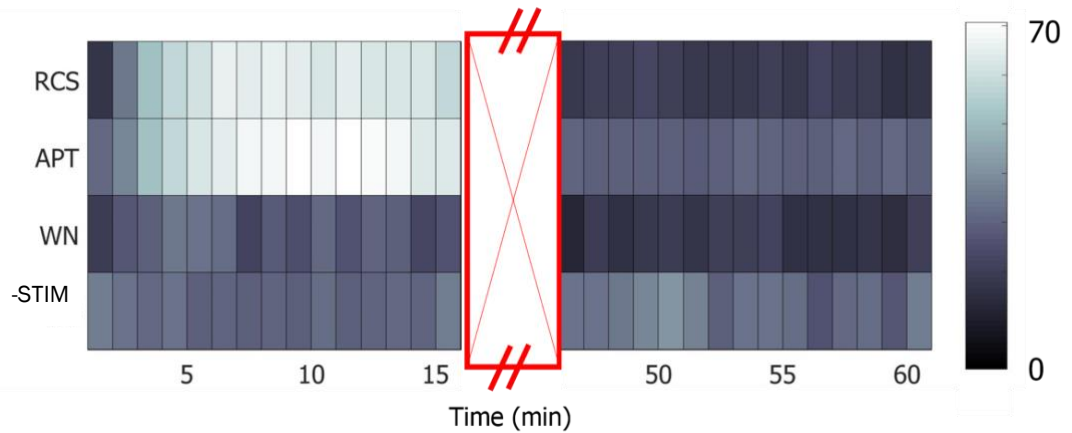
Figure 32: Tile plot to show the difference in activity magnitude of male wild-type flies during the baseline and stimulus presentation interval for -STIM, WN, APT & RCS.

5.3.4: Grouped conditions lead to increased locomotor output in response to sound stimuli

Since acoustic signals are used in a variety of social contexts, classical auditory behavioural assays in *Drosophila* are done in grouped conditions (Eberl et al., 1997; Yoon et al., 2013; Zhou et al., 2015). The results presented within this chapter thus far have been conducted with flies in grouped conditions, where there were 3 males per sampling tube. To assess whether grouping influences responsiveness to the sound stimuli; the responses to APT stimulus of flies in grouped and individually housed conditions were compared.

Naturally, it was expected that the individually housed flies would have a lower activity count due to there being fewer flies within the sampling tube and less opportunity to generate beam breaks. This presented a challenge when directly comparing to the activity in grouped conditions. To address this problem, it was assumed that there is a linear relationship between the number of flies in the tube and activity count. Based upon this assumption, an estimate of activity of animals in grouped conditions was constructed by multiplying the sampled data from the individually housed flies by 3. This predicted activity was called grouped estimate. By cross-comparison of the activity between the observed grouped conditions and grouped estimate, it was possible to determine whether a 'social effect' was reflected in the activity of grouped flies.

Individually housed flies showed significant increases in locomotor activity in response to APT stimulus presentation. The mean activity at baseline was 173 ± 86 which was significantly lower compared to the mean activity during stimulus presentation 306 ± 125 [t(27)= -7.410, p<0.0001, Paired t-test]. This shows that presentation of APT sound stimulus can produce increases in locomotor activity in grouped and individually housed conditions.

There was no significant difference in the baseline activity between the observed group and the estimate. The median baseline activity count for the observed grouped conditions was 483, whereas for the grouped estimate it was 454 [U= 947.000, p=0.798, Mann-Whitney U test] (**Fig: 33A, Table 8**). This indicates that the baseline activity pattern follows a linear relationship between number of flies within a sampling tube and activity count. The median activity during stimulus presentation for the observed group was 985 which was higher compared to the calculated estimate (847) however the difference between the groups was not found to be statistically significant (**Fig: 33B**).

Significant differences in the baseline subtracted activity were found between the observed group and the calculated estimate (**Fig: 33C**). The observed group median was 384, which was significantly higher compared to the calculated estimate of 209 [U=348.500, p<0.001, Mann-Whitney U test].

The activity gain is a measure of relative change so this metric was compared between grouped observed, grouped estimate and individually housed flies. The activity gain for the grouped observed was 65.5% whereas the calculated grouped estimate was 34.1% and the individually housed flies had an activity gain of 31.6% to APT stimulus presentation [χ_2 (2)=16.557, p<0.001, Kruskal-Wallis one-way ANOVA on ranks]. Post hoc comparisons using the Dunn's method showed that the activity gain for the grouped observed was significantly higher compared to both calculated estimate and individually housed condition (p=0.002 & p=0.006 respectively) (**Fig: 33D**).
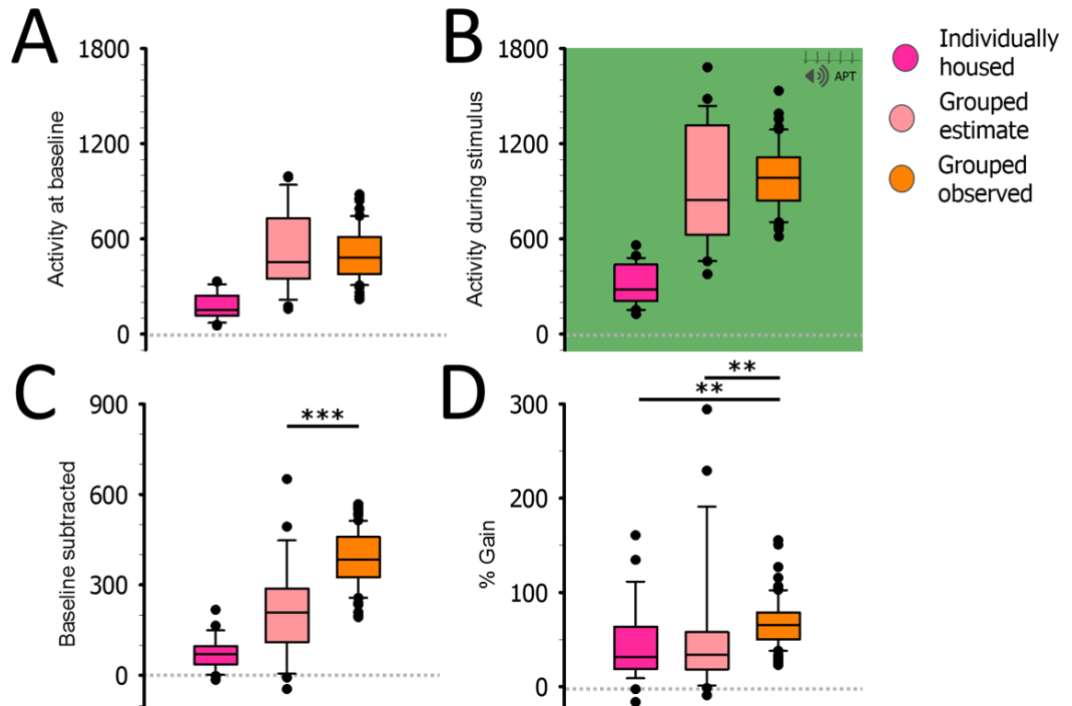
Figure 33: Box plots to show the differences in auditory-induced locomotor activity of male wild-type flies in response to APT for grouped and individually housed conditions. A grouped estimate is also shown.

A: Box plot showing the activity at baseline for wild-type flies in grouped observed, grouped estimate and individually housed conditions. There were no significant differences between baseline activity of grouped observed and grouped estimate. B: Box plots to show the activity during APT stimulus presentation. Baseline subtracted activity in response to APT stimulus presentation was significantly higher for grouped observed compared to grouped estimate (C). D: Box plots to show the activity gain for the individually housed, grouped observed and grouped estimate (*** = p <0.001, ** = p <0.01). Data shown is of male flies tested in LD environmental conditions.

Table 8: Summary of median baseline and auditory-induced activity of male wild-type flies in response to APT stimulus for individually housed, grouped estimate and grouped observed conditions.

	Individually housed (n= 28)	Grouped estimate	Grouped observed (n=70)
Activity at baseline	151	454	483
Activity during stimulus	282	847	985
Baseline subtracted activity	70	209	384
Activity gain (%)	31.6	34.1	65.5

The differences between the conditions in the baseline subtracted and activity gain indicate that there is a non-linear relationship between the number of flies in the sampling tube and the locomotor activity in response to APT sound stimuli. Since the baseline subtracted activity and activity gain were greater for grouped observed conditions it is suggestive that grouping results in an increased auditory-induced locomotor response to APT stimulus (**Fig: 33 C&D**).

To examine whether there were differences in the response dynamics between grouped and individually housed flies, the circadian-corrected hourly activity for the conditions was normalised to correct for the disparity in activity magnitude. The circadian-corrected hourly activity was normalised and scaled from 0 to 1 (**Fig 34A**). The response kinetics for the individually housed condition does not follow the same pattern as for the grouped condition. In the individually housed condition, the activity peak appears to be after the offset of sound stimulus. However, this is hard to quantify as the individually housed circadian corrected hourly activity is noisy.

Collectively, these findings indicate that grouping effects auditory-induced locomotor activity. This socially determined component results in an increased propensity to show a greater locomotor response to the sound stimulus (**Fig 34B**). This outcome demonstrates the complexity of auditory-induced locomotor activity and how the response behaviour is not only a direct readout of auditory sensory input. It is evident that there are a number of factors modulating this response.
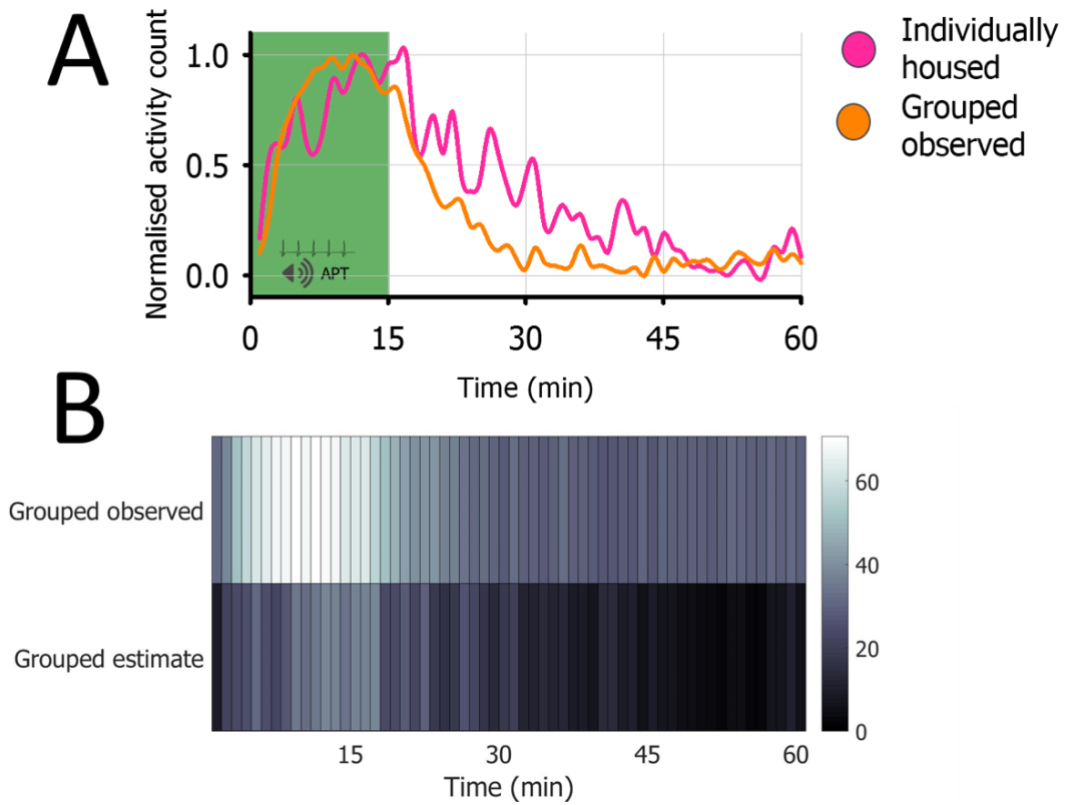
Figure 34: Time-series graph and tile plot to show the response dynamics of male wild-type flies to APT sound stimulus of individually housed, grouped observed and grouped estimate.
A: Line plot to show the median activity count of individually housed and grouped flies over an hour (data averaged over a 24-h period). For ease of comparison between the conditions, the activity counts have been scaled. There is no observable difference in the activity pattern between groups. **B:** Tile plot to compare the distribution of median activity counts for grouped observed and grouped estimate. Observed condition shows higher magnitude in responsiveness to stimuli within the first 15 min and elevated baseline. Grouped conditions n=70, individually housed n=28. Data shown is of male flies tested in LD environmental conditions.

5.3.5: Sex differences are observed in response behaviour to APT & RCS stimulus presentation

Several studies have reported sexual dimorphism in locomotor behavioural patterns as well as courtship behaviour in *Drosophila* (Helfrich-Förster, 2000; Tompkins, Gross, Hall, Gailey, & Siegel, 1982; von Philipsborn et al., 2011). To assess whether this sexual dimorphism can be detected in the auditory-induced locomotor responses, male and female flies were tested in the behavioural assay. Furthermore, to investigate whether the mated state of the animal modulates the response to stimulus, both mated and virgin animals were tested. Additionally, responses of virgin and mated males and females to APT and RCS stimulus were tested to explore whether there were differential behavioural responses to the sound stimulus.

Previous reports have described that auditory courtship signals produce inhibitory effects on female locomotor activity (Hall, 1994; von Schilcher, 1976). There was no evidence of such behaviour within this assay. On the contrary, both virgin and mated females showed significant increases in locomotor activity during APT and RCS stimulus presentation compared to baseline.

Virgin females showed similar increases in locomotor activity to both APT and RCS stimulus. Mean activity during APT stimulus presentation was 744 ± 144 which was significantly greater compared to the activity at baseline 552 ± 149 [$t(29)$ = -14.125, $p < 0.001$, Paired t-test] (**Fig 35A, Table 9**). The mean activity during RCS stimulus presentation was 796 ± 167 which was significantly greater compared to activity at baseline 600 ± 120 [$t(7)$ = -9.183, $p < 0.001$, Paired t-test] (**Fig 36A**).
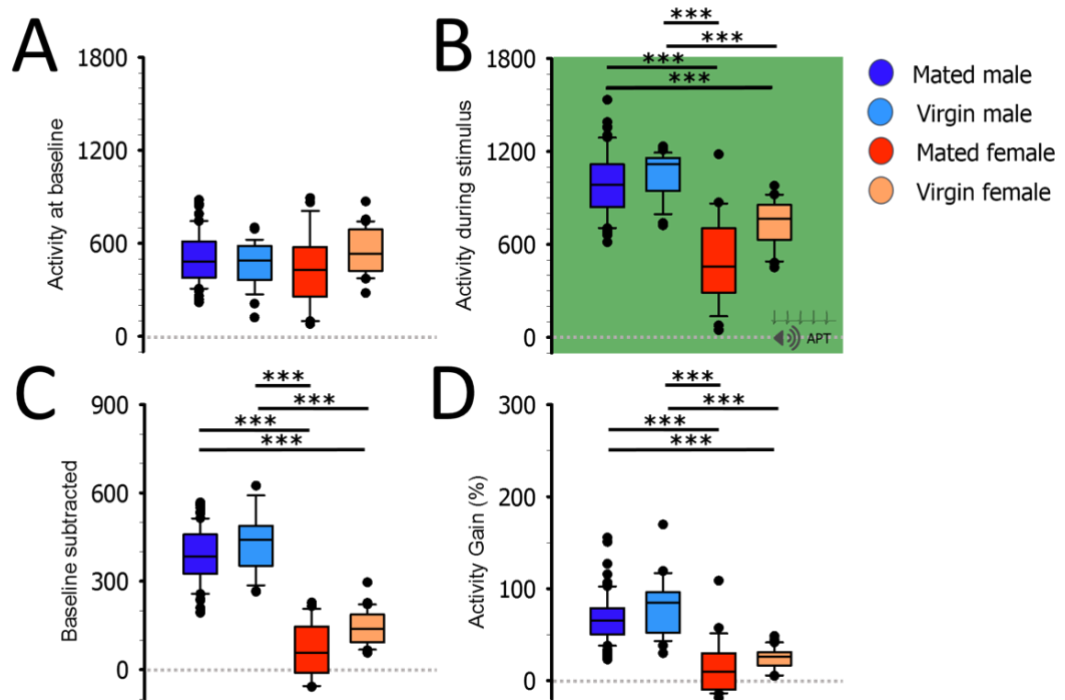
Figure 35: Box plots to show the differences in auditory-induced locomotor activity of mated and virgin, female and male flies in response to APT sound stimulus presentation.
A: Box plot showing the activity at baseline for mated and virgin, female and male wild-type flies. **B:** Box plots to show the activity during APT stimulus presentation. Virgin and mated males showed highest levels of activity during stimulus presentation Baseline subtracted activity demonstrates the locomotor response was greater for virgin and mated males compared to females (**C**). **D:** Box plots showing males responses to APT stimulus had larger activity gain compared to females (*** = *p<0.001*). Experiments were conducted in LD environmental conditions.

Mated females also exhibited significant increases in locomotor activity in response to both sound stimuli. Activity during APT sound stimulus presentation was 504 ± 277 which was significantly greater compared to activity at baseline 430 ± 226 [t(21)= -2.928, p= 0.008, Paired t-test] (**Fig 35B**). Activity during RCS stimulus presentation was 782 ± 151 which was significantly greater compared to activity at baseline 535 ± 137 [t(7)= -8.416, p<0.001, Paired t-test] (**Fig 36B**).These findings demonstrate that virgin and mated female flies respond to both APT and RCS stimuli by increasing locomotor activity.

Comparing between APT and RCS, baseline subtracted activity showed mated female flies had significantly greater increases in locomotor activity to RCS 196 ± 60 compared to APT 59 ± 91 [t(28)= 3.946, p<0.001, t-test] (**Fig 37 & 38 C**). This effect was also reflected in the activity gain. The median activity gain for RCS was

31.8% which was significantly higher compared to APT 9.71% [U=42, p=0.033, Mann-Whitney U test] (**Fig 35 & 36 D**). Interestingly, there were no significant differences in the baseline subtracted activity and activity gain of virgin females in response to APT and RCS stimulus.
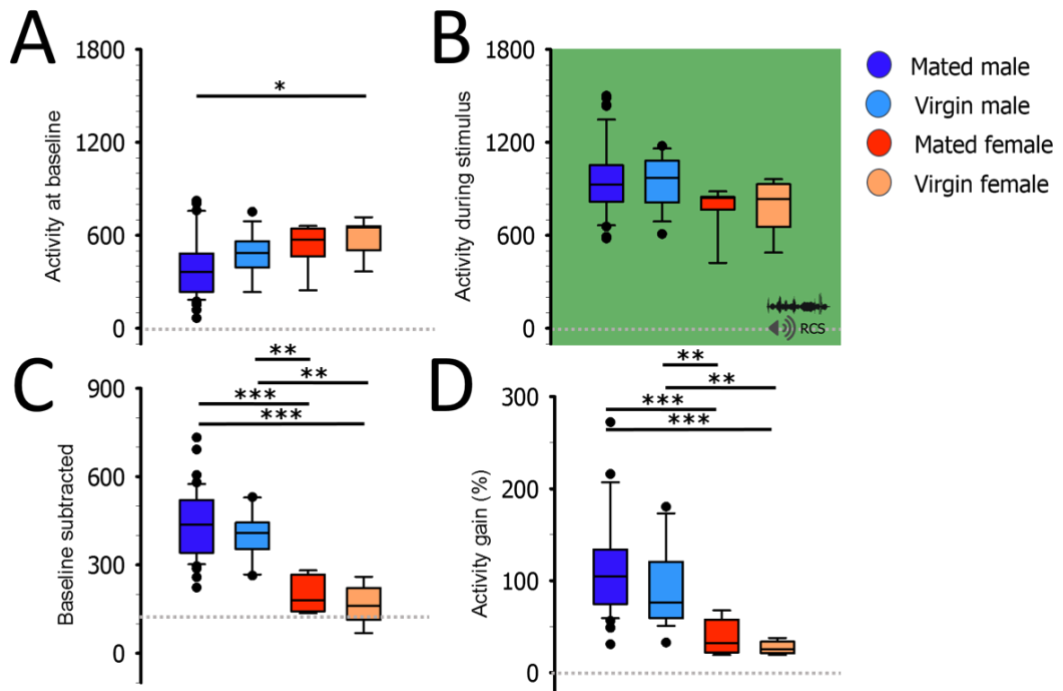
Figure 36: Box plots to show the differences in auditory-induced locomotor activity of mated and virgin, female and male flies in response to RCS sound stimulus presentation.
A: Box plot showing the activity at baseline for mated and virgin, female and male wild-type flies. **B:** Box plots to show the activity during RCS stimulus presentation. Virgin and mated males showed highest levels of activity during stimulus presentation Baseline subtracted activity demonstrates the locomotor response was greater for virgin and mated males compared to females (**C**). **D:** Box plots showing males responses to RCS stimulus had larger activity gain compared to females (*** = *p<0.001*). Experiments were conducted in LD environmental conditions.

Mated males were also found to show larger increases in locomotor activity in response to RCS over APT. The mean baseline subtracted activity for RCS was 443 ± 114 which was significantly greater compared to APT 385 ± 94 [t(114)= 2.996, p=0.003, t-test] (**Fig 36D**). This effect was also evident in the activity gain. The median activity gain for mated males in RCS conditions was 104.4% whereas for APT the median activity gain was 65.5% [U=652, p<0.001, Mann-Whitney U test]. Interestingly, as seen for virgin females, there were no significant differences in baseline subtracted activity and activity gain in virgin males in responses to RCS

and APT (**Table 9**).

Males and females showed comparable levels of baseline activity but there was sexual dimorphism in the response to sound stimuli. Males exhibited greater auditory-induced locomotor activity in response to both sound stimuli compared to females. All comparisons and statistical significances are shown in **Figure 35 & 36**. Statistical comparisons performed using the Kruskal-Wallis one-way ANOVA on ranks with post hoc pairwise comparisons using the Dunn's method.

Table 9: Summary table of the average activity at baseline, during stimulus, baseline subtracted activity and activity gain for virgin and mated male and female wild-type flies. Comparisons are made between the responses to APT and RCS stimulus.

	APT				RCS			
	Virgin		Mated		Virgin		Mated	
	M (n=28)	F (n=30)	M (n=70)	F (n=22)	M (n=18)	F (n=8)	M (n=46)	F (n=8)
Activity at baseline	468 ± 141	552 ± 149	503 ± 162	430 ± 226	487	652	363	572
Activity during stimulus	1119	766	985	457	970	835	929	841
Baseline subtracted activity	441	139	384	57	409	162	438	180
Activity gain (%)	84.9	25.9	65.5	9.71	76.1	25.1	104.4	31.8

In summary, males show greater auditory-induced locomotor activity in response to both APT and RCS stimuli. Virgin male and female wild-type flies did not show differences in response between APT and RCS stimulus. Yet, both mated females and males show greater responses to RCS sound stimuli. This suggests that the discrimination between the two stimuli is dependent on the mating state of the animal.

5.4 Discussion

Within this chapter, I have outlined and quantified a new behavioural paradigm to test auditory behaviour in *Drosophila*. Robust increases in locomotor activity were observed in Canton-S and Oregon-R wild-type flies during the presentation of an auditory stimulus. This is complementary to early work researching the effect of auditory courtship signals on males that found the observed activity changes to be most striking (Kowalski, Aubin, & Martin, 2004; von Schilcher, 1976).

The method taken within the current body of work is notably different compared to previous approaches used to assess auditory-induced locomotor behaviour. Von Schilcher (1976) took a binary approach to classifying this response. Within a chamber, it was qualified how many male flies within a cohort become active after exposure to the auditory courtship stimulus. Despite this being a robust measure, it does not quantify the observed increases in activity. Further work by Kowalski et al (2004) used video tracking to quantify the locomotor response to auditory courtship signals by measuring the distance moved and movement duration. This approach gives greater insight into the finer details of the response behaviour, but presents some practical challenges. Extracting the relevant parameters from the videos takes a significant amount of pre-processing and computation. These issues are avoided in the current work since the activity counts provide a direct readout of locomotor activity. Additionally, through using this measure, the data is more manageable allowing for the assay to be used over longer periods of time.

Locomotor increases in response to prolonged auditory stimulation was observed in both behavioural paradigm presented in this chapter and the behavioural assay used in Kowalski et al (2004) however, the response dynamics between the two studies are found to be different. Kowalski et al (2004) observed locomotor activity of individual male flies in response to a selected natural courtship song representative of the species and the same song filtered by a 160-600 Hz bandpass filter to isolate the pulse song. In that study males show an initial peak in locomotor activity in response to stimulus onset, followed by a rapid decline of activity despite the continued presence of sound stimulus. Whereas within the current work, a more sustained response is observed. Activity of male wild-type flies

followed an exponential increase from stimulus onset leading to a plateaued response during stimulus presentation (**Fig 34A, page 86**). The main discrepancy between the studies is the age of the experimental flies. Kowalski et al (2004) explored this behaviour in flies that were 1-4 days old whereas in the current work, animals were tested at day 7-12 post-eclosion. Possibly, age influences auditory induced locomotor behaviour.

Ablation of the arista results in deafness and an inhibition of auditory-induced behaviours (Ishikawa & Kamikouchi, 2016; Kyriacou & Hall, 1982; Nichols, Becnel, & Pandey, 2012; von Schilcher, 1976). Thus, it was no surprise that the antenna-ablated flies did not show auditory-induced locomotor activity in response to stimulus presentation within the current work. The behavioural response to sound stimulus was also greatly attenuated in pymetrozine-treated flies. Since pymetrozine did not fully abolish the auditory-induced locomotor response, this finding could suggest that there is *nan-iav* independent mechanotransduction within the antenna. Or, that there are non-chordotonal organ sensors in the body contributing to the response. Taking these findings together, it is possible to conclude that, firstly, the behaviour is antenna-dependent and secondly, that the behavioural response is primarily conditional on the function of *nan-iav* channels.

In **5.3.3** (**page 77**), I presented findings which show that white noise stimulus presentation elicits auditory-induced locomotor activity. This could seem at odds with previous studies that used mating chain and copulation analysis, which found white noise stimulus does not induce a behavioural response (Eberl et al., 1997; Schilcher, 1976a). Based on this, it can be assumed that sound with no courtship signal is capable of having a stimulating effect on *Drosophila* locomotor behaviour, yet be ineffectual at eliciting a courtship-specific response. This demonstrates that the behavioural readout of the assay presented in this chapter is not tied solely to courtship and is more of a broad auditory sensitivity test. Since the most optimal behavioural responses were elicited by courtship-specific stimuli, it still shows that there is a preference within the system. The activity readout in this assay is similar to previous findings demonstrating that pulse stimuli with a species-specific IPI induce largest behavioural responses, whereas divergence from this optimal IPI results in a gradient reduction in response (Zhou et al., 2015).

Playback of RCS stimuli resulted in increased auditory-induced locomotor activity compared to exposure to APT sound stimulus. Meanwhile, Kowalski et al (2004) did not detect any differences in response behaviour between pulse and courtship song stimulus. This discrepancy in the observations between Kowalski et al (2004) and the current work can be attributed to the mating state of the animal. As shown in **section 5.3.5** (**page 87**), mated males had larger increases in locomotor activity in response to RCS stimuli, whereas for virgin males the response magnitude to both stimuli was comparable. Within the work of Kowalski et al (2004), experimental flies were segregated at 4 hours post-eclosion and tested after 3 days. Typically, males need 12 hours to reach sexual maturity (Stromnaes, 1959). Thus, it can be assumed that the experimental flies used by Kowalski et al (2004) were virgins.

Collectively, these findings indicate that the mating state impacts the animal's sensitivity to the presented auditory stimulus. There are a number of factors which can contribute to these observations. Possibly, previous experience of courtship encounters primes the animals to only respond to more 'naturalistic' stimuli. Or mated animals are more sensitive to the sine component which is present in RCS stimuli. Similarly, the heightened locomotor response could be due to the unique interaction between the two song components within a natural courtship song. These factors are challenging to test but could be assessed by investigating auditory-induced locomotor activity in response to varying augmented RCS stimuli.

Both virgin and mated females showed significant locomotor increases in response to APT and RCS stimulus presentation. This response of females is, however ,significantly reduced compared to the auditory-induced locomotor activity observed in males. The magnitude of the female response is reminiscent of the behaviour induced by white noise stimulus in males. Drawing on this comparison, it is possible to speculate that the stimulating effect of the sound on females is a manifestation of general responsiveness to auditory stimuli rather than as a courtship signal.

Social interactions rely on a variety of sensory cues to inform behavioural output. It has been characterized that based on these signals, social space between the animals can increase, thus resulting in avoidance (Fernandez et al, 2014) or

decrease, resulting in grouping and aggregation (Parrish & Edelstein-Keshet, 1999). Playback of courtship song to groups of males has been shown to result in aggregation of flies interacting in exploratory courtship of nearby males (Eberl, 1997; Inagaki et al., 2010). There is a non-linear relationship between the number of males in a chamber and the number of courtship interactions as observed in chaining assays (Yoon et al., 2013).

This non-linearity was also observed within the current work. The locomotor response to sound stimuli was greater for males in grouped conditions. It cannot be verified with the current data, but it is possible that the grouped flies show chaining behaviour within the sampling tubes which results in this increase in activity amplitude. These findings support that other sensory modalities influence locomotor activity in response to playback of auditory courtship stimuli. For the mating chain assay, the optimal cohort number was found to be 6 (Yoon et al., 2013). Further work can investigate the range of responses for different population densities to find the optimal grouped number with largest responses to auditory stimuli within the behavioural assay presented within this chapter.

5.5 Critical analysis of method

This chapter has introduced and quantified the use of a new protocol to test auditory behaviour in *Drosophila*. Arguably, the greatest advantage of this method is that there is a direct readout of locomotor activity which does not involve interpretation. Quantifying locomotor activity through 'activity counts' (number of beam breaks) is a highly reproducible metric. Previous methods used to explore auditory sensitivity and auditory-induced behaviours rely on attributing points to observed courtship interactions (Eberl et al., 1997; von Schilcher, 1976). This method can lead to misinterpretation of interactions between flies to be falsely attributed to stimulus presentation thus making it prone to type I errors.

Nonetheless there are limitations to the auditory behavioural assay introduced in this chapter. Firstly, it does not capture the finer details in the responsiveness to stimuli. Perhaps a certain stimulus might not induce increases or decreases in locomotor activity, yet it might have an equally pronounced effect on behaviour. In

this case, output from this assay could suggest there is no effect leading to type II errors.

Secondly, there are many factors which contribute to auditory-induced activity. Hence, auditory-induced locomotor activity cannot be taken as a proxy for auditory sensitivity and processing. The effect of other sensory modalities other than auditory inputs cannot be excluded since, as has been shown in this chapter factors such as grouping and mating state influence the observed behavioural response. It is possible that some of the factors which modulate auditory-induced locomotor behaviour affect the function of the primary sensory organ, although further investigation by other means is necessary before validating these assumptions.

Thirdly, it is not possible to differentiate between auditory and courtship induced locomotor activity. Since it was found that flies respond to both white noise and courtship-specific signals, it is impossible to determine what is the underlying process which results in increases in locomotor activity. Further study using stimulus with the courtship signal removed by augmenting the IPI of the pulse train can extricate the auditory part of the signal from the courtship part. This could help distinguish between the contribution of the two underlying processes.

Fourthly, in this behavioural assay, the animal is freely moving inside the tubes, this makes it difficult to determine how much the animal can hear at any one point. Since the *Drosophila* antennal ear is a particle velocity sensor, it is highly direction and distance sensitive (Batchelor & Wilson, 2019). In effect, in the acoustic near-field, the particle velocity of the sound radiated by the *Drosophila* wing drops steeply by 18dB per doubling distance (Bennet-Clark, 1971). Furthermore, flagellar auditory organs are only optimally stimulated by sound sources from specific angles (Batchelor & Wilson, 2019). Taking these factors into account, it cannot be assumed that the sound stimulus is uniform for all sampled animals.

Finally, this assay does not capture naturalistic behaviour in response to auditory stimulus. The courtship stimulus is presented for lengthy periods throughout a number of experimental days. Hourly playback of courtship stimulus undoubtedly results in adaptation and changes in stimulus perception. Furthermore, animals

are wing-clipped which could affect their response to the stimulus. It is hard to quantify the effect of these but awareness of the advantages as well as the limitations of this assay could help with how this test can be best exploited in further study.

Chapter 6

Key modulators of auditory-induced locomotor behaviour

6.1 Introduction

6.1.1 Sensory modalities involved in courtship behaviours

Courtship behaviours are reliant on the integration of multiple sensory signals via different sensory modalities (Krstic, Boll, & Noll, 2009; von Schilcher, 1976). Wing clipped chemosensory mutants (*OrfD*) maintained in the dark show no courtship behaviours and no progeny (Gailey, Lacaillade, & Hall, 1986) demonstrating that inhibiting all sensory modalities in *Drosophila* (auditory, olfaction and vision) results in behavioural sterility. Inhibiting these sensory modalities individually has also been consistently shown to result in increased courtship duration and decreased success rate (Crossley & Zuill, 1970; Gailey et al., 1986; Manning, 1967; Rybak et al., 2002; von Schilcher, 1976). However, the relationship between the sensory pathways and their contribution to courtship interactions are hard to determine.

Since males play a more active role in the courtship ritual, most studies have focused on male behaviour. As established within this work already, exposure to auditory courtship signals induces behaviours that are not dependent on the presence of a female nor on visual input; demonstrating that auditory signals can independently induce behaviour (Boekhoff-Falk & Eberl, 2014; von Schilcher, 1976).

It has been hypothesised that signals from the visual pathway are redundant in courtship but allow the process to be more effective (Gailey et al., 1986). Mutants lacking input from photoreceptors and *Drosophila* kept in darkness demonstrate courtship behaviours when presented with a female. However, there is a change in locomotor behaviour in these flies since they compensate for the visual deficit by scanning the environment (Krstic, Boll, & Noll, 2009). Presenting isolated female fat bodies, which are known to be involved in the production of chemosensory signals, have also been shown to induce courtship behaviours (Jallon & Hotta, 1979; Tompkins, Hall, & Hall, 1980). Interestingly, mutants with chemosensory deficits display virtually no courtship behaviours in dark conditions indicating that integration of signals from the visual and olfactory pathway are crucial for the initiation of courtship behaviours (Krstic, Boll, & Noll, 2009).

Collectively, these findings demonstrate that presenting a courtship stimulus to each sensory modality independently readily provokes displays of courtship behaviours (Rings & Goodwin, 2019). However, it is also evident that there is integration between sensory inputs (visual and olfactory) that are required to trigger and sustain these behaviours. Conceivably there is a hierarchy to which sensory input is relevant at which point in the courtship ritual. The auditory pathway might play a differential role in courtship behaviour since this signal is an innate feedback behaviour which is relevant to the males' performance rather than a cue to seek out a partner. By independently manipulating the function of these sensory modalities, it is possible to make inferences regarding the interactions between these pathways.

6.1.2 A mechanosensory pathway to the clock

Within this thesis it has already been discussed that light and temperature sensory inputs are capable of synchronizing endogenous biological rhythms (Glaser & Stanewsky, 2005; Helfrich-Förster et al., 2001). Additionally, mechanosensory stimuli have also been shown to entrain the circadian clock (Simoni et al., 2014). Exposing *Drosophila* to 12-h vibration/no-vibration cycles has been found to induce shifts in behavioural and molecular rhythms to synchronize to the given mechanosensory stimuli (Simoni et al., 2014). This suggests that there is a

mechanosensory input pathway to the clock specifically for proprioceptive feedback which is capable of entrainment.

Mechanosensory processes underlies both auditory and proprioceptive feedback yet these sensory modalities can have a differing role within the clock. In *Drosophila* it has not been determined whether auditory signals can be used as an entrainment cue. However, work on other species has found that auditory feedback can regulate circadian rhythms. House sparrows showed shifts in their locomotor behaviour in response to playback of bird songs (Menaker & Eskin, 1966). Furthermore, it has been reported that core body temperature cycles in humans can be shifted with auditory cues (Goel, 2005).

Nevertheless, these findings should be examined with caution as there could be strong differences between and even amongst species. It is possible that the efficacy of a mechanosensory stimulus as a zeitgeber is based on the importance of the sensory modality. Furthermore, it is well documented that auditory cues can induce behaviours such as increases and decreases in locomotion (von Schilcher, 1976). This property of the mechanosensory stimulus to directly impact behaviour can result in an indirect influence on circadian rhythms. So, instead of the animal entraining directly to the mechanosensory stimulus, the effect arises through the stimulus having a concomitant effect on behaviour, with subsequent feedback driving changes to the clock.

6.1.3 Circadian modulation of mechanosensory processing

The interaction between mechanosensory processing and the circadian clock can be bi-directional. As well as there being a mechanosensory pathway to the clock; processing of mechanosensory stimuli can also be under circadian regulation. Self-sustained oscillations of key clock genes have been found to be maintained in isolated cultured antennae (Plautz, Kaneko, Hall, & Kay, 1997). Since many tissues also show rhythmic changes in function based on these molecular oscillations- this raises the question, of whether auditory function is also regulated by the circadian clock.

Multiple studies have shown that there is a change in the sensitivity to auditory stimuli throughout a 24-h cycle. In mice, it has been found that the amplitude of the fast motor reflex in response to sound stimuli shows circadian modulation (Basinou, Park, Cederroth, & Canlon, 2017). Additionally, diurnal changes in the startle response have also been observed in humans (Miller & Gronfier, 2006). Nonetheless, from these findings it is hard to determine whether there is a direct circadian change in auditory processing since changes in sensitivity to a given auditory stimuli can be due to higher function processing of the primary sensory input.

The behavioural assay presented in the previous chapter allows to observation of auditory-induced locomotor behaviour over prolonged periods of time. Thus, it is well placed to investigate its relationship to the circadian clock. Aside from determining whether there is circadian regulation of auditory-induced behaviours, the focus of this chapter is to explore other modulators of auditory-induced locomotor activity. Identifying these regulators of auditory-induced locomotor behaviour, firstly, gives insight into the interactions in higher order auditory processing and secondly, allows to speculate on the pathways involved in primary auditory function.

6.2 Methods

Drosophila melanogaster were tested on the auditory behavioural assay presented in **chapter 5**. Only male flies were used for the experiments outlined in this chapter. Experimental flies were wing clipped several days before experimental onset. The experimental flies were 7-12 days old on the first experimental day and flies were sampled in cohorts of 3 per tube. Each fly was only exposed to one experimental condition so all comparisons were done between different groups of flies. For further details on experimental setup, sound stimulus, other procedures and data analysis protocols, please refer to **chapter 4** (**page 46**).

6.2.1 Experiments relating to circadian regulation of sound-induced locomotor behaviour

As with all circadian studies investigating the locomotor activity patterns, the animals were exposed to a variety of environmental conditions which are described below.

6.2.1.1 Experiments under Light: Dark (LD) cycles

Within this environmental condition, wild-type *Canton-S* flies were exposed to a 12-h light, 12-h dark (LD) cycle. The LD cycle during the experiment was aligned with the previous entrainment regime during rearing of the animals. The temperature was kept at a constant 25°C.

6.2.1.2 Experiments under Dark: Dark (DD) cycles

Within this environmental condition, wild-type *Canton-S* flies were placed into constant darkness for the duration of the experiment. The first day of constant darkness was on the first experimental day. Prior to the experiment, flies within this condition were kept in an LD regime. The temperature was kept at a constant 25°C.

6.2.1.3 Experiments under Light: Light (LL) cycles

Drosophila kept in constant light show arrhythmic behaviour and demonstrate a breakdown of the molecular clock, which is essential for circadian function (Marrus et al., 1996). This process has been reported as gradual and to fully impair the clock, flies need to be exposed to constant light over a number of days (Emery, Stanewsky, Hall, & Rosbash, 2000). Thus, in this environmental condition, Canton-S flies were kept in constant light over several generations and during the experiment. The temperature was kept at a constant 25°C.

6.2.2 Fly strains

Glass₆₀ⱼ flies lacking all major external visual input structures, were tested in the auditory behavioural assay. *Glass* encodes a transcription factor essential for the formation of the fly's visual system. The phototransduction machinery in external photoreceptor cells, ocelli and primary and secondary photoreceptor cells is missing a homozygous loss-of-function allele for the *glass* gene (Moses, Ellis, & Rubin, 1989). *Glass₆₀ⱼ* mutants are known to lack all retinal eye structures as well as the H-B eyelets (Helfrich-Förster, Winter, Hofbauer, Hall, & Stanewsky, 2001).

The *per₀₁* strain is a null mutant of the *per* gene, which is fully arrhythmic in its behaviour and molecular oscillators that regulate the circadian cycle (Konopka & Benzer, 1971a). The oscillatory behaviour observed in wild-type flies in entrainment and freerun conditions is abolished in *per₀₁* mutants. The locomotor behaviour of these flies can mimic that of wild-type flies when observed under an LD cycle, which enforces behavioural rhythmicity (Wheeler et al., 1993a). To prevent this interference, for all the data presented within this chapter, *per₀₁* flies were tested in DD conditions. The *per₀₁ W+* strain rather than *per₀₁ YW* was used for the behavioural experiments since *per₀₁ W+* is in a *Canton-S* genetic background. Thus, the *Canton-S* wild-type strain was taken as control

6.3 Results

6.3.1 Changes in baseline and auditory-induced locomotor activity over a 24-h period

Observing the behaviour in the auditory behavioural assay over a two-day period, both baseline and auditory-induced locomotor activity showed changes throughout a circadian day. Raw behavioural data was analysed in accordance with the protocol described in **methods 4.6.4 (page 62)** to maintain a time component in the recorded data.

6.3.1.1 Baseline rhythms

Robust locomotor rhythms were observed in the baseline activity of wild-type flies in entrainment conditions (**Fig 37A**). The highest baseline activity was observed at ZT12 whereas the lowest activity was at ZT6 for both experimental days. For the first experimental day, the median activity at baseline at ZT6 was 175 whereas at ZT12 there was a >5-fold increase in median baseline activity to 999 [Z=6.735, p<0.001, Wilcoxon Rank Sum test] (**Fig 37B**). For the second experimental day, the difference in median baseline activity between the time points was maintained [ZT6: 162, ZT12: 881, Z=7.178, p<0.001, Wilcoxon Signed Rank test]. There was also a peak in baseline activity around the morning light transition, however this increase in activity was not as prominent as the evening activity peak.
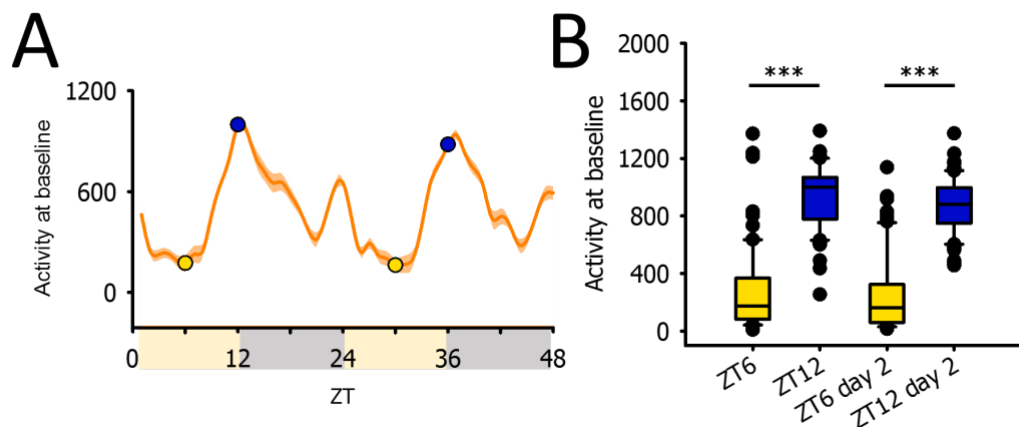
Figure 37: Line and box plots to show the changes in median baseline activity throughout a 48-h cycle in LD conditions.
A: An actogram to show the median baseline activity of male wild-type flies in LD conditions over two consecutive experimental days (n=70). **B:** Box plot to show the activity at baseline for two points within a 24-h cycle which were determined as having the lowest and highest levels of activity. The differences between ZT6 (lowest point of baseline activity) and ZT12 (highest point of baseline activity) were found to be significantly for both experimental days.

These observed changes in baseline locomotor activity are in line with previous reports on circadian activity patterns in *Drosophila* (Klarsfeld et al., 2003; Rosato & Kyriacou, 2006). This validates the use of activity at baseline as a reliable readout of endogenous locomotor activity. Additionally, this demonstrates that hourly sound stimulus exposure does not impact the basic circadian patterns of locomotor activity.

6.3.1.2 Auditory-induced locomotor rhythms

Baseline subtracted activity provides an accurate representation of auditory-induced locomotor activity normalised to baseline. This response activity was also found to change throughout a 24-h cycle (**Fig 38A**). Similar to activity at baseline, lowest baseline subtracted activity was observed at ZT6. To assess whether this trough in baseline subtracted locomotor activity is significant, the activity at ZT6 was compared to the higher levels observed at ZT19. The mean baseline subtracted activity at ZT6 was 99 ± 313 which was found to be significantly lower compared to the activity observed at ZT19 494 ± 334 [t(69)= -4.859, p<0.0001, Paired t-test] (**Fig 38B**). This difference between the time points was as robust on the second experimental day [ZT6: 200 ± 331, ZT19 587 ± 468, t(69)= -5.599, p<0.0001, Paired t-test].
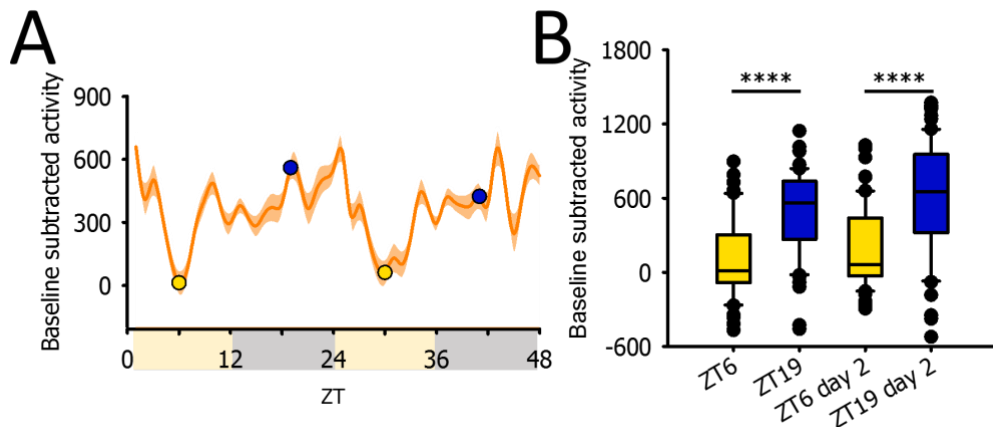
Figure 38: Line and box plots to show the changes in median baseline subtracted locomotor activity in response to APT stimulus throughout a 48-h cycle in LD conditions.
A: An actogram to show the median baseline subtracted activity in response to APT stimulus of male wild-type flies in LD conditions over two consecutive experimental days (n=70). **B:** Box plot to show the baseline subtracted locomotor activity for two points within a 24-h cycle which were determined as having the lowest and highest levels of activity. The differences between ZT6 (lowest point of baseline activity) and ZT19 (highest point of baseline activity) were found to be significantly for both experimental days.

These findings demonstrate that there is modulation of auditory-induced locomotor activity, however the data is inherently noisy. To account for the noise, I applied a simple moving average to the data with a 3-hour time window to smooth the data (**Eq. 4**).

Equation 4: Formula for a simple moving average applied to smooth behavioural data

$$SMA = \frac{A_1 + A_2 + .. A_n}{n} \qquad (4)$$

The purpose of this was to allow to focus on the broader pattern rather than to be distracted by the finer changes within the data. It is possible that these finer variabilities in the signal are underpinned by biological processes, but this was considered unlikely and out of the scope of this project.

The rest of the data presented within this chapter has been smoothed with a moving average to reduce the presence of noise in the signal.

6.3.2 Baseline & auditory-induced locomotor activity characterised by a single or dual sinusoidal function

Least squares regression of a sinusoidal function can be used to characterise the best fit parameters quantifying the periodicity and amplitude of oscillatory behaviour over a given time course. The raw behavioural output from the auditory behavioural assay was processed using the protocol in the **methods 4.6.4 (page 62**) to maintain the time component and sinusoidal functions were fitted to this data to better characterise the observed periodic behaviour.

Two primary sinusoidal functions were used:

Equation 5 & 6: Single & dual 4 parameter sinusoidal functions fitted to baseline and auditory-induced locomotor activity.

$$f(t) = y0 + A sin\left(\frac{2\pi}{T}t + C\right) \qquad (5)$$

or

$$f(t) = y0 + A1 sin\left(\frac{2\pi}{T1}t + C1\right) + y02 + A2 sin\left(\frac{2\pi}{T2}t + C2\right) \qquad (6)$$

Equation 5 is a single term sinusoidal function. *y0* is the constant displacement of the function, *A* denotes the amplitude of the waveform, *T* determines the periodicity of the oscillation and *C* is the phase offset of the waveform. As with all trigonometric fits, these parameters stay constant over time.

Equation 6 is a dual term sinusoidal function. This function consists of two sinusoidal waveforms in series. The same parameters were used as for equation 6 but since two sine waves in series have independent coefficients, *y01, A1, T1, C1* characterise the properties of the first sine wave; *y02, A2, T2 and C2* characterise the properties of the second sine wave.

The harmonics of the activity data can be modelled by a single or dual-term sinusoidal equation. Undoubtedly, increasing the complexity of a model allows for a better fit yet, this risks fitting to the noise. The Akaike information criterion corrected for small samples (AICc) was used to inform model selection not only based on goodness of fit, but also adjusted for model complexity. AICc estimates the information loss through fitting with consideration of those factors, so the lower the AICc value, the better the relative quality of the model. Consequently, for each metric and condition, both models were fitted to a small representative sample and the AICc values were compared to determine which model is best applied to the median activity. If one model was associated with significantly lower AICc values, that model was selected.

Table 10: Summary table to show which sinusoidal model was fitted to which measure.

	LD	DD	LL
Baseline activity	Dual-term function	Dual-term function	Dual-term function
Baseline subtracted activity	Dual-term function	Single-term function	Dual-term function
Activity gain	Single-term function	Single-term function	Single- erm function

Reported alongside the parameters for the fits is the R^2 coefficient of determination. This measure describes how well the regression model fits the data. The closer R^2 is to 1, the better the independent variables predict the dependent variables. Generally, within the field a R^2= 0.95 or above is considered a good fit. However, since the regression fitting of the sinusoidal function was done to gain insights on the relationship between the variables, lower levels of R^2 were tolerated.

Lastly, the coefficient which determines phase in the sine function can provide valuable information about locomotor behaviour in this instance, this parameter is

not reported since a running average was applied to the data prior to fitting and would skew this outcome. Additionally, it is unknown how to best interpret circadian phase when these multiple frequency components can themselves be misaligned relative to one another.

6.3.2.1 Baseline activity in LD, DD & LL environmental conditions

Figure 39: Time series plots to show the baseline activity of male wild-type flies in LD, DD and LL conditions overlaid with a sinusoidal regression fit.

Sinusoidal fits to the baseline locomotor activity in different environmental conditions. **A** & **B** show the median baseline locomotor activity of wild-type flies in LD overlaid with a dual sinusoidal function. **C** & **D** show the median baseline locomotor activity of wild-type flies in DD overlaid with a dual sinusoidal function. **E** & **F** show the median baseline locomotor activity of wild-type flies in LL also fitted with a dual sinusoidal function. The left column shows the baseline activity recorded in APT stimuli conditions and the right shows the baseline activity recorded in RCS stimulus conditions.

Table 11: Table to summarise the *A* and *T* parameters from the regression fits for baseline activity of male wild-type flies in LD, DD and LL conditions.

	APT				RCS			
	1st Oscillation		2nd Oscillation		1st Oscillation		2nd Oscillation	
	A1 (amplitude)	*T1 (period in h)*	*A2 (amplitude)*	*T2 (period in h)*	*A1 (amplitude)*	*T1 (period in h)*	*A2 (amplitude)*	*T2 (period in h)*
LD	236.37	24.05	191.19	12.09	252.1	24.71	207.4	11.7
DD	257.4	24.33	148.64	12.06	287.64	22.9	1566.77	274.83
LL	459.56	69.93	302.48	51.31	1244.94	245.39	90.71	28.05

Light/Dark (LD) conditions

There are many lines of evidence to show that the locomotor activity of *Drosophila* is best characterised as a dual-oscillator (Helfrich-Förster, 2000, 2001). Baseline activity of entrained wild-type flies was fitted with both sinusoidal functions and in support of this premise, the AICc values for the dual-term model was 236.97 ± 15.99, which was significantly lower compared to the single-term model 248.81 ± 11.72 [t(7)=2.806, p=0.0263, Paired t-test]. Consequently, the dual-term model (**Eq. 6**) was applied to the median baseline activity of animals in LD conditions.

For LD conditions, the fit to baseline activity resulted in an R^2 value of 0.952 and 0.947 for APT and RCS respectively. The oscillatory baseline activity in these two stimulus conditions had similar periods and amplitudes. In APT conditions, a 24.05-h period was associated with a larger 236.37 amplitude, this is aligned to the evening peak. Another 12.09-h periodicity was associated with a smaller 191.19 amplitude (**Fig 39A, Table 11**). This characterises the morning peak. For RCS conditions, the larger amplitude of 252.1 was associated with a 24.71-h periodicity and a smaller peak had an amplitude of 207.4 was associated with a 11.7-h oscillation (**Fig 39B**).

Constant darkness (DD) conditions

DD conditions are associated with a decrease in morning activity peak (Helfrich-Förster, 2000). Despite this, comparing the AICc values for the two sinusoidal models, suggests that the dual sinusoidal model is a better predictor of the baseline activity [single term model: 247.16 ± 13.45; dual-term model: 235.05 ± 11.55, t(7)=2.411, p=0.046, Paired t-test]. Since the AICc was significantly lower, the dual-term function was fitted to baseline activity in DD conditions (**Eq. 6**).

The R_2 value for the fit to baseline activity was 0.953 for APT and 0.887 for RCS. Similar to the activity pattern in LD conditions, for APT a larger 257.4 amplitude peak was found to have a 24.33-h period which describes the evening peak whereas a smaller 148.64 amplitude peak was associated with a 12.06-h period describing the morning activity peak (**Fig 39C**).

When comparing baseline activities between LD and DD conditions, the diminished amplitude of the morning peak demonstrates the effect of DD conditions on the behavioural activity patterns. In LD conditions, the 12-h frequency peak was associated with 191.19 whereas in DD this dropped to 148.64.

For RCS, the larger 294.92 amplitude peak had a periodicity of 22.83-h. However, the second sinusoid did not show reliable fit parameters. It can be hypothesized that due to the inhibitory effect of DD on the morning activity peak, the second oscillation is no longer detectable in the fit. Alternatively, the fit is impaired by the slight baseline drift in the data (**Fig 39D**).

Constant light (LL) conditions

The baseline activity pattern of LL flies appears arrhythmic on visual inspection. To ensure there is no underlying periodicity, the dual-term sinusoidal function was fitted to the baseline activity of wild-type flies in LL conditions (**Eq. 6**).

The resulting R_2 was 0.925 and 0.885 for APT and RCS respectively. As shown in **Table 11**, the periodicity of the baseline activity waveforms did not reveal any potential for biologically relevant frequencies. This finding suggests that the

baseline activity of wild-type flies in LL is arrhythmic and had no circadian oscillations (**Fig 39 E&F**).

In summary, these findings show that in LD, there are prominent evening and morning activity peaks in baseline activity. The morning peak is diminished in freerun conditions and in LL, the baseline locomotor activity becomes arrhythmic. The observed changes in baseline activity between the different environmental conditions are consistent with previous reports (Helfrich-Förster, 2001; Wheeler, Hamblen-Coyle, Dushay, & Hall, 1993b)

6.3.2.2 Auditory-induced locomotor activity in LD, DD & LL environmental conditions

To characterise the oscillatory behaviour of the response to sound stimuli, the baseline subtracted activity in varying environmental conditions was calculated using the protocol in **methods 4.6.4.** This data was then fitted with a sinusoidal model.

Light/Dark (LD) conditions

For entrained conditions, the AICc was significantly lower for the dual-term sinusoidal model 505.65 ± 18.82 compared to the single term model 514.61 ± 18.56 [$t(7)$=5.394, $p<0.01$, Paired t-test]. So, the dual sinusoidal function was fitted to baseline subtracted activity of wild-type flies in LD (**Eq. 6**).

For APT, the fit had an R^2 value of 0.791. One of the oscillatory processes was found to have a 22.35-h cycle with an amplitude of 138.35. The second oscillation with a 12.235-h periodicity had an amplitude of 98.799 (**Fig 40A**).

A similar frequency pattern was observed for the RCS locomotor responses. The fit to RCS baseline subtracted locomotor had an R^2 value of 0.855. A 164.23 amplitude peak had a 23.01-h periodicity and another 11.87-h oscillatory process was associated with a 53.54 amplitude peak (**Fig 40B**).
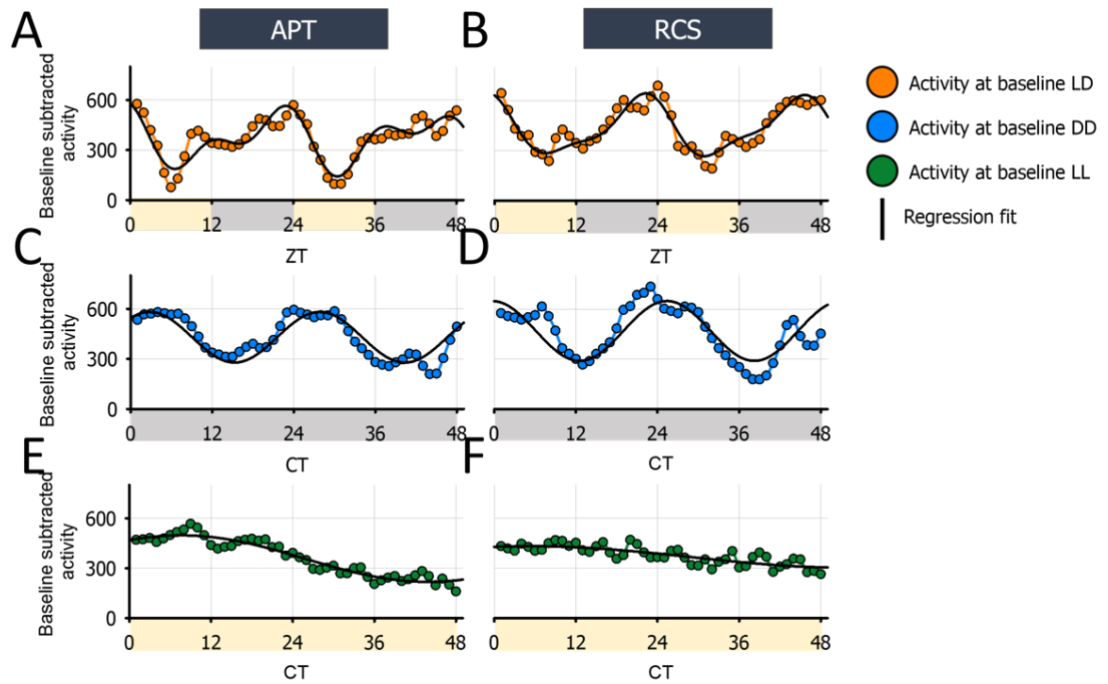
Figure 40: Time series plots to show the auditory-induced baseline subtracted locomotor activity of male wild-type flies in LD, DD and LL conditions overlaid with a sinusoidal regression fit.

Sinusoidal fittings to the auditory-induced locomotor activity in different environmental conditions. **A** & **B** show the median baseline subtracted locomotor responses of wild-type flies in LD overlaid with a dual sinusoidal function. **C** & **D** show the median baseline subtracted locomotor responses of wild-type flies in DD overlaid with a single sinusoidal function. **E** & **F** show the median baseline subtracted locomotor responses of wild-type flies in LL also fitted with a dual sinusoidal function. The left column shows the baseline activity recorded in APT stimuli conditions and the right shows the baseline activity recorded in RCS stimulus conditions.

Table 12: Table to summarise the *A* and *T* parameters from the regression fits to baseline subtracted activity of wild-type flies in LD, DD and LL conditions.

| | APT | | | | RCS | | | |
| | 1st Oscillation | | 2nd Oscillation | | 1st Oscillation | | 2nd Oscillation | |
	A1 (amplitude)	T1 (period in h)	A2 (amplitude)	T2 (period in h)	A1 (amplitude)	T1 (period in h)	A2 (amplitude)	T2 (period in h)
LD	138.346	22.35	98.8	12.24	164.23	23.01	53.54	11.87
DD	151.783	25.03			179.48	25.67		
LL	139.497	72.59			94.19	64.71		

Constant dark (DD) conditions

Baseline subtracted activity in DD conditions was found to be better characterised by a single sinusoidal function (**Eq. 5**). There was no significant differences between AICc values for the single and dual term sinusoidal models [single-term function: 248.88 ± 13.01; dual-term function: 248.55 ± 14.51, t(12)=0.223, p=0.83, Paired t-test]. Since the AICc values were so similar between the two fits, the simpler single term function was used as there was no significant advantage of applying the dual-term model.

The fitting of a single sinusoidal function to APT baseline subtracted locomotor responses resulted in a R_2 of 0.79. The response behaviour had a 25.03-h periodicity associated with a 151.78 amplitude (**Fig 40C**). The fit to RCS baseline subtracted locomotor responses had an R_2 of 0.677. This oscillation had a periodicity of 25.67-h and an amplitude of 179.48 (**Fig 40D, Table 12**).

Constant light (LL) conditions

As with baseline activity, baseline subtracted activity for both sound stimuli did not show periodic changes in LL conditions. As shown in **Table 12**, there was no circadian periodicity evident in the fitting to this data.

Shown in **Figure 41** is a comparison of the fits between the three environmental conditions. It is evident that the periods of baseline subtracted activity were widened in DD conditions in comparison to LD. Additionally, a reduction of the activity amplitude during the light phase of an LD cycle was observed which falls below the amplitude of DD activity amplitude.

In conclusion, these findings demonstrate that the baseline subtracted auditory-induced locomotor activity shows periodic changes in magnitude which is confined to a specific temporal pattern. The periodic changes in LD conditions are best characterised by a dual oscillator model whereas in DD, a single oscillator is a better determinant of the response behaviour. Furthermore, this auditory-induced behaviour is arrhythmic in LL conditions. Since 24-h oscillatory behaviour was observed in LD and DD conditions and was then abolished in LL (**Fig 41**), these

findings suggest that auditory-induced locomotor behaviour shows circadian modulation.
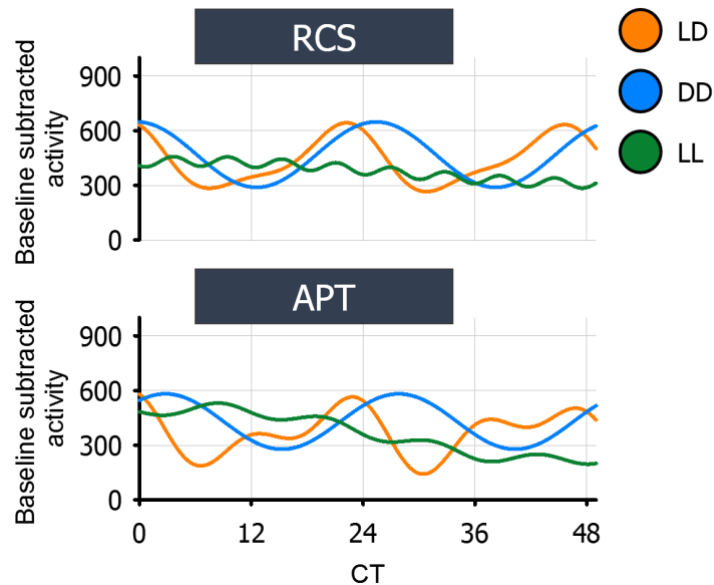
Figure 41: Sinusoidal fits of baseline subtracted activity in response to APT & RCS stimuli for male wildtype flies in LD, DD and LL conditions.
Regression fits to the baseline subtracted locomotor activity to show the differences in the response properties amongst the different environmental conditions.

6.3.2.3 Circadian changes of relative responsiveness to auditory stimuli

Activity gain is the relative change in locomotor activity in response to sound stimuli. The activity gain in varying environmental conditions was calculated using the protocol in **methods 4.6.4.** Fitting a sinusoidal function allowed to characterise the oscillatory properties of this response.
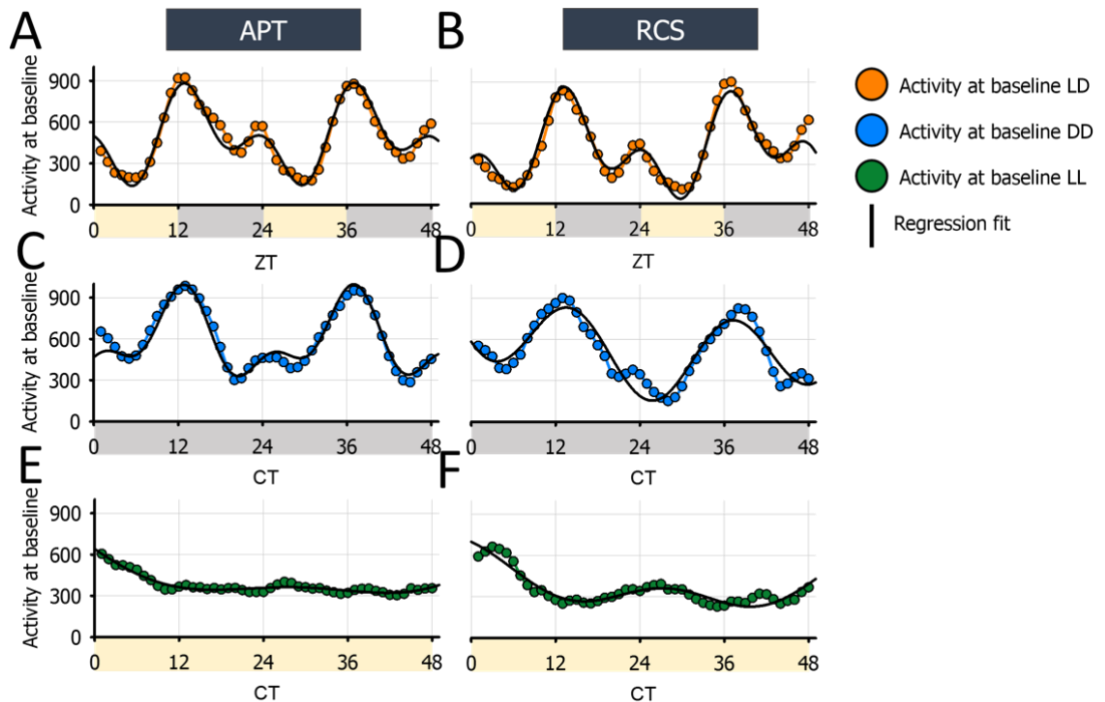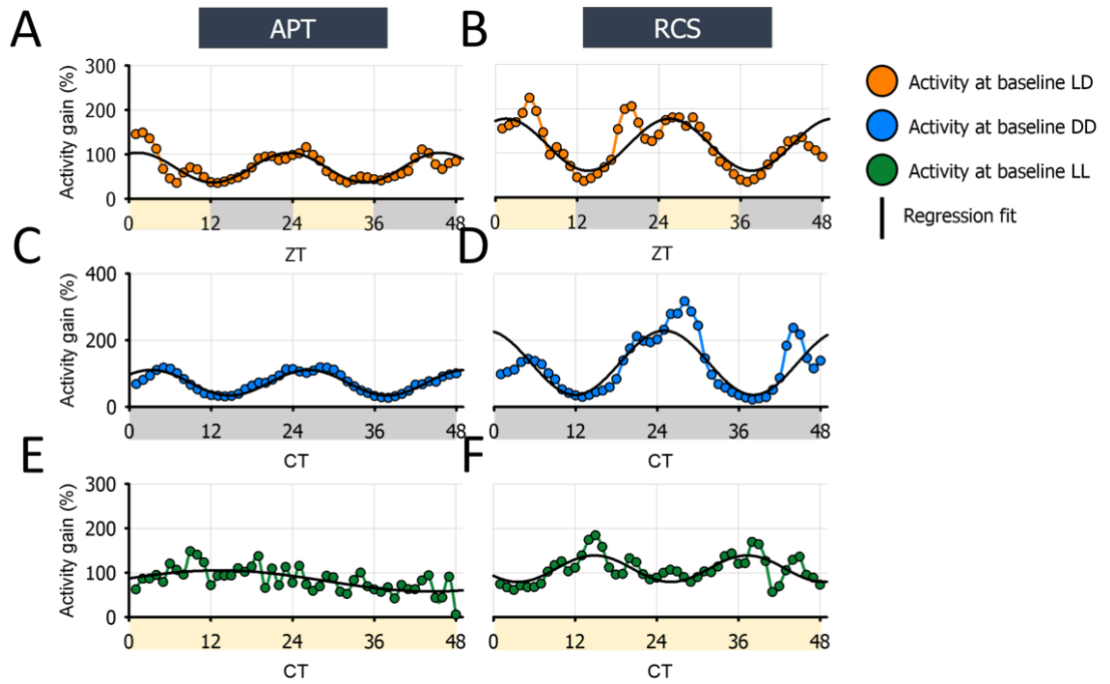
Figure 42: Time series plots to show the auditory-induced activity gain of male wild-type flies in LD, DD and LL conditions overlaid with a sinusoidal regression fit.
Sinusoidal fittings to the auditory-induced locomotor activity in different environmental conditions. **A** & **B** show the median auditory-induced activity gain of wild-type flies in LD overlaid with a single sinusoidal function. **C** & **D** show the median auditory-induced activity gain of wild-type flies in DD overlaid with a single sinusoidal function. **E** & **F** show the median auditory-induced activity gain of wild-type flies in LL also fitted with a single sinusoidal function. The left column shows the baseline activity recorded in APT stimuli conditions and the right shows the baseline activity recorded in RCS stimulus conditions.

Light/Dark (LD) conditions

Fitting a single and dual-term function to the activity gain of wild-type flies in LD conditions, there was no significant differences between the AICc values [single-term model: 31.78 ± 56.88; dual-term model: 32.88 ± 57.36, t(7)= -0.784, p=0.46, Paired t-test]. Since there was no advantage to using the dual-term sinusoidal function, the single-term model was applied to the activity gain (**Eq. 5**).

The fit to APT activity gain had an R_2 of 0.663. The activity gain for APT conditions showed a 22.24-h oscillation of a 33.5% amplitude (**Fig 42A**). For RCS the R_2 was 0.629. A 24-h oscillation was associated with a 58.6% amplitude peak (**Fig 42B**).

These findings demonstrate that there is ~24-h modulation of activity gain in response to sound stimuli in LD conditions.

Table 13: Table to summarise the A and T parameters from the regression fits to the activity gain of male wild-type flies in LD, DD and LL conditions.

	APT		RCS	
	1st Oscillation		1st Oscillation	
	A (amplitude in %)	*T (period in h)*	*A (amplitude in %)*	*T (period in h)*
LD	33.5	22.24	58.6	24
DD	38.3	23.11	96.4	26.15
LL	23.8	62.25	29.8	22.46

Constant dark (DD) conditions

The single oscillator function was also found to best characterize the activity gain in freerun conditions (**Eq. 5**). There were no significant differences between the AICc values for single and dual-term sinusoidal model [single term model: 24.42 ± 33.75; dual-term model: 24.85 ± 34.75, t(7)= -0.173, p=0.87, Paired t-test].

The fit to APT activity gain had an R_2 of 0.862. The oscillatory pattern had a 23.11-h periodicity and an amplitude of 38.3% (**Fig 42C**). For RCS, the fit had an R_2 of 0.641. The period of 26.15-h which was associated with a 96.4% amplitude (**Fig 42D**).

Constant light (LL) conditions

A single term sinusoidal function was also fitted to the activity gain in LL conditions (**Eq. 5**). Similar to other measurements in constant light, the periodicity of the fit did not correspond with biologically relevant oscillations for APT (**Fig 42E, Table 13**). For RCS, the period of the oscillation was found to be 22.46-h (**Fig 42F**). Despite this being within the biological range, there are a number of factors which suggest this is an artefact rather than circadian oscillatory behaviour. Firstly, this frequency is associated with a very low amplitude, suggesting that this behaviour is part of the noise floor. Secondly, the activity gain in APT conditions shows a period of 62.25-h. This disparity between the two stimulus conditions raises questions. Apart from changes in response magnitude, this period only indicates baseline drift. Thus, it was considered that this was a fitting to noise artefact.

6.3.3 Loss of rhythmic auditory-induced locomotor activity in *per₀₁* mutants

Similar to wild-type flies, *per₀₁* mutants show increases in locomotor activity in response to APT stimulus presentation (discussed further in **6.3.4 page 127**). The baseline activity of this mutant recorded within the behavioural assay is distinctly different to wild-type. In DD conditions, this mutant lacks the sinusoidal 24-h activity pattern observed in wild-type flies in equivalent environmental conditions.

To assess whether the *per₀₁* mutants display oscillatory response behaviours to sound stimuli, baseline subtracted activity and activity gain were calculated using the protocol described in **methods 4.6.4** which was then fitted with a sinusoidal function. Since it was determined that baseline subtracted and activity gain of wild-type flies in DD conditions is best characterised using the single sinusoidal function (**Eq. 5**), the same approach was taken here, since the mutant flies were in the same environmental conditions.

Fitting the single sinusoidal function (**Eq. 5**) to the baseline subtracted activity resulted in an R^2 of 0.467 (**Fig 43A**). A 9.82-h periodicity was associated with a 62.21 amplitude peak (**Table 14**). It is evident that *per₀₁* mutants show arrhythmic response behaviour similar to the responses of wild-type flies kept in constant light conditions.

Performing the regression fit to the activity gain had a lower R^2 of 0.36 (**Fig 43B**). A 9.71-h period was associated with a 11.9% amplitude peak (**Table 14**).

These outcomes demonstrate that the auditory-induced locomotor activity of *per₀₁* does not show circadian rhythmicity. The absence of this cycling within these mutants and wild-type flies in constant light suggests that the rhythmic response behaviour observed in wild-type flies in LD and DD conditions is mediated by the circadian clock.
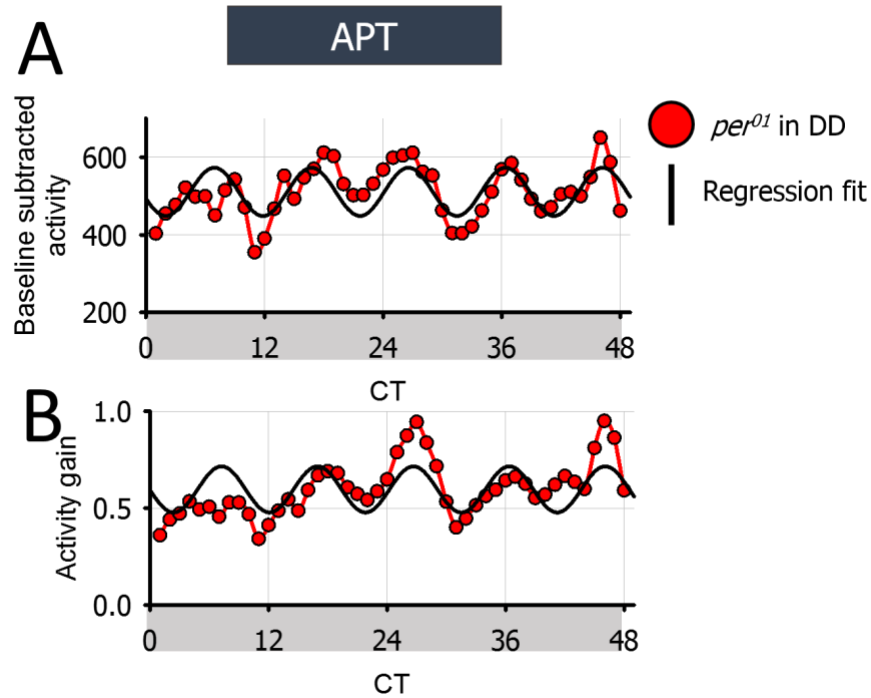
Figure 43: Time series plots to show the baseline subtracted and activity gain of male *per01* mutants in DD conditions overlaid with a sinusoidal regression fit.
A: Shows the median baseline subtracted activity of *per01* mutants over a 48-h period with a single sinusoidal function overlaid. B: Shows the median activity gain for *per01* mutants over a 48-h period with a single sinusoidal function fitted on top. Both traces show high frequency, low amplitude changes in behaviour over the given time period. The measured data is in response to APT sound stimulus presentation.

Table 14: Table to summarise the *A* and *T* parameters from the regression fits baseline subtracted activity and activity gain of male *per01* mutants.

	per01 response to APT stimulus in DD conditions	
	1st Oscillation	
	A (amplitude)	*T (period in h)*
Baseline activity	1629.66	439.99
Baseline subtracted activity	62.21	9.82
Activity gain (%)	11.9	9.71

6.3.4 Loss of rhythmic auditory-induced behaviour in wild-type flies in response to white noise (WN) sound stimulus

The findings from the previous sections of this chapter suggest that auditory-induced locomotor activity rhythmicity is clock-dependent. Both APT and RCS stimuli encode courtship signals. To probe whether this circadian rhythmicity of

auditory-induced locomotor activity is specific to courtship signals; wild-type flies response behaviour to WN stimulus was investigated in a circadian context. The raw data collected from the auditory behavioural assay for this sound condition was processed using the protocol described in **methods 4.6.4.** Following this, a sinusoidal function was fitted to the activity data to characterize the periodicity and amplitude of the response.

Table 15: Table to summarise the *A* and *T* parameters from the regression fits to baseline, baseline subtracted activity and activity gain of male wild-type flies in response to WN stimulus.

	WN			
	1st Oscillation		2nd Oscillation	
	A1 (amplitude)	T1 (period in h)	A2 (amplitude)	T2 (period in h)
Baseline activity	254.31	22.73	175.85	12.13
Baseline subtracted activity	48.48	1.636E-004	441.34	371.31
Activity gain (%)	1.05	202.16		

Since WN flies were in LD conditions, a dual-term sinusoidal function was fitted to the data (**Eq. 6**). Fitting the function resulted in a R^2 of 0.939. The model picked up both morning and evening oscillatory peaks in baseline activity. A larger amplitude of 254.31 was associated with a 22.73-h period peak which characterised the evening activity and a smaller 175.85 amplitude peak was associated with a 12.13-h period (**Fig 44A, Table 15**). These findings demonstrate that the WN stimulus does not affect the circadian pattern of baseline activity.

Visually inspecting the pattern of response behaviour to WN, baseline subtracted activity had no discernible rhythmicity. Fitting the dual sinusoidal function to baseline subtracted activity resulted in an R^2 of 0.481. The fit did not pick up any biologically relevant oscillatory patterns within the signal (**Fig 44B**). Equally, the activity gain also did not show any rhythmic properties (**Fig 44C**).

These findings indicate that the auditory-induced locomotor activity in response to WN stimulus does not show circadian rhythmicity. This is in contrast to the rhythmic response behaviour observed in wild-type flies presented with APT and RCS stimulus. Collectively, these findings suggest that the rhythmic modulation of

response behaviour is specific to reception of auditory courtship signals.
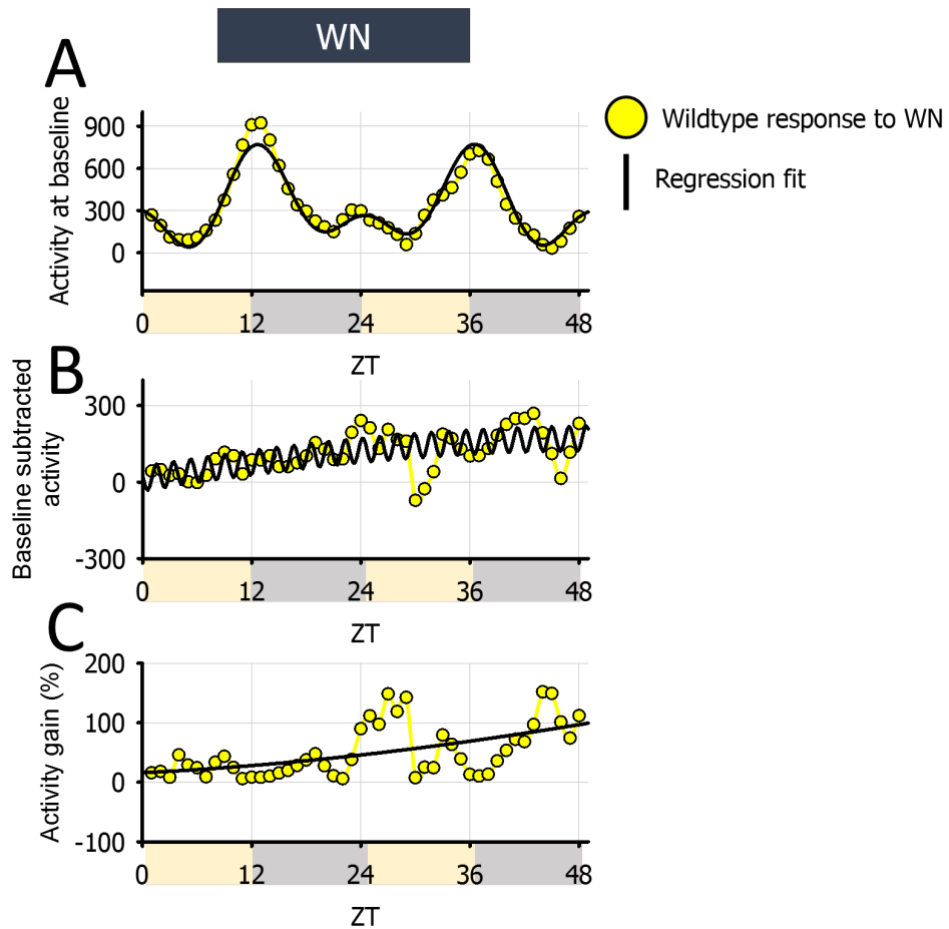
Figure 44: Time series plots to show baseline, baseline subtracted and activity gain of wild-type flies in LD conditions in response to WN stimulus; overlaid with a sinusoidal regression fit.
A: Shows the median baseline activity of wild-type flies over a 48-h period with a dual sinusoidal function overlaid. **B:** Shows the median baseline subtracted activity in response to WN over a 48-h period with a dual sinusoidal function fitted on top. **C:** Shows the median activity gain of wild-type flies in response to WN stimulus overlaid with a single sinusoidal function fit.

6.3.5 Comparison between baseline & auditory-induced locomotor activity rhythms

From the findings in the previous sections, it is evident that there are multiple oscillatory processes present in the activity measured within the auditory behavioural assay. By plotting the sinusoidal fits generated to the original behavioural data, it was possible to compare the differences in the oscillatory pattern between activity at baseline, baseline subtracted activity and activity gain.

121
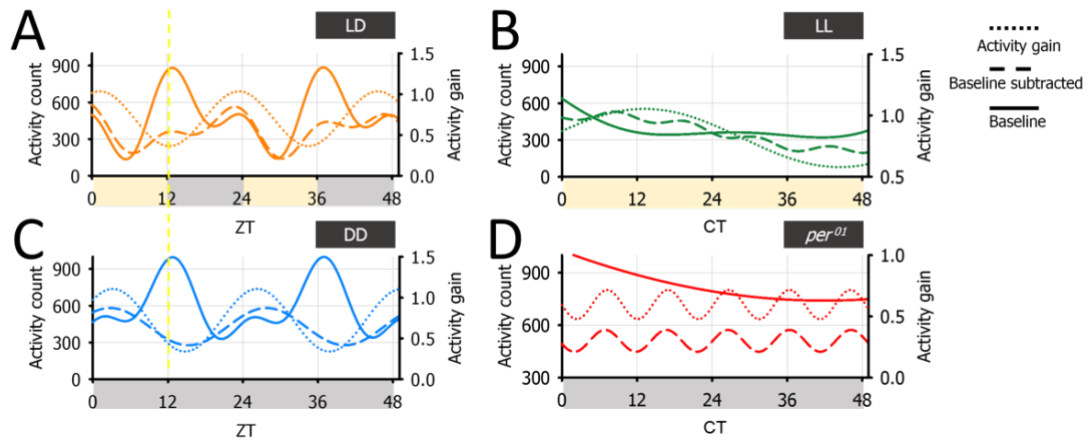
Figure 45: Sinusoidal fits plotted on a time series to compare the differences in periodicity in baseline, baseline subtracted activity and activity gain in male wild-type flies in LD, DD, LL conditions and *per01*.
A: A 48-h time series to show the derived sinusoidal fits from the baseline and auditory-induced activity of wild-type flies in LD. The graph shows baseline, baseline subtracted activity and activity gain superimposed. **B:** Shows the same measurements for the flies in constant light, **C** For DD conditions and **D** shows the fits for *per01* mutants. The peaks of the auditory-induced locomotor behaviour appear antiphase compared to baseline activity peaks in LD (**A**) and DD (**C**), whereas the circadian periodicity is lost in LL (**B**) and *per01* (**D**) conditions. All the sinusoidal fittings are derived from the responses to APT sound stimulus.

The most prominent peak in both baseline subtracted activity and activity gain is around the morning light transition (ZT24, dark-to-light transition) in LD and DD conditions (**Fig 45 A&C**). This indicates that flies in LD and DD conditions are most responsive to sound stimuli around this time window. Additionally, activity at baseline and auditory-induced locomotor activity is arrhythmic in LL conditions and *per01* mutants. Both these conditions show deficits in clock function whereby there are no molecular oscillations of the core molecular clock components; suggesting that the inhibition of activity cycling is due to the inhibition of the clock (**Fig 45 B&D**).

By assessing which model best characterised the behaviour for the different activity readouts, it is possible to make inferences about the number of oscillatory processes underlying the behaviour. Since baseline activity was best modelled by a dual sinusoidal function in LD and DD conditions, this indicates that there are two underlying oscillatory processes. This assumption is complementary to previous findings which determined that there are different molecular structures which underlie the regulation of the morning and evening activity peaks (Helfrich-

Förster, 2000).

Interestingly, the baseline subtracted activity was found to best be modelled by a dual-term sinusoidal function for measurements in LD conditions and a single term function for freerun conditions (**Fig 45 A&C**). From this it can be inferred that there are two oscillatory processes within response behaviour in entrained conditions and only one remains in freerun. Since the only disparity between LD and DD experimental conditions is the presents of a light phase in the LD condition, it can be assumed that the second oscillatory process with a 12-hourly periodicity is mediated by exposure to environmental light.

The activity gain for all environmental conditions was best modelled by a single term sinusoidal function. This suggests that there is one oscillatory process captured within this activity measurement. The activity gain is the relative change in auditory-induced locomotor activity. It can be hypothesised that this metric provides a more robust measure of the changes in the auditory processing of the auditory signal. Given the ~24-h periodicity of the activity gain in LD and DD conditions, it can be hypothesised that the process underlying this behaviour is also under circadian control.
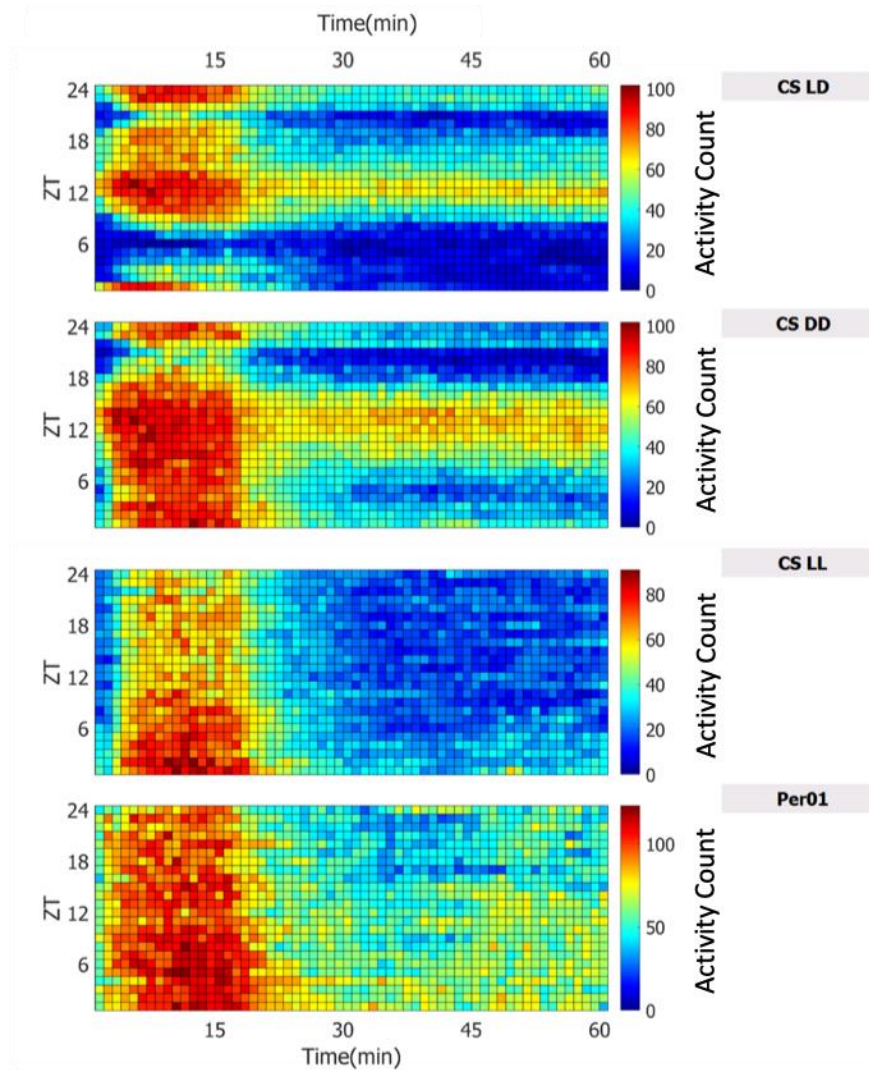
Figure 46: Heat map to show the median locomotor activity over a 24-h period for male wild-type flies in LD, DD, LL and *per01* mutants.

Heatmaps to show the median locomotor activity in LD (n=70), DD (n= 54), LL (n= 50) and *per01* (n= 18) conditions. The X axis shows the time in minutes of every hour with the Y axis showing the time in hours in a 24-hr cycle. The color of each square represents the intensity of locomotor activity (with blues representing low levels of locomotor activity and reds representing high) in that moment in time which is calculated by taking the median activity for each time point for each experimental group. There is an increase in activity during the first 15-min of each hour in all the conditions however this behavior is found to have an oscillatory pattern in LD and DD and be arrhythmic is LL and *per01* mutants.

Collectively, these findings demonstrate that auditory-induced locomotor activity shows periodic changes over a 24-h period in LD and DD conditions. This response pattern appears to be mediated by the clock since the response behaviour is arrhythmic in LL conditions and *per01* mutants (**Fig 46**).

124

6.3.6 Circadian changes to the sensitivity to acoustic stimuli

Circadian regulation of auditory-induced behaviours can manifest in a number of ways. Thus far, I have presented findings demonstrating that there is modulation in response magnitude to a given stimulus throughout a 24-h period. Another way to probe the system is to query whether there are differences in the sensitivity to the sound stimulus. As shown in **chapter 5.3.1** (**page 71**), presentation of an APT stimulus results in an exponential rise in locomotor activity throughout the 15 min presentation period. The sensitivity of the system can manifest itself in the rate at which the animal reaches its activity maxima in response to stimulus presentation. Based on this it is assumed that increased sensitivity to the auditory stimulus results in a faster response and a decrease in sensitivity would result in slower response.

The hourly median activity from all the samples in LD, DD, LL and *per01* conditions was calculated over a 48-h period. To investigate the changes in the speed of responsiveness, a single exponential function was fitted to this median activity for the first 10 min interval of every hour for each of these experimental conditions (**Fig 48**). The initial 10 minutes was chosen to enable a good fit since there was a slight decrease in response observed towards the latter part of stimulus presentation of every hour. By fitting this function, the time constant could be extracted from the activity.

Equation 7: Two-parameter single exponential function used to characterize the increase in activity in response to sound stimuli.

$$f(t) = a(1 - e^{-\tau t}) \hspace{2cm} (7)$$

A simple two-parameter single-exponential function was used for the fit (**Eq. 7**), where *a* is the amplitude of the exponent and the time constant is denoted by τ. This model was selected since it accurately characterised the behaviour observed in response to sound stimulus presentation.
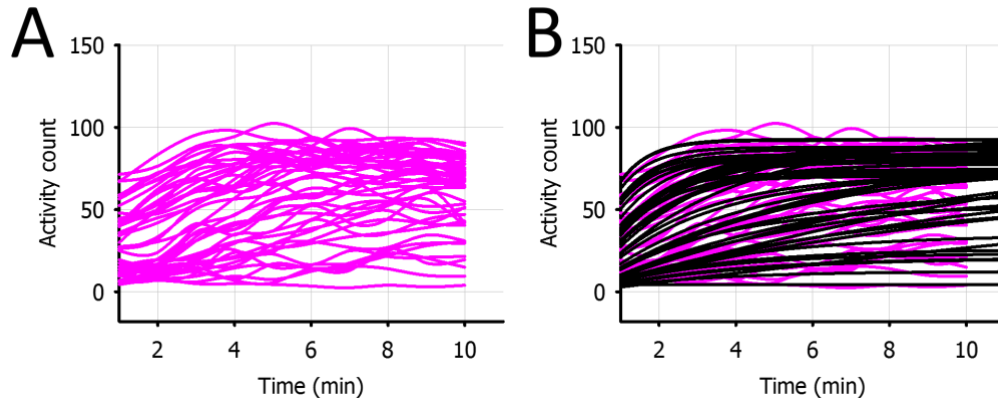
Figure 47: Time series to show the fitting of the exponential function to the first 10-min hourly median activity of wild-type flies in LD conditions
A: The median activity for every hour over a 48-h period of wild-type flies in LD conditions (n=70). This segment shows the ramping of locomotor activity in response to APT sound stimulus presentation. The same plot is superimposed with the regression fits of the single-term single exponential function (**B**).

Extracting the time constants from the fits, there was an overall difference in response properties between the conditions. Overall *per01* mutants had shorter time constants over the 48-h sampling period [χ^2 (3)= 80.608, p<0.001, Kruskal-Wallis one-way ANOVA on ranks] (**Table 16**). The median time constant for *per01* mutants over the two experimental days was 1.166 min (**Fig 48**). This was found to be significantly shorter as compared to wild-type flies in entrained, freerun and constant light conditions [p<0.001 for all post hoc comparisons using Dunn's method]. Wild-type flies in LL had the longest time constants of 3.373 min which was significantly longer compared to DD conditions 2.077 min (p<0.001).

Table 16: The median time constants over a 48-h period of male wild-type flies in response to APT of LD, DD, LL conditions and *per01* mutants.

	LD	DD	LL	*per01*
Time constant ,τ (min)	2.506	2.077	3.373	1.166
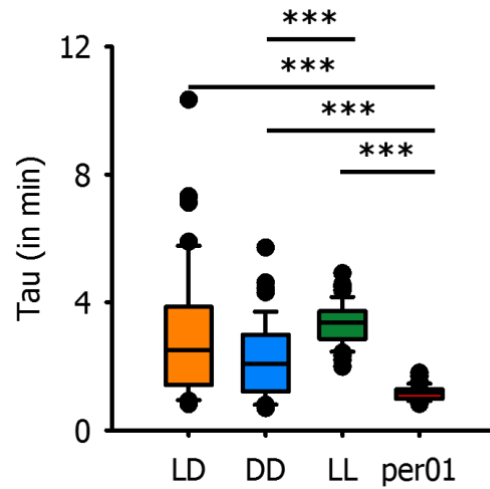
Figure 48: Box plots to show the differences in the median time constants of male wild-type in LD, DD & LL conditions and *per01* mutants derived over a 48-h period in response to APT.
per01 mutants showed faster response properties to APT sound stimulus compared to the time constants of the wild-type flies in LD, DD and LL conditions.

In entrained conditions, the response time constant showed periodic changes throughout the circadian day (**Fig 49A**). The observed response pattern was similar to that of the activity gain. The time constants were found to be lower around ZT12 and higher at ZT24. A similar response pattern was observed for wild-type flies in DD conditions (**Fig 49C**).
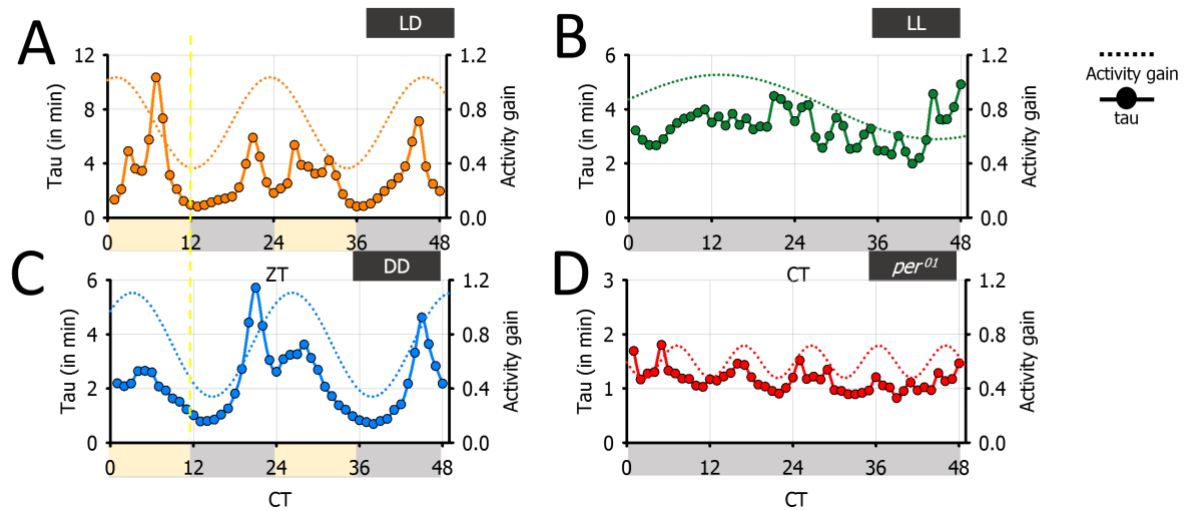
Figure 49: Time series graphs to show the changes in response sensitivity to APT sound stimulus throughout a 48-h period for male wild-type flies in LD, DD, LL conditions and *per01* mutants.
A: Time series of the derived time constant in response to APT sound stimulus for every hour over a 48-h period. The larger the time constant, the longer it takes the locomotor activity to reach its asymptotic peak. Increases in time constant indicate decreases in sensitivity to the sound stimuli. **B:** Shows the derived time constants for LL conditions, **C** for DD conditions and **D** for *per01* mutants. The dotted lines indicate the oscillatory pattern of the activity gain for comparison.

Visually inspecting the time constants for LL and *per01* conditions over the time course, no indication of periodicity in this measure was found (**Fig 49 B&D**).

In summary, these findings suggest that there is a change in sensitivity to the sound stimulus throughout the circadian day. This periodic modulation was observed in LD and DD conditions yet was not evident in LL conditions and *per01* mutants. Surprisingly, the largest time constants align to the peaks in baseline subtracted activity and activity gain (**Fig 49 A&B**). Indicating that the response rate was slower for the largest amplitudes in response activity.

6.3.7: Locomotor responses to sound stimuli in clock-disrupted conditions

In this section, I investigate whether the overall responsiveness to APT sound stimuli is changed in wild-type flies in LD, DD and LL environmental conditions and in per_{01} mutants. To assess the overall changes in behaviour between these conditions, the protocol described in **methods section 4.6.3 (page 59)** was used to process the raw data.
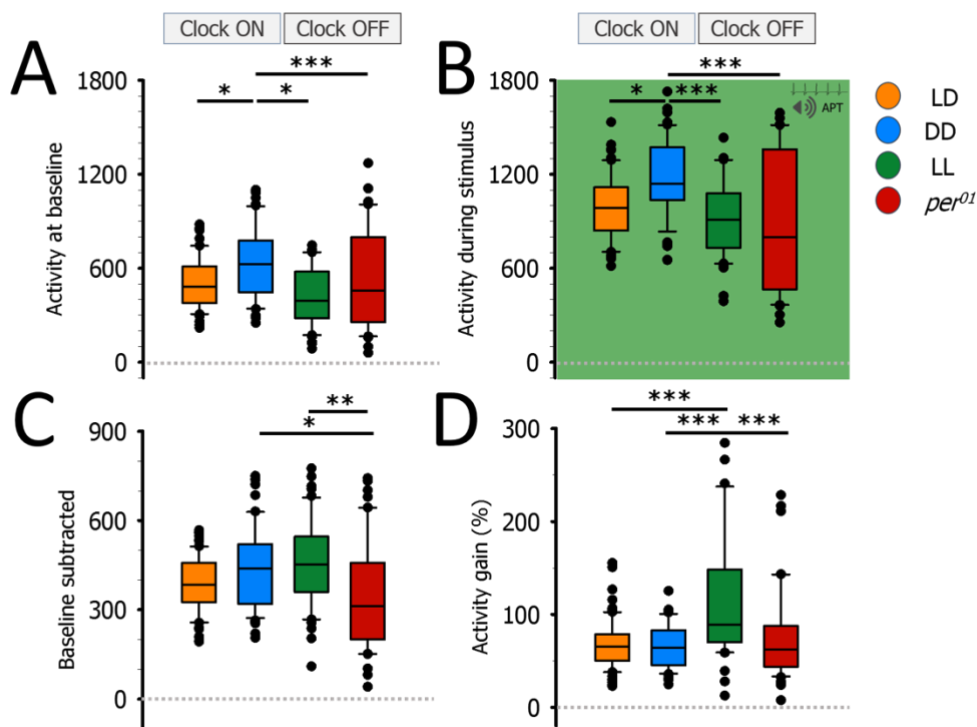
Figure 50: Box plots to show the activity at baseline, during stimulus, baseline subtracted and activity gain of male wild-type flies in LD, DD, LL and *per01* mutants over the first experimental day.

The baseline activity is shown in the box plots in panel **A** comparing between the baseline activity of LD, DD, LL and *per01* taken from the first experimental day. DD shows the highest baseline activity levels over the whole day. **B:** Box plots to show the activity during stimulus for the four conditions. **C:** Baseline subtracted activity shown for the four conditions where LL shows the highest auditory-induced locomotor activity. Activity gain is shown in **D** for the four conditions. LL flies also have the largest activity gain relative to baseline locomotor activity.

There were significant differences in the baseline activity between LD, DD, LL and per_{01} conditions [χ_2 (3)=23.363, p<0.001, Kruskal-Wallis one-way ANOVA on

ranks] (**Fig 50A**). Wild-type flies in DD were found to have the highest baseline activity of 627. This was significantly greater compared to the baseline activity of flies in LL, 393 (p<0.001), LD conditions, 483 (p=0.025) , and *per01* mutants (456, p= 0.032. Dunn's method used for post hoc comparisons).

Similar differences between the conditions were found for activity during APT stimulus presentation [χ_2 (3)=28.07, p<0.001, Kruskal-Wallis one-way ANOVA on ranks] (**Fig 50B**). Flies in DD conditions had the highest levels of activity during APT stimulus at 1140. This was significantly higher compared to LL (910, p<0.001), LD conditions (985, p=0.002) and *per01* mutants (798, p<0.001. Dunn's method used for post hoc comparisons).

Baseline subtracted activity was found to be different between conditions [χ_2 (3)=17.003, p<0.001, Kruskal-Wallis one-way ANOVA on ranks] (**Fig 50C**). *per01* mutants had the lowest median baseline subtracted activity of 313 which was found to be significantly lower compared to the median baseline subtracted activity of LL (453, p=0.002) and DD (439, p=0.011).

The activity gain also differed between conditions [χ_2 (3)=30.368, p<0.001, Kruskal-Wallis one-way ANOVA on ranks] (**Fig 50D**). The median activity gain for LL flies was 88.8% whereas DD, LD and *per01* conditions were all found to have similar, lower levels of activity gain (63.8%, 65.5% & 62.6% respectively). This difference was found to have a significance value of p<0.001 for all the pairwise comparisons between LL and other experimental conditions.

Although animals in LL conditions showed lower levels of baseline activity, the response to stimulus was found to be most pronounced amongst the experimental conditions. Both the baseline subtracted activity and the activity gain indicate that wild-type flies exposed to constant light conditions have a larger response to APT sound stimulus. Wild-type flies in DD showed increased levels of baseline activity compared to wildtype flies in LD. This rise was accompanied by higher levels of activity in response to APT sound stimulus but relative to baseline, there was no greater locomotor response in DD conditions. The overall activity of *per01* mutants was on a similar level for what was observed for wild-type flies in LD conditions.

Table 17: Table to summarise the median activity output over the first experimental day for male wild-type flies in LD, DD, LL conditions and *per01* mutants. Activity at baseline and activity during APT stimulus, baseline subtracted and activity gain are shown.

	APT			
	Clock on		Clock off	
	LD (n=70)	DD (n=54)	LL (n=50)	*per01*(n=18)
Activity at baseline	483	627	393	456
Activity during stimulus	985	1140	910	798
Baseline subtracted activity	384	439	453	313
Activity gain (%)	65.5	63.8	88.8	62.6

6.3.8: Light as a modulator of auditory-induced locomotor activity

Wild-type flies in entrained conditions appear to show differing behaviour between the two hemispheres of a circadian day. Both baseline and auditory-induced activity appears suppressed during the light phase and there is a subsequent increase in activity during the dark phase (refer to **figure 37, 39, 40**). To test this assumption, raw data was processed using the protocol described in **methods section 4.6.3** (**page 59**) however instead of averaging across the whole day; the data was split between the two hemispheres of the day and averages were calculated for ZT/CT 1-12 and ZT/CT 13-24 for LD, DD and LL conditions. Comparisons were made within and between the different environmental conditions.
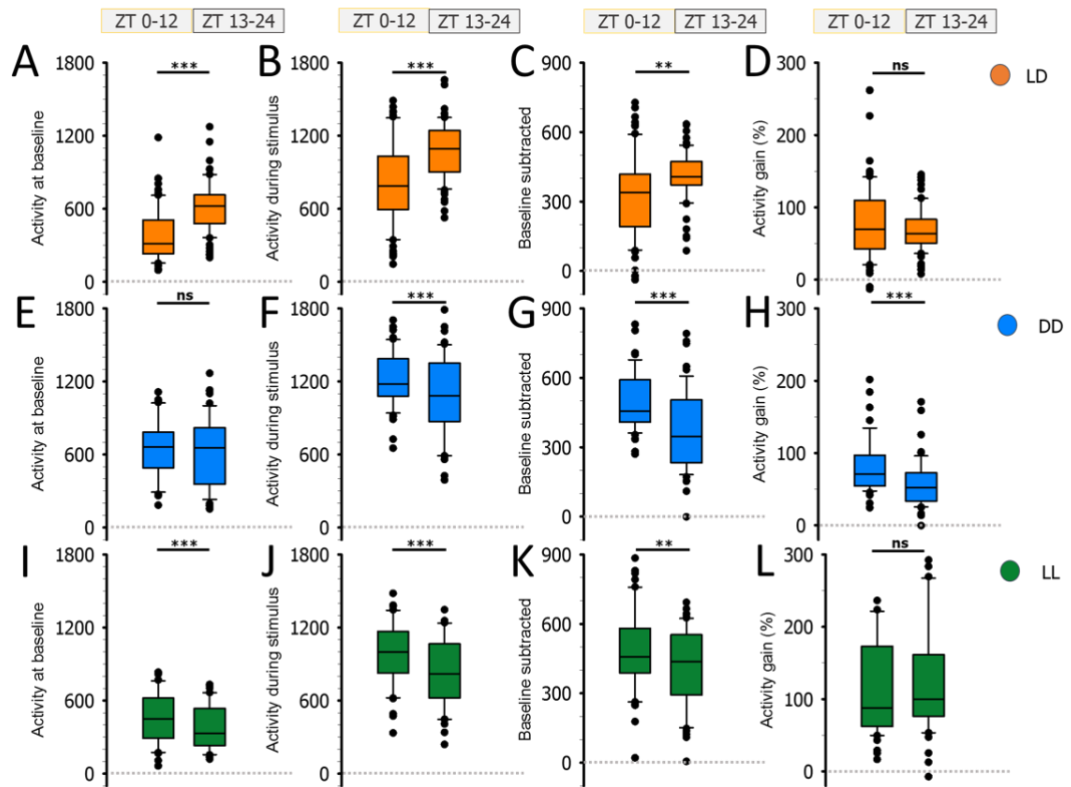
Figure 51: Series of box plots to show the differences in the locomotor activity between CT/ZT1-12 and ZT/ZT13-24 for male wild-type flies LD, DD and LL conditions.
A-D: show the activity at baseline (**A**), activity during stimulus (**B**), baseline subtracted activity (**C**) and activity gain (**D**) for animals in LD environmental conditions. The box plots show the measurement for either ZT 1-12 and ZT13-24. Comparisons are made between the two phases and between conditions. **E-H:** shows the same measurements but for DD conditions and **I-L** is for LL environmental conditions (**= p<0.01, ***= p<0.001)

Table 18: Table to summarise the median activity at baseline, during stimulus, baseline subtracted and activity gain for male wild-type flies in LD, DD, LL conditions. Comparisons are made between the median activity for ZT/CT1-12 and ZT/CT 13-24. The stimuli induced activity is in response to APT sound presentation.

	LD (n= 70)		DD (n= 54)		LL (n=50)	
	ZT 1-12	ZT 13-24	CT 1-12	CT 13-24	CT 1-12	CT 13-24
Activity at baseline	314	623	661	655	449	331
Activity during stimulus	786	1093	1179	1081	1000	821
Baseline subtracted activity	331 ± 180	408	506 ± 135	347	487 ± 180	438
Activity gain (%)	69.6	63.6	71.1	52	88	99.7

In LD conditions, the median activity at baseline for ZT1-12 was 314 which was significantly lower compared to ZT13-24 [623, Z=5.381, p<0.001, Wilcoxon Signed Rank test] (**Fig 51A**). No differences in median baseline activity were observed between the two hemispheres for DD conditions (**Fig 51E**). Whereas for LL, baseline activity during CT13-24 was found to be significantly greater compared to CT0-12 [CT0-12: 449, CT13-24: 331, Z= -3.437, p<0.001, Wilcoxon Signed Rank test] (**Fig 51I**).

Comparing the same phase of the day between experimental conditions, significant differences were found between the groups for ZT/CT 1-12 [χ_2 (2)=36.064, p<0.001, Kruskal-Wallis one-way ANOVA on ranks]. The highest median activity at baseline was observed for DD conditions (661). This was over double the baseline activity recorded for flies in LD conditions during this phase (314, p<0.001). Furthermore, the baseline activity for DD was also significantly greater in comparison to LL conditions (449, p<0.001). After the light transition, the baseline activity of flies in LD conditions shifted higher. Thus, for ZT13-24, the activity at baseline for LD and DD was alike. The baseline activity in the constant light condition remained low during CT13-24 (331). Hence, the baseline activity for LL conditions was significantly lower compared to LD and DD [χ_2 (2)= -32.391, p<0.001, Kruskal-Wallis one-way ANOVA on ranks].

These findings demonstrate that the baseline activity is stable between the two hemispheres of the day in DD and LL conditions, whereas in LD there is an increase in baseline activity during the dark phase; suggesting that there is suppression of baseline activity during light exposure.

In LD conditions, activity during APT stimulus presentation was found to be significantly higher for ZT1-12: 315 ± 334 compared to ZT13-24: 1083 ± 236 [t(69)= -5.866, p<0.001, Paired t-test] (**Fig 51B**). In DD, the median activity during stimulus was 1179 for CT1-12 which was significantly greater compared to the activity for CT13-24 [1001, Z= -3.866, p<0.001, Wilcoxon Signed Rank test] (**Fig 51F**). Similarly, in LL conditions, the median activity during stimulus was 1000 for CT0-12 which was significantly greater compared to CT13-24 [821, Z= -5.866, p<0.001, Wilcoxon Signed Rank test] (**Fig 51J**).

There were significant differences in the activity during APT stimulus presentation between the conditions for ZT/CT 1-12 [χ_2 (2)=45.532, p<0.001, Kruskal-Wallis one-way ANOVA on ranks]. The activity during stimulus was significantly higher for DD compared to LL and LD (p<0.001 for both). Furthermore, in LL the activity during stimulus was significantly higher compared to LD (p=0.034, all pairwise comparisons obtained using the post hoc Dunn's method). For ZT/CT13-24, similar to the changes observed for baseline activity post light transition, the activity during stimulus for LD increased within the dark phase. The activity during stimulus for LD was significantly higher in comparison to LL and DD [p<0.001 for both, χ_2 (2)=25.078, p<0.001, Kruskal-Wallis one-way ANOVA on ranks, all post hoc comparisons were done using the Dunn's method].

In LD conditions, the baseline subtracted activity was significantly higher during the dark phase (ZT0-12: 331 ± 180, ZT13-24: 409 ± 106, t(69)= -2.945, p=0.004, Paired t-test) (**Fig 51C**). Whereas for DD conditions, the reverse was observed where the baseline subtracted activity was greater for CT0-12 (506 ± 135) compared to CT13-24 (373 ± 176, t(53)= 5.460, p<0.001, Paired t-test) (**Fig 51G**). Similarly for LL, where the baseline subtracted activity was greater in the first part of the day (CT0-12: 487 ± 180, CT13-24: 420 ± 168, t(49)=2.485, p=0.016, Paired t-test) (**Fig 51K**).

For ZT/CT 1-12, the baseline subtracted activity was significantly higher for flies in LL and DD in comparison to LD [F(2,171)=20.751, p<0.001, one way ANOVA, Holm-Sidak method used for all post hoc pairwise comparisons]. No statistically significant differences were detected between the conditions for the latter phase of the day (ZT/CT13-24) between the three experimental conditionals.

There were no significant differences in the activity gain between the two phases of the day for LD and LL conditions (**Fig 51 D&L**). However, for DD, the activity gain was significantly lower for CT13-24 at 52.5%, compared to CT0-12 at 81.8%, [t(53)=3.889, p<0.001, Paired t-test] (**Fig 51H**).

Comparing the activity gain between the experimental conditions, for CT/ZT 1-12 the activity gain was highest for LL conditions at 88% [χ_2 (2)=11.058, p=0.004, Kruskal-Wallis one-way ANOVA on ranks, all post hoc comparisons performed using

the Dunn's method]. This was significantly higher compared to LD (69.6%, p=0.004) but was not statistically significant in comparison to DD (71.1%). For CT/ZT13-24, LL activity gain was 99.7%, which was significantly higher compared to LD (63.6%, p<0.001) and also significantly higher compared to DD (52%, p<0.001) [χ^2 (2)=40.977, p=0.004, Kruskal-Wallis one-way ANOVA on ranks, all post hoc comparisons performed using the Dunn's method].

The differences reported here between CT/ZT 1-12 and CT/ZT 13-24 and between conditions were maintained on the second experimental day (**Supplementary 2**).

In conclusion, a suppression of baseline and auditory-induced locomotor activity was observed during the light phase in LD conditions. Since this effect was not observed in DD and LL, this outcome suggests that the light transition has an effect on behaviour.

6.3.9: Auditory-induced locomotor activity of *glass₆₀ⱼ* mutants

Within the previous section, it was evidenced that there is suppression of auditory-induced activity during the light phase in LD conditions (**Fig 51**). This suppressive behaviour was not evident in the responses of wild-type flies assayed in DD, which suggests transitory light changes can have a suppressive effect on the system. To test whether this effect is dependent on the input through the visual phototransduction pathway, *glass₆₀ⱼ* mutants were tested on the auditory behavioural assay. As per for the previous section, the raw behavioural output from the assay of *glass₆₀ⱼ* flies was processed using the protocol described in **methods section 4.6.3 (page 59**). However, instead of averaging across the whole day; the data was split between the two hemispheres of the day and averages were calculated for ZT/CT 1-12 and ZT/CT 13-24.
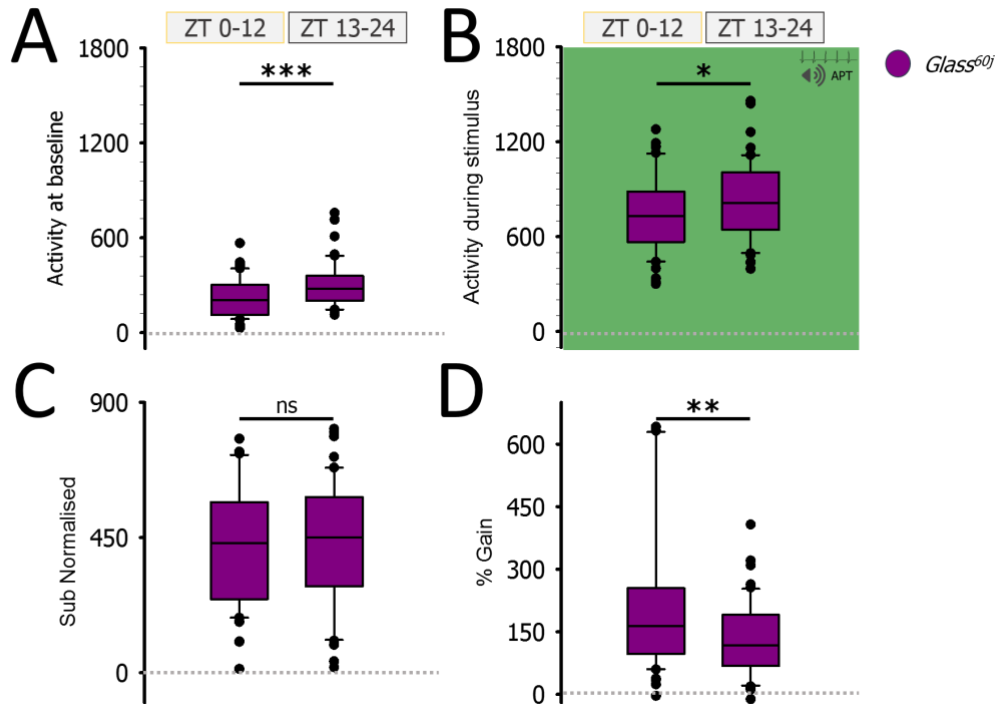
Figure 52 Box plots to show the differences in activity between ZT1-12 &ZT13-24 for *glass60j* mutants in LD conditions on the first experimental day.
A: Box plots to show the median baseline activity of *glass60j* mutants in LD conditions on the first experimental day. The activity during APT stimulus presentation is shown in panel **B** and the baseline subtracted auditory-induced locomotor activity is shown in **C**. Box plots in panel **D** show the differences in activity gain between ZT1-12 and ZT13-24 for the *glass60j* mutants.

The activity at baseline was found to be significantly lower during ZT1-12 in comparison to ZT13-24 in *glass60j* mutants. The median baseline activity for ZT1-12 was 224 ± 120 whereas for the dark phase it was 302 ± 144 [t(49)= -4.946, p<0.001, Paired t-test] (**Fig 52A**). This activity is comparable to wild-type flies in LD condition which were found to have lower baseline activity in the light part of the circadian cycle.

The activity during APT stimulus presentation was also found to be significantly higher for the dark phase compared to the light. The activity during APT stimulus presentation for ZT1-12 was 786 ± 243 which was significantly lower than the activity observed during the dark phase ZT13-24 821 ± 251 [t(49)= -2.234, p=0.03, Paired t-test] (**Fig 52B**). This outcome is also similar to the activity observed in wild-type flies in the same environmental conditions.

For the baseline subtracted activity, there were no significant differences between the two parts of the day. During the light phase, the mean baseline subtracted activity was found to be 438 ± 216, whereas for the dark phase, the mean was 426 ± 217 (**Fig 52C**). This is different to the observed behaviour of wild-type flies in LD conditions, where it was observed that there was suppression in the locomotor response to sound stimulus during the light phase.

Comparing the activity gain between the two phases of the circadian day, it was found that during the light phase, there was a significant increase in activity gain. The activity gain for the light phase was 163.2% compared to an activity gain during the dark phase of 118.1% [Z= -2.891, p=0.003, Wilcoxon Rank Sum test] (**Fig 52D**).

From the observations above, it can be concluded that *glass$_{60j}$* mutants showed similar suppression of baseline activity during the light phase, however this effect of light was not evident on the activity induced by sound stimuli. This suggests that the suppression in auditory-induced locomotor activity in wild-type flies during the light phase in LD conditions is mediated by the visual transduction pathway whereas the suppression of baseline activity is modulated by other non-visual phototransduction pathways.

Although it was found that there was a significant increase in activity gain during the light phase, this effect was not observed during the second experimental day (**Supplementary 3**). Since this measure was not found to be consistent, this outcome was considered to be a type I error.

To establish whether the sound-induced locomotor oscillations are regulated by the visual transduction pathway via its input to the clock; the periodicity of *glass$_{60j}$* mutants was assessed. The raw data collected from the auditory behavioural assay for *glass$_{60j}$* flies was processed using the protocol described in **methods 4.6.4** (**page 62**). Following this, a sinusoidal function was fitted to the activity data to characterize the periodicity and amplitude of the response.

glass$_{60j}$ mutants in the same environmental conditions showed robust periodic oscillations of baseline locomotor activity. A dual sinusoidal function was fitted to

characterize the periodicity and amplitude of activity at baseline (**Eq. 6**). The fit to baseline activity resulted in a R_2 of 0.770. The periodicity of the two oscillations was consistent to the frequencies observed for wild-type flies. An amplitude of 183.4 was associated with a 23.54-h period and a second waveform has a period of 11.66-h associated with a 121.5 amplitude peak (**Fig 53A, Table 19**). Thus, *glass60j* mutants display both morning and evening activity peaks. This behaviour is comparable to wild-type flies in the same environmental conditions. However, the morning activity peak is diminished in *glass60j* mutants since the amplitude of baseline activity at this frequency range was observed to be larger in wild-type flies.
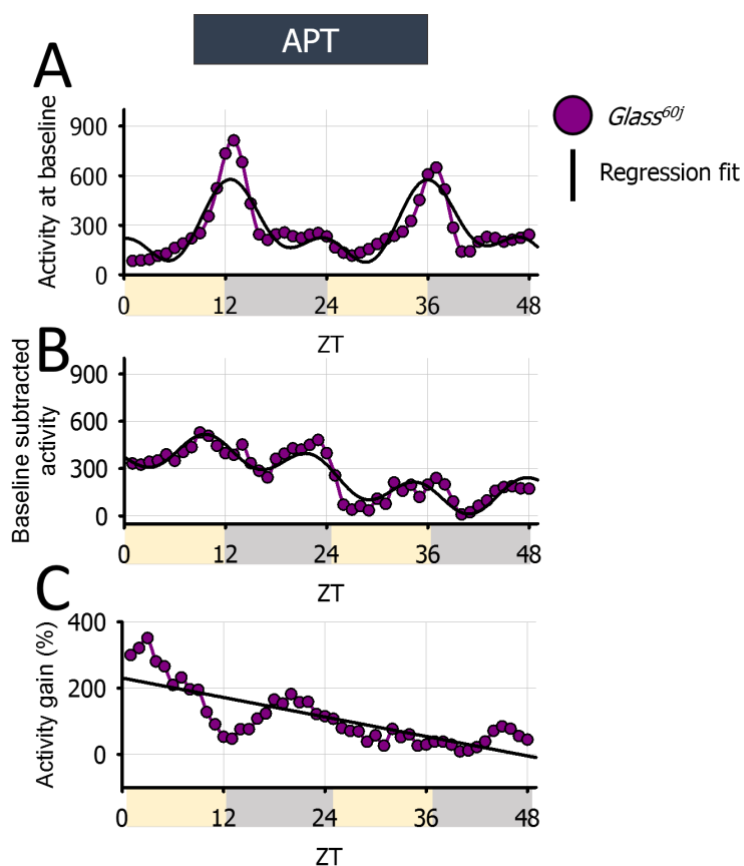
Figure 53: Time series to show the median baseline, baseline subtracted and activity gain for *glass60j* mutants over a 48-h period in LD conditions. Sinusoidal functions are fitted on top of the response to quantify oscillatory behaviour.
A: The median baseline activity for *glass60j* mutants in LD conditions modelled with a dual sinusoidal function. The median baseline subtracted activity is shown in panel **B** also fitted with a dual sinusoidal function. The auditory-induced behaviour is in response to APT sound stimulus. **C:** shows the median activity gain over a 48-h period with a single sinusoidal function fitting superimposed. The activity at baseline shows clear circadian oscillation but the 24-h fluctuations are no present in the baseline subtracted (**B**) and activity gain (**C**) (n=50).

Table 19: Summary of the *A & T* parameters derived from the sinusoidal fittings to the locomotor activity of *glass60j* mutants.

	glass$_{60j}$ in response to APT sound stimulus			
	1st Oscillation		2nd Oscillation	
	A1 (amplitude)	T1 (period in h)	A2 (amplitude)	T2 (period in h)
Baseline activity	183.4	23.54	121.5	11.66
Baseline subtracted activity	91.25	12.5	162.45	61.41
Activity gain (%)	33.78	4325.75		

Fitting the dual sinusoidal function to the baseline subtracted activity resulted in an R_2 of 0.860. A 91.25 amplitude peak had a periodicity of 12.53-h and a second process was associated with an amplitude of 162.45 had a biologically irrelevant period of 61.41-h (**Fig 53B**). So, baseline subtracted activity of *glass60j* flies did not show circadian rhythmicity. Furthermore, no circadian oscillations were observed in the activity gain for *glass60j* mutants in LD conditions (**Fig 53C**).

These findings suggest that circadian rhythmicity of auditory-induced locomotor activity is inhibited in *glass60j* mutants. Based on this, it can be speculated that the visual light input pathway is essential for the circadian regulation of auditory-induced locomotor activity.

6.4 Discussion

Drosophila show diurnal patterns of activity in LD and DD conditions (Fujii, Krishnan, Hardin, & Amrein, 2007). Wild-type flies time their activity maxima towards the morning and evening light transitions (Rieger et al., 2007) resulting in a bimodal locomotor activity pattern (Helfrich-Förster, 2000). In the results presented within this chapter, baseline activity of wild-type flies in equivalent environmental conditions showed the same bimodality. Additionally, it was observed that the baseline activity was significantly greater during the dark phase when flies were in LD conditions. This increase in locomotor activity during the dark

phase is not a behaviour which is typically observed in classical LD studies (Klarsfeld et al., 2003). However, very low levels of iridescence have been shown to shift the activity levels of wild-type flies to make them nocturnal (Kempinger, Dittmann, Rieger, & Helfrich-Förster, 2009). The activity observed within the current work showed all the key hallmarks of animals exposed to light/ simulated moonlight conditions with increases in activity during the dark phase, diminished midnight trough and more pronounced widening of the midday siesta.

The behavioural experiments presented within this thesis were conducted in a room rather than an environmentally controlled incubator. Though the environmental monitor was not sensitive enough to pick up any iridescence during the dark phase, these outcomes suggest that the LD within the current work are more comparable to light/ moonlight environmental conditions.

These findings suggest a sensitivity of the system to extremely low levels of light. Since this work investigates circadian regulation of behaviour, it raises the question of whether light/moonlight environmental conditions affect the clock? Bachleitner et al (2007) reported that exposure to light/'moonlight' conditions does not interfere with the cycling of molecular clock proteins within peripheral tissue. Nonetheless, under these light/dim light cycles, it was found that there was a shift in the expression of key clock proteins within the central pacemaker cells. Peak expression of PER and TIM was shifted by two hours from ZT23 to ZT21 in the central pacemakers regulating the morning activity peak. Whereas peak expression of PER and TIM proteins shifted forwards by 2 hours in the central pacemakers regulating the evening activity peak (Bachleitner et al., 2007). Hence, although there are shifts in the molecular function of the clock, the oscillations remain stable in light/'moonlight' conditions.

Auditory-induced locomotor activity in response to APT and RCS stimuli also showed rhythmic changes throughout a 24-h period. The response pattern was different to baseline activity. The most prominent increases in auditory-induced locomotor activity were found to be around the morning light transition in LD and DD conditions. The oscillatory pattern of sound-induced locomotor activity was similar to the locomotor rhythms observed in the courting pairs by Fujii et al (2007) (**Fig 54B**). Male- female paired flies were found to have a distinct locomotor-activity

pattern, termed a 'courtship rhythm' whereby they were most active during the subjective night and early morning and least active around the CT12.
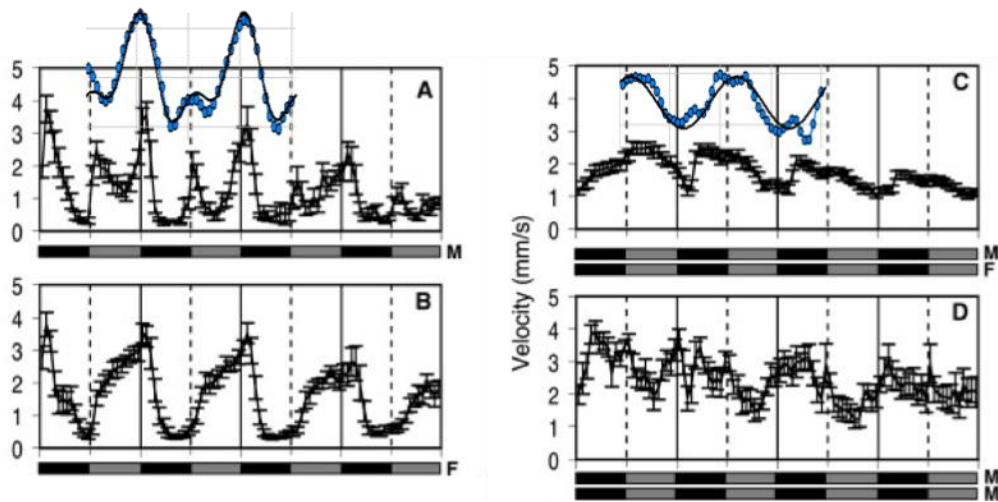
Figure 54: Actograms of courtship rhythms as found by Fujii *et al* (2007) overlaid with the observed baseline and auditory induced locomotor activity of wildtype flies in DD conditions.
A: shows the activity rhythm of a single male fly. The blue trace above demonstrates the baseline locomotor activity of grouped male wildtype flies in DD conditions as observed in the experiments reported in this chapter. **B** is the locomotor rhythm for a single female fly in a chamber. **C:** shows the locomotor rhythms in male with female pairings where there is a courtship rhythm, the locomotor pattern changes and the peak in activity is around the previously entrained morning light transition. The blue trace presented above demonstrates the auditory induced locomotor activity of grouped male wildtype flies in DD conditions as observed in the experiments reported in the current chapter. **D:** are the locomotor rhythms of paired males in a chamber (Figure from (Fujii et al., 2007)).

Interestingly, in the same paper Fujii et al (2007) reported that male-male pairings result in a disruption of locomotor activity. Within these conditions the males displayed erratic activity patterns with indistinguishable peaks. This observation is contradictory to the outcomes presented within this thesis since the baseline activity of wild-type flies displayed a clear oscillatory bimodal pattern in DD conditions (**Fig 54A**). All the behavioural experiments were conducted with 3 male flies within one sampling tube, so it can be presumed that the interactions between the flies presented here should be comparable to the male-male interactions observed in Fujii et al (2007). Initially it was considered whether the regular exposure to the sound stimulus stabilises baseline locomotor activity patterns. However, in experiments where no sound stimulus was presented, rhythmic patterns of activity were still observed (**Supplementary 4**). Possibly the observation

in Fujii et al (2007) is specific for paired rather than increased numbers of socially interacting flies.

Moreover, Fujii et al (2007) concluded that auditory input does not play a role in determining the unique courtship locomotor rhythm since the removal of the aristae did not disturb this behaviour in male-female paired flies. Since auditory-induced locomotor activity observed in this chapter is antenna-dependent and similar to the courtship rhythms observed in Fujii et al (2007), it is evident that this structure is crucial in determining this oscillatory pattern of behaviour. Still, it is possible that in courtship interactions where there are courtship signals via other sensory modalities (such as male-female pairings), auditory signals are made redundant.

Several previous studies have shown a link between courtship rhythms and the circadian clock. Sakai & Ishida (2001) found daily fluctuations in mating activity to be under circadian control. Similarly, the courtship patterns observed in Fujii et al (2007) were also found to be regulated by clock genes. Within the current work, I also presented findings to show that auditory-induced locomotor activity rhythms are inhibited in per_{01} mutants and LL conditions. The similarities in the outcomes of these studies suggest that collectively these investigations are describing the same behavioural process which is mediated by the clock.

There were no prominent differences in auditory-induced locomotor activity rhythms in response to RCS and APT however these oscillations were not present in response to WN stimulus. Taking this with the findings discussed in the previous paragraph suggests that the auditory-induced behavioural rhythms are specific to courtship signals rather than being an overall rhythmic modulation to auditory stimuli. This raises the question of whether these courtship specific changes are determined in the function of the primary auditory sensory organ or whether they are a manifestation of higher order changes in the system.

Comparing the overall response of wild-type flies in LD conditions, I found that during the light phase there was a suppression of auditory-induced locomotor activity. $glass_{60j}$ mutants did not show suppression nor was this effect observed in DD conditions. This suggests that light has a direct effect on the responsiveness of

the system to the auditory stimulus. Since it was suggested at the beginning of this discussion that the environmental conditions in the current work are more comparable to light/'moonlight' conditions and these evidently have an effect on baseline locomotor activity (Bachleitner et al., 2007); it was considered whether this might be the cause of the observed suppression of auditory-induced locomotor activity. The baseline activity in *glass60j* mutants was found to be reduced during the light phase in LD cycles, which is similar to the behaviour observed for wild-type flies in the same environmental conditions in this work. These findings lead to two primary conclusions. Firstly, this demonstrates that the visual phototransduction pathway is not the determinant of 'moonlight' effects on baseline activity. Given this finding, it is likely that these environmental conditions affect behaviour via other light feedback pathways to the clock. Secondly, since there was no reduction of auditory-induced behaviour in *glass60j* mutants, it suggests that this activity is modulated by the input from the visual pathway. This is complementary to the hypothesis I made in this chapter that baseline subtracted activity in LD conditions is a behaviour which is contributed to by two processes since this activity in response to APT and RCS stimuli was best characterised by a dual sinusoidal function. Collectively, these findings suggest that both light and the circadian clock are modulators of auditory-induced behaviour elicited by sounds with a courtship signal.

Interestingly, *glass60j* flies did not show robust circadian oscillation of auditory-induced locomotor activity. This suggests that the visual phototransduction pathway regulates auditory-induced locomotor rhythms. It is known that activity rhythms are entrained by several photoreceptive pathways which interact with the central pacemaker neurons (Helfrich-Förster et al., 2001). Inhibition of the visual pathway has been shown to specifically impact the morning activity peak (Helfrich-Förster, 2000; Nippe et al., 2017; Yang, Emerson, Su, & Sehgal, 1998). *glass60j* mutants do not show any cycling of PER and TIM in the dorsal neurons (DN1) neurons. Based on this, it is possible to speculate that auditory-induced locomotor rhythms are functionally connected to this subset of pacemaker cells. To test this assumption, commonly used DN1 drivers such as Clk4.1M-GAL4 and R18H11-GAL4 can be used to express a synaptic neurotransmitter blocker such as tetanus toxin light chain (TNT) to inhibit the output of these neurons. By using this system, it would be possible to probe whether auditory-induced locomotor rhythms are

dependent upon the function of these specific pacemaker neurons.

Relative to baseline, wild-type flies in LL conditions show the largest increases in locomotor activity in response to APT and RCS stimuli throughout the whole-time range. This effect is independent on the clock since the relative response of *per01* mutants was comparable to wild-type in LD and DD conditions. Additionally, *glass60j* mutants also show overall higher levels of activity gain in response to sound stimuli. Constant light exposure even at low intensity leads to retinal damage and blindness in wild-type animals (Lee & Montell, 2004). Given that the wild-type flies in LL were in constant light for several generations, it is reasonable to assume that these environmental conditions have resulted in damage to the visual structures. Thus, the similarity between the overall gain in responsiveness of wild-type flies in LL and *glass60j* mutants could be attributed to the defects in the compound eye.

Previous reports have found the lack of visual input results in a significant change to locomotor activity during courtship behaviours (Krstic et al., 2009). During light conditions, males are able to use visual tracking to approach a female within the chamber, whereas in darkness males would zig-zag across the chamber as a form of scanning to locate the potential mate (Krstic et al., 2009). This change in behaviour naturally results in an increased distance of travel. This observation serves as a possible explanation as to why wild-type flies in LL and *glass60j* mutants demonstrate greater auditory-induced locomotor activity.

In conclusion, this chapter has explored some of the key modulators of sound-induced locomotor activity. The response behaviour to auditory stimuli containing courtship signals has been found to have a unique temporal pattern which is dissimilar to baseline locomotor activity rhythms. This unique activity rhythm has a similar topology to 'courtship rhythms' which have been observed in other studies which have also shown that this behaviour has clock dependent modulation (Kempinger et al., 2009; Sakai & Ishida, 2001). Since auditory-induced activity rhythms where also not observed in *glass60j* mutants, it is possible that DN1 neurons specifically drive this behaviour. Furthermore, based on the findings within this chapter, it is proposed that light is also a key modulator of auditory-induced activity. To test this assumption, further investigations are needed to test this light induced behavioural switch. For example, if suppression of auditory-induced

locomotor activity is a direct effect of light independent of the clock, shifting the light phase or introducing light pulses at various time points should also result in a reduction of this behaviour.

6.5 Limitations of findings

As established in **chapter 5.3.2** (**page 74**) the sound-induced locomotor behaviour is antenna-dependent. However, locomotor behaviour cannot be taken as a direct readout of auditory processing. Are there changes in the function of the primary sensory organ which results in changes in behaviour or does auditory processing remain constant and the key modulators explored in this chapter act somewhere upstream within the system? Further study is required to address these questions. It is clear that baseline subtracted activity and activity gain are two measures which characterise auditory-induced locomotor activity however the physiological mechanisms driving these two readouts of activity are not known. It is assumed that activity gain reflects the changes in auditory sensitivity although again, it is not clear at which point in the system this occurs.

It is surprising that the highest levels of activity gain were found to be aligned with the largest time constants. This seems counterintuitive since if there were an increase in response to the sound stimulus it would be assumed that this response would also be faster. This inverse relationship between speed of responsiveness and the magnitude of the response is confusing. Perhaps there is some biological relevance to show a slower ramping in activity when the animal is particularly sensitive to the presented auditory stimulus. Thus, the relationship between auditory input and behavioural output needs to be further explored.

All the outcomes investigating circadian rhythmicity in this chapter were done on the median activity of all the samples of that particular experimental condition. Individual samples showed highly variable auditory-induced locomotor activity. The data is noisy which presents a significant challenge. It is possible that some of this

noise is due to the adopted experimental approach. *Drosophila* only demonstrate auditory-induced behaviour upon reception of the sound stimulus. Thus, this behaviour is dependent upon the animal perceiving the sound. In an experiment where the animal is freely moving, it is difficult to assess how much the animal can hear. Since *Drosophila* antennal ears are highly direction and distance-sensitive, it is likely that there is a large disparity in the level of sound each fly is exposed to. This could account for some of the noise within the data. Perhaps adopting a different behavioural approach where this can be controlled would be advantageous. Though challenging, I propose that key modulators identified in the current work can be investigated by using tethered flies on a trackball. Trackball experiments in *Drosophila* use a small ball on which the animal can still move its legs while the wings are tethered. By using this type of protocol, it would be possible to direct the sound stimulus directly at the arista while investigating the movement of the animal. Assuming the animal can be kept in good health for prolonged periods of time, this approach could reduce the signal-to-noise ratio and help test some of the assumptions presented within this chapter.

As discussed within the first part of this chapter, the baseline activity readout indicates that the experiments were done in light/'moonlight' conditions. Most circadian studies have been done in LD conditions and even though it could be argued light/'moonlight' conditions have more ecological relevance, this limits the generalisability of the findings presented in this work. To address this, the experiments should be repeated in environmentally controlled incubators.

Finally, the regression fits to the behavioural data allowed me quantify the periodicity and amplitude of the response behaviour. However, this process could be optimised. Levine at al (2002), proposed more advanced methods involving digital filtering of the signal to extract and clarify features of interest. It was not possible to apply this method on the current data set due to the insufficient number of data points. By running the experiments for longer periods of time, it could yield enough data to apply pre-existing toolboxes allowing for better filtering and assessment of the data.

Chapter 7

The effect of key modulators of auditory behaviour on the function of JO neurons

7.1 Introduction

The structural, mechanical and electrophysiological properties of the auditory system have been investigated by various means. Sound intensity increase of the stimulus is accompanied by a decrease in compliance of the antennal sound receiver. The mechanical response of the receiver is modulated by decreasing the stiffness towards the dominating frequencies within the courtship song (Albert & Göpfert, 2015; Ewing, 1983; Göpfert & Robert, 2002). This property of the antenna demonstrates that the sound receiver is pre-primed for detection of specific signals.

Specificity in signal detection is not only reflected within the mechanical structure of the *Drosophila* antennal ear but also within the electrophysiological response of the organ. Direct single-cell recordings have not been obtained from the mechanosensory neurons within the JO, as there are several practical challenges with adopting this method. Firstly, the organ is encased by a thick, waxy cuticle. Secondly, the JO stretch receptors are anchored to the underside of the epidermis making it difficult to gain access while preserving the structural properties of this organ. However, compound action potentials (CAPs) have been recorded by

inserting an electrode the base of the antennae close to the nerve. These signals reflect the bulk spiking of JONs. By using this method, the JO has been found to be the source of sound evoked potentials (Eberl et al., 2000).
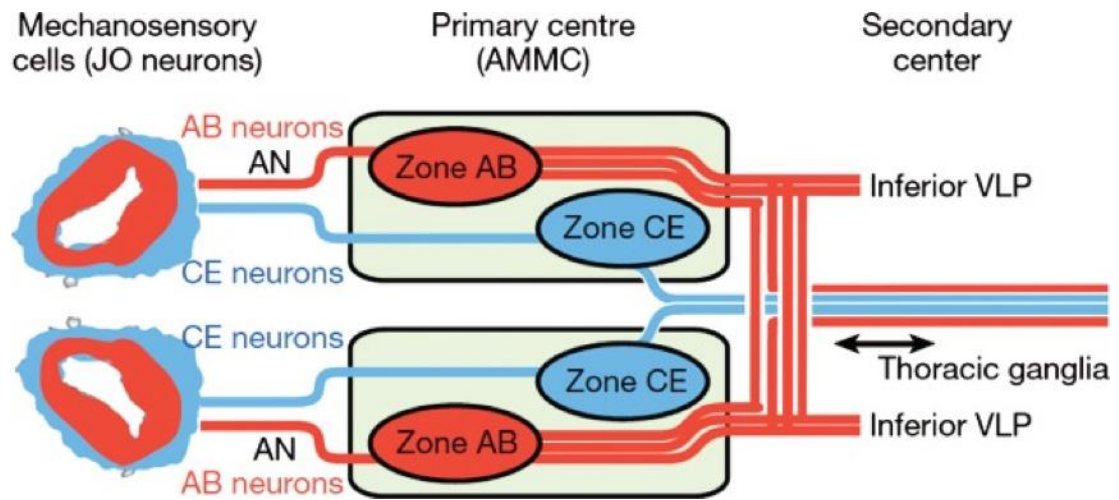
Figure 55: Illustration to show the two distinctions of mechanosensory receptors within the JO.
The AB population project to a distinct region within the AMMC and are considered to be sound sensitive mechanoreceptors. CE are sensory neurons which are found to be unresponsive to auditory stimuli but are activated by static stimuli on the arista. CE neurons are classed as 'wind/gravity' sensory neurons and also project to a distinct region within the AMMC (Reference for illustration (Kamikouchi et al., 2009)).

The JO contains a heterogenous population of mechanosensory neurons (Kamikouchi et al., 2009). Five anatomically distinct neuronal subdivisions have been found to preferentially respond to different stimuli. Sub-population A has been characterised as preferentially responding to high-frequency sound and sub-population B to low-frequency sound (Kamikouchi et al., 2009) whereas sub-population D is highly responsive to mid-frequency sounds (Yorozu et al., 2009). C and E sub-populations are most responsive to tonic deflections of the arista. Inhibition of these deflection sensitive neurons results in impairments in gravity-mediated behaviours, hence these sub-population neurons have been primarily described as gravity sensors (Kamikouchi et al., 2009) (**Fig 55**).

These distinctions between JONs however do not explain the behavioural preference of *Drosophila* specific inter-pulse intervals (IPI) in courtship signals (Yoon et al., 2013). Differential response properties have been found further upstream in the postsynaptic cells of sub-population A and B JONs (Azevedo & Wilson, 2017). The vibration-sensitive JON-A sub-population make connections

with A2 cells and JON-B's synapse onto the B1 cells within the AMMC. By performing direct *in vivo* single-cell recordings, it was found that A2 cells encode the overall vibration energy of the signal whereas B1 cells function as bandpass filters by modulating their membrane potential (Azevedo & Wilson, 2017). All B1 cells were found to respond to frequencies of <200Hz yet there were still differential preferences within that cluster of neurons (Lai, Lo, Dickson, & Chiang, 2012). Courtship-evoked behaviours have been specifically linked to the function of B1 postsynaptic cells. The inhibition of these neurons and silencing of their postsynaptic partners has been observed to diminish sound-induced courtship behaviours (Vaughan, Zhou, Manoli, & Baker, 2014; Zhou et al., 2015).

An efficient sensory system allows for adaptation to the statistics of its surroundings. Sensory systems can be described to possess both fast and slow adaptation properties. CAP amplitudes are strongly scaled by the intensity of the presented stimulus however post-stimulus onset, the response settles into a steady state which is intensity invariant (Clemens, Ozeri-Engelhard, & Murthy, 2018). This is a demonstration of a fast adaptation process whereby there is dynamic processing of the sensory input.

Circadian modulation can be categorised as a slow adaptation process since changes to the response properties may prime the system to better detect signal. Diurnal rhythms were identified in the electrophysiological responses to odorants (Krishnan et al., 1999) and visual processing in *Drosophila* have also been shown to have robust changes in the electrophysiological responses throughout a circadian day (Nippe et al., 2017). Clearly this adaptation process is directly relevant in sensory systems but has not been demonstrated in auditory processing.

All the above findings demonstrate the complexity and the dynamics of sensory systems. **In chapter 6,** I showed key regulators of auditory-induced locomotor activity. To probe whether the modulation of behaviour by these factors is reflective of the modulation of the function of JO neurons; calcium imaging was performed on JO neurons.

7.2 Methods

7.2.1 Calcium Imaging

There are changes in intracellular calcium produced by neural activity. Calcium imaging allows to visualise the excitation of neurons by non-invasive means. Through the use of genetically encoded calcium indicators (GECIs), it is possible to express calcium protein indicators in specific subsets of neurons to monitor their activity. Neurons have fast calcium dynamics and low calcium accumulation which the calcium sensors must account for. The development of the next generation GECIs ultrasensitive GCaMP-6f sensors account for these properties (Chen et al., 2013).

GCaMP-6f sensors function as follows. Changes in intracellular calcium of a cell with expression of a GCaMP-6f reporter result in a conformational change of the sensor protein matrix. The calcium binding protein calmodulin (CaM) and its interacting peptide (M13) undergo calcium-dependent conformational change, whereby there is modulation of solvent access to the chromophore allowing for increased brightness upon calcium binding. This results in an increase in fluorescence signal (Chen et al., 2013).

7.2.2 Fly strains

To visualise the calcium transients within the JO, the UAS-GAL4 system was used to drive the expression of GCaMP-6f in specific cell types. This binary method utilizes a yeast transcriptional activator protein, Gal-4, as a promoter for tissue specific genes. Gal-4 specifically binds to an upstream activation sequence (UAS) enhancer which activates gene transcription. This system allows for temporal and spatial targeting of gene expression. Targeted expression of the signalling reporter UAS-GCaMP-6f males were crossed with GAL-4 females to explore neuronal calcium transients within the JO.

I used UAS-GCaMP-6f (42747, Bloomington, US) as the GECI reporter strain. Four Gal-4 lines were used within the current chapter. JO1 (also known as NP0761) drives the expression of GCaMP-6f in all JONs. For simplicity, animals with expression of this driver are referred to as **JO-all** within this text. JO15 was used to target the A and B sub-population sound sensitive neurons. Experimental animals with these selectively labelled neurons are referred to as **JO-AB** within the text. JO29 was used to express GCaMP-6f specifically in JO D sub-population neurons and NP6250 which drives expression in JO C-E neurons. Experimental animals with the expression of these sub-population specific drivers are referred to as **JO-D** and **JO-CE** respectively.

7.2.3 Functional imaging set up

Images were captured at the rate of 2Hz using an upright Zeiss (Germany) LSM510 confocal microscope (Axioscop II platform) coupled to an Argon ion laser using the 488nm wavelength line. The laser power was set to 2.5% and the emission light was collected through a dichroic filter capturing all light above 505nm. A 25x air objective was used for sampling with a numerical aperture (NA) of 0.4. The excitation area of 420μm x 420μm and the pinhole was set maximally to try to aggregate the signal from the whole JO.

7.2.4 Sample preparation for functional imaging

The experimental fly was anesthetised on CO_2 and its body immobilised onto a glass microscope slide using dental glue. The dental glue was then cured using a blue light-curing gun. At this stage the head was left suspended and positioned facing upwards. Then the head would be tilted backwards around 30° and fixed onto the thorax to allow for the antenna to be fully exposed. To ensure there is no movement artefact in the recordings, the second antennal segment was also fixed using the dental glue. The arista and the funiculus were left suspended.

7.2.5 Protocol

The stimulus was delivered using a modified ear bud speaker connected to a basic

amplifier running off a 5V battery. A pipette tip was attached to the end of the ear bud to allow for the sound to be directed straight onto the sound receiver. Once the sample was in position underneath the objective, using a micromanipulator, the opening of the pipette tip was manoeuvred into close proximity and pointed perpendicularly to the arista (**Fig 56**).
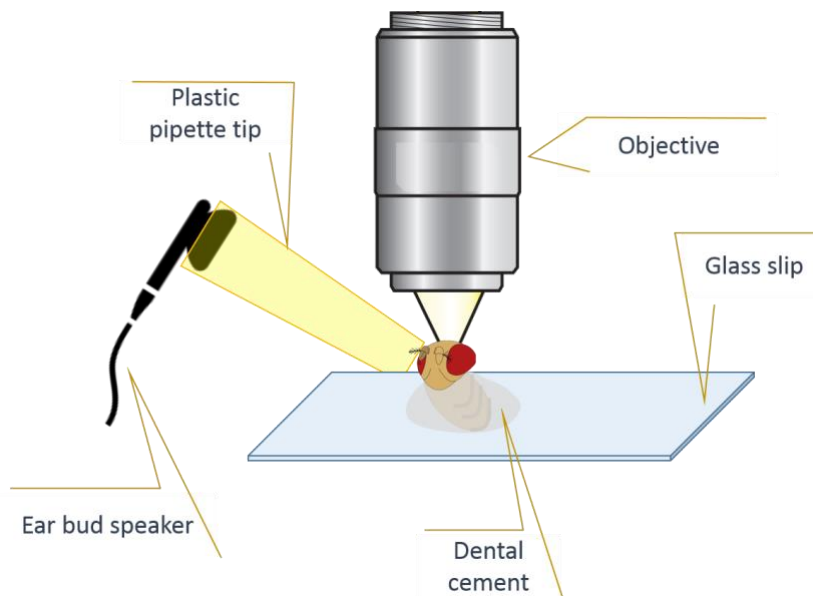
Figure 56: Schematic to show the set up for functional imaging of the JO in a live preparation.

To be able to compare the signal between samples, the gain, pinhole and other settings were kept constant within and between experiments. Furthermore, the amplitude of the sound stimulus was also left unchanged between experiments.

First, the displacement of the arista was measured by performing a line-scan. The sound receiver was brought into view using the 633 laser and a line bisecting the structure was selected (**Fig 57A**). The displacement of the arista could be observed in the movement artefact of the line scan (**Fig 57 B&C**). Through this procedure, it was possible to ensure that the opening of the pipette which carries the sound was was correctly positioned to produce distortions of the arista. It was found that upon triggering the sound, the displacement of the arista accurately reflected the properties of the given stimulus.
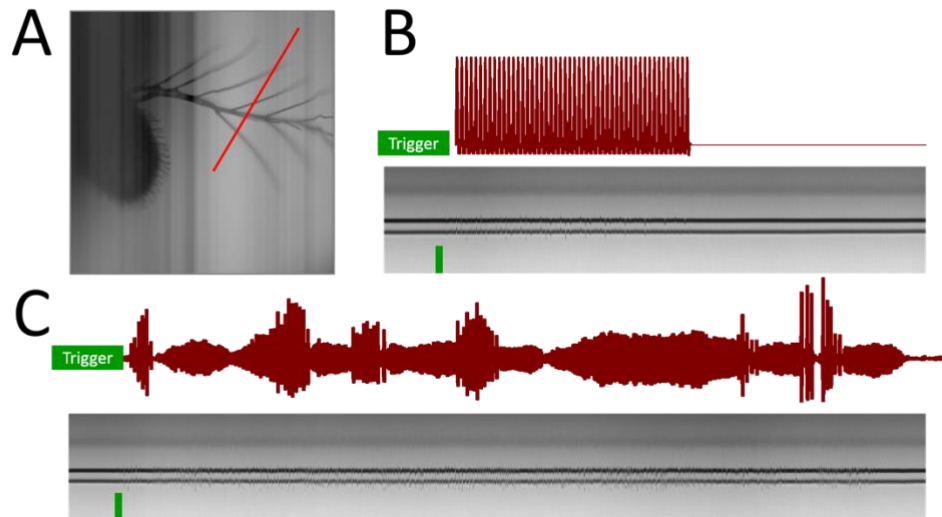
Figure 57: Line-scan of the arista to assess the displacement of the sound receiver in response to APT and RCS stimuli.
A: Shows a bisection of the arista which was then imaged using the line scan to assess the displacement of the sound receiver in response to stimulus. B: Shows the waveform of the stimulus presented via a small loudspeaker with the associated displacement of the arista and captured by the line scan below. C: Shows the waveform of the 9 second real courtship song (RCS) extract also tested. Underneath shows the associated displacement of the arista as captured by the line scan bisection.

To observe the calcium transients in response to sound stimulus presentation, a time series function was used to capture images. Two images were captured every second. The stimulus waveform had a trigger signal placed within the first 50ms of stimulus onset (**Fig 57 B&C**). This trigger was generated by pClamp and sent to the image capturing software LSM 510 to signal the start of image collection. Every stimulus round generated a trigger which was then encoded into the data file allowing to have a precise measure of which frames are associated with the presented stimulus.

7.2.6 Sound stimulus

The command waveform was controlled using pClamp software. Via a digitizer (Digidata 440A), the output signal fed into the amplifier connected to the earbud speaker. The sound stimulus presented in this series of experiments was based on the same stimulus given in the behavioural experiments in **chapter 5 & 6.** Each fly tested was exposed to all of the following stimuli once.

7.2.6.1 2s APT stimulus

The averaged pulse presented in **Figure 17** (**page 51**) was used to construct a continuous pulse train for 2s with an IPI of 40-ms. An 8s silence interval followed this stimulus to allow for the calcium signal to return back to baseline. During a single trial, this stimulus was repeated 30 times with the recording lasting roughly 4 min per trial.

7.2.6.2 Saturating APT stimulus

The averaged pulse (same as above) was used to construct a saturating stimulus. A continuous pulse train lasting for the duration of 16 and 32 seconds was presented to the experimental animals. The IPI of this pulse train was 40ms (**Fig 17, page 51**). This saturating stimulus was presented only once per trial.

7.2.6.3 Real courtship song (RCS) stimulus

The same real courtship song (RCS) extract as described in **Figure 18** (**page 52**) was presented as a stimulus during calcium imaging. The stimulus lasting 9s was followed by a 11s period of silence to allow the signal to drop back to baseline. This was looped for 12 times during a single trial lasting around 4 min. Within the text, this stimulus is referred to **RCS**.

7.2.6.4 9s APT stimulus

To be able to directly compare between the responses to APT and RCS stimulus, a continuous pulse train lasting 9s constructed out of the averaged pulse mentioned above was presented to the experimental animal. As with the RCS stimulus, 9s of the APT stimulus was followed by a 11s period of silence. This was looped for 12 times during a single trial lasting around 4 min.

7.2.7 Troubleshooting

To ensure that the signal delivered to the experimental animal was coherent with the command signal, input channels feeding back into the digitizer were enabled to get a readout of a) the signal generated by the digitizer b) the signal outflowing

from the amplifier and c) a recording of the output at the pipette tip opening. The sound stimulus output from the pipette tip was recorded by using a particle velocity microphone. The microphone was positioned at the approximate distance to the pipette tip opening as the arista. The velocity of all given stimuli was attenuated equally however the key features of the stimulus were preserved (**Fig 58,59**).
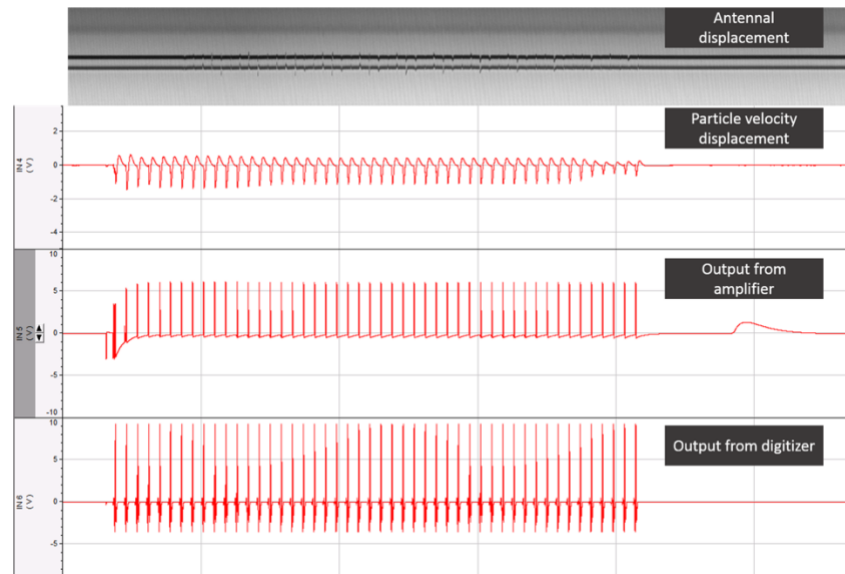
Figure 58: Output of the APT stimulus from the signal generator & recording by a particle velocity meter from the earbud speaker.

Though the stimulus is attenuated as the signal goes from the digitizer to the amplifier, the output waveform recorded by the particle velocity meter is reflective of the original APT stimulus.
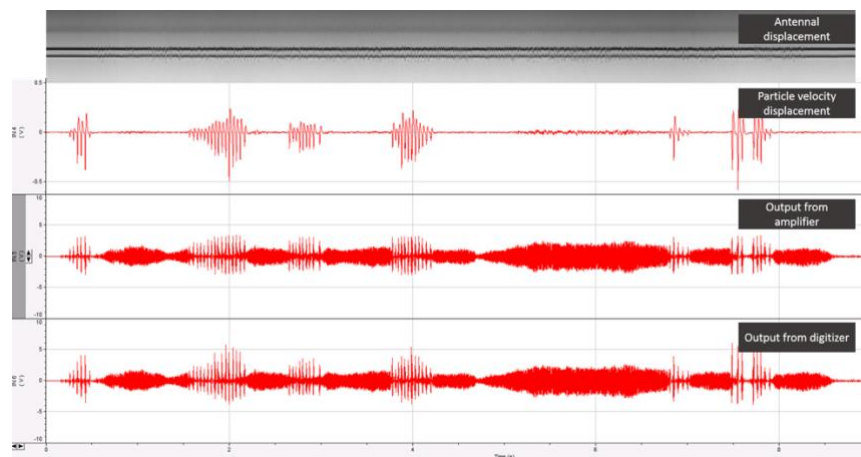
Figure 59: Output of the RCS stimulus from the signal generator & recording by a particle velocity meter from the earbud speaker.

Though the stimulus is attenuated as the signal goes from the digitizer to the amplifier, the output waveform recorded by the particle velocity meter is reflective of the original RCS stimulus. However the sine component is greatly reduced.

7.2.8 Image handling & analysis

The time series data was analysed using ImageJ software. A single region of interest (ROI) to encompass the whole organ was selected for each sample (**Fig 60A**). To select the ROI, key landmarks such extra cuticular bristles and areas of most fluorescence signal were used to detect the positioning of the JO within the image. ROI selection was maintained the same between the separate trials per sample. The time series analyser plugin for ImageJ was used to calculate the average signal intensity per frame in a time series (**Fig 60B**). Trigger points from the time series were manually extracted using ZEN software and matched to the output from ImageJ. Further processing and analysis was done using MATLAB.
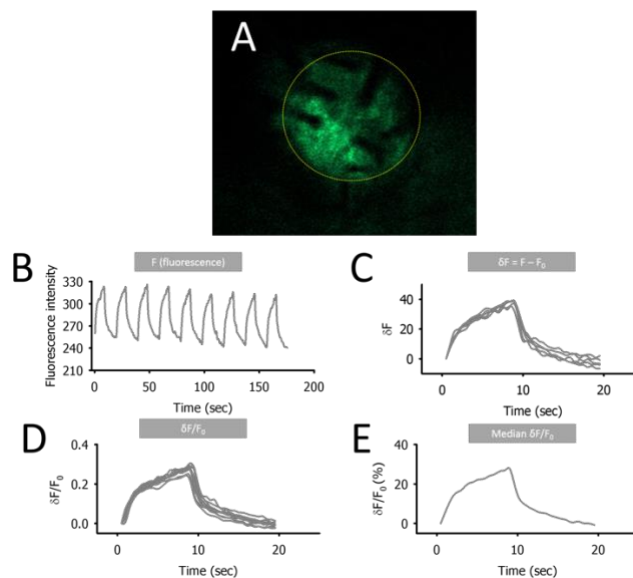
Figure 60: Protocol for extracting the changes in signal fluorescence in response to repeated sound stimulus in a series.
A: Shows the ROI selection. For all the tested samples, a ROI of the whole organ was taken.
B: From the ROI, the average intensity for each frame was calculated. Since for many protocols the stimulus was repeated multiple times, the data was visualised to assess whether there was any corruption in the recording. Each calcium transient was aligned based on the trigger signal encoded in the file and normalised to baseline (**C & D**). Then a median response of the stimulus was taken from the series and multiplied by 100 to give the % change in fluorescence signal (**E**).

During some trials where there was repeated exposure to the same stimulus (like the 2s APT, 9s APT and 9s RCS stimulus), the responses within the trace were separated into individual columns and each signal peak was normalised to baseline (F_0) (**Fig 60C**). Since there was a shift in baseline throughout the

recordings, the baseline for each individual stimulus presentation was calculated independently. Hence, F_0 was taken as the average fluorescence intensity of the 4 frames prior to each stimulus trigger. This change in signal intensity was then divided by F_0 to provide a ratiometric measure relative to baseline fluorescence (*ΔF/F₀*) (**Fig 60D**) This value was then multiplied by 100 to provide a percentage change in fluorescence intensity.

Response to repeated stimuli did not show decay over a period of a recording trial therefore, an average of the signal was constructed by folding the response along the trace to create one median response (**Fig 60 D&E**).

There were 3 primary ways in which the fluorescence signal was quantified:

Peak *ΔF/F₀* **:** This readout is the maximum *ΔF/F₀* of the response. This measure is
reported as a %.

Total *ΔF/F₀* **:** The total *ΔF/F₀* was calculated by taking the area integral of the *ΔF/F₀*
of the response from stimulus onset till stimulus offset. This measure is
reported as a %.

Time constant of the response

To better characterize the response, a three-parameter single exponential rise to maximum function and an exponential decay function were fitted to the response fluorescence signal (**Eq. 8 & 9**). *y0* is the constant displacement of the function, *a* denotes the amplitude and τ. The time constant measure is reported in seconds.

Equation 8: A three parameter single exponential function used to quantify the rise time of the response.

$$f(t) = y0 + a * (1 - e^{-\tau t})$$

(8)

Equation 9: A three parameter single exponential function used to quantify the decay time of the response.

$$f(t) = y0 + a * e^{(-\tau t)}$$

(9)

7.3 Results

7.3.1 Exposure to sound stimuli results in observable calcium transients within the JO
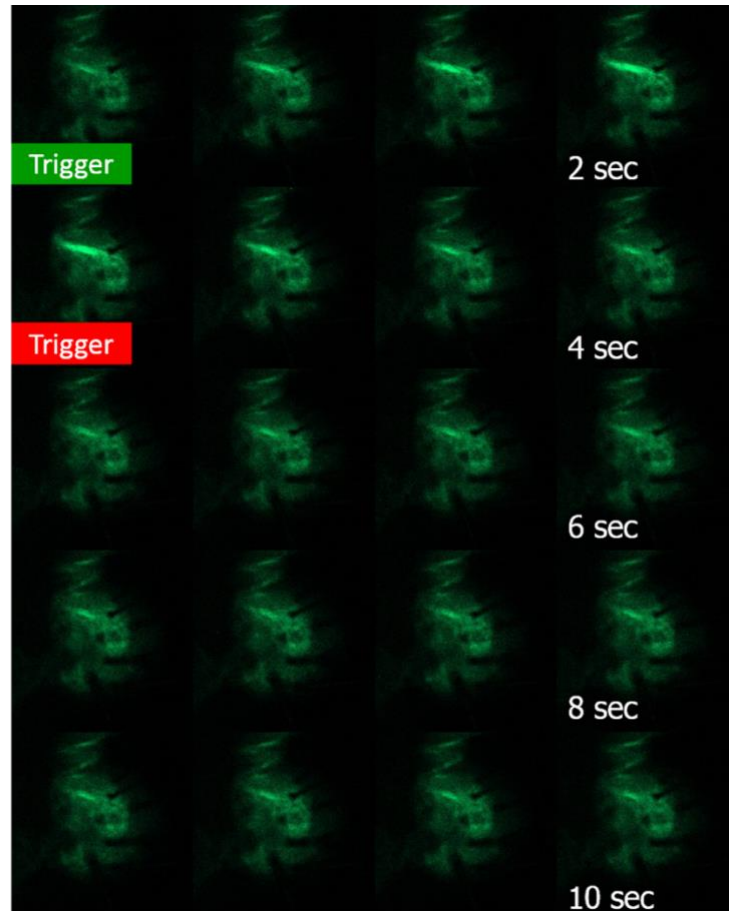
Figure 61: A series of time lapse images to show the changes in fluorescence signal in response to sound stimulus presentation of a single experimental fly expressing UAS-GCamp-6f in JO-all neurones.
A series of images captured showing the changes in fluorescence intensity of a single fly expressing GCaMP in JO-all neurons. The response is to the presentation of a 2s APT sound stimulus is in the first row. Images were captured at the rate of 500ms. As shown in the first two rows, there is a prominent increase in fluorescence when the sound stimulus is triggered and a decay in fluorescence is observed from stimulus offset.

Robust changes in fluorescence signal were observed within the JO in response to sound stimulus presentation (**Fig 61**). All variants of sound stimuli elicited calcium transients in JO-all flies. To probe the dynamics of the response, a comparison was made between the exposure to 2, 16 and 32s of continuous APT stimulus.

A summative effect of the signal was observed during prolonged exposure to the stimulus (**Fig 62A**). The average peak *ΔF/F0* for 2-s of APT stimulus presentation was 8.8% ± 2.87% whereas the average peak *ΔF/F0* for 16s and 32s of APT stimulus was 19.9% ± 6.54% and 20.7% ± 5.27% respectively. Significant differences between the peaks were found [$F_{(2,26)}= 17.632$, $p<0.001$, Repeated measures ANOVA] (**Fig 62B**). The response to 2s was significantly lower compared to the response to 16s and 32s of APT sound stimulus exposure ($p<0.001$ for both, post hoc comparisons using the Holm-Sidak method). Since there were no significant differences in the average peak *ΔF/F0* between 16s and 32s, it can be hypothesised that there is a saturation of response to the given sound stimulus somewhere between 2s and 16s.
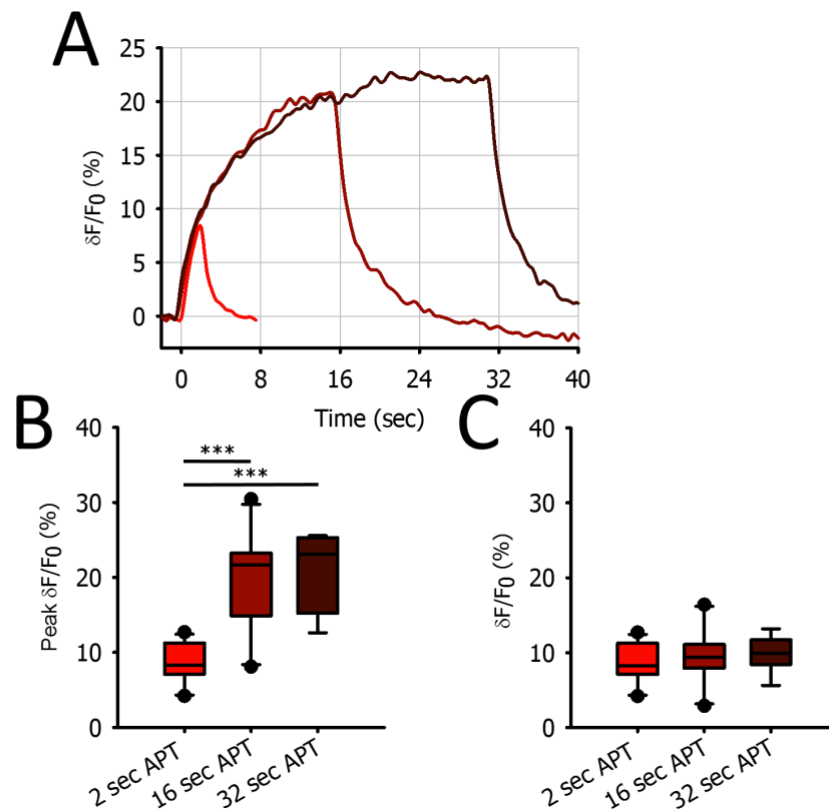
Figure 62: Fluorescence signal in response to 3 different lengths of the same stimuli.
A: Demonstrates the exponential rise of fluorescence intensity of JO-all flies in response to 3 stimuli: 2 sec, 16s and 32s APT stimulus presentation. **B:** The box plot presents the peak fluorescence intensity in response to the 3 stimuli. Calcium transients in response to prolonged stimuli were of higher magnitude. Box plots to show the level of fluorescence intensity at 2 seconds after sound stimulus trigger for the 3 conditions. The fluorescence intensity is comparable at this time point for all 3 conditions meaning that the increased peak in fluorescence levels for prolonged stimulus summate over a similar time course (**C**).

There was an exponential increase in fluorescence signal following from stimulus onset. The response kinetics were found to be the same for the 3 lengths of stimulation (**Fig 62A**). Comparing the response magnitude at 2s between these three lengths of stimuli, no significant differences were found [$F_{(2,26)}$= 0.267, p=0.768 ,one way ANOVA] (**Fig 62C**). At 2s into the stimulus presentation, average peak $\Delta F/F_0$ was 8.8% ± 2.87% for 2s stimulus, 9.52% ± 2.81% for 16-s and 9.8% ± 2.33% for 32s conditions. Each experimental animal was presented with all the sound stimuli in series with -2 min breaks between trials to allow for recovery. Since there were no significant changes in $\Delta F/F_0$, this outcome indicates that the system did not sensitize to the repeated exposures to the same stimulus.

7.3.2 Pymetrozine inhibits calcium influx in JO mechanosensory neurons

The response to sound stimulus of pymetrozine-treated flies is comparable to antenna-ablated flies (**chapter 5.3.2, page 74**). To test whether this deaf phenotype was due to the mechanism of action of the drug on JO function; JO-all expressing flies were administered with pymetrozine. Using the same protocol as used for the behavioural experiment (**methods 5.2.1, page 70**), experimental flies were placed onto food topped with the insecticide 24-h prior to the experiment, thus the method of administration of the drug was through ingestion.

There was no detectable change in fluorescence signal during the presentation of stimulus in pymetrozine-treated flies (**Fig 63B**). This was inherently different to the response of untreated JO-all flies (**Fig 63 A&C**) as this treatment group was found to be unresponsive to all sound stimuli. 32s of APT stimulus was also insufficient to induce calcium transients. This shows that pymetrozine has a full inhibitory effect on the JO sound-sensitive neurons rather than just a change in the relative sensitivity.
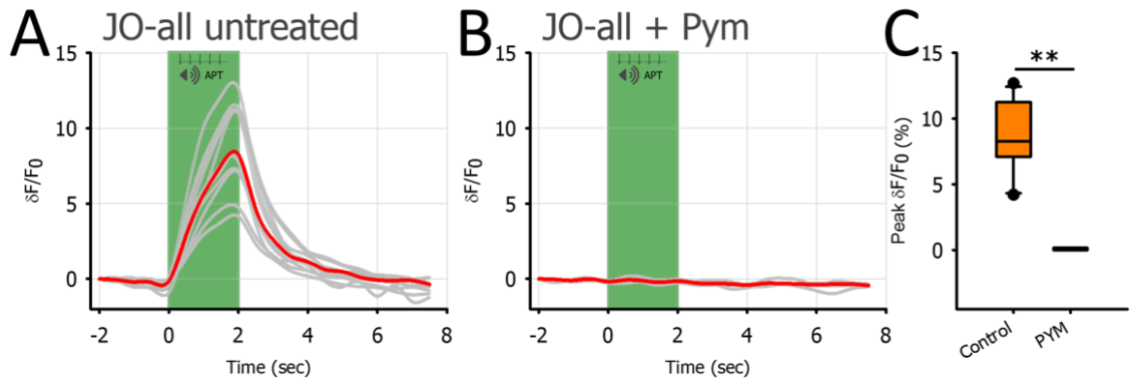
Figure 63: Sound-induced calcium transients in JO-all flies are abolished when the sample is treated with pymetrozine.

> Time series plots to show the calcium transient response recorded in JO-all flies. **A** shows responses of untreated flies and **B** of flies treated with pymetrozine. Pymetrozine-treated flies do not show calcium transients in response to sound stimulus presentation (**C**).

Visually inspecting the JO of the treatment group, the cells appeared swollen in all the pymetrozine-treated animals (n=5) (**Fig 63B**). This evident blebbing could be an indicator of apoptotic processes (Charras 2008). These findings provide an explanation for the inhibition of auditory-induced locomotor activity discussed in **chapter 5.3.2 (page 74)**. Additionally, these findings are consistent with previous reports on pymetrozine having selective effects on chordotonal mechanoreceptors (Ausborn et al., 2005).
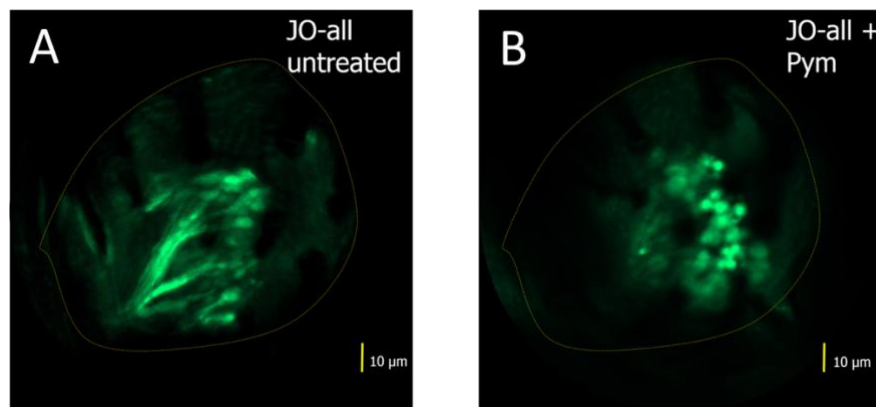
Figure 64: Captured images of the neurons & processes labelled with GCaMP in untreated and pymetrozine-treated flies.

> The images show the whole organ with the GCaMP-6f signal from all JO neurons. Imaging through the cuticle it is possible to see the cell bodies and processes. In pymetrozine-treated flies, the cell bodies appear brighter, circular and 'bloated' compared to untreated flies. These visual observations of the organ could be indicative of the apoptotic processes induced as a result of insecticide exposure.

7.3.3 Calcium transients in response to sound stimuli are dependent on JO sub-populations

Previous reports have demonstrated that the JO consists of a heterogenous population of neurons (Kamikouchi et al., 2009; Kamikouchi, Shimada, & Ito, 2006). To evaluate whether the presented sound stimuli induce calcium transients from specific sub-populations of JO neurons, the GCaMP-6f reporter was crossed with JO sub-population-specific drivers.
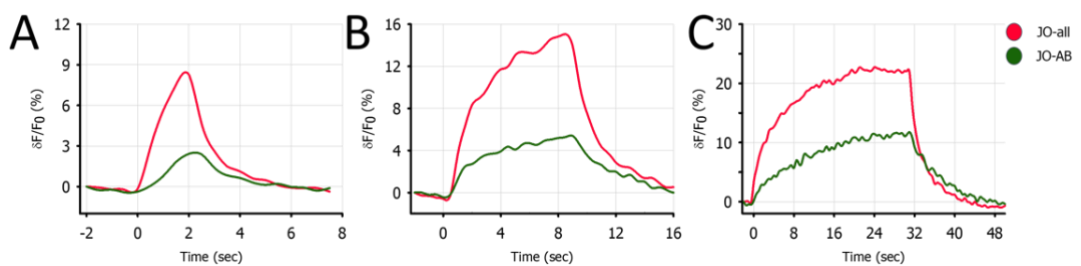
Figure 65: Time series plots to show the differential response calcium transients of GCaMP expressed in JO-all & JO-AB driver lines.
A: Shows the response to 2s APT stimulus presentation, **B** is the response observed to RCS stimuli and **C** is the response to a prolonged 32s APT stimulus. The response of JO-all is greater in magnitude compared to JO-AB for all the presented sound stimuli.

JO-AB flies showed robust calcium transients in response to sound stimuli. Similar to the responses observed for JO-all, there was an exponential increase in fluorescence signal following sound stimulus onset. For all stimuli presentations, JO-AB consistently showed lower response magnitude compared to JO-all flies (**Fig 65**). Comparisons indicated in **Table 20**. This relative difference between the driver lines indicates that the calcium signal observed in JO-all is not substantiated only by the JO-AB sub-population neurons expressed in the JO-AB driver.

Table 20: Summary table of the peak *ΔF/F$_0$* for JO-AB & JO-all in response to varying stimuli.

	2s APT stimulus		9s RCS stimulus		32s APT stimulus	
	JO-AB	JO-all	JO-AB	JO-all	JO-AB	JO-all
Peak *ΔF/F$_0$* (%)	2.46	8.27	5.03 ± 2.77	20.4 ± 13.1	12.2	23.1
Significance	U= 1, p= 0.002, Mann-Whitney U test		t(10)= 2.814, p=0.0184, t-test		U= 5, p= 0.0018, Mann-Whitney U test	

JO-AB showed significant differences in the average peak $\Delta F/F_0$ between stimulus conditions [$F_{(5,2)}$= 20.794, p<0.001, Repeated measures ANOVA]. The mean peak response to 32s APT stimuli was 11.4% ± 4.8%, which was significantly higher compared to RCS 5.03% ± 2.77% (p=0.002) and 2s of APT stimulus 2.7% ± 1.14% (p<0.001). The difference in the mean response between RCS and 2s APT was found to be insignificant (p=0.129).

For JO-all this comparison between stimulus conditions was also found to be significant [$F_{(10,2)}$= 9.225, p=0.004, Repeated measures ANOVA]. The mean peak $\Delta F/F_0$ response for 2s APT presentation was 8.8% ± 0.86% which was significantly lower compared to RCS 20.4% ± 5.35% (p=0.016) and 32s APT stimulus 20.7% ± 1.86% (p=0.008) (**Fig 66**). There are two assumptions that can be made from these findings. Firstly, this restates that the response observed in JO-all consists of more than what is captured by the expression of the JO-AB driver. And secondly that the activation properties for JO-AB expressing neurons differ to the neurons which additionally contributed to the JO-all response.
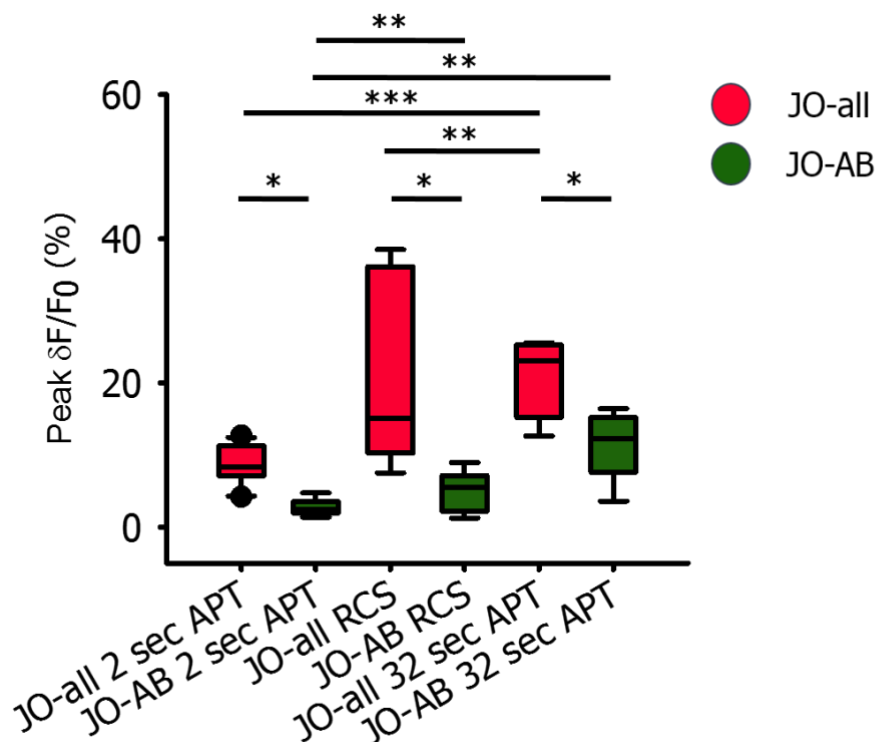
Figure 66: Box plots to show the differences in peak $\Delta F/F_0$ for JO-all & JO-AB flies in response to varying sound stimuli.

To dissect out the differences in the response properties between JO sub-populations and test the above assumptions; the JO-AB response was subtracted from JO-all for the 32s APT stimuli (**Fig 67 A&B**). The derived group was referred to as **JO-other** and represents the neurons additionally contributing to the response in JO-all expression. By subtracting one response from the other, it becomes evident that JO-AB and JO-other contribute proportionally to the response observed in the JO-all to 32s APT stimuli (**Fig 67B**).
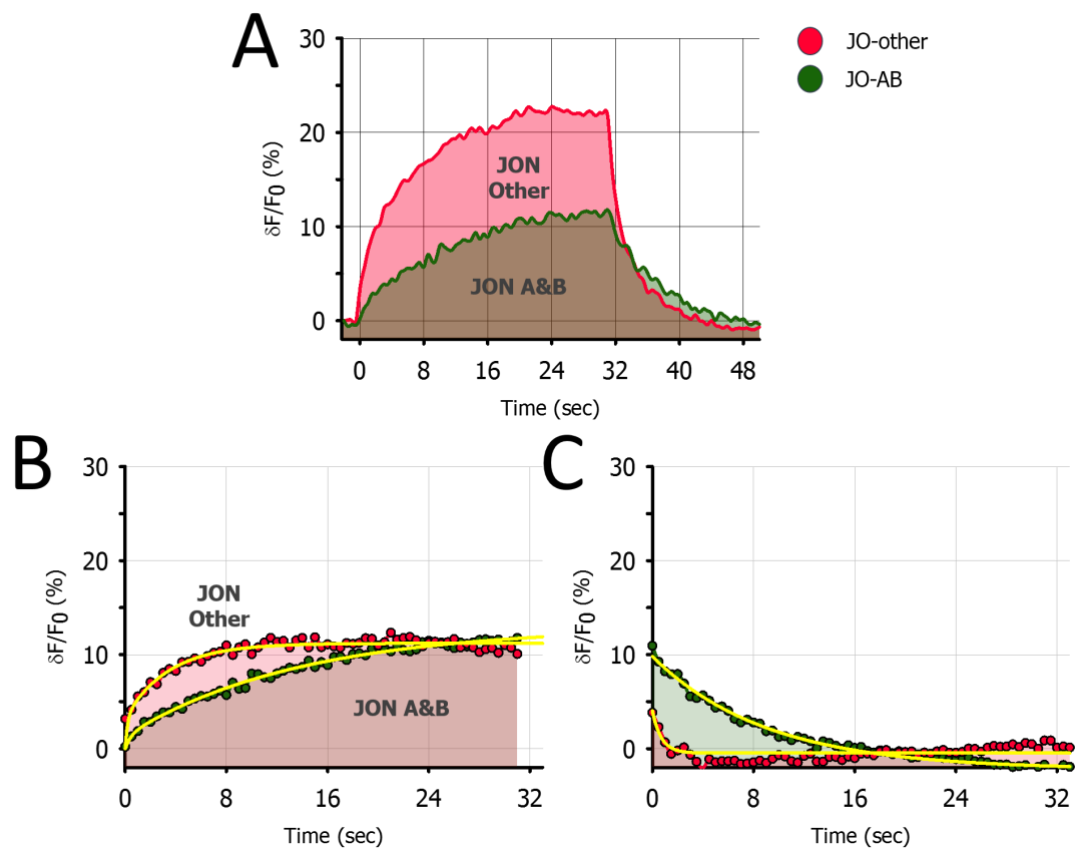
Figure 67: Area plots to compare the rise & decay time constants of the response of JO-AB & JO-other neurons (JO-other derived by subtracting JO-AB from JO-all).
A: Area plot to show the response of JO-all and JO-other in response to 32 sec APT sound stimuli. JO-other is derived by subtracting the response of JO-AB from JO-all. **B:** Double exponential function fitted to characterize the rise time properties of the JO-AB and JO-other responses. **C:** shows the fitting of the decay function to the decay of the fluorescence signal after stimulus offset.

The rise time constant for JO-other (3.41-s) exceeded the time constant of the response for JO-AB (12.66-s) (**Fig 67B, Eq. 8**). This demonstrates that response kinetics for JO-other was faster at reaching its asymptote. Similarly, fitting the decay function to the latter portion of the response starting from stimulus offset (**Fig 67C,**

Eq. 9). JO-other was found to have a time constant of 0.71 seconds whereas for JO-AB the time constant was 9s.

These findings show that JO-other and JO-AB have different response and adaptation properties. JO-other shows fast activation and rectification whereas the JO-AB response is slower and reaches its asymptotic peak later during prolonged stimulation.

Other JON sub-population specific driver lines were used to investigate whether the JO-other response can be attributed to other neuronal subtypes. JO-CE is specifically expressed in the C-E sub-population neurons. This sub-population is not thought to contribute to the processing of auditory signals (Effertz, Wiek, & Göpfert, 2011; Kamikouchi et al., 2009; Matsuo et al., 2014).

Consistent with previous reports, flies expressing GCaMP in JO-CE neurons did not show any calcium transients in response to sound stimulus presentation. Despite the sound producing tonic displacements of the sound receiver as evidenced by the line scan (described in protocol **section7.2.5, page 150**) this sub-population was found to be insensitive to this type of vibratory stimulus. Thus, the JO-other response cannot be attributed to the C-E sub-population neurons.

Next, another driver line was tested which is specific to the D sub-population neurons. This sub-population has been shown to be vibration sensitive with a specificity towards midrange frequencies of 100-200 Hz (Matsuo et al., 2014). However, no calcium transients were detected in response to any of the sound stimuli in JO-D flies. Based on this finding it can be concluded that the JO sub-population D is not sensitive to the presented sound stimuli within this study hence does not contribute to the observed response in JO-all expressing flies.

7.3.4 Differential response properties to APT & RCS stimuli

In **chapter 5.3.3 (page 77**) it was found that wild-type flies presented with RCS sound stimuli demonstrated greater auditory-induced locomotor activity compared to APT. To test whether this gain in responsiveness is related to changes in JO function, pairwise comparisons of calcium transients in response to APT and RCS

stimulus exposure were made for each experimental animal.

For JO-all flies, significant differences were found in the response properties for APT and RCS stimuli (**Fig 68A, Table 21**). In response to RCS, the median total *ΔF/F₀* was 256.1% which was significantly higher compared to APT stimuli [245.4%, Z=3.102, p=0.002, Wilcoxon Signed Rank test] (**Fig 68B**). There were also significant differences in the median peak *ΔF/F₀* between the stimulus conditions (**Fig 68B**). For RCS, the median peak *ΔF/F₀* was 16.3% which was significantly higher compared to APT [15.6%, Z=3.224, p=0.001, Wilcoxon Signed Rank test].

Figure 68: Comparison of the response to APT & RCS stimulus of JO-all flies
    A: Time series graph to show the changes in fluorescence intensity in response to APT and RCS stimulus presentation of JO-all flies. The response to RCS stimulus was of a significantly greater magnitude (**B & C**). The rise time constant was also significantly smaller for RCS stimuli indicating that the rise in the fluorescence intensity to asymptotic peak was faster (**D**). (** = p<0.01, ***= p<0.001, ****= p<0.0001).

Table 21: Summary of the response properties to APT & RCS stimuli of flies expressing GCaMP in JO-all & JO-AB neurons.

		JO-all (n=23)		JO-AB (n=8)	
		APT	RCS	APT	RCS
Total (%)	$\Delta F/F_0$	245.4	256.1	59.2 ± 20.5	59.5 ± 31.6
Peak (%)	$\Delta F/F_0$	15.6	16.3	4.95 ± 2.51	5.24 ± 1.77
Time constant (s)		3.6 ± 0.52	3.08 ± 0.49	3.29 ± 1.36	1.95 ± 1.43

The rise time constant of the JO-all responses was also found to be smaller for RCS in comparison to APT. The average time constant for the response to RCS stimuli was 3.07 ± 0.46 sec which was significantly faster compared to the average time constants for APT stimuli [3.6s ± 0.52s, t(22)= 5.584, p<0.001, Paired t-test] (**Fig 68C**).

Taking these findings together suggests that there is a differential response to RCS and APT stimulus in JO-all expressing flies. The calcium transients observed in response to RCS were found to have significantly larger amplitudes and reach the asymptotic peak faster in comparison to the responses recorded to APT sound stimuli.

To test whether these differences in the responses between the two stimuli are dependent upon the output of A&B sub-population JO neurons, the same comparisons were made for flies expressing the JO-AB driver line (**Fig 69A**).

Interestingly, there were no significant differences in response magnitude between APT and RCS stimulus conditions in JO-AB flies (**Fig 69 B&C**, **Table 21**). However, the differences in the rise time constants were maintained in the responses between the two stimuli. The mean time constant in response to RCS stimulus (1.95s ± 1.43s) was significantly faster compared to the average rise time constant in response to APT stimuli [3.29s ± 1.36s, t(7)= 4.121, p=0.004, Paired t-test] (**Fig 69D**). This demonstrates that the fluorescence intensity approaches its asymptotic peak faster in response to RCS stimuli.
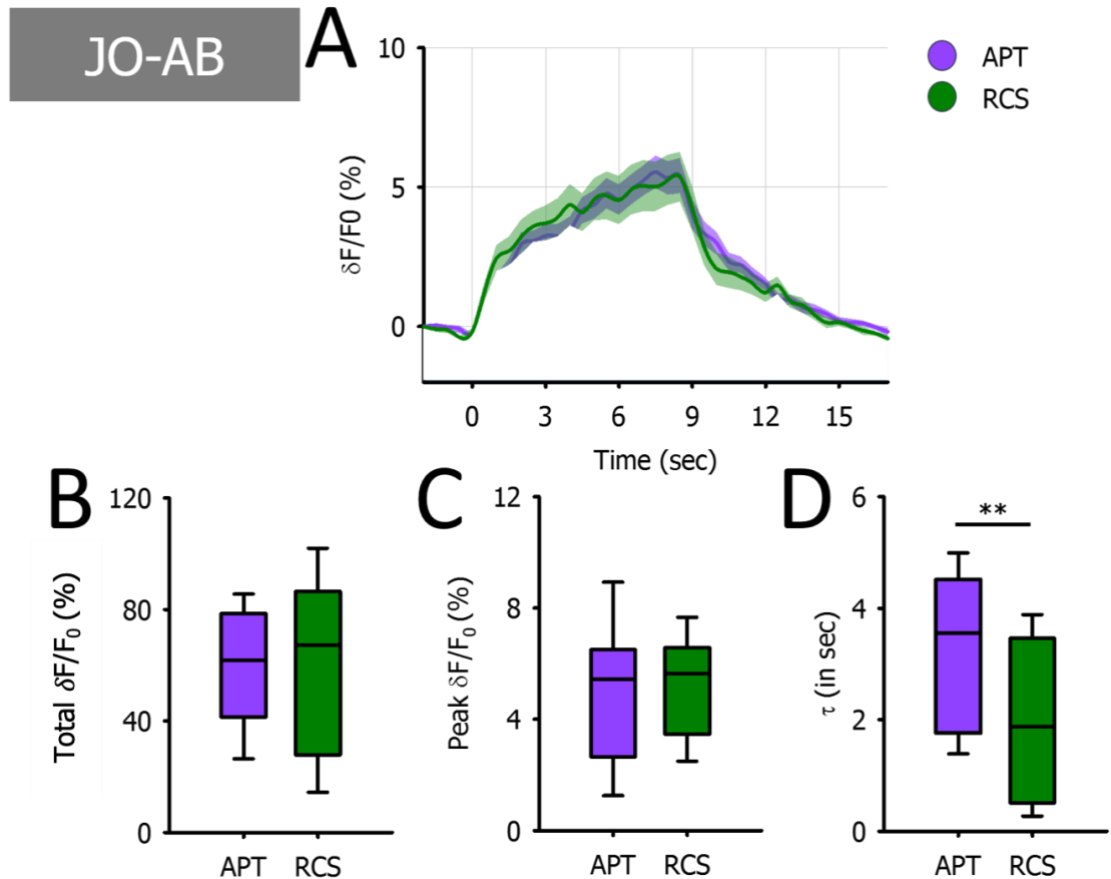
Figure 69: Comparison of the response to APT & RCS stimulus of JO-AB flies

A: Time series graph to show the changes in fluorescence intensity in response to APT and RCS stimulus presentation of JO-AB flies. The magnitude of the response of JO-AB flies was comparable to both presented stimuli (**B & C**). The rise time constant was significantly smaller for RCS stimuli indicating that the rise in the fluorescence intensity to asymptotic peak was faster (**D**). (** = $p < 0.01$).

In conclusion, similar to auditory-induced locomotor activity observed in the auditory behavioural assay, there is a gain in the calcium transients in response to RCS stimuli. The faster rise time constant of this response is a property shared by all JO neurons. Interestingly, JO-AB sub-population neurons which have previously been characterised as the sound sensitive sub-population, did not show increases in magnitude in the fluorescence intensity in response to RCS stimuli. This suggests that the larger response magnitude observed in JO-all elicited by RCS stimuli is due to the activation of neurons not captured by the expression of the JO-AB driver.

168

7.3.5 Calcium transients in response to APT & RCS at different time points in a circadian cycle

In **chapter 6.3.2** (**page 105**), it was found that auditory-induced locomotor activity undergoes periodic changes throughout the circadian day. Here, I investigate whether this behavioural modulation is due to changes in primary auditory function. It was hypothesised that if there is circadian modulation of JON function, presenting the same stimulus at different points throughout a 24-h period would result in observed differences in the response calcium transients. Groups of entrained JO-all flies were sampled at ZT3, ZT9 and ZT13. Furthermore, comparisons were made between APT and RCS responses at these time points to explore whether there is a change amongst these responses.

As anticipated, JO-all showed robust calcium transients in response to APT and RCS stimulus at ZT3 (**Fig 70A**). At this time point there were no significant differences in the total $\Delta F/F_0$ or the peak $\Delta F/F_0$ between APT and RCS responses [for peak $\Delta F/F_0$: t(6)= -1.384, p=0.216, Paired t-test. For total $\Delta F/F_0$: Z= 0.338, p= 0.813, Wilcoxon Signed Rank] (**Fig 70 B&C, Table 22**). However, the median rise time constant for RCS was faster compared to APT. For RCS the median time constant was 3.17s, whereas for APT stimuli it was 3.53s [Z= -2.366, p=0.0016, Wilcoxon Signed Rank test] (**Fig 70D, Table 22**). These findings suggest that there are no differences in response magnitude in JO-all at ZT3 for the two sound stimuli. However, the change in fluorescence signal was observed to be faster in response to RCS presentation.
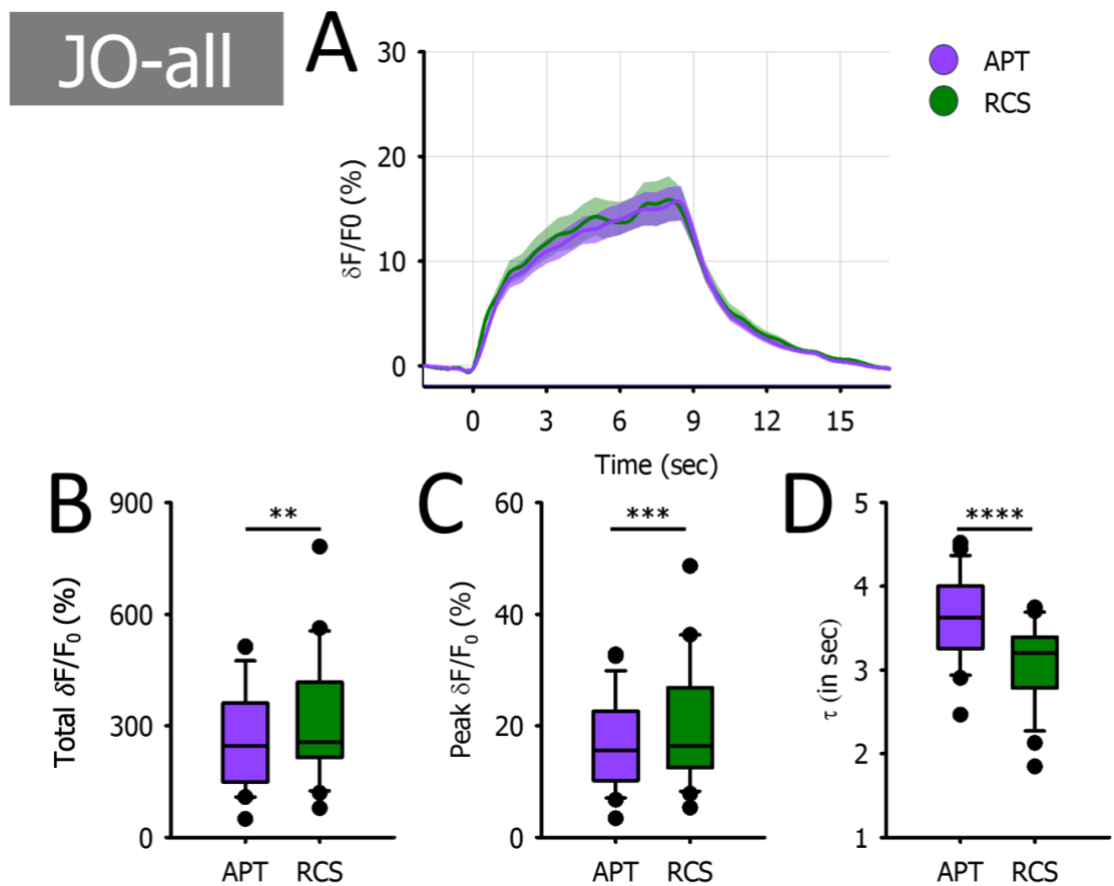
Figure 70: Comparison of the response to APT & RCS stimuli of JO-all flies at ZT3.
A: Time series graph to show the changes in fluorescence intensity in response to APT and RCS stimuli of JO-all flies at ZT3. There are no significant differences in the magnitude of the response to the two stimuli (**B & C**), however the rise time constant for RCS stimuli was found to be significantly smaller (**D**). (******=p<0.01).

Table 22: Summary table of the response properties to APT & RCS stimuli of JO-all flies at ZT3.

	JO-all ZT3 (n=8)	
	APT	RCS
Total $\Delta F/F_0$ (%)	243.4	250.8
Peak $\Delta F/F_0$ (%)	12.7	14.1
Time constant (s)	3.53	3.17

Visually inspecting the response characteristics in the time series graph (**Fig 70A**), it is evident that there are a series of prominent dips in the fluorescence signal recorded in response to RCS stimulus presentation. When aligning the response time series with the RCS trace waveform, the graph suggests that the depressions in response align to the presentation of the sine components within the sound stimulus (**Fig 71**). It is possible that the neurons expressed in JO-all are

unresponsive to these sine components within the natural courtship song, thus resulting in depressions in the signal. Or as seen in **figure 59** (**page 153**), it is possible that the sine component is greatly attenuated during stimulus delivery resulting in a reduction of fluorescence signal. This assumption would however require further investigation.
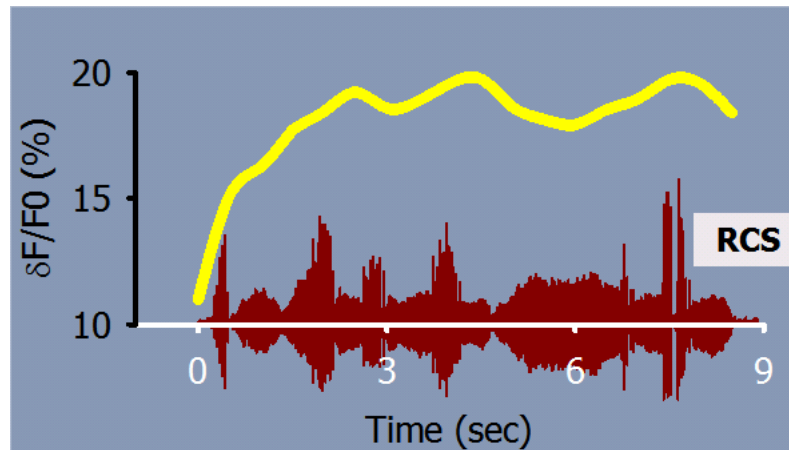
Figure 71: Finer details of the changes in fluorescence intensity shown in relation to RCS stimuli waveform.
The dips in the calcium signal align to the presentation of the sine components of the given stimulus.

At ZT9, there was also no differences found in the total $\Delta F/F_0$ in response to APT and RCS stimuli [t(6)= -2.201, p=0.07, Paired t-test] (**Fig 72B, Table 23**). However, there were significant differences in the peak $\Delta F/F_0$ (**Fig 72C**). The mean peak $\Delta F/F_0$ for APT was 19.3% ± 9.47% whereas for RCS the mean peak in the response was 21.7% ± 10.4% [t(6)= -2.691, p=0.036, Paired t-test]. Unlike what was observed at ZT3, there were no significant differences in the rise time constants between APT and RCS stimuli [t(6)=1.438, p=0.2, Paired t-test] (**Fig 72D**).

Table 23: Summary table of the response properties to APT & RCS stimuli of JO-all flies at ZT9.

|	JO-all ZT9 (n=7)	
	APT	RCS
Total $\Delta F/F_0$ (%)	309.9 ± 153.6	343.8 ± 165
Peak $\Delta F/F_0$ (%)	19.3 ± 9.47	21.7 ± 10.4
Time constant (s)	3.3 ± 0.64	3 ± 0.56
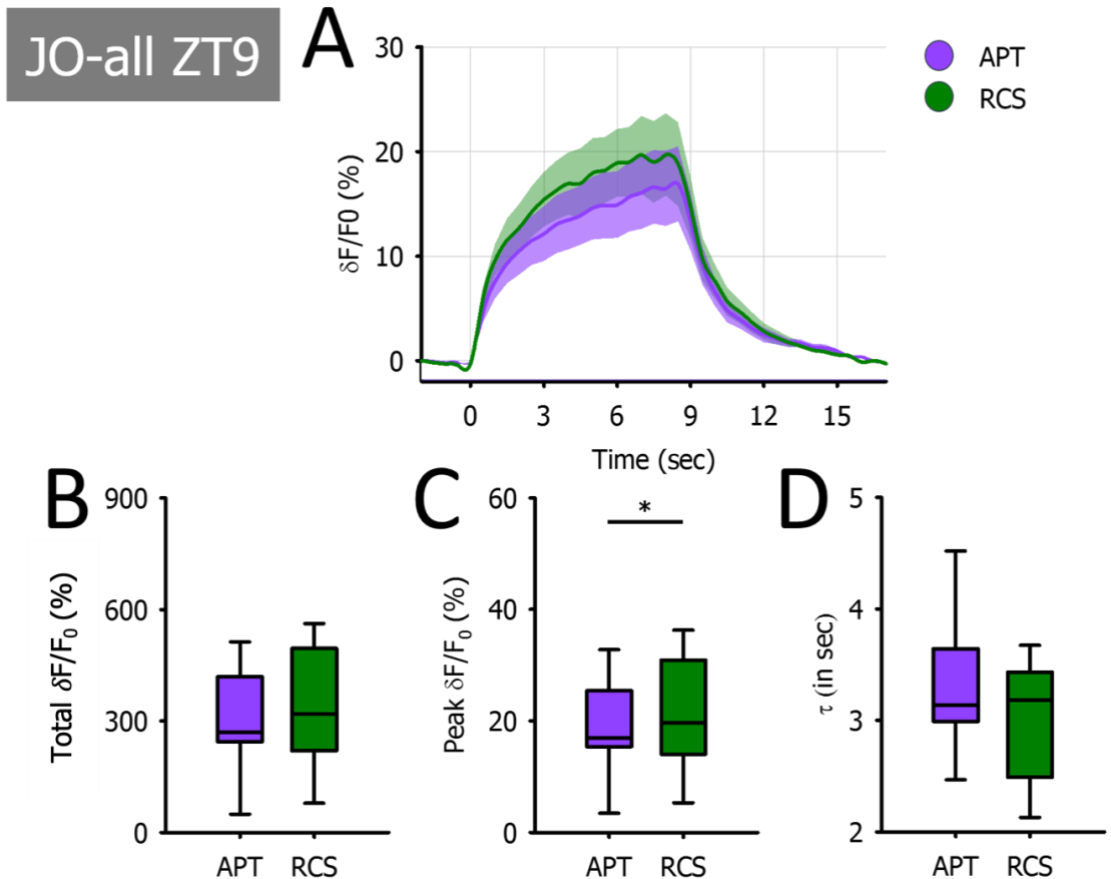
Figure 72: Comparison of the response to APT & RCS stimuli of JO-all flies at ZT9.
A: Time series graph to show the changes in fluorescence intensity in response to APT and RCS stimuli of JO-all flies at ZT9. There are no significant differences in the total $\Delta F/F_0$ signal however the peak $\Delta F/F_0$ to RCS stimuli was found to be significantly larger (**B & C**). No significant differences were found in the rise time constants between the responses to the two stimuli (**D**). (*=p<0.05).

At ZT13, JO-all showed differences in the response to APT and RCS stimuli (**Fig 73A, Table 24**). The median total $\Delta F/F_0$ was significantly greater for RCS (256.1%) compared to APT [245.4%, Z=2.666, p=0.004, Wilcoxon Signed Rank test] (**Fig 73B**). The mean peak $\Delta F/F_0$ was also significantly greater for RCS responses (21.9% ± 13.9%) in comparison to APT [17% ± 8.81%, t(8)= -2.737, p=0.026, Paired t-test] (**Fig 73C**). Lastly, the mean rise time constant for RCS was 3.24s ± 0.38s which was significantly faster compared to the mean rise time constant for APT [3.94s ± 0.35s, t(8)= 4.495, p=0.002, Paired t-test] (**Fig 73D**).
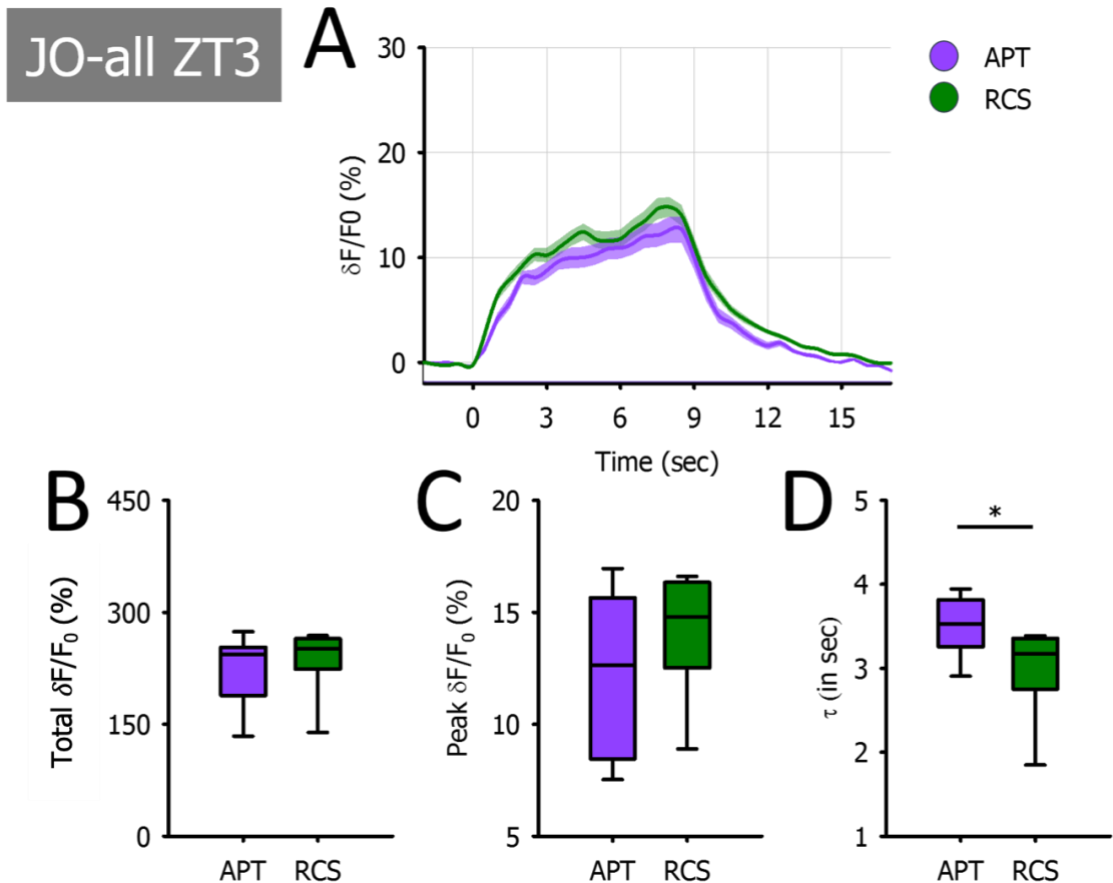
172
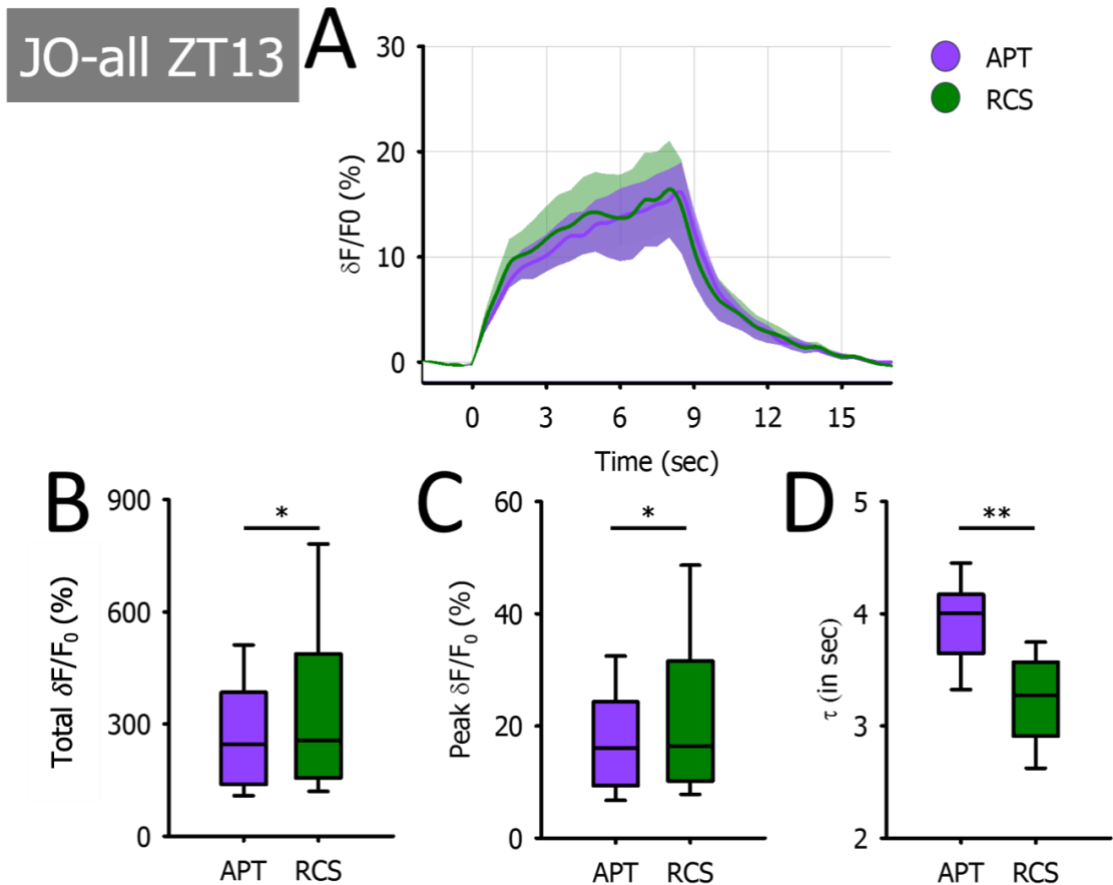
Figure 73: Comparison of the response to APT & RCS stimuli of JO-all flies at ZT13.
A: Time series graph to show the changes in fluorescence intensity in response to APT and RCS stimuli of JO-all flies at ZT13. There were significant differences in the total $\Delta F/F_0$ and the peak $\Delta F/F_0$ between the responses to APT and RCS stimuli. The magnitude of the response was greater for RCS stimuli (**B & C**). The rise time constant was also significantly smaller in response to RCS stimuli (**D**). (*=p<0.05, **=p<0.01).

Table 24: Summary table of the response properties to APT & RCS stimuli of JO-all flies at ZT13.

	JO-all ZT13 (n=9)	
	APT	RCS
Total $\Delta F/F_0$ (%)	245.4	256.1
Peak $\Delta F/F_0$ (%)	17 ± 8.81	21.9 ± 13.9
Time constant (s)	3.94 ± 0.35	3.24 ± 0.38

Next, the response properties for RCS and APT stimuli were compared between ZT3, ZT9 and ZT13 (**Fig 74, Table 25**). Though there was variation in the total and peak $\Delta F/F_0$, there were no significant differences between the group means between the sampled time points (**Fig 74A,B,D,E**). The rise time constant for RCS also didn't show significant variation between the groups. However, there were

significant differences in the mean rise time constants for APT [F(2,20)= 4.149, p=0.031, One way ANOVA]. The mean rise time constant for the response at ZT9 was 3.3s ± 0.64s which was significantly faster compared to ZT13 3.94s ± 0.35s (p=0.037, Halm-Sidak method used for post hoc comparisons) (**Fig 74C**). This demonstrates that the change in fluorescence signal at ZT9 was significantly faster compared to the responses recorded at ZT13.

Table 25: Summary of the response properties to APT & RCS stimuli at ZT3, ZT9 & ZT13.

	Total $\Delta F/F_0$ (%)		Peak $\Delta F/F_0$ (%)		Time constant (s)	
	APT	RCS	APT	RCS	APT	RCS
ZT3	2.19 ± 0.49	2.34 ± 0.45	12.7 ± 3.59	14.1 ± 2.69	3.48 ± 0.358	2.94 ± 0.55
ZT9	3.1 ± 1.54	3.44 ± 1.65	19.3 ± 9.47	21.7 ± 10.4	3.3 ± 0.64	3 ± 0.55
ZT13	2.64 ± 1.41	3.42 ± 2.2	17 ± 8.81	21.9 ± 13.9	3.94 ± 0.35	3.24 ± 0.38
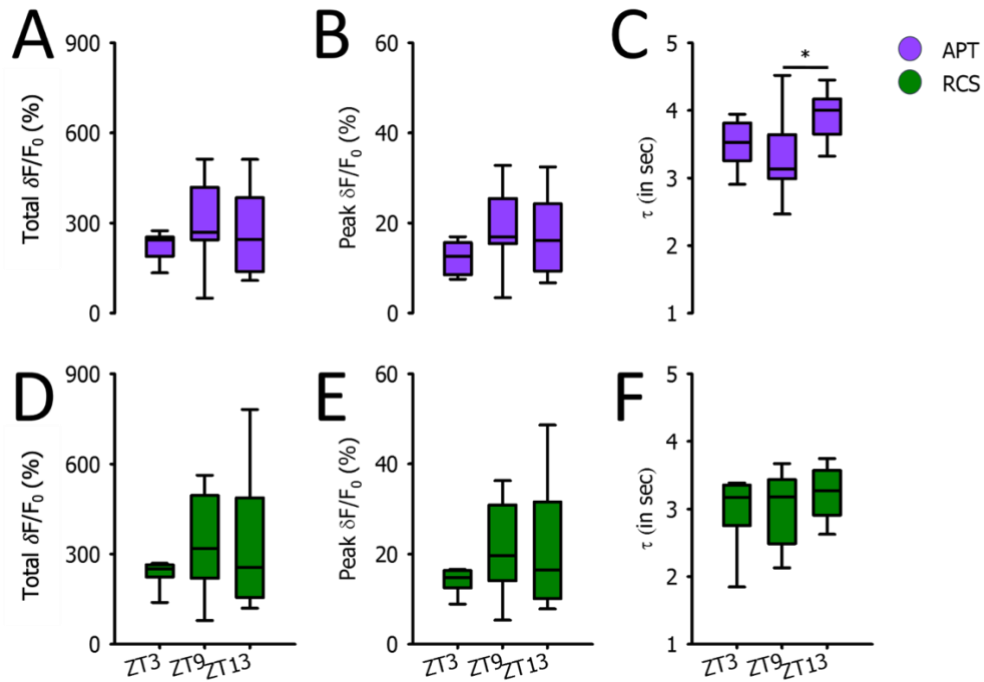
Figure 74: Series of box plots to compare the response properties to APT & RCS stimuli at 3 different assayed time points.
A-C: Shows the response properties to APT stimulus for 3 time points, ZT3, ZT9 and ZT13. The rise time constant for ZT13 was found to be significantly greater compared to ZT9 (**C**). There were no significant differences in the response properties to RCS stimuli at the different assayed time points.

There are two main conclusions to be drawn from the above findings. Firstly, the signal magnitude in response to APT and RCS does not show significant differences between the assayed time points. Still, there were significant differences found in the rise time constants between ZT9 and ZT13 for APT stimuli; suggesting that at ZT9 the fluorescence signal has a faster rate of change. Secondly, there was a change in differences between APT and RCS at the tested time points. This suggests that there is a change in the relationship between the responses throughout this time course. Taken together, these findings suggest that rather than there being a difference in the response properties between the time points, there is circadian modulation of the relative change in sensitivity between APT and RCS.

7.3.6 Calcium transients in response to APT and RCS in flies kept in constant light conditions
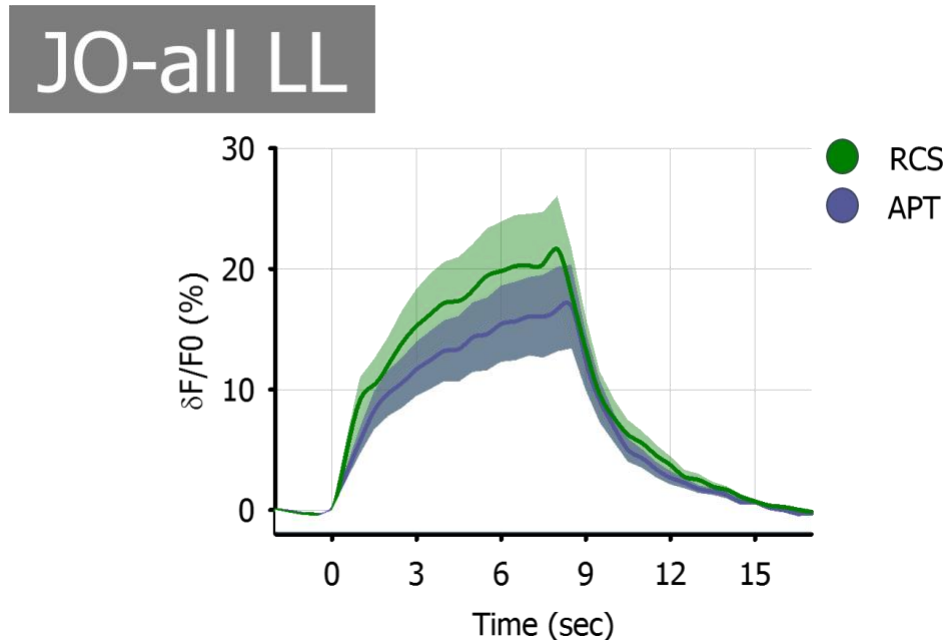
Figure 75: Time series graph to show the response to APT & RCS stimuli of JO-all flies kept in constant light conditions.

In **chapter 6.3.2** (**page 105**) it was found that wild-type flies kept in LL conditions showed an increase in auditory-induced locomotor activity gain in comparison to flies reared and tested in LD. To probe whether this behavioural effect can be attributed to changes in JO function, the calcium transients in response to APT and RCS stimuli of JO-all expressing flies kept in LL were compared to JO-all flies kept in LD conditions.

JO-all LL flies showed robust calcium transients in response to both APT and RCS stimuli (**Fig 75**) and as observed for JO-all LD flies, the responses to RCS were of greater magnitude and displayed faster rise time constants (**Table 26**). The median total $\Delta F/F_0$ for RCS was 339.5% which was significantly larger compared to APT [267.5%, Z= 3.419, p<0.001, Wilcoxon Signed Rank test]. The median peak $\Delta F/F_0$ for responses to RCS was also significantly greater at 21.6% compared to 16.9% [Z= 3.549, p<0.001, Wilcoxon Signed Rank test]. And finally the mean rise time constant was faster for RCS (2.22s ± 0.674s) compared to responses to APT [2.76-s ± 0.59s, t(16)= 4.624, p<0.001, Paired t-test].

Table 26: Summary table of the response properties to APT & RCS stimuli of JO-all flies kept in constant light conditions.

	JO-all LL (n=18)	
	APT	RCS
Total $\Delta F/F_0$ (%)	267.5	339.5
Peak $\Delta F/F_0$ (%)	16.9	21.6
Time constant (s)	2.76 ± 0.59	2.22 ± 0.67

When comparing these measurements between JO-all LL and JO-all LD, there were no significant differences in the means between the conditions for total $\Delta F/F_0$ and peak $\Delta F/F_0$ (**Fig 76A,B,D,E**). Nevertheless, JO-all LL showed significantly smaller time constants in the response to both APT and RCS. In response to RCS stimuli, the mean rise time constant for JO-all LL was 2.22s ± 0.67s which was significantly faster compared to the mean rise time constant of JO-all LD flies in response to the same sound stimulus [3.08s ± 0.49s, t(39)=4.789, p<0.0001, t-test] (**Fig 76F**). Similarly, the mean time constant in response to APT stimulus was 2.76s ± 0.59s for JO-all LL conditions and 3.6-s ± 0.52-s for JO-all LD conditions [t(39)=4.726, p<0.0001, t-test] (**Fig 76C**).
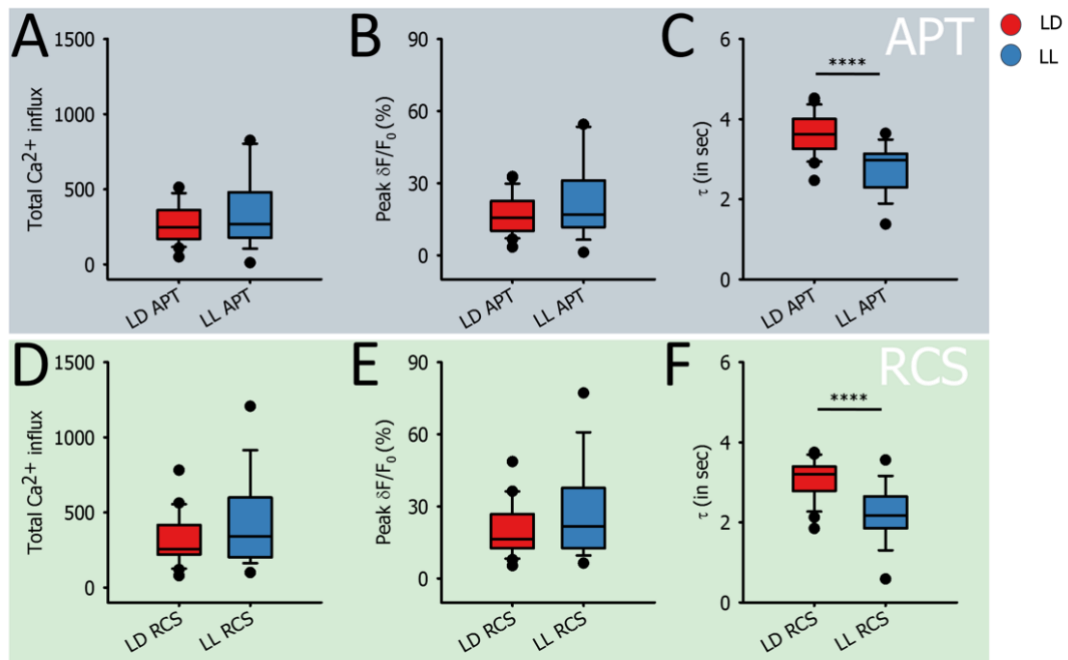
Figure 76: Series of box plots comparing the response properties to APT & RCS stimuli of JO-all flies kept in LD & in LL conditions.
A-B. D-E: There are no significant differences in the magnitude of the response to APT and RCS stimulus between entrained and constant light exposed JO-all flies. However the rise time constant in response to both sound stimuli was significantly smaller for JO-all flies exposed to constant light (**C,E**).

In summary, as was observed in JO-all flies in LD conditions, JO-all flies in LL conditions also demonstrate larger calcium transients with faster activation kinetics in response to RCS stimuli compared to APT. Thus, it can be concluded that constant light does not affect the relationship of these responses between the two sound stimuli. Also, interestingly JO-all flies in LL conditions showed faster change in fluorescence signal in response to both APT and RCS stimuli. This change was found to be significant compared to JO-all flies kept in LD conditions.

7.3.7 Response behaviour to sound stimuli during environmental light/ dark conditions

A suppression of auditory-induced locomotor activity was observed during the light phase in LD conditions in the auditory behavioural assay (**chapter 6.3.8, page 129**). To probe whether exposure to light has an effect on the function of JO neurons, a comparison was made of responses to sound stimuli in light and in dark conditions. The experimental sample was exposed to the either light or dark for 20 min prior to testing. The ambient light in the room was used as the independent variable. Measurements of the light conditions using a DAMSystem monitor were comparable with the environmental conditions in the behavioural experiments.

JO-all did not show significant differences in the total $\Delta F/F_0$, peak $\Delta F/F_0$ or rise time constants in response to 2s APT stimulus in light and dark environmental conditions (**Fig 77,78, Table 27**). From this, it is possible to conclude that environmental light conditions do not have an effect on the magnitude or kinetics of the calcium transients elicited in response to sound stimuli. Yet it should be emphasised that the experimental animals were only exposed to the environmental light conditions for 20 minutes prior to testing, so perhaps this length of exposure is insufficient to produce changes to JO response properties.
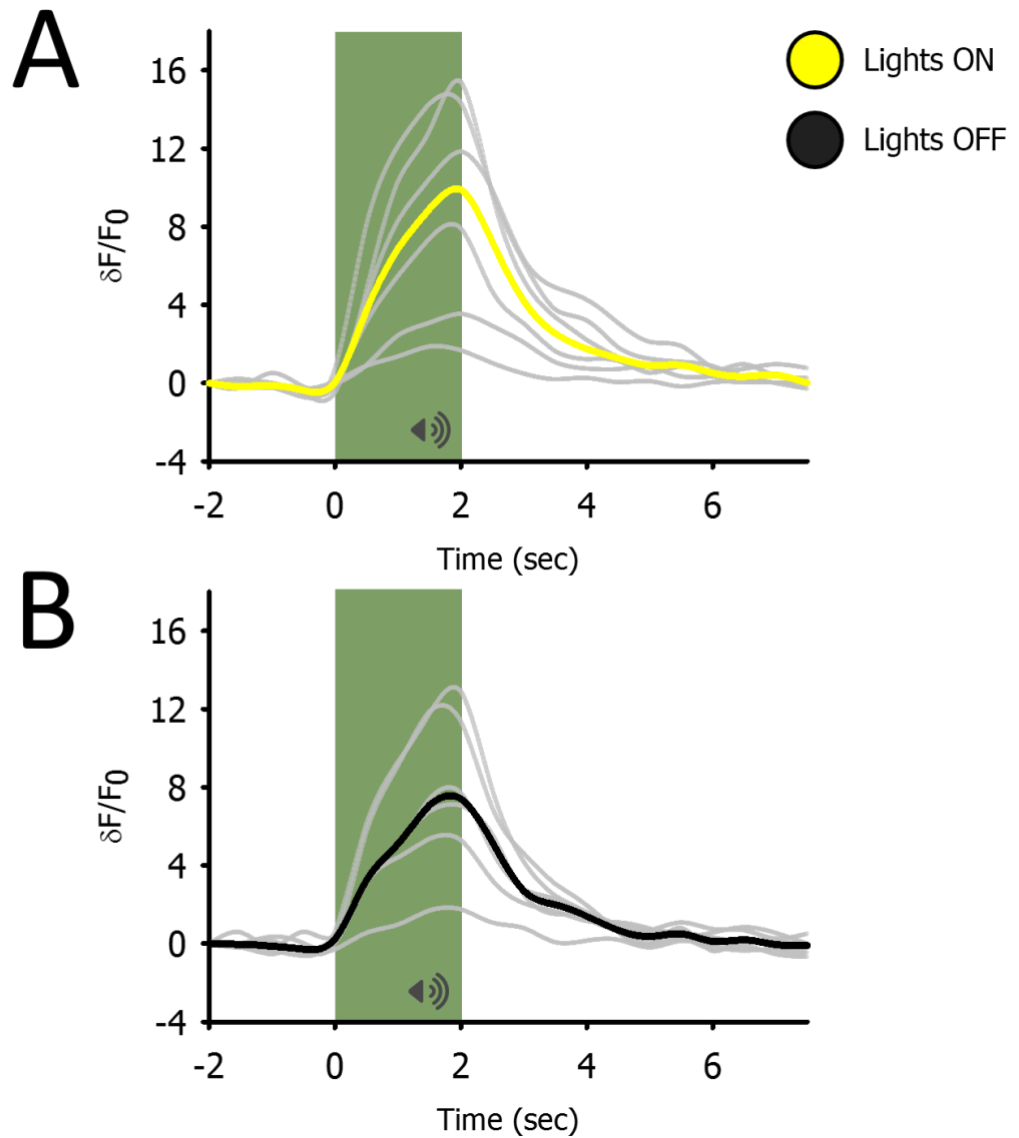
Figure 77: Time series graphs to show the individual & average response to sound stimuli exposure of JO-all flies in light & in dark environmental conditions.
A: Individual responses to 2s of APT stimulus shown in grey and the average change in fluorescence intensity is shown in yellow for JO-all flies responding to the stimulus in light environmental conditions. **B:** Shows the individual (in grey) and average (in black) response of JO-all flies to 2s of APT stimulus in dark environmental conditions. Observable calcium transients are found in both experimental conditions.

Table 27: Summary of the response properties to APT stimulus of JO-all flies in light & dark environmental conditions.

	JO-all (n=6)	
	Light	Dark
Total $\Delta F/F_0$ (%)	43.4 ± 27.1	36 ± 18.6
Peak $\Delta F/F_0$ (%)	9.18 ± 5.64	7.79 ± 4.13
Time constant (s)	1.4 ± 0.64	1.26 ± 0.78
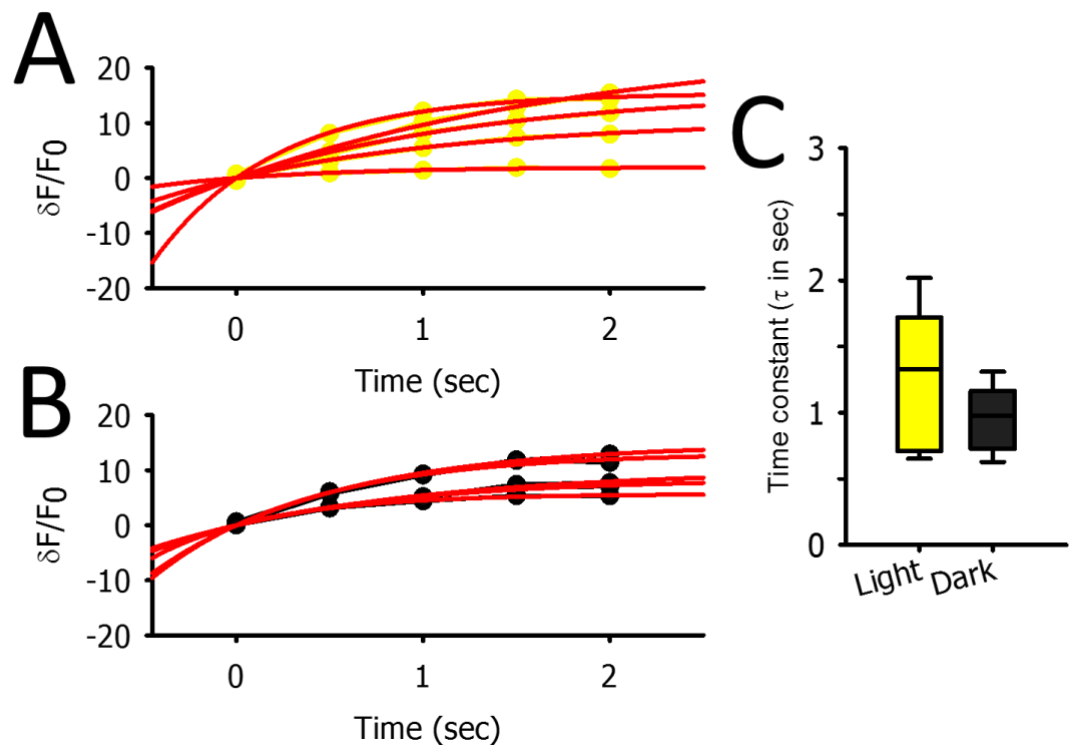
Figure 78: Rise time constants in response to APT stimulus of JO-all flies in light & in dark environmental conditions.
A&B: Show the first part of the time trace where the stimulus is presented from 0. A single exponential function is fitted to this rise to extract the time constant. There were no significant differences in the time constants for the responses between these two conditions (**C**

7.4 Discussion

The developed live-fly preparation presented within this chapter has allowed for the assessment of intracellular calcium signals from JO sensory neurons by imaging through the cuticle of the second antennal segment. By expressing the genetically encoded calcium sensor GCaMP-6f, it was possible to visualise the response properties of the neurons within the organ and probe how this response varied dependent on the presented stimulus and environmental conditions.

Changes in signal fluorescence were elicited by presentation of sound stimuli in JONs. Total *ΔF/Fo* and peak *ΔF/Fo* were used as measures to quantify the magnitude of the response whereas the rise time constant was used to quantify the kinetics of the signal. Changes in these parameters represent changes in intracellular calcium levels which underlie neuronal activity of JONs. While the temporal resolution of the GCaMP-6f is reduced, these recordings provide an arguably direct, albeit slow readout of JON spiking.

Here, I make some general assumptions on how neuronal activity is reflected in the calcium transients. This will help with interpreting what changes in the recorded signal parameters suggest about the electrophysiological function of JONs. GCaMP-6f has its own inherent properties which should be factored into this. The magnitude of the signal is not only determined by the number of spike bursts but also the frequency at which these occur. With the GCaMP-6f sensor, individual spikes within a burst result in an exponential increase in fluorescence levels unless separated by 50-75ms intervals (Chen et al., 2013). Thus, if the frequency of the spiking events (which results in changes in intracellular calcium) exceeds the decay constant of the GCaMP-6f sensor, there is non-linear summation of the signal. This synchronous release of intracellular calcium is reflected in the rise time constants of the signal. Hence it can be assumed that the larger the inter-spike interval gap, the slower the rate of change of the fluorescence signal (**Fig 80**).
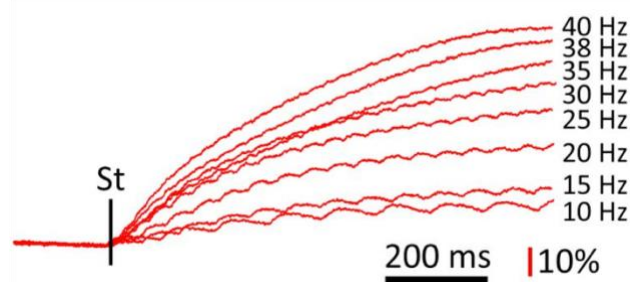
Figure 79: Example of summation of GCaMP-6f signal in high frequency firing from hippocampal neurons stimulated at different rates.
This time series plot demonstrates the properties of the GCaMP-6f calcium indicator in response to increases in firing rate. (Reference for figure: (Li et al., 2019)).

Due to the structure of the JO, there are no single cell recordings of JONs. However, extracellular potentials recorded from the antennal nerve, which include axons

projecting from JO mechanosensory neurons, provide insight into the electrophysiological properties of the system. Both sine and pulse components of a courtship stimulus elicit sound-evoked potentials upon presentation (Eberl et al., 2000; Effertz, Nadrowski, Piepenbrock, Albert, & Göpfert, 2012).
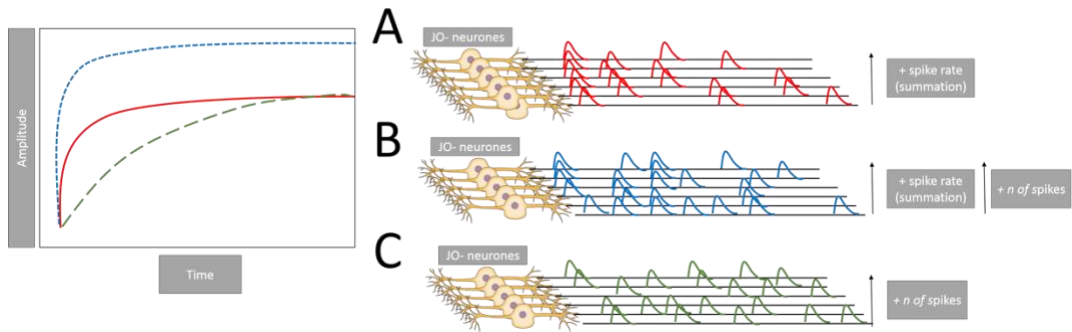
Figure 80: Proposed model to explain the electrophysiological basis of the changes in fluorescence intensity during stimulus presentation.
Two independent variables contribute to the response properties of the fluorescence signal; the number of spike bursts and the frequency of firing. Neural activity results in intracellular calcium transients which change the levels of fluorescence signal based on the concentration of calcium ions. In a system where there is an increase in the firing rate of the neuron, there is a summation of the calcium signal, resulting in faster time constants of the response signal (**A**). However, if there are the same amount of spike bursts but a decrease in the rate of firing, the calcium indicator has time to drop back towards baseline between bursts, resulting in a response which is of the same magnitude as **A** but with an increased rise time (**C**). If there is an increase in both the firing rate and the number of bursts, this results in a fluorescence signal which is both larger in magnitude and has a greater rate of change (**B**).

It is well established that sub-population A and B JONs consist of sound-sensitive mechanoreceptors (Kamikouchi et al., 2009). Considering there were no calcium transients in response to sound stimuli with GCaMP expressed in JO-D and JO-CE neurons; it was surprising to find that there was a discrepancy between the responses of the JO-all and JO-AB to sound stimuli. JO-all showed significantly larger increases in fluorescence signal in response to sound stimulus presentation.

These differences in response can be partly explained by the differences in the driver lines. Extensive classification of the varying JO driver strains specific to all or some sub-populations has been described in Kamikouchi et al (2006). The JO-all strain (referred to as JO1 and NP0761 within the reference paper) was found to be expressed in nearly all ~500 JO neurons. Visualising the expression of this driver

saw the projections of the JO neuron terminals distributed throughout all of the AMMC. The JO-AB driver (also referred to as JO15 in the reference paper) was found to be expressed only in the A and B sub-populations, with the JO neuron projections synapsing in zones A and B in the AMMC accordingly. By systemic analysis of labelled neurons in the JO, it was predicted that there are ~159 population A neurons and ~141 population B. Whereas counting the labelled neurons in JO-AB, roughly ~145 cells were found. Thus, not all the neurons in the associated zones are labelled. The JO-AB strain was found to label all subareas in zone A but a distinct lack of expression was found in the central part of zone B. JO A and B sub-populations can further be subdivided into groups based on anatomic and physiologic distinctions (Carr et al., 2017). Sub-population B can be subdivided into two clusters of JO-B1 and JO-B0. JO-B1 is sparsely contributed by the JO-AB driver line. Taking these findings together, it shows that the JO-AB driver, though captures the two sub-populations, it is incomplete in its expression of sub-population B1.

In section **7.3.3 (page 160)**, the response fluorescence signal in JO-all was found to be double that of JO-AB. This is consistent with the findings presented in the previous paragraphs denoting that there are roughly half the cells, primarily from JO sub-population B1, unaccounted for within the JO-AB driver line. Thus, this suggests that the signal response properties of JO-other discussed in **section 7.3.3** can be attributed to the JO-B1 sub-population. JO-other was derived by subtracting the signal of JO-AB from JO-all. This derived signal was found to have the same response magnitude as the JO-AB driver. Additionally, the JO-other response had faster rise time kinetics. From this it can be assumed that the JO-B1 sub-population had increased synchrony in neuronal activity leading to a faster rate of change of the fluorescence signal. Yet, the number of spike bursts is presumably similar to the activity captured by the JO-AB driver since the magnitude of the response signal was similar.

Calcium transients in response to RCS stimuli were significantly higher in magnitude and had faster rise time kinetics compared to the responses to APT in flies expressing JO-all. This suggests that RCS stimuli elicited a greater number of synchronously-aligned spike bursts. Apart from encoding different courtship signals, the two stimuli have different sound properties. It has been found bulk spiking represented by the compound action potentials (CAPs) strongly scales in

amplitude by the size of the displacement of the arista (Effertz et al., 2012). Thus, it is possible to speculate that this effect is due to RCS simply producing greater deflections on the sound receiver. However, the root mean squared (RMS) value for RCS was 0.04 and for APT was 0.07 which shows that at the point of the arista, APT actually generated greater velocities. This demonstrates that the effect cannot be explained by a simple bias in the presented stimulus.

There are a number of hypotheses which could explain the observed differences in the response to APT and RCS stimuli. It can be proposed that the lower response magnitude and slower kinetics in response to APT are due to fast adaptation. The reduction of response to repeated stimuli allows for the sensory system to extend its operating range. There is dynamic adjustment of the response gain where amplitude is a function of the number of the repeats of the stimulus signal (Clemens et al., 2018). Thus, repeated presentations of pulse stimuli over a given time frame perhaps result in diminished responses. Alternatively, RCS has a different temporal sequence and stimulus evolution pattern which could result in these observed differences.

The obvious differential factor between RCS and APT stimuli is that RCS contains sine song components. This in itself could contribute to the increased response observed to this stimulus. Though sub-population A and B respond to a variety of phasic stimuli, there is heterogeneity in the sensitivity and response properties to sound stimuli. Sub-population A was found to have a preference for high frequency vibrations whereas sub-population B for lower frequency stimuli (Kamikouchi et al., 2009). Consulting a power spectrum of the recorded APT and RCS stimuli by a particle velocity meter; more lower frequency components are evident in the RCS stimulus (**Fig 81**). Thus, it is possible that the greater response to RCS is due to the activation of more JO-B neurons.
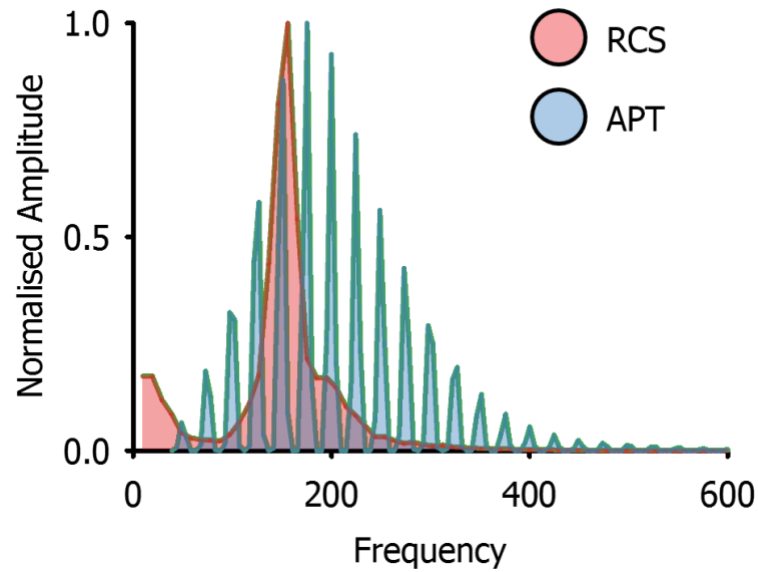
Figure 81: Power spectrum of APT & RCS stimuli demonstrating that RCS signal contains a greater number of low-frequency components.

It is difficult to conclusively determine what contributes to these differential response properties without performing intracellular recordings of the varying JONs. But, based on the current and previous findings, it can be hypothesised that there is an increased output from the JO in response to more naturalistic RCS stimuli which is determined by a combination of changes in adaptation properties and sensitivity of JONs to the signal.

Interestingly, the response properties of JO-AB to RCS and APT had no significant differences. Relating this finding to the differences in the responses observed for JO-all, it can be hypothesised that the observed gain in response to RCS is mediated by the activity of the JO-B1 sub-population. The rise time constants for RCS remain smaller compared to APT in the response of JO-AB. Based on the assumptions made at the beginning of this discussion, this indicates that there is an increased rate of spike bursts which results in a summation of the fluorescence signal. Thus, it can be hypothesised that the spike rate is increased in JO-AB expressing neurons in response to RCS stimuli.

In **chapter 5.3.3** (**page 77**), it was found that presentation of RCS stimuli results in an increased gain in responsiveness and greater auditory-induced locomotor activity. The findings within the current chapter suggest that there is a direct link

between the auditory processing of the signal within the JO and auditory-induced locomotor behaviours.

By assessing the calcium transients of JO-all flies at 3 different timepoints throughout an LD cycle, there was little evidence of circadian changes in response to APT and RCS sound stimuli. However, it was found that the relationship between the response to APT and RCS stimuli changed at these assayed time points. Based on the hypothesis presented in the previous paragraph suggesting that the difference in response to APT and RCS stimulus is dependent on the JO-B1 subpopulation; it is possible to speculate further that the circadian modulation of only this one sub-population which modulates the response signal in relation to APT. The difference in the magnitude of the response between APT and RCS becomes more prominent throughout the day (**Table 26**). This indicates that there is an increase in response to RCS relative to APT towards ZT12. Possibly this change is specifically dependent on the output of the JO-B1 neurons.

Table 28: Changes in the differences between the responses to APT & RCS stimuli throughout different timepoints.

	ZT3	ZT9	ZT13
Difference between APT & RCS Total $\Delta F/F_0$ (%)	5.13	49.5	69.7
Difference between APT and RCS Peak $\Delta F/F_0$ (%)	0.433	2.81	4.18

Bringing these findings together, I propose a model where sub-populations C-E do not contribute to the sound-induced calcium transients observed, but sub-populations A and B do. The contribution of the JO-A and JO-B0 remains constant, however JO-B1 is modulated by the type of stimulus and potentially by the time of day. The sensitivity of the JO-B1 sub-population to properties within the naturalistic stimulus increases throughout the day. Potentially the sensitivity of this subtype of neurons is circadian-modulated (**Fig 82**). This model is based on the collective findings within this chapter, however further investigation is necessary to validate these assumptions.
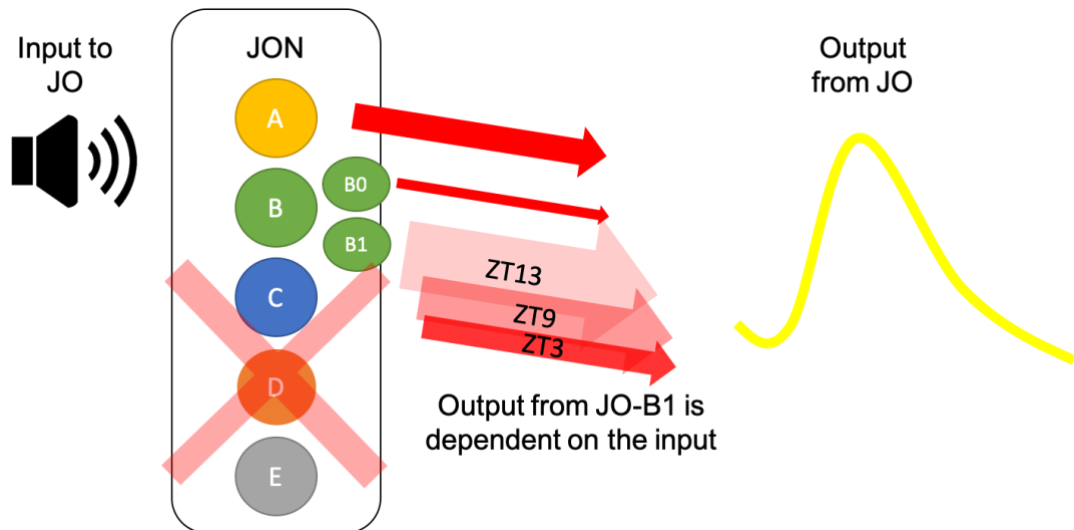
Figure 82: Proposed model of the contribution of the JO sub-populations to the observed calcium transients in response to sound stimuli.

This model proposes that in response to auditory stimuli, there is activation of sub-population JO-A and B neurons. Sound stimuli elicit changes in intracellular calcium which is reflected in the fluorescence signal of a GCamp reporter. Sub-populations C-E do not contribute to the observed response and JO-A and JO-B0 output is maintained throughout the day. However, the response of JO-B1 neurons is dependent on the sound stimulus and on the time of day. There is a greater output at ZT13 from JO-B1 neurons compared to ZT3. The thicker arrows demonstrate the changes in the contribution of these neurons to the response signal.

There are a number of experiments which can be conducted to test some of the hypothesis presented in this discussion so far. Using drivers which have specific expression in individual sub-populations, it is possible to test the contribution of JO-A and JO-B neurons separately. From the current findings it has been hypothesised that JO-B1 sub-population neurons firstly respond more to the presented naturalistic stimuli and also potentially modulate their activity throughout the day. To test the first assumption, driver lines such as JO2 JO28, JO29 and JO24, which have specified expression in JO sub-populations, need to be tested to assess their responses to RCS and APT stimuli. To further delineate which differences in the given stimulus result in the observed changes, different sound components (both pulse and sine song) can be tested separately as well as at different frequencies to test biases in sensitivity of the sub-populations to certain signals. Following this, the animals can be assayed at various time points to investigate whether there are any systematic changes in the response throughout a circadian day. If an oscillatory change in responsiveness to the same stimulus is found, further experiments with arrhythmic flies can be conducted to establish

whether these changes are regulated by the output of the central and/or peripheral clock.

Furthermore, to test the link between JO output and behaviour, specific sub-populations of neurons can be silenced with UAS-Hid-RPR to determine whether these increases in locomotor gain or periodicity of auditory-induced locomotor activity is determined by specific sub-populations of JONs such as JO-B1.

Comparing the responses of JO-all kept in constant light conditions and JO-all LD samples, JO-all LL demonstrated significantly lower rise time constants in response to both APT and RCS stimuli. This indicates that there was an increased rate of spike bursts in JO-all LL flies. It may be that animals kept in constant light have changes in the adaptation properties of the system which results in the faster build-up of intracellular calcium. Obtaining CAP recordings from the antennal nerve could probe this assumption.

Sound-induced calcium transients were compared for animals presented to the sound stimulus in light and dark environmental conditions. From the previous chapter (**chapter 6.3.8 page 129**), it was proposed that light can prompt auditory-induced locomotor activity suppression. Though this effect could be observed in the behavioural paradigm, there were no evident changes in fluorescence signal between animals tested in light and in dark. This suggests that environmental light conditions do not have a significant effect on the processing of a sound stimulus in JO. It should also be noted that functional imaging is perhaps not the most optimal method of investigation of this since the 488nm laser was used for point excitation, which falls into the visual range of the fly. As a secondary effect, the light from the laser could be disrupting the effect of environmental dark conditions. Red shifted GECIs can be used instead, since the excitation range of RFP is closer to 580nm, outside of the optical range of *Drosophila* (Zhu, 2013)*.*

7.5 Limitations of findings

In all the experiments presented in this chapter, the sound stimulus was delivered through a piece of tubing connected to a small earbud speaker. By using the line

scan before recording GCamp responses, it was possible to quantify whether or not the presented sound stimulus elicited sound receiver deflections. Nonetheless, this was a binary readout which did not have the resolution to quantify the extent of the displacement. With this mode of stimulus delivery, it is likely that there was variability in the positioning of the opening of the tubing in relation to the arista between experimental animals. Due to this, it is probable that between samples there was some variability in the received intensity of the sound signal. There was large variation in response seen between samples in the same conditions and this could have been one of the contributing factors. To address this problem, future experiments could use electrostatic actuation to deliver the sound stimulus which provides a more precise mode of stimulus delivery (Albert, Nadrowski, & Göpfert, 2007).

There are other practical considerations which could increase the variability in the recordings. The animal was fixed in position manually thus, minor positional differences between experimental animals are highly likely. This could result in changes in the cross section at which the organ was imaged. Since the imaging was done through the cuticle surface, the poor image resolution did not allow to precisely determine that image capture occurred on the same plane of the JO between experimental animals. To omit some of this effect, the pinhole was set maximally to aggregate the signal from the JO however it is likely this did not fully account for this limiting practical factor.

To address some of these issues, future studies should have a greater n number to offset the variability in the recorded responses. Furthermore, where possible, the same sample could be exposed to different conditions to allow for within sample comparisons. This method has been applied to test circadian changes in response. Preliminary results show that it is possible to keep a sample alive over a prolonged time and sample every hour (**Supplementary 5**).

In the discussion, I made assumptions about what the changes in calcium transients represent on the electrophysiological level of the JONs. Though calcium imaging is a powerful tool, it does not provide a direct readout of the electrophysiological activity of neurons within the JO. There is a limited amount known about the neuronal architecture of the JO and its adaptation properties thus

these hypotheses must be tested further by other means. As it is technically challenging to conduct single cell recording in the JO, recordings from the antennal nerve could help supplement the findings within this chapter

Chapter 8

Conclusions & final remarks

By developing a new approach to assay auditory-induced behaviour, within this thesis I have presented findings that demonstrate auditory-induced locomotor activity is governed by a number of key modulators. I have also determined that some of these regulators of auditory behaviour have a direct effect on the function of JO neurons. Suggesting that some of the observed behavioural changes are, at least in part, mediated by the changes to primary sensory processing of the sound within the hearing organ.

One of the first major outcomes of this research is that playback of naturalistic sound stimuli is most effective at eliciting auditory-induced locomotor activity in male *Drosophila.* The presentation of a repeated uniform pulse also induces observable changes in behaviour but this behavioural response is weaker in comparison. These differential effects of the stimuli were also evident in the function of JONs where it was observed that naturalistic stimuli elicit, both larger and faster calcium transients. This demonstrates that there is an increased sensitivity of the system to naturalistic stimuli and that the gain in behavioural responsiveness can be related back to the initial processing of the sound stimulus.

Secondly, I have established a link between auditory-induced behaviour and the circadian clock. Auditory-induced locomotor activity was observed to have robust periodic changes throughout a 24-h cycle. This behavioural pattern was lost in clock impaired conditions. Intriguingly, these rhythms follow a distinct pattern unlike that of baseline locomotor activity observed in *Drosophila.* Additionally, I found that this oscillatory behaviour is only elicited by the playback of sound stimuli containing biologically relevant courtship signals. Whether auditory-induced locomotor rhythms are regulated by the peripheral clock or central pacemakers and where these circadian changes take place is yet to be determined. Future

research can build on the link established within this thesis between the clock and auditory-induced behaviour.

Lastly, I found that light is a key regulator of auditory-induced behaviour. Specifically, exposure to constant light results in an increased auditory-induced locomotor response to sound stimuli. Exposure to these environmental conditions was also found to induce significantly faster calcium transients in response to sound stimuli from JONs. From this it can be inferred that constant light changes the sensitivity of the system.

This research has opened up multiple new avenues of enquiry. Collectively, these findings call for further assessment of the interactions between behaviour and physiology and how molecular mechanisms could affect auditory-induced behaviour and JO function.

Bibliography

Albert, Joerg T., & Kozlov, A. S. (2016). Comparative Aspects of Hearing in Vertebrates and Insects with Antennal Ears. *Current Biology*, *26*(20), R1050–R1061. https://doi.org/10.1016/j.cub.2016.09.017

Albert, Jörg T., & Göpfert, M. C. (2015). Hearing in Drosophila. *Current Opinion in Neurobiology*, *34*, 79–85. https://doi.org/10.1016/j.conb.2015.02.001

Albert, Jörg T., Göpfert, M. C., & Kamikouchi, A. (2010). *Mechanical feedback amplification in Drosophila hearing is independent of synaptic transmission*. *31*, 697–703. https://doi.org/10.1111/j.1460-9568.2010.07099.x

Albert, Jörg T., Nadrowski, B., & Göpfert, M. C. (2007a). Mechanical Signatures of Transducer Gating in the Drosophila Ear. *Current Biology*, *17*(11), 1000–1006. https://doi.org/10.1016/j.cub.2007.05.004

Albert, Jörg T., Nadrowski, B., & Göpfert, M. C. (2007b). Mechanical Signatures of Transducer Gating in the Drosophila Ear. *Current Biology*, *17*(11), 1000–1006. https://doi.org/10.1016/J.CUB.2007.05.004

Albert, Jörg T, Nadrowski, B., & Göpfert, M. C. (2007). Drosophila mechanotransduction--linking proteins and functions. *Fly*, *1*(4), 238–241. https://doi.org/10.4161/fly.4990

Allada, R., & Chung, B. Y. (2011). Circadian Organization of Behavior and Physiology in Drosophila. *Neurobiology*, 605–624. https://doi.org/10.1146/annurev-physiol-021909-135815.Circadian

Armstrong, J. D., Texada, M. J., Munjaal, R., Baker, D. A., & Beckingham, K. M. (2006). Gravitaxis in Drosophila melanogaster: a forward genetic screen. *Genes, Brain and Behavior*, *5*(3), 222–239. https://doi.org/10.1111/j.1601-183X.2005.00154.x

Ausborn, J., Wolf, H., Mader, W., & Kayser, H. (2005). The insecticide pymetrozine selectively affects chordotonal mechanoreceptors. *The Journal of Experimental Biology*, *208*(Pt 23), 4451–4466. https://doi.org/10.1242/jeb.01917

Azevedo, A. W., & Wilson, R. I. (2017). Active mechanisms of vibration encoding and frequency filtering in central mechanosensory neurons. *Neuron*, *96*(2), 446. https://doi.org/10.1016/J.NEURON.2017.09.004

Bachleitner, W., Kempinger, L., Wü, C., Rieger, D., & Helfrich-Fö, C. (2007). *Moonlight shifts the endogenous clock of Drosophila melanogaster*. Retrieved

from www.pnas.orgcgidoi10.1073pnas.0606870104

Basinou, V., Park, J.-S., Cederroth, C. R., & Canlon, B. (2017). Circadian regulation of auditory function. *Hearing Research*, *347*, 47–55. https://doi.org/10.1016/j.heares.2016.08.018

Batchelor, A. V, & Wilson, R. I. (2019). *Sound localization behavior in Drosophila melanogaster depends on inter-antenna vibration amplitude comparisons*. https://doi.org/10.1242/jeb.191213

Bodmer, R., Barbel, S., Sheperd, S., Jack, J. W., Jan, L. Y., & Jan, Y. N. (1987). Transformation of sensory organs by Mutations of the cut locus of D. melanogaster. *Cell*, *51*(2), 293–307. https://doi.org/10.1016/0092-8674(87)90156-5

Boekhoff-Falk, G., & Eberl, D. F. (2014). The Drosophila auditory system. *Wiley Interdisciplinary Reviews: Developmental Biology*, *3*(2), 179–191. https://doi.org/10.1002/wdev.128

Bretman, A., Rouse, J., Westmancoat, J. D., & Chapman, T. (2017). The role of species-specific sensory cues in male responses to mating rivals in Drosophila melanogaster fruitflies. *Ecology and Evolution*, *7*(22), 9247–9256. https://doi.org/10.1002/ece3.3455

Carr, C., Gopfert, M., Bibikov, N., Seeds, A. M., Ishikawa, Y., Kamikouchi, A., … Kim, H. (2017). Anatomic and Physiologic Heterogeneity of Subgroup-A Auditory Sensory Neurons in Fruit Flies. *Frontiers in Neural Circuits | Www.Frontiersin.Org*, *1*, 46. https://doi.org/10.3389/fncir.2017.00046

Charras G.T. (2008). A short history of blebbing. *Journal of Microscopy*, *231*(3), 466–478. https://doi.org/10.1111/j.1365-2818.2008.02059.x

Chen, T.-W., Wardill, T. J., Sun, Y., Pulver, S. R., Renninger, S. L., Baohan, A., … Kim, D. S. (2013). Ultrasensitive fluorescent proteins for imaging neuronal activity. *Nature*, *499*(7458), 295–300. https://doi.org/10.1038/nature12354

Cheng, L. E., Song, W., Looger, L. L., Jan, L. Y., & Jan, Y. N. (2010). The role of the TRP channel NompC in Drosophila larval and adult locomotion. *Neuron*, *67*(3), 373–380. https://doi.org/10.1016/j.neuron.2010.07.004

Clemens, J., Ozeri-Engelhard, N., & Murthy, M. (2018). Fast intensity adaptation enhances the encoding of sound in Drosophila. *Nature Communications*, *9*(1), 134. https://doi.org/10.1038/s41467-017-02453-9

Cocroft, R. B. (2001). *Vibrational Communication and the Ecology of Group-Living, Herbivorous Insects 1* (Vol. 41). Retrieved from https://academic.oup.com/icb/article-abstract/41/5/1215/343867

Crossley, S., & Zuill, E. (1970). Courtship Behaviour of some Drosophila melanogaster Mutants. *Nature*, *225*(5237), 1064–1065. https://doi.org/10.1038/2251064a0

Crozatier, M., & Vincent, A. (2007). *Control of multidendritic neuron differentiation in Drosophila: The role of Collier*. https://doi.org/10.1016/j.ydbio.2007.12.030

Darlington, T. K., Wager-Smith, K., Ceriani, M. F., Staknis, D., Gekakis, N., Steeves, T. D., … Kay, S. A. (1998). Closing the circadian loop: CLOCK-induced transcription of its own inhibitors per and tim. *Science (New York, N.Y.)*, *280*(5369), 1599–1603. Retrieved from http://www.ncbi.nlm.nih.gov/pubmed/9616122

Dubruille, R., & Emery, P. (2008). A Plastic Clock: How Circadian Rhythms Respond to Environmental Cues in Drosophila. *Molecular Neurobiology*, *38*(2), 129–145. https://doi.org/10.1007/s12035-008-8035-y

Eatock, R. A., Corey, D. P., Hudspeth, A. J., & Fettiplace, R. (1987). Adaptation of mechanoelectrical transduction in hair cells of the bullfrog's sacculus. *The Journal of Neuroscience : The Official Journal of the Society for Neuroscience*, *7*(9), 2821–2836. https://doi.org/10.1523/jneurosci.2188-06.2006

Eberl, D. F., Duyk, G. M., & Perrimon, N. (1997). A genetic screen for mutations that disrupt an auditory response in Drosophila melanogaster. *Proceedings of the National Academy of Sciences*, *94*(26), 14837–14842. https://doi.org/10.1073/pnas.94.26.14837

Eberl, D. F., Hardy, R. W., & Kernan, M. J. (2000). Genetically similar transduction mechanisms for touch and hearing in Drosophila. *The Journal of Neuroscience : The Official Journal of the Society for Neuroscience*, *20*(16), 5981–5988. https://doi.org/10.1523/JNEUROSCI.20-16-05981.2000

Effertz, T., Nadrowski, B., Piepenbrock, D., Albert, J. T., & Göpfert, M. C. (2012). Direct gating and mechanical integrity of Drosophila auditory transducers require TRPN1. *Nature Neuroscience*, *15*(9), 1198–1200. https://doi.org/10.1038/nn.3175

Effertz, T., Wiek, R., & Göpfert, M. C. (2011). NompC TRP Channel Is Essential for Drosophila Sound Receptor Function. *Current Biology*, *21*(7), 592–597. https://doi.org/10.1016/J.CUB.2011.02.048

Emerson, K. J., Bradshaw, W. E., & Holzapfel, C. M. (2009). Complications of complexity: integrating environmental, genetic and hormonal control of insect diapause. *Trends in Genetics*, *25*(5), 217–225. https://doi.org/10.1016/j.tig.2009.03.009

Emery, P., Stanewsky, R., Hall, J. C., & Rosbash, M. (2000). A unique circadian-

rhythm   photoreceptor.   *Nature*,   *404*(6777),   456–457.
https://doi.org/10.1038/35006558

Ewing, A. W. (1983). Functional aspects of Drosophila courtship. *Biological Reviews*, *58*(2), 275–292. https://doi.org/10.1111/j.1469-185X.1983.tb00390.x

Field, L. H., & Matheson, T. (1998). Chordotonal Organs of Insects. *Matheson Advances in Insect Physiology*, *27*. Retrieved from https://www2.le.ac.uk/departments/npb/people/matheson/matheson-neurobiology/images/publications/chordotonal.pdf

Frisch, B., Hardin, P. E., Hamblen-Coyle, M. J., Rosbash, M., & Hall, J. C. (1994). A promoterless period gene mediates behavioral rhythmicity and cyclical per expression in a restricted subset of the drosophila nervous system. *Neuron*, *12*(3), 555–570. https://doi.org/10.1016/0896-6273(94)90212-7

Fujii, S., Krishnan, P., Hardin, P., & Amrein, H. (2007). Nocturnal Male Sex Drive in Drosophila. In *Curr Biol* (Vol. 17). Retrieved from https://www.ncbi.nlm.nih.gov/pmc/articles/PMC2239012/pdf/nihms38366.pdf

Gailey, D. A., Lacaillade, R. C., & Hall, J. C. (1986). Chemosensory Elements of Courtship in Normal and Mutant, Olfaction-Deficient Drosophila melanogaster. In *Behavior Genetics* (Vol. 16). Retrieved from https://link.springer.com/content/pdf/10.1007%2FBF01071319.pdf

Giebultowicz, J. M., Stanewsky, R., Hall, J. C., & Hege, D. M. (2000). Transplanted Drosophila excretory tubules maintain circadian clock cycling out of phase with the host. *Current Biology*, *10*(2), 107–110. https://doi.org/10.1016/S0960-9822(00)00299-2

Gillespie, P. G., & Walker, R. G. (2001). Molecular basis of mechanosensory transduction. *Nature*, *413*(6852), 194–202. https://doi.org/10.1038/35093011

Glaser, F. T., & Stanewsky, R. (2005). Temperature Synchronization of the Drosophila Circadian Clock. *Current Biology*, *15*, 1352–1363. https://doi.org/10.1016/j.cub.2005.06.056

Goel, N. (2005). Late-night presentation of an auditory stimulus phase delays human circadian rhythms. *American Journal of Physiology-Regulatory, Integrative and Comparative Physiology*, *289*(1), R209–R216. https://doi.org/10.1152/ajpregu.00754.2004

Göpfert, M C, & Robert, D. (2003). Motion generation by Drosophila mechanosensory neurons. *PNAS, 100*(9), 5514–5519. Retrieved from http://www.pnas.org/content/pnas/100/9/5514.full.pdf

Göpfert, Martin C., & Robert, D. (2001). Biomechanics: Turning the key on Drosophila audition. *Nature*, *411*(6840), 908–908. https://doi.org/10.1038/35082144

Göpfert, Martin C, & Robert, D. (2002). *The mechanical basis of Drosophila audition*. *1208*, 1199–1208.

Grima, B., Chélot, E., Xia, R., & Rouyer, F. (2004). Morning and evening peaks of activity rely on different clock neurons of the Drosophila brain. *Nature*, *431*(7010), 869–873. https://doi.org/10.1038/nature02935

Grunert, U., & Gnatzy, W. (1987). K+ and Ca++ in the receptor lymph of arthropod cuticular mechanoreceptors. *Journal of Comparative Physiology A*, *161*(2), 329–333. https://doi.org/10.1007/BF00615253

Hall, J. C. (1994). *The Mating of a Fly*. https://doi.org/10.1126/science.8209251

Hamblen-Coyle, M., Konopka, R. J., Zwiebel, L. J., Colot, H. V, Dowse, H. B., Rosbash, M., & Hall, J. C. (1989). A new mutation at the period locus of Drosophila melanogaster with some novel effects on circadian rhythms. *Journal of Neurogenetics*, *5*(4), 229–256. Retrieved from http://www.ncbi.nlm.nih.gov/pubmed/2509652

Helfrich-Förster, C. (2004). Neurobiology of the fruit fly's circadian clock. *Genes, Brain and Behavior*, *4*(2), 65–76. https://doi.org/10.1111/j.1601-183X.2004.00092.x

Helfrich-Förster, Charlotte. (2000a). Differential Control of Morning and Evening Components in the Activity Rhythm of Drosophila melanogaster-Sex-Specific Differences Suggest a Different Quality of Activity. In *Helfrich-Förster / SEXUAL DIMORPHISM IN DROSOPHILA'S RHYTHMIC BEHAVIOR JOURNAL OF BIOLOGICAL RHYTHMS* (Vol. 15). Retrieved from https://journals.sagepub.com/doi/pdf/10.1177/074873040001500208

Helfrich-Förster, Charlotte. (2000b). Differential Control of Morning and Evening Components in the Activity Rhythm of Drosophila melanogaster-Sex-Specific Differences Suggest a Different Quality of Activity. In *Helfrich-Förster / SEXUAL DIMORPHISM IN DROSOPHILA'S RHYTHMIC BEHAVIOR JOURNAL OF BIOLOGICAL RHYTHMS* (Vol. 15). Retrieved from https://journals.sagepub.com/doi/pdf/10.1177/074873040001500208

Helfrich-Förster, Charlotte. (2001). *The locomotor activity rhythm of Drosophila melanogaster is controlled by a dual oscillator system*. *47*, 877–887.

Helfrich-Förster, Charlotte, & Homberg, U. (1993). Pigment-dispersing hormone-immunoreactive neurons in the nervous system of wild-type *Drosophila melanogaster* and of several mutants with altered circadian rhythmicity. *Journal of Comparative Neurology*, *337*(2), 177–190.

https://doi.org/10.1002/cne.903370202

Helfrich-Förster, Charlotte, Winter, C., Hofbauer, A., Hall, J. C., & Stanewsky, R. (2001a). The Circadian Clock of Fruit Flies Is Blind after Elimination of All Known Photoreceptors. *Neuron*, *30*(1), 249–261. https://doi.org/10.1016/S0896-6273(01)00277-X

Helfrich-Förster, Charlotte, Winter, C., Hofbauer, A., Hall, J. C., & Stanewsky, R. (2001b). The Circadian Clock of Fruit Flies Is Blind after Elimination of All Known Photoreceptors. *Neuron*, *30*(1), 249–261. https://doi.org/10.1016/S0896-6273(01)00277-X

Helfrich-Förster, C., Winter, C., Hofbauer, A., Hall, J. C., & Stanewsky, R. (2001). The Circadian Clock of Fruit Flies Is Blind after Elimination of All Known Photoreceptors. In *Neuron* (Vol. 30). Retrieved from https://ac.els-cdn.com/S089662730100277X/1-s2.0-S089662730100277X-main.pdf?_tid=f6d1d963-c103-4edb-9f3e-6eb44e04c4a7&acdnat=1537533093_83b2da0d172c4b1b38fe4c3aee0df0cb

Inagaki, H. K., Kamikouchi, A., & Ito, K. (2010). Protocol for quantifying sound-sensing ability of Drosophila melanogaster. *Nature Protocols*, *5*(1), 26–30. https://doi.org/10.1038/nprot.2009.206

Ishikawa, Y., Okamoto, N., Yoneyama, Y., Maeda, N., & Kamikouchi, A. (2019). A single male auditory response test to quantify auditory behavioral responses in Drosophila melanogaster. *Journal of Neurogenetics*, *33*(2), 64–74. https://doi.org/10.1080/01677063.2019.1611805

Ito, C., & Tomioka, K. (2016a). Heterogeneity of the Peripheral Circadian Systems in Drosophila melanogaster: A Review. *Frontiers in Physiology*, *7*, 8. https://doi.org/10.3389/fphys.2016.00008

Ito, C., & Tomioka, K. (2016b). Heterogeneity of the Peripheral Circadian Systems in Drosophila melanogaster: A Review. *Frontiers in Physiology*, *7*, 8. https://doi.org/10.3389/fphys.2016.00008

Jallon, J. M., & Hotta, Y. (1979). Genetic and behavioral studies of female sex appeal in Drosophila. *Behavior Genetics*, *9*(4), 257–275. Retrieved from http://www.ncbi.nlm.nih.gov/pubmed/117791

Kamikouchi, A. (2013). Auditory neuroscience in fruit flies. *Neuroscience Research*, *76*(3), 113–118. https://doi.org/10.1016/j.neures.2013.04.003

Kamikouchi, A., Inagaki, H. K., Effertz, T., Hendrich, O., Fiala, A., Göpfert, M. C., & Ito, K. (2009a). The neural basis of Drosophila gravity-sensing and hearing. *Nature*, *458*(7235), 165–171. https://doi.org/10.1038/nature07810

Kamikouchi, A., Inagaki, H. K., Effertz, T., Hendrich, O., Fiala, A., Göpfert, M. C., & Ito, K. (2009b). The neural basis of Drosophila gravity-sensing and hearing. *Nature*, *458*(7235), 165–171. https://doi.org/10.1038/nature07810

Kamikouchi, A., & Ishikawa, Y. (2016). *Hearing in Drosophila*. https://doi.org/10.1007/978-3-319-28890-1_10

Kamikouchi, A., Shimada, T., & Ito, K. (2006). Comprehensive classification of the auditory sensory projections in the brain of the fruit fly Drosophila melanogaster. *The Journal of Comparative Neurology*, *499*(3), 317–356. https://doi.org/10.1002/cne.21075

Kempinger, L., Dittmann, R., Rieger, D., & Helfrich-Förster, C. (2009). The Nocturnal Activity of Fruit Flies Exposed to Artificial Moonlight Is Partly Caused by Direct Light Effects on the Activity Level That Bypass the Endogenous Clock. *Chronobiology International*, *26*(2), 151–166. https://doi.org/10.1080/07420520902747124

Kernan, M. J. (2007). Mechanotransduction and auditory transduction in Drosophila. *Pflügers Archiv - European Journal of Physiology*, *454*(5), 703–720. https://doi.org/10.1007/s00424-007-0263-x

Kim, J., Chung, Y. D., Park, D., Choi, S., Shin, D. W., Soh, H., … Kim, C. (2003). A TRPV family ion channel required for hearing in Drosophila. *Nature*, *424*(6944), 81–84. https://doi.org/10.1038/nature01733

Klarsfeld, A., Leloup, J.-C., & Rouyer, F. (2003). Circadian rhythms of locomotor activity in Drosophila. *Behavioural Processes*, *64*(2), 161–175. https://doi.org/10.1016/S0376-6357(03)00133-5

Koh, K., Zheng, X., & Sehgal, A. (2006). JETLAG Resets the Drosophila Circadian Clock by Promoting Light-Induced Degradation of TIMELESS. *Science*, *312*(5781), 1809–1812. https://doi.org/10.1126/science.1124951

Kondratov, R. V, Chernov, M. V, Kondratova, A. A., Gorbacheva, V. Y., Gudkov, A. V, & Antoch, M. P. (2003). BMAL1-dependent circadian oscillation of nuclear CLOCK: posttranslational events induced by dimerization of transcriptional activators of the mammalian clock system. *Genes & Development*, *17*(15), 1921–1932. https://doi.org/10.1101/gad.1099503

Konopka, R. J., & Benzer, S. (1971). Clock mutants of Drosophila melanogaster. *Proceedings of the National Academy of Sciences of the United States of America*, *68*(9), 2112–2116. Retrieved from http://www.ncbi.nlm.nih.gov/pubmed/5002428

Kowalski, S., Aubin, T., & Martin, J.-R. (2004). *Courtship song in Drosophila melanogaster: a differential effect on male-female locomotor activity*. https://doi.org/10.1139/Z04-102

Krishnan, B., Dryer, S. E., & Hardin, P. E. (1999). Circadian rhythms in olfactory responses of Drosophila melanogaster. *Nature*, *400*(6742), 375–378. https://doi.org/10.1038/22566

Krstic, D, Boll, W., & Noll, M. (2009). Sensory Integration Regulating Male Courtship Behavior in Drosophila. *PLoS ONE*, *4*(2), 4457. https://doi.org/10.1371/journal.pone.0004457

Krstic, Dimitrije, Boll, W., & Noll, M. (2009). Sensory integration regulating male courtship behavior in Drosophila. *PLoS ONE*, *4*(2). https://doi.org/10.1371/journal.pone.0004457

Lai, J. S.-Y., Lo, S.-J., Dickson, B. J., & Chiang, A.-S. (2012). Auditory circuit in the Drosophila brain. *Proceedings of the National Academy of Sciences*, *109*(7), 2607–2612. https://doi.org/10.1073/pnas.1117307109

Lee, J., Moon, S., Cha, Y., & Chung, Y. D. (2010). Drosophila TRPN(=NOMPC) channel localizes to the distal end of mechanosensory cilia. *PLoS ONE*, *5*(6). https://doi.org/10.1371/journal.pone.0011012

Lee, S.-J., & Montell, C. (2004). Suppression of Constant-Light-Induced Blindness but Not Retinal Degeneration by Inhibition of the Rhodopsin Degradation Pathway. *Current Biology*, *14*(23), 2076–2085. https://doi.org/10.1016/j.cub.2004.11.054

Lehnert, B. P., Baker, A. E., Gaudry, Q., Chiang, A.-S., & Wilson, R. I. (2013). Distinct Roles of TRP Channels in Auditory Transduction and Amplification in Drosophila. *Neuron*, *77*(1), 115–128. https://doi.org/10.1016/J.NEURON.2012.11.030

Levine, J. D., Funes, P., Dowse, H. B., & Hall, J. C. (2002). Signal analysis of behavioral and molecular cycles. *BMC Neuroscience*, *3*(1), 1. https://doi.org/10.1186/1471-2202-3-1

Li, P., Geng, X., Jiang, H., Caccavano, A., Vicini, S., & Wu, J. (2019). Measuring Sharp Waves and Oscillatory Population Activity With the Genetically Encoded Calcium Indicator GCaMP6f. *Frontiers in Cellular Neuroscience*, *13*, 274. https://doi.org/10.3389/fncel.2019.00274

Li, T., Bellen, H. J., & Groves, A. K. (2018). Using Drosophila to study mechanisms of hereditary hearing loss. *Disease Models & Mechanisms*, *11*(6), dmm031492. https://doi.org/10.1242/dmm.031492

Manning, A. (1967). Antennae and sexual receptivity in Drosophila melanogaster females. *Science (New York, N.Y.)*, *158*(3797), 136–137. https://doi.org/10.1126/SCIENCE.158.3797.136

Markow, T. A., & O'Grady, P. M. (2005). Evolutionary Genetics of Reproductive

Behavior in Drosophila: Connecting the Dots. *Annu. Rev. Genet*, 263–191. https://doi.org/10.1146/annurev.genet.39.073003.112454

Marrus, S. B., Zeng, H., & Rosbash, M. (1996). Effect of constant light and circadian entrainment of perS flies: evidence for light-mediated delay of the negative feedback loop in Drosophila. In *The EMBO Journal* (Vol. 15). Retrieved from https://www.ncbi.nlm.nih.gov/pmc/articles/PMC452514/pdf/emboj00024-0107.pdf

Matsuo, E., Yamada, D., Ishikawa, Y., Asai, T., Ishimoto, H., & Kamikouchi, A. (2014). Identification of novel vibration- and deflection-sensitive neuronal subgroups in Johnston's organ of the fruit fly. *Frontiers in Physiology*, *5*, 179. https://doi.org/10.3389/fphys.2014.00179

Menaker & Eskin. (1966). Entrainment of Circadian Rhythms by Sound in Passer domesticus. *Science*, *154*(3756), 1579–1581. https://doi.org/10.1126/science.154.3756.1579

Miller, M. W., & Gronfier, C. (2006). Diurnal variation of the startle reflex in relation to HPA-axis activity in humans. *Psychophysiology*, *43*(3), 297–301. https://doi.org/10.1111/j.1469-8986.2006.00400.x

Moses, K., Ellis, M. C., & Rubin, G. M. (1989). The glass gene encodes a zinc-finger protein required by Drosophila photoreceptor cells. *Nature*, *340*(6234), 531–536. https://doi.org/10.1038/340531a0

Moulin, B., Aubin, T., & Jallon, J.-M. (2004). Why there is a one-way crossability between. In *Genetica* (Vol. 120). Retrieved from https://link.springer.com/content/pdf/10.1023%2FB%3AGENE.0000017650.45464.f4.pdf

Myers, E. M., Yu, J., & Sehgal, A. (2003). Circadian Control of Eclosion: Interaction between a Central and Peripheral Clock in Drosophila melanogaster. *Current Biology*, *13*, 526–533. https://doi.org/10.1016/S

Nadrowski, B., Albert, J. T., & Göpfert, M. C. (2008). Transducer-Based Force Generation Explains Active Process in Drosophila Hearing. *Current Biology*, *18*(18), 1365–1372. https://doi.org/10.1016/j.cub.2008.07.095

Nesterov, A., Spalthoff, C., Kandasamy, R., Katana, R., Rankl, N. B., Andrés, M., … Göpfert, M. C. (2015). TRP Channels in Insect Stretch Receptors as Insecticide Targets. *Neuron*, *86*(3), 665–671. https://doi.org/10.1016/J.NEURON.2015.04.001

Nippe, O. M., Wade, A. R., Elliott, C. J. H., & Chawla, S. (2017a). Circadian Rhythms in Visual Responsiveness in the Behaviorally Arrhythmic Drosophila Clock Mutant ClkJrk. *Journal of Biological Rhythms*, *32*(6), 583–592. https://doi.org/10.1177/0748730417735397

Nippe, O. M., Wade, A. R., Elliott, C. J. H., & Chawla, S. (2017b). Circadian Rhythms in Visual Responsiveness in the Behaviorally Arrhythmic Drosophila Clock Mutant ClkJrk. *Journal of Biological Rhythms*, *32*(6), 583–592. https://doi.org/10.1177/0748730417735397

Nitabach, M. N., & Taghert, P. H. (2008). Organization of the Drosophila Circadian Control Circuit. *Current Biology*, *18*(2), R84–R93. https://doi.org/10.1016/J.CUB.2007.11.061

Pittendrigh, C. S. (1954). ON TEMPERATURE INDEPENDENCE IN THE CLOCK SYSTEM CONTROLLING EMERGENCE TIME IN DROSOPHILA. *Proceedings of the National Academy of Sciences of the United States of America*, *40*(10), 1018–1029. Retrieved from http://www.ncbi.nlm.nih.gov/pubmed/16589583

Plautz, J. D., Kaneko, M., Hall, J. C., & Kay, S. A. (1997a). Independent photoreceptive circadian clocks throughout Drosophila. *Science (New York, N.Y.)*, *278*(5343), 1632–1635. https://doi.org/10.1126/science.278.5343.1632

Plautz, J. D., Kaneko, M., Hall, J. C., & Kay, S. A. (1997b). Independent photoreceptive circadian clocks throughout Drosophila. *Science (New York, N.Y.)*, *278*(5343), 1632–1635. https://doi.org/10.1126/SCIENCE.278.5343.1632

Renn, S. C., Park, J. H., Rosbash, M., Hall, J. C., & Taghert, P. H. (1999). A pdf neuropeptide gene mutation and ablation of PDF neurons each cause severe abnormalities of behavioral circadian rhythms in Drosophila. *Cell*, *99*(7), 791–802. https://doi.org/10.1016/s0092-8674(00)81676-1

Riabinina, O., Dai, M., Duke, T., & Albert, J. T. (2011). Active Process Mediates Species-Specific Tuning of Drosophila Ears. *Current Biology*, *21*, 658–664. https://doi.org/10.1016/j.cub.2011.03.001

Rieger, D., Fraunholz, C., Popp, J., Bichler, D., Dittmann, R., & Helfrich-Förster, C. (2007). The Fruit Fly Drosophila melanogaster Favors Dim Light and Times Its Activity Peaks to Early Dawn and Late Dusk. *JOURNAL OF BIOLOGICAL RHYTHMS*, *22*(5), 387–399. https://doi.org/10.1177/0748730407306198

Rings, A., & Goodwin, S. F. (2019). To court or not to court – a multimodal sensory decision in Drosophila males. *Current Opinion in Insect Science*, *35*, 48–53. https://doi.org/10.1016/J.COIS.2019.06.009

Rosato, E., & Kyriacou, C. P. (2006). Analysis of locomotor activity rhythms in Drosophila. *Nature Protocols*, *1*(2), 559–568. https://doi.org/10.1038/nprot.2006.79

Rosato, E., Tauber, E., & Kyriacou, C. P. (2006). Molecular genetics of the fruit-fly

circadian clock. *European Journal of Human Genetics*, *14*(6), 729–738. https://doi.org/10.1038/sj.ejhg.5201547

Rybak, F., Sureau, G., & Aubin, T. (2002). *Functional coupling of acoustic and chemical signals in the courtship behaviour of the male Drosophila melanogaster*. https://doi.org/10.1098/rspb.2001.1919

Saarikettu, M., Liimatainen, J. O., & Hoikkala, A. (2005). The Role of Male Courtship Song in Species Recognition in Drosophila montana. *Behavior Genetics*, *35*(3), 257–263. https://doi.org/10.1007/s10519-005-3218-z

Sakai, T., & Ishida, N. (2001). Circadian rhythms of female mating activity governed by clock genes in Drosophila. *Proceedings of the National Academy of Sciences of the United States of America*, *98*(16), 9221–9225. https://doi.org/10.1073/pnas.151443298

Sehgal, A. (2016). *Control of Metabolism by Central and Peripheral Clocks in Drosophila*. https://doi.org/10.1007/978-3-319-27069-2_4

Simoni, A., Wolfgang, W., Topping, M. P., Kavlie, R. G., Stanewsky, R., & Albert, J. T. (2014). A Mechanosensory Pathway to the Drosophila Circadian Clock. *Science*, *343*. https://doi.org/10.1126/science.1245710

Siwicki, K. K., Eastman, C., Petersen, G., Rosbash, M., Hall, J. C., Zerr, D. M., … Young, M. W. (1971). Rhythmic Expression of timeless: A Basis for Promoting Circadian Cycles in period Gene Autoregulation. In *Z. J. Huang, I. Edery, M. Rosbash* (Vol. 68). Retrieved from http://science.sciencemag.org/

Sokolowski, M. B. (2001). Drosophila: Genetics meets behaviour. *Nature Reviews Genetics*, *2*(11), 879–890. https://doi.org/10.1038/35098592

Somers, J., Harper, R. E. F., & Albert, J. T. (2018). *How Many Clocks , How Many Times ? On the Sensory Basis and Computational Challenges of Circadian Systems*. *12*(September), 1–8. https://doi.org/10.3389/fnbeh.2018.00211

Spieth, H. T. (1974). *COURTSHIP BEHAVIOR IN DROSOPHILA*. Retrieved from www.annualreviews.org

Stanewsky, R., Kaneko, M., Emery, P., Beretta, B., Wager-Smith, K., Kay, S. A., … Hall, J. C. (1998). The cryb Mutation Identifies Cryptochrome as a Circadian Photoreceptor in Drosophila. *Cell*, *95*(5), 681–692. https://doi.org/10.1016/S0092-8674(00)81638-4

Stern, D. L. (2014). Reported Drosophila courtship song rhythms are artifacts of data analysis. *BMC Biology*, *12*(1), 38. https://doi.org/10.1186/1741-7007-12-38

Stromnaes, O. (1959). Sexual Maturity in Drosophila. *Nature*, *183*(4658), 409–410. https://doi.org/10.1038/183409a0

Tang, C.-H. A., Hinteregger, E., Shang, Y., & Rosbash, M. (2010). Light-mediated TIM degradation within Drosophila pacemaker neurons (s-LNvs) is neither necessary nor sufficient for delay zone phase shifts. *Neuron*, *66*(3), 378–385. https://doi.org/10.1016/j.neuron.2010.04.015

Tataroglu, O., & Emery, P. (2014). Studying circadian rhythms in Drosophila melanogaster. *Methods*, *68*(1), 140–150. https://doi.org/10.1016/j.ymeth.2014.01.001

Tompkins, L., Gross, A. C., Hall, J. C., Gailey, D. A., & Siegel, R. W. (1982). The Role of Female Movement in the Sexual Behavior of Drosophila melanogaster. In *Behavior Genetics* (Vol. 12). Retrieved from https://link.springer.com/content/pdf/10.1007%2FBF01067849.pdf

Tompkins, L., Hall, J. C., & Hall, L. M. (1980). Courtship-stimulating volatile compounds from normal and mutant Drosophila. *Journal of Insect Physiology*, *26*(10), 689–697. https://doi.org/10.1016/0022-1910(80)90042-6

Tootoonian, S., Coen, P., Kawai, R., & Murthy, M. (2012). Neural Representations of Courtship Song in the Drosophila Brain. *Journal of Neuroscience*, *32*(3), 787–798. https://doi.org/10.1523/JNEUROSCI.5104-11.2012

Vaughan, A. G., Zhou, C., Manoli, D. S., & Baker, B. S. (2014). Neural Pathways for the Detection and Discrimination of Conspecific Song in D. melanogaster. *Current Biology*, *24*(10), 1039–1049. https://doi.org/10.1016/J.CUB.2014.03.048

Veleri, S., Brandes, C., Helfrich-Förster, C., Hall, J. C., & Stanewsky, R. (2003). A Self-Sustaining, Light-Entrainable Circadian Oscillator in the Drosophila Brain and CYCLE (CLK/CYC). PER and TIM proteins subse-quently repress their own expression by inhibiting CLK/ CYC function in the nucleus and thereby closing the. *Current Biology*, *13*, 1758–1767. https://doi.org/10.1016/j.cub.2003.09.030

von Philipsborn, A. C., Liu, T., Yu, J. Y., Masser, C., Bidaye, S. S., & Dickson, B. J. (2011). Neuronal Control of Drosophila Courtship Song. *Neuron*, *69*(3), 509–522. https://doi.org/10.1016/J.NEURON.2011.01.011

von Schilcher, F. (1976). The role of auditory stimuli in the courtship of Drosophila melanogaster. *Animal Behaviour*, *24*(1), 18–26. https://doi.org/10.1016/S0003-3472(76)80095-4

Vosshall, L., Price, J., Sehgal, A., Saez, L., & Young, M. (1994). Block in nuclear localization of period protein by a second clock mutation, timeless. *Science*, *263*(5153), 1606–1609. https://doi.org/10.1126/science.8128247

Walker, R. G., Willingham, A. T., & Zuker, C. S. (2000). A Drosophila mechanosensory transduction channel. *Science (New York, N.Y.), 287*(5461), 2229–2234. https://doi.org/10.1126/SCIENCE.287.5461.2229

Wheeler, D. A., Hamblen-Coyle, M. J., Dushay, M. S., & Hall, J. C. (1993a). Behavior in Light-Dark Cycles of Drosophila Mutants That Are Arrhythmic, Blind, or Both. *Journal of Biological Rhythms, 8*(1), 67–94. Retrieved from https://journals.sagepub.com/doi/pdf/10.1177/074873049300800106

Wheeler, D. A., Hamblen-Coyle, M. J., Dushay, M. S., & Hall, J. C. (1993b). Behavior in Light-Dark Cycles of Drosophila Mutants That Are Arrhythmic, Blind, or Both. *Journal of Biological Rhythms, 8*(1), 67–94. Retrieved from https://journals.sagepub.com/doi/pdf/10.1177/074873049300800106

Yack, J. E. (2004). The structure and function of auditory chordotonal organs in insects. *Microscopy Research and Technique, 63*(6), 315–337. https://doi.org/10.1002/jemt.20051

Yang, Z., Emerson, M., Su, H. S., & Sehgal, A. (1998). Response of the Timeless Protein to Light Correlates with Behavioral Entrainment and Suggests a Nonvisual Pathway for Circadian Photoreception. In *Neuron* (Vol. 21). Retrieved from https://www.cell.com/action/showPdf?pii=S0896-6273%2800%2980528-0

Yoon, J., Matsuo, E., Yamada, D., Mizuno, H., & Morimoto, T. (2013). Selectivity and Plasticity in a Sound-Evoked Male-Male Interaction in Drosophila. *PLoS ONE, 8*(9), 74289. https://doi.org/10.1371/journal.pone.0074289

Yorozu, S., Wong, A., Fischer, B. J., Dankert, H., Kernan, M. J., Kamikouchi, A., … Anderson, D. J. (2009). Distinct sensory representations of wind and near-field sound in the Drosophila brain. *Nature, 458*(7235), 201–205. https://doi.org/10.1038/nature07843

Zerr, D. M., Hall, J. C., Rosbash, M., & Siwickil, K. K. (1990). Circadian Fluctuations of period Protein Immunoreactivity in the CNS and the Visual System of Drosophila. In *The Journal of Neuroscience*. Retrieved from http://www.jneurosci.org/content/jneuro/10/8/2749.full.pdf

Zhou, C., Franconville, R., Vaughan, A. G., Robinett, C. C., Jayaraman, V., & Baker, B. S. (2015). Central neural circuitry mediating courtship song perception in male Drosophila. *ELife, 4*, e08477. https://doi.org/10.7554/eLife.08477

Zhu, Y. (2013). The Drosophila visual system: From neural circuits to behavior. *Cell Adhesion & Migration, 7*(4), 333–344. https://doi.org/10.4161/cam.25521

Supplementary

Supplementary 1: The MATLAB script that I developed to be used for data processing and analysis of auditory-induced locomotor activity. This script allowed to extract the relevant findings from the raw DAMSystem output. This was used alongside tools within Sigmaplot to process, analyse and visualise the data. Some variables were manually changed between different experimental conditions.

```
%%
ALL_day1 = [file_20190405_day1];
ALL_day2 = [file_20190405_day2];
%%
clearvars -except ALL_day1 ALL_day2

ALL_raw = ALL_day1;
ALL_reshaped = [];

%% Splits all columns into hourly responses
% i.e. (,1:25) = vial 1 hourly responses
ALL = ALL_raw;
[u,a] = size(ALL_raw);
for j = 1:a;
    c = j*25;
    d = c-24;

    ALL_reshaped(:,d:c) = reshape(ALL(:,j), 60, []);

end
%% Creates a daily 24 hour median activity for each vial
ALL_medians = [];
```

```matlab
[u,z] = size(ALL_raw);
for i = 1:z;
    b = i*25;
    a = b-23;

    ALL_medians = [ALL_medians, median(ALL_reshaped(:,a:b),2)];

end

% At this point ALL_medians gives the hourly median activity for
all
% individual vials.
%  PLOT ALL_medians into line graph to see responsiveness to
stimuli.

%% Normalise  hourly  median  activity  to  baseline  to  check
responsiveness
clear ALL a b i u

for i = 1:z ;

    ALL_subtraction(:,i)   =   median(ALL_medians(1:15,i))   -
median(ALL_medians(46:60,i));
end

clear i

%% After identifying the peak of the distribution of noramlised
activity values,
% Find the indicies of the final sample to be used.

a = 39; % this is the peak distribution value of sample
peak_plus = [];
for i = a:0.5:100;

    peak_plus = [peak_plus, find(ALL_subtraction==i)]
end

peak_minus = [];
for i = a:-0.5:-70;

    peak_minus = [peak_minus, find(ALL_subtraction==i)];
end
clear a i
% At the end of this, you will have the indecies of the closest
to furthest
% peak normalised values within the dataset
%% Collect the sample to be used for further processing from the
original raw data.
[u,a] = size(ALL_raw);
a = a/4;
ALL_new_minus_sample = [];
for i = 1:a;
    b = peak_minus(i)
    ALL_new_minus_sample = [ALL_new_minus_sample, ALL_raw(:,b)]
end
```

```
ALL_new_plus_sample = [];
for i = 1:a;
    b = peak_plus(i)
    ALL_new_plus_sample = [ALL_new_plus_sample, ALL_raw(:,b)]
end

NEW_SAMPLE_raw  =  [ALL_new_plus_sample,  ALL_new_minus_sample]
%THIS IS THE SAMPLE TO BE USED FOR DURTHER DATA PROCESSING

clear a b i u
%% Test the normality distribution of new sample
clear ALL_reshaped
ALL = NEW_SAMPLE_raw;
[u,a] = size(NEW_SAMPLE_raw);
for j = 1:a;
    c = j*25;
    d = c-24;

    ALL_reshaped(:,d:c) = reshape(ALL(:,j), 60, []);

end
%%
NEW_SAMPLE_medians = [];
for i = 1:a;
    b = i*25;
    a = b-23;
    NEW_SAMPLE_medians(:,i) = median(ALL_reshaped(:,a:b),2);

end

%% ANALYSIS

% IF NORMALITY TEST PASSED

NSR = NEW_SAMPLE_raw;

[n,m] = size(NSR)
for i = 1:n/60;
    a = i*2;
    b = a-1;
   for j = 1:m;

   NSR_median(a,j) = sum(NSR(46:60,j));


    NSR_median(b,j) = sum(NSR(1:15,j));


    end

NSR = NSR(61:end,:);

end
clear n m NSR b i j a
```

```
%%
NSR_absolute_stimulus = NSR_median(3:2:end,:)  % stimulus matrix
NSR_absolute_baseline = NSR_median(2:2:end,:)  % baseline matrix

%%
NSR_interpolating_baseline  = [];
[u,z] = size(NSR_absolute_baseline);


for i = 1:24;
a = i+1;

NSR_sub                                              =
(NSR_absolute_baseline(i,:)+NSR_absolute_baseline(a,:))/2;
NSR_interpolating_baseline    =    [NSR_interpolating_baseline;
NSR_sub];
end

NSR_sub_normalised       =       NSR_absolute_stimulus       -
NSR_interpolating_baseline;

NSR_div_normalised       =          NSR_sub_normalised     ./
NSR_interpolating_baseline;
%NSR_interpolating_baseline;

%%
NSR_median_median = median(NSR_median,2);
NSR_median_SEM = std(NSR_median,0,2);
NSR_median_SEM = NSR_median_SEM / sqrt(50);

NSR_stim_median = median(NSR_absolute_stimulus,2);
NSR_stim_SEM = std(NSR_absolute_stimulus,0,2);
NSR_stim_SEM  = NSR_stim_SEM / sqrt(24);

NSR_baseline_median = median(NSR_interpolating_baseline,2);
NSR_baseline_SEM = std(NSR_interpolating_baseline,0,2);
NSR_baseline_SEM = NSR_baseline_SEM / sqrt(24);

NSR_sub_median = median(NSR_sub_normalised,2);
NSR_sub_SEM = std(NSR_sub_normalised,0,2);
NSR_sub_SEM  = NSR_sub_SEM / sqrt(24);

NSR_div_median = median(NSR_div_normalised,2);
NSR_div_SEM = std(NSR_div_normalised,0,2);
NSR_div_SEM  = NSR_div_SEM / sqrt(24);

clear a aa i u z NSR_sub
%%
z_base = NSR_absolute_baseline(2:25,:);
[u,z] = size(NSR_interpolating_baseline);
b = z*8;
z_baseline = reshape(z_base,[],b);
z_baseline = median(z_baseline);
z_baseline = reshape(z_baseline,[],z);
z_baseline = z_baseline'
```

209

```
z_stim = NSR_absolute_stimulus(1:24,:);
[u,z] = size(NSR_interpolating_baseline);
b = z*8;
z_stimulus = reshape(z_stim,[],b);
z_stimulus = median(z_stimulus);
z_stimulus = reshape(z_stimulus,[],z);
z_stimulus = z_stimulus'

z_sub = z_stimulus - z_baseline;
z_gain = z_sub ./ z_baseline;

z_gain_avr = median(z_gain);
z_sub_avr = median(z_sub);
z_base_avr = median(z_baseline);
z_stim_avr = median(z_stimulus);
clear b c d u z z_base z_stim

%%
average_baseline = median(NSR_interpolating_baseline)
average_stimulus = median(NSR_absolute_stimulus)
average_sub = median(NSR_sub_normalised)
average_gain = median(NSR_div_normalised)


%% Light dark testing

a_light_div = NSR_div_normalised(1:12,:);
a_dark_div = NSR_div_normalised(13:24,:);
aa_light_sub = NSR_sub_normalised(1:12,:);
aa_dark_sub = NSR_sub_normalised(13:24,:);
aaa_light_baseline = NSR_interpolating_baseline(1:12,:);
aaa_dark_baseline = NSR_interpolating_baseline(13:24,:);
aaaa_light_stim = NSR_absolute_stimulus(1:12,:);
aaaa_dark_stim = NSR_absolute_stimulus(13:24,:);

b_light_div_avr = median(a_light_div);
b_dark_div_avr = median(a_dark_div);
bb_light_sub_avr = median(aa_light_sub);
bb_dark_sub_avr = median(aa_dark_sub);
bbb_light_base_avr = median(aaa_light_baseline);
bbb_dark_base_avr = median(aaa_dark_baseline);
bbbb_light_stim_avr = median(aaaa_light_stim);
bbbb_dark_stim_avr = median(aaaa_dark_stim);
```
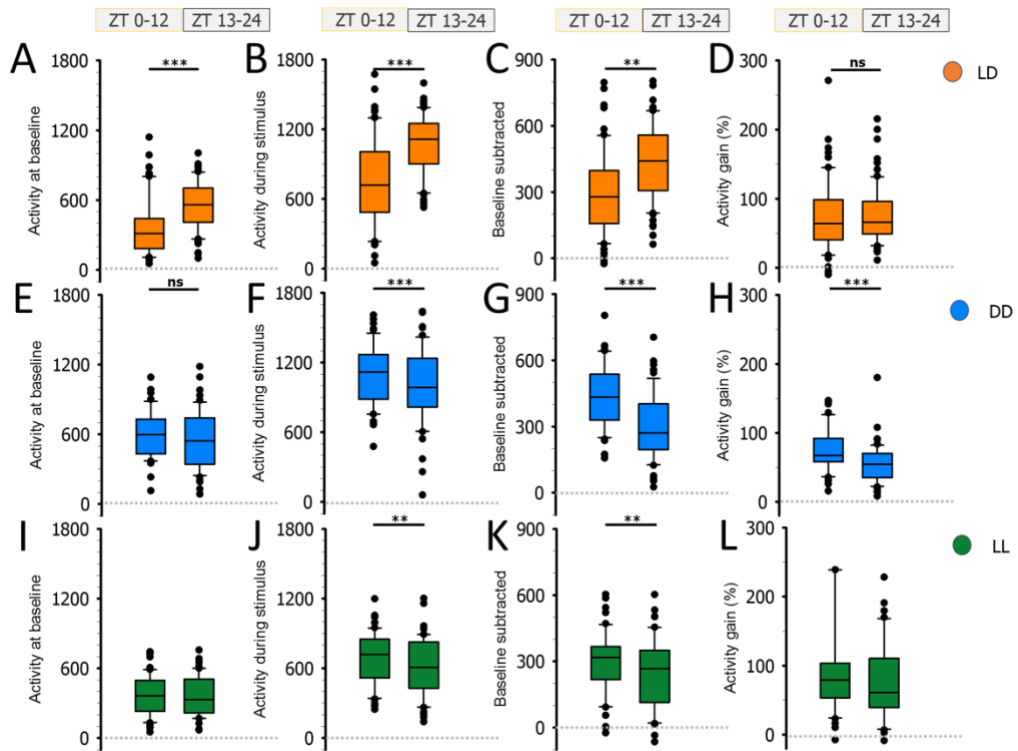
Supplementary 2: Series of box plots to show the differences in the locomotor activity between CT/ZT1-12 and ZT/ZT13-24 for male wild-type flies LD, DD and LL conditions on the second experimental day. **A-D:** show the activity at baseline (**A**), activity during stimulus (**B**), baseline subtracted activity (**C**) and activity gain (**D**) for animals in LD environmental conditions. The box plots show the measurement for either ZT 1-12 and ZT13-24. Comparisons are made between the two phases and between conditions. **E-H:** shows the same measurements but for DD conditions and **I-L** is for LL environmental conditions (**= p<0.01, ***= p<0.001)

Supplementary 3: Box plots to show the activity gain for *glass60j* flies for the second experimental day. There were no significant differences in the activity gain between ZT1-12 and ZT13-24 for this experimental day. The first box is the median activity gain for ZT1-12 of *glass60j* flies and the second box is the median activity gain for ZT13-24. (n= 18)
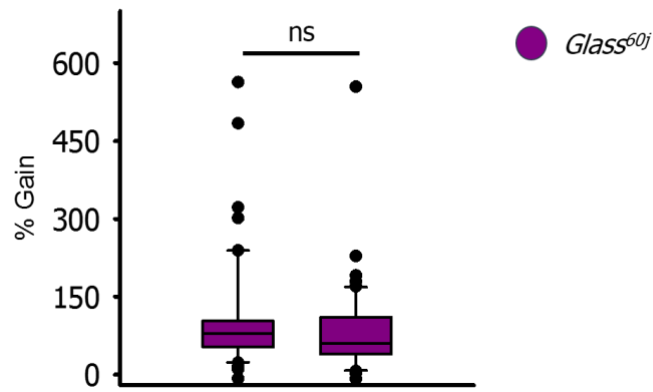
Supplementary 4: Area plot to show the median baseline locomotor activity of male wild-type flies that were not exposed to sound stimuli. The activity of these flies was simply monitored over a 24-h period. The animals were sampled in grouped conditions of 3. (n= 18).
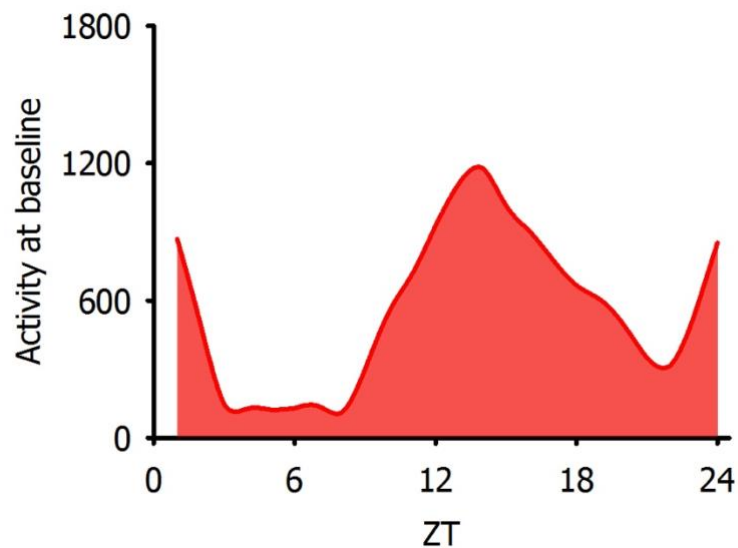
Supplementary 5: Scatter plots to show the response properties to APT and RCS stimuli of two flies expressing UAS-GCamp-6f in JO-all neurons assayed each hour from ZT3 to ZT12/ZT13. There are changes in the peak $\Delta F/F_o$, total $\Delta F/F_o$, and the time constants in the responses recorded throughout the tested period. Interestingly both sampled flies show increases in signal magnitude around ZT6.

The purple dots show the responses to APT stimuli and the green are the responses to RCS. These preliminary findings demonstrate that it is possible to perform calcium imaging on a fly over a prolonged period of time.